CHARACTERIZATION OF THE ROLE OF PROTEIN ARGININE METHYLTRANSFERASE 5 (PRMT5) IN MAMMALIAN DEVELOPMENT

MARCO BEZZI

(*Master in Molecular Biotechnology (Hons),*

Alma Mater Studiorum Bologna, Italy)

A THESIS SUBMITTED

FOR THE DEGREE OF DOCTOR OF PHILOSOPHY

DEPARTMENT OF BIOCHEMISTRY

NATIONAL UNIVERSITY OF SINGAPORE

2014

DECLARATION

I hereby declare that the thesis is my original work and it has been written by me in its entirety.

I have duly acknowledged all the sources of information which have been used in the thesis.

This thesis has also not been submitted for any degree in any university previously.

Marco Bezzi

23 January 2014

MARCO BEZZI

22/05/2014

ACKNOWLEDGEMENTS

First of all, I would like to thank my supervisor, Dr. Ernesto Guccione for having me in his lab, for his continuous support, motivation and most of all for constantly believing in me. I am indebted to A*STAR and to the National University of Singapore for giving me the opportunity to embark on a PhD. I am thankful to the members of my Thesis Advisory Committee, Dr. Xin-Yuan Fu and Dr. Huck Hui Ng for the precious advices. I owe much to the IMCB histopathology facility and to the proteomic facility for the constant technical support. A big thank you to the Kaldis lab for sharing reagents and protocols.

My sincere thanks go to all the current and past members of the EG lab, particularly Shun Xie, Wei Chuen and Julius for the incredible help on all my projects.

Finally, I want to thank my two women, the crazy beast and my closet friends all around the world for making everything worthwhile.

TABLE OF CONTENTS

SUMMARY

The tight control of gene expression at the level of both transcription and post-transcriptional RNA processing is essential for mammalian development and altered in a multitude of human pathologies. We here investigate the role of protein arginine methyltransferase 5 (PRMT5), a putative splicing regulator and transcriptional cofactor, of high-interest to the cancer and drug discovery fields, yet of unclear function during mammalian development.

We demonstrate that selective deletion of *Prmt5* during organogenesis, in a conditional mouse model, is embryonically lethal causing widespread apoptosis and cell cycle arrest. Actively proliferating organs such as the liver, which during embryonic development is populated by Hematopoietic Stem Cells (HSCs), are particularly affected. Consistently, *ex vivo* PRMT5 depletion in HSCs impairs hematopoiesis. Since a variety of developmental diseases of the Central Nervous System (CNS) have been linked to either epigenetic or splicing defects we next focus our efforts on brain development in order to gain further insights into the physiological and molecular basis of PRMT5 function in safeguarding proliferating cells homeostasis. PRMT5 depletion in the developing CNS leads to postnatal death in mice. Notably, Neural Stem/ Progenitor cells (NPCs) homeostasis is compromised and the activation of the apoptotic response can be fully rescued by deletion of the tumor suppressor protein p53. At the molecular level, the absence of PRMT5 results in reduced methylation of Sm proteins, aberrant constitutive splicing, and the alternative splicing of specific mRNAs with weak 5’ donor sites. Intriguingly, the products of these mRNAs are, among others, several proteins regulating cell cycle progression. We identify *Mdm4* as one of these key mRNAs that senses the defects in the spliceosomal machinery and transduces the signal

to activate the p53 response, providing a mechanistic explanation of the phenotype observed in vivo. Finally, we describe a correlation between the severity of the growth arrest phenotype, the rate of cell proliferation and the severity of the splicing defects. The identified mechanism is fully conserved in human cells.

Our data demonstrate that PRMT5 is a master regulator of splicing in mammals and uncover a new early-warning system based on *Mdm4* pre-mRNA, which could be exploited for anti-cancer therapy.

LIST OF FIGURES

LIST OF TABLES

LIST OF PUBLICATIONS

Regulation of constitutive and alternative splicing by PRMT5 reveals a role for Mdm4 pre-mRNA in sensing defects in the spliceosomal machinery.
Genes Dev., vol. 27, no. 17, pp. 1903–1916, Sep. 2013.
Bezzi M, Teo SX, Müller J, Mok WC, Sahu SK, Vardy LA, Bonday ZQ, and Guccione E.

p53-Independent regulation of p21Waf1/Cip1 expression and senescence by PRMT6.
Nucleic Acids Res., vol. 40, no. 19, pp. 9534–9542, Oct. 2012.
Phalke S, Mzoughi S, **Bezzi M**, Jennifer N, Mok WC, Low DHP, Thike AA, Kuznetsov VA, Tan PH, Voorhoeve PM, and Guccione E.

Hairless promotes PPARγ expression and is required for white adipogenesis.
EMBO Rep., vol. 13, no. 11, pp. 1012–1020, Nov. 2012.
Kumpf S, Mihlan M, Goginashvili A, Grandl G, Gehart H, Godel A, Schmidt J, Müller J, **Bezzi M**, Ittner A, Guccione E, Wolfrum C, and Ricci R.

Symmetric dimethylation of H3R2 is a newly identified histone mark that supports euchromatin maintenance.
Nat. Struct. Mol. Biol., vol. 19, no. 2, pp. 136–144, Feb. 2012.
Migliori V, Müller J, Phalke S, Low D, **Bezzi M**, Mok WC, Sahu SK, Gunaratne J, Capasso P, Bassi C, Cecatiello V, De Marco A, Blackstock W, Kuznetsov V, Amati B, Mapelli M, and Guccione E.

Arginine/lysine-methyl/methyl switches: biochemical role of histone arginine methylation in transcriptional regulation.
Epigenomics, vol. 2, no. 1, pp. 119–137, Feb. 2010.
Migliori V, Phalke S, **Bezzi M**, and Guccione E.

Chapter 1

INTRODUCTION

1.1 Arginine Methylation

Post-translational modifications (PTMs) have been shown to be crucial modulators of every known cellular process. By changing the biochemical and biophysical features of proteins, PTMs deeply impact on the proteome complexity fine-tuning and regulating protein fate, localization, stability, activity and interaction. Protein methylation is one of the most studied and abundant PTM and almost 2% of protein coding genes in prokaryotes and eukaryotes encode methyltransferases (Katz et al., 2003; Petrossian and Clarke, 2009; Petrossian and Clarke, 2011; Wlodarski et al., 2011). In eukaryotes, the most commonly methylated residues are lysines and arginines and a study conducted in rat liver nuclei estimates that 2% of arginine residues are methylated (Boffa et al., 1977).

The two terminal guanidino-groups (NH2) of the arginine side chain mediate protein-protein, protein-DNA and protein-RNA interaction by formation of hydrogen bonds (Luscombe et al., 2001). Addition of methyl moieties to the guanidino-groups does not change the cationic charge of the residue, but rather increases its hydrophobicity and reshape the amino acid making it bulkier. Moreover, each methyl group abolishes a potential hydrogen bond donor (Hughes and Waters, 2006; Stetler et al., 2006). The methylation of one guanidino-group generates a ω-N^G-monomethylarginine (MMA), which can be dimethylated either on the same guanodino-group giving rise to ω-N^G,N^G-asymmetric dimethylarginine (ADMA), or on the other guanidine group generating ω-N^G,N'^G-symmetric dimethylarginine (SDMA) **(Fig.1.1)** (Bedford and Clarke, 2009).

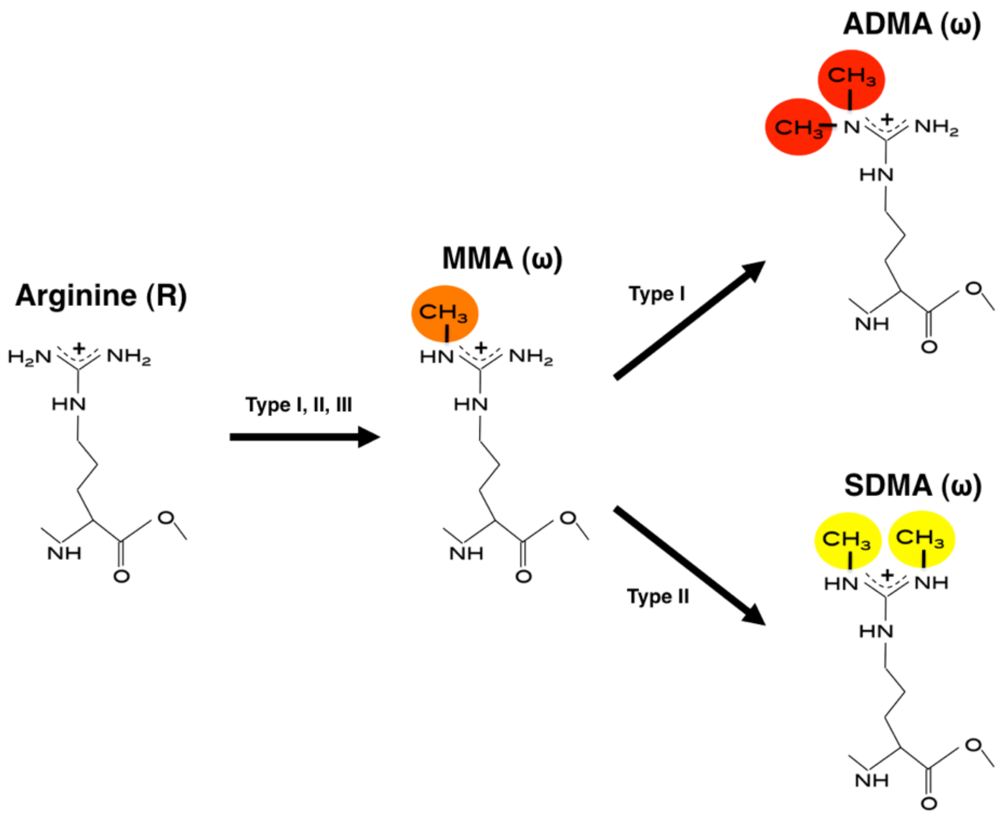

Figure 1.1: Types of arginine methylation. Adapted from (Yang and Bedford, 2013). All protein methyltranferases (Type I, II and III) can methylate arginine one of the terminal (ω) guanidino nitrogen atoms generating monomethylarginine (MMA). The generation of symmetric dimethylraginine (SDMA) is catalyzed by Type II enzymes, whereas Type I PRMTs generate asymmetric dimethylarginine methylating the same terminal (ω) guanidino nitrogen atom methylated in the first methylation event.

1.2 Protein arginine methyltransferases

Arginine methylation is catalyzed by the protein arginine methyltransferase (PRMT) family of proteins. Nine seven-beta-strand PRMTs have been identified in mammals until now, PRMT1-9, and we cannot exclude that other PRMTs have yet to be discovered. These enzymes have been grouped in three different classes: type I, type II and type III PRMTs. All the PRMTs are able to catalyze MMA, while type I PRMTs (PRMT1, 2, 3, 4, 6 and 8) specifically dimethylate arginines asymmetrically. On the other hand type II PRMTs catalyze symmetric arginine dimethylation. PRMT5 is unquestionably the better studied type II PRMT (Yang and Bedford, 2013), whereas it is not clear whether PRTM7 is a type II PRMT or a type III PRMT simply able to monomethylate arginines (Zurita-Lopez et al., 2012; Bedford and Clarke, 2009). The catalytic specificity of PRMT9 has not been characterized **(Fig. 1.1) (Fig. 1.2)**.

The most active type I and type II PRMTs, PRMT1 and PRMT5 respectively, are conserved from yeast to human and are essential for mouse and cell viability (Yu et al., 2009; Tee et al., 2010; Wang and Li, 2012). PRMTs appear to be ubiquitously expressed, with the exception of PRMT8, a brain specific prologue of PRMT1, conserved in vertebrates (Lee et al., 2005; Wang and Li, 2012).

PRMTs display high activity *in vitro*, they are able to methylate multiple target proteins on multiple arginine sites and their substrate specificity is much broader compared to that of lysine methyltransferases (Bedford and Clarke, 2009). These enzymes preferentially methylates arginines within the glycine-arginine-rich (GAR) motif and within the proline-glycine-methionine-rich (PGM) motif. Despite the absence of a specific consensus targeted by individual PRMTs and the fact that most of the PRMTs share substrates *in vitro*, they are not redundant *in vivo*, as they affect cell growth and differentiation in different ways (Hyllus et al., 2007; Swiercz et al., 2007; Yadav et al., 2003; Yu et al., 2009).

Initial attempts to identify arginine-methylated proteins have generated lists of putative PRMT targets (Boisvert et al., 2003; Ong et al., 2004; Bremang et al., 2013). These studies failed to identify residues methylated by specific PRMT family members and to distinguish between symmetric and asymmetric dimethylation. However, they did shed light on the relevance of arginine methylation in numerous cellular processes including cytoskeleton formation, signaling, DNA transcription, protein translation and pre-mRNA processing. Key methylated targets regarding the latter are components of the constitutive splicing machinery (e.g., Sm proteins), several additional regulators of alternative splicing (e.g., FUS/TLS, SF2, and members of the heterogeneous nuclear ribonucleoprotein [hnRNP] family).

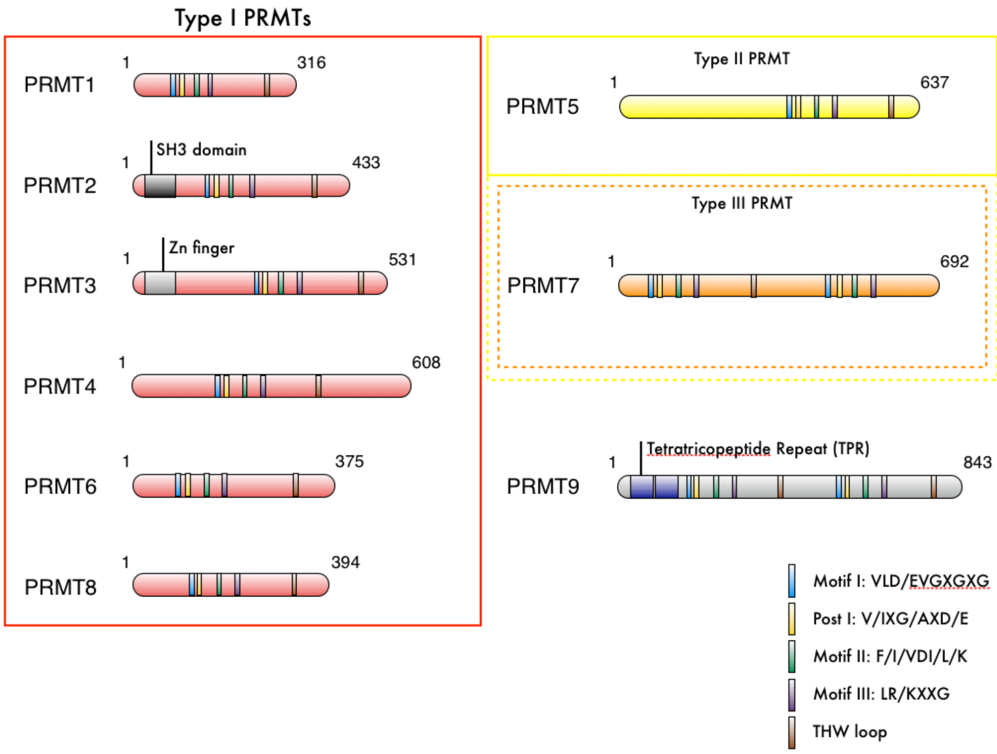

Figure 1.2: The mammalian PRMT family. Adapted from (Yang and Bedford, 2013). Type I enzymes PRMT1, PRMT2, PRMT3, PRMT4, PRMT6, PRMT8, are in the red box. The only Type II enzyme, PRMT5, is in the yellow box. It is not clear whether PRMT7 is either a Type II or a Type III PRMT (yellow and orange dashed box). PRMT9 catalytic activity has not been characterized yet. The vertical lines represent the typical PRMT motifs indicated in the legend.

1.3 PRMT5 structure and activity

PRMT5 is the human homolog of the *Schizosaccaromyces pombe* Skb1, and *Saccharomyces cerevisiae* Hsl7 protein. It was discovered in a yeast two-hybrid screening as a Janus kinase 2 binding protein and therefore called JBP1 (Pollack et al., 1999). After the discovery of its catalytic activity as an arginine methyltransferase towards Myelin basic protein, Fibrillarin and histones H2A and H4 *in vitro,* JBP1 has been renamed PRMT5 (Rho et al., 2001). Sequence homology analysis, and concomitant biochemical studies unveiled that the C-terminal PRMT5 domain contains the domains I

(GXGRGP motif), II, III and the post-I domain typical of the S-Adenosyl-L-Methionine (SAM) binding proteins. SAM is the most common methyl group donor cofactor and mutation in the PRMT5 SAM-binding domain motif I dramatically reduced PRMT5 catalytic activity. Finally, the N-terminal domain is necessary for the interaction with the C-terminal domain and the formation of functional homo-oligomeric complexes (Branscombe et al., 2001; Pollack et al., 1999; Rho et al., 2001). PRMT5 has been described as a binding partner for several proteins and this is partially explained by the recent finding that PRMT5 is a major contaminant of the FLAG immunoprecipitation (Nishioka and Reinberg, 2003). MEP50 (methylosome protein 50) is a WD-repeat-containing protein which has been constantly detected as a PRMT5 binding partner in different experimental conditions and is now considered and essential PRMT5 coactivator (Antonysamy et al., 2012; Friesen et al., 2002). Further evidence regarding the decisive contribution of MEP50 to PRMT5 activity have been recently collected by Liu and colleagues. While focusing on the role of constitutive active mutants of JAK2 in myeloproliferative neoplasms they discovered that phosphorylation of PRMT5 disrupted the PRMT5 MEP50 association impairing PRMT5 catalytic activity (Liu et al., 2011). In addition to MEP50, other proteins associate with PRMT5 conferring its context-dependent substrate specificity. COPR5 redirect PRMT5 activity specifically towards histone H4 (Lacroix et al., 2008) while DAL-1/4.1B stimulates PRMT5-mediated methylation of myelin basic protein (Jiang et al., 2005). pICln is a key component of the PRMT5 complex responsible for the methylation of the spliceosome Sm proteins (Grimm et al., 2013) while RioK1, which is mutually exclusive with pICln, redirects PRMT5 methylation towards Nucleolin (Guderian et al., 2011).

Recent structural studies generated significant insights into PRMT5 dimerization properties, interaction with MEP50, active site and substrate recognition (Antonysamy et al., 2012; Ho et al., 2013; Sun et al., 2011).

Human PRMT5 has been co-crystallized in complex with MEP50 and the structure revealed the formation of a hetero-octamer $(PRMT5)_4(MEP50)_4$ in which the four PRMT5 monomers are tightly packed in the central catalytic core of the complex and the four MEP50 molecules bind the outer surface (Antonysamy et al., 2012). PRMT5 is composed of four domains: the N-terminal TIM barrel domain, the middle Rossmann-fold domain, and the C-terminal β-barrel domain containing a small dimerization domain **(Fig. 1.3)**. MEP50 adopts a seven bladed WD40 β-propeller conformation and interacts with PRMT5 solely through the PRMT5 N-terminal TIM barrel domain (Antonysamy et al., 2012; Ho et al., 2013). The TIM barrel domain is also required for PRMT5 homo-dimerization enabling head-to-tail interactions with the C-terminal β-barrel domain of a different PRMT5 monomer. Another important event in PRMT5 homo-dimerization is the direct interaction between the two dimerization domains of adjacent PRMT5 monomers.

PRMT5-substrate interaction has been explored using a peptide mimicking the N-terminal tail of histone H4. The H4 peptide contacts a cavity on the PRMT5 β-barrel domain and the arginine side chain enters the active site through a narrow tunnel where hydrogen bonds between protein backbones stabilize the interaction of the H4 peptide with residues within the PRMT5 β-barrel domain and the Rossmann-fold domain (Antonysamy et al., 2012). Moreover, electron microscopy studies suggest a crucial role for MEP50 in substrate recognition as they revealed direct contact between MEP50 and the substrate Nucleophosmin (NPM) (Ho et al., 2013). The catalytic site has been identified by co-crystallization of PRMT5 with different SAM analogs and lies in the Rossmann-fold domain. Two glutamate residues (in human Glu 435 and Glu 444) conserved among all the PRMTs and located on a double-E loop are necessary for the enzymatic activity. They contact the substrate arginine forming salt bridges and are likely responsible for the activation of the nitrogen atom. Furthermore, the most important residue determinant of the symmetry of methylation has been identified in the active site. The phenylalanine 375, in human PRMT5, is replaced by a methionine residue in the type I PRMTs and ensure the correct orientation of the arginine to be symmetrically dimethylated (Antonysamy et al., 2012; Sun et al., 2011).

Importantly, in contrast to the asymmetric dimethylation catalyzed by PRMT1, the methylation reaction carried out by PRMT5 is not a processive mechanism. PRMT5 methylates the substrate in a distributive fashion with a rapid equilibrium random kinetic. Two distinct methylation events occur with release of the substrate prior the second methylation. Thus the concentration of un-methylated and mono-methylated substrate are crucial (Antonysamy et al., 2012; Wang et al., 2013).

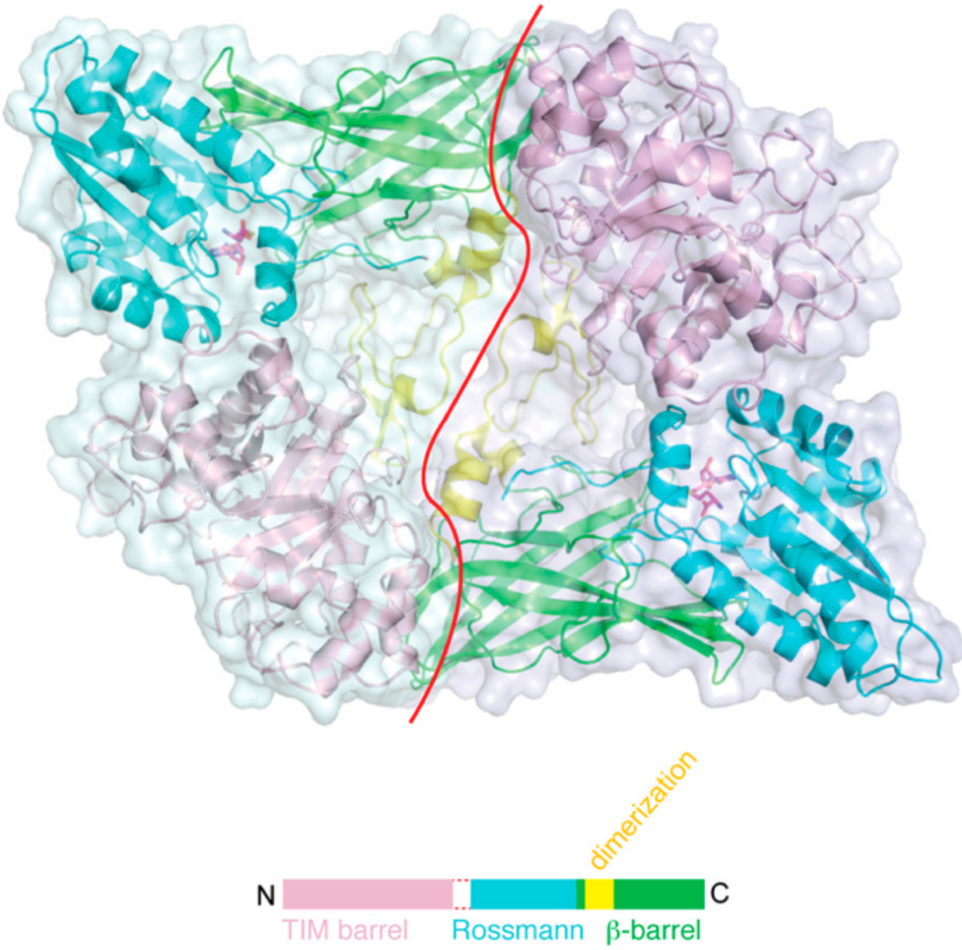

Figure 1.3: Structure of PRMT5. Adapted from (Sun et al., 2011). A ribbon representation of *C. elegans* PRMT5 dimer. The SAH is shown in the Rossmann-fold domain (pink). The dimer surface is traced by the red line.

1.4 PRMT5 and transcriptional regulation

PRMT5 is a highly versatile enzyme and participates in the regulation of many cellular processes methylating a multitude of substrates. PRMT5 role in transcriptional regulation is undoubtedly its most studied function and it is clear that it acts as a transcriptional cofactor modifying histones and modulating the activity of several transcription factors. In contrast to the majority of the chromatin remodeling enzymes, PRMT5 is not univocally classified as coactivator or corepressor of gene expression, but the transcriptional outcome rather depends on the arginine residue being methylated, on PRMT5 binding partners and in some cases on the chromatin landscape.

1.4.1 PRMT5 and histone methylation

Eukaryotes condense the DNA into highly ordered chromatin fibers. The basic repeating unit of chromatin is the nucleosome, consisting of a core of eight histones ($(H2A)_2(H2B)_2(H3)_2(H4)_2$) around which 147 base pairs of DNA wrap (Kornberg and Lorch, 1999; Luger et al., 1997). Besides packaging the DNA, allowing its storage into the nucleus, chromatin plays a fundamental role in regulating DNA accessibility during several processes such as replication, DNA repair as well as transcription initiation, elongation and pre-mRNA splicing. Histone post translational modifications, DNA methylation and ATP-dependent chromatin remodelers modify the chromatin landscape determining nucleosome-DNA interaction, therefore chromatin condensation, and recruiting factors essential for the regulation of the genetic information (Strahl and Allis, 2000; Workman and Kingston, 1998). PRMT5 is an unusual histone-modifying enzyme, as it is able to catalyze symmetric dimethylation of at least four different arginine residues of different histones: arginine 3 on histone H4 (H4R3me2s), arginine 3 on histone H2A (H2AR3me2s), arginine 8 on histone H3 (H3R8me2s) and arginine 2 on histone H3 (H3R2me2s) **(Fig. 1.4)**.

1.4.1.1 H4R3me2s

Since its discovery, H4R3me2s has been associated with transcriptional repression. The first study describing H4R3me2s identifies PRMT5 as a component of an atypical E2F complex which represses cyclin E1 promoter via histone methylation resulting in inhibition of cell proliferation (Fabbrizio et al., 2002). The Sif group later co-purified PRMT5 in association with the Brg1 and hBrm-based hSWI/SNF chromatin remodeler complex, and with the mSin3A histone deacetylase (HDAC) 2. As part of this complex PRMT5 catalyses both H4R3me2s and H3R8me2s ensuring repression of the c-Myc target genes *Nucleolin* and *Cad* as well as of the tumor suppressor genes *St7*, *Nm23*, and some genes of the RB family of tumor suppressors in lymphoid cancer cells, hence supporting tumor proliferation (Pal et al., 2007; 2004; 2003; Wang et al., 2008). The direct mechanism linking H4R3me2s to transcriptional silencing has been recently elucidated. Zhao and colleagues showed that DNMT3A directly interacts with H4R3me2s through the PHD finger motif within its ADD domain. As a consequence, PRMT5-mediated dimethylation of histone H4 is required for DNA methylation, a well-established mechanism of gene repression (Zhao et al., 2009). Moreover, in erythroid cells PRMT5 binds the promoter of the ɣ–globin gene and methylation of histone H4 is required not only for DNMT3A DNA methylation, but also for the establishment of a repressive chromatin landscape through the recruitment of multiple repressor proteins such as the histone H4 lysine 20 methyltransferase SUV4-20h1, casein kinase 2α, HDAC1 and mSin3A (Rank et al., 2010).

Additional evidence supporting the repressive role of H4R3me2s has been collected in other cell systems and more tumor suppressor and cell cycle regulator genes, such as *Smad7*, *Cul4A/B*, *Cdnka* and *Cdh*, have been identified as PRMT5 targets (Aggarwal et al., 2010; Gurung et al., 2013; Patel et al., 2011; Tabata et al., 2009) **(Fig. 1.4)**. However, all the above-mentioned studies rely on PRMT5 knock-down experiments and focus on a limited number of genomic loci. Tee and colleagues described the role of PRMT5 in mouse embryonic stem (mES) cells and PRMT5 knock-down experiments, which phenocopied the PRMT5 knock-out mES cells (as will be discussed later), did not show any reduction in H4R3me2s (Tee et al., 2010). Furthermore, the Feil group recently took advantage of chromatin immunoprecipitation coupled with DNA deep sequencing in order to elucidate the genome wide distribution of H4R3me2s. Surprisingly, their data show that the observed enrichment of H4R3me2s at G+C-rich regions does not correlates with transcriptional levels or chromatin silencing (Girardot et al., 2014).

1.4.1.2 H3R8me2s

H3R8me2s, in combination with H4R3me2s, has been associated with gene silencing in lymphoid cancer cells (Pal et al., 2004; 2007), whereas during myogenic differentiation and adipogenesis it is required for gene expression and PRMT5 acts as a transcriptional coactivator (Dacwag et al., 2009; 2006; LeBlanc et al., 2012). The nature of this dual function is still unclear, since no direct H3R8me2s binding partner has been identified and genome-wide studies have yet to be performed. Moreover, whether there is a PRMT5 cofactor specifically restricting PRMT5 activity towards H3R8 is still unknown. A possible explanation could be found considering the crosstalk between

H3R8 and the proximal residues within the N-terminal tail of histone H3. Histone acetylation positively regulates gene transcription and PRMT5 preferentially methylates hypoacetylated histones. *In vitro*, H3R8 methylation is inhibited by acetylation of both lysine 9 (H3K9) and lysine 14 on histone H3 and this observation is consistent with repression of gene expression induced by co-recruitment of PRMT5 and HDACs (Pal et al., 2003; 2004; Rank et al., 2010).

Conversely, H3K9 methylation is a hallmark of silent chromatin and the trimethylated form of H3K9 is directly bound by HP1 which promote chromatin condensation. H3R8me2s blocks G9a-mediated methylation of lysine 9 on histone H3 *in vitro* (Rathert et al., 2008). Moreover, HP1 co-crystallization with histone H3 revealed structural insights about the requirement for unmethylated arginine 8 **(Fig. 1.4)**. In this context H3R8me2s likely interferes with the establishment of repressed chromatin therefore acting as an activator of transcription (Jacobs and Khorasanizadeh, 2002; Nielsen et al., 2002). However, *in vivo* evidence is still missing.

1.4.1.3 H2AR3me2s

Despite PRMT5 ability to methylate histones H2A and H4 *in vitro* has been described more than a decade ago (Rho et al., 2001), it is only recently that *in vivo* evidence of H2AR3me2 existence has been collected (Ancelin et al., 2006) and its function has been investigated (Tee et al., 2010). Notably, the N-terminal of histone H2A and the N-terminal tail of histone H4 have significant sequence similarity, and we now know that many commercial antibodies raised against H4R3me2s cross-react with H2AR3me2s.

Consequently, it is possible that chromatin immunoprecipitation and immunofluorescence experiments investigating H4R3me2s have been misinterpreted. PRMT5 knock-down in mES cells showed the conspicuous reduction of H2AR3me2s rather than H4R3me2s. Interestingly, PRMT5 in mES cells localizes and methylates H2A in the cytoplasm. H2AR3m2s is dispensable for chromatin assembly and its deposition on repressed promoters appears to be required for maintenance of transcriptional inhibition **(Fig. 1.4)**. Nevertheless, how H2AR3s contributes to gene expression is not clear.

1.4.1.3 H3R2me2s

H3R2me2s has been discovered in our lab. It is conserved throughout evolution and marks open chromatin regions. H3R2me2 inhibits recruitment of several transcription co-repressors and is directly bound by WDR5, a component of the MLL complex which trimethylates lysine 4 on histone H3 (H3K4me3) (Migliori et al., 2012). H3K4me3 is a hallmark of gene activation and its genomic distribution correlates with H3R2me2s distribution in yeast and mouse (Yuan et al., 2012). Both PRMT5 and PRMT7 are able to produce H3R2me2s *in vitro* and the double knock-down results in a dramatic reduction of this histone modification *in vivo* (Migliori et al., 2012) **(Fig. 1.4)**. This result can be explained considering the controversial nature of PRMT7 catalytic activity as type II or type III PRMT, and the distributive fashion of PRMT5 catalytic activity.

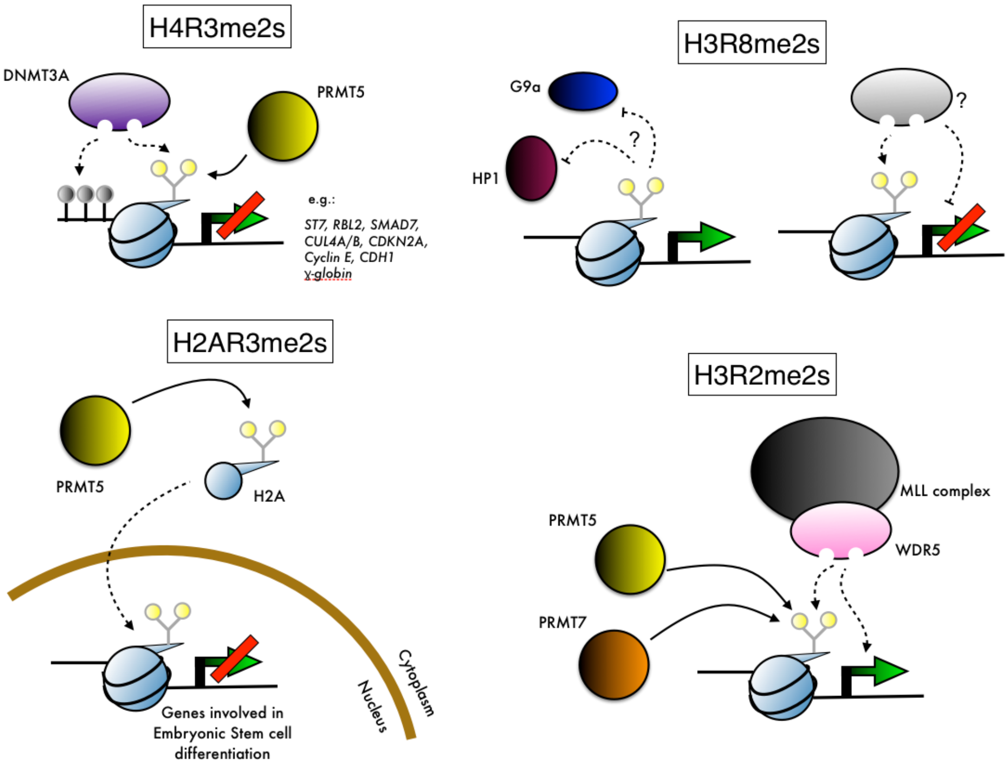

Figure 1.4: PRMT5-mediated histone modifications. Schematic representation of the mechanism of action of the histone modification catalyzed by PRMT5. H4R3me2s has been shown to be recognized by DNMT3A (dashed line) which in turn methylates (dashed line) the DNA (grey) establishing a repressive chromatin landscape. Few illustrative examples of repressed target genes in different cell lines are indicated. H2AR3me2s is catalyzed in the cytoplasm, then imported into the nucleus (dashed line) and assembled into nucleosomes which mark repressed genes. H3R8me2s has been linked with both activation and repression of transcription. H3R8me2s - mediated activation of transcription is thought to occur by the inhibition of the association between chromatin and repressive components such as HP1 and the enzyme G9a. The mechanism through which H3R8me2s inhibits transcription has not been characterized. H3R2me2s has been shown to be catalyzed by both PRMT5 and PRMT7. It is bound by WDR5, a component of the MLL complex, a well characterized activator of transcription.

1.4.2 PRMT5 and transcription factors

PRMT5 is overexpressed in many cancer types and appears to be essential for cancer cells, not only for its role as a chromatin-modifying enzyme, but also for its direct regulation of transcription factors involved in regulation of growth, inflammation and development.

p53, also called "the guardian of the genome", is a transcription factor considered to be the master regulator of DNA damage and stress response. Its targets are apoptotic genes and cell cycle inhibitors. The *p53* gene is ubiquitously expressed and its protein levels are finely regulated by a feedback loop with the protein that regulates its stability, the E3 ubiquitin ligase MDM2. MDM2 acts in combination with its heterodimeric partner MDM4 which is also involved in inhibition of p53 transcriptional activity (Wade et al., 2010).

Through the interaction with the p53 cofactor Strap, PRMT5 modulates the p53 DNA damage-induced response directly methylating p53 on three adjacent arginine residues. In human cancer cell lines, following DNA damage, PRMT5 depletion appears to restrict p53 transcriptional activation towards apoptotic genes, inducing cell death rather than cell cycle arrest. However, it is not yet clear the molecular mechanism by which arginine methylation directs p53 activity (Jansson et al., 2008).

PRMT5 has been shown to methylate another transcription factor involved in cell cycle progression and induction of apoptosis, E2F-1. The absence of PRMT5 stabilizes E2F-1 and induces apoptosis through activation of E2F-responsive genes, such as p73. Consistently, in several human tumor cell lines, reduction of E2F-1 by PRMT5-mediated arginine methylation has been observed upon DNA damage allowing the activation of the DNA damage response (Cho et al., 2012). A recent study clarifies that upon DNA damage, PRMT1 asymmetrically dimethylates E2F-1 counteracting methylation by PRMT5. Moreover, PRMT1-E2F-1 association is inhibited by Cyclin A. The E2F-1 symmetric dimethyl arginines are recognized by the tudor domain of p100-TSN, which binds E2F-1, reduces its half-life and modulates its apoptotic activity targeting a subset of E2F-responsive genes (Zheng et al., 2013).

In analogy with what has been observed for p53 and E2F-1, PRMT5 regulates the transcriptional activity of NF-κB and HOXA9 in a stimulus-dependent manner. NF-κB is a transcription factor critical for immune and inflammatory response as well as for tumorigenesis. Following stimulation with IL-1β, PRMT5 binds and methylates the arginine 30 of the NF-κB subunit p65. This methylation event reduces the binding of p65 to the κB element causing changes in gene expression. Notably, microarray analysis revealed that overexpression of the NF-κB R30A mutant leads to dowregulation of many NF-κB responsive genes, and approximately 85% of them are downregulated also in cells lacking PRMT5 (Wei et al., 2013).

Similarly, inflammation signal in endothelial cells (EC) induces PRMT5 association with the transcription factor HOXA9, following its methylation on arginine 140. This association is transient and occurs on selective target gene promoters. It does not affect HOXA9 DNA recognition, but rather modulates its transcriptional activity promoting the expression of pro-inflammatory endothelial-leukocytes adhesion molecules (ELAM) such as E-selectin and VCAM1. Thus, PRMT5 is potentially important in inflammation and cardiovascular inflammatory diseases (Bandyopadhyay et al., 2012).

1.5 PRMT5 and RNA splicing

As they are transcribed into precursor mRNAs (pre-mRNAs), most eukaryotic genes need to be edited in order to remove non coding regions (introns) ligating together regions destined to become a part of mature messenger (m) RNA sequence (exons). This essential multistep editing process called splicing is carried out by the spliceosome, a multi-megadalton ribonucleoprotein (RNP) complex. Importantly, not all the exons are constitutively included in the mature transcript. Proper functioning of all splicing-associated proteins allows a highly coordinated spatiotemporal exon selection (alternative splicing) generating multiple mRNA isoforms that significantly increase the complexity of the cell proteome. On the other hand, mutations in proteins involved in RNA processing have been causally linked to many human diseases such as spinal muscular atrophy (SMA) and amyotrophic lateral sclerosis (ALS), to mention a few (Da Cruz and Cleveland, 2011; Novoyatleva et al., 2006; Vance et al., 2009; Ward and Cooper, 2010; Zhang et al., 2008).

The spliceosome contains the small nuclear RNPs (snRNPs) U1,U2, U5, U4 (which belong to the Sm class of snRNP), U6 and a multitude of non-snRNP proteins. U6 belongs to the LSm-like class of snRNPs. The core of each Sm snRNP is formed by a unique snRNP-specific small nuclear RNA (snRNA) and seven Sm proteins (B/B', D3, D2, D1, E, F and G). In the cytoplasm, PRMT5 acts together with pICln and MEP50 as part of the methylosome, which mainly methylates Sm proteins B/B', D1, and D3 regulating snRNPs biogenesis and assumably plays a pivotal role in splicing efficacy (Matera et al., 2007).

1.5.1 Arginine methylation and core snRNPs biogenesis

The maturation pathway of the Sm-class snRNPs is summarized in **Fig. 1.5** and reviewed by (Matera et al., 2007). The uridine-rich, non-polyadenylated U snRNAs are transcribed by RNA Polymerase II (Pol II) and exported to the cytoplasm by a specialized snRNA-export complex. In the cytoplasm the Sm proteins are assembled as a heptameric ring around the Sm motif of the snRNAs. This fundamental step is orchestrated by the Spinal Motor Neuron (SMN) protein complex which recognizes the 3' stem-loop and the Sm protein binding site of the snRNAs, and the symmetrically dimethylated arginines of the Sm proteins B/B', D1 and D3. Subsequently the 5' ends of the snRNAs are hypermethylated by trimethylguanosine syntase-1 (TGS1) forming the 2,2,7-trimethylguanosine (TMG) cap. The Sm core and the TMG cap are necessary signals for the import into the nucleus carried out by the import complex which is comprised of snurportin-1 (SPN) and importin-b (Imp-b). Following the import, the core snRNPs localize in the nuclear compartments called Cajal bodies where small Cajal body-specific RNAs (scaRNAs) guide site-specific modification of the snRNAs and where a variable number of particle-specific proteins bind the core snRNPs completing the maturation process. Notably, also Coilin, which is the structural scaffold protein of the Cajal bodies, contains symmetrically dimethylated arginines required for SMN binding and essential for Cajal bodies formation (Boisvert, 2002; Hebert et al., 2002).

Symmetrically dimethylated arginines within the RG repeats located in the C-terminal regions of SmB/B', D1 and D3 were identified by the Luhrmann group (Brahms et al., 2001; 2000). PRMT5, the catalytic component of the methylosome, binds the RG domain of the Sm proteins and catalyses these methylations in the cytoplasm. Whereas MEP50 appears to be a general coactivator of PRMT5, stimulating its activity, the role played by pICln is multifaceted, specifically required for snRNP maturation process and inhibition of histone methylation (Friesen et al., 2001b; 2002; Meister et al., 2001; Meister and Fischer, 2002; Pesiridis et al., 2009).

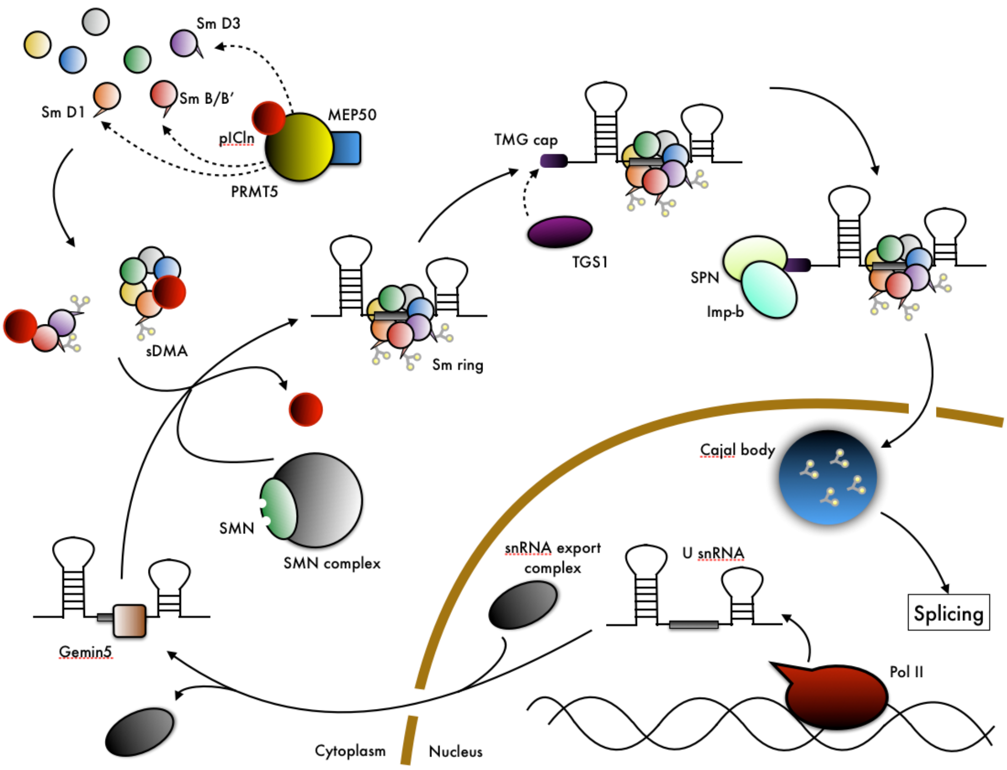

Figure 1.5: The maturation pathway of small nuclear RNPs. Adapted from (Matera et al., 2007). Following transcription by RNA Polymerase II (Pol II), a specialized snRNA-export complex, exports the Sm-class snRNA to the cytoplasm. Gemin5, a component of the SMN complex, recruits the snRNA and the SMN complex assembles the Sm proteins, three of which (SmB/B', D1 and D3) pre-methylated by the methylosome (PRMT5/pICln/MEP50), around the snRNA in a ring-like structure. Next, TGS1 hypermethylates the 5'end of the snRNA, forming the so called TMG cap. Both the Sm ring and the TMG cap are necessary signals for the import into the nucleus, carried out by SPN and Imp-b. On nuclear re-entry, the snRNPs localize in the Cajal bodies where further maturation steps take place before the snRNPs participate in splicing.

pICln binds the Sm domain of the Sm proteins and gel filtration studies revealed that it is part of two complexes, the 20S and the 6S complex, composed of different subset Sm proteins. The 20S complex, also known as the PRMT5 complex, is formed by PRMT5, MEP50, and all the Sm proteins recruited by pICln. The formation of this complex is considered as the beginning of the Sm ring formation and as the step required for the methylation of SmB/B', D1 and D3 (Grimm et al., 2013). The Sm proteins D1, D2, released by the 20S complex, and SmE, F, G are the other constituent of the 6S complex. pICln preferentially binds Sm D1 and D2 stabilizing their interaction with SmE, G and F to form the 6S complex unable to associate with the U snRNAs (Fischer, 2008). X-ray crystallography uncovered that such complex adopts a ring-like structure, very similar to the assembled Sm ring, in which pICln mimics the SmB/B', D3 heterodimer (Grimm et al., 2013). Subsequently, the SMN complex recruits both the 6S and the heterotrimer pICln, SmB/B', D3, and dissociates pICln to assemble the Sm ring onto snRNA (Fischer, 2008; Grimm et al., 2013). Importantly, seven other proteins are part of the SMN complex, the Gemins, which are critical for binding the U snRNAs (Gemin5) and for associating with the Sm proteins (Gemin2) (Battle et al., 2006; Gubitz et al., 2004).

The first evidence that suggested a crucial role for the C-terminal RG domain of Sm D1 and D3 in snRNP biogenesis was the finding of their interaction with the Tudor domain of SMN (Friesen and Dreyfuss, 2000; Selenko et al., 2001). Concomitant experiments highlighting the importance of symmetrically dimethylated arginines for the recognition of the Sm proteins by SMN (Friesen et al., 2001b; 2001a; Meister et al., 2001; Meister and Fischer, 2002) led to the discovery of the functional role of the basic SMN Tudor domain as a methyl-arginine binding protein module (Côté and Richard, 2005). The aromatic cage formed by this Tudor domain specifically favors the recognition of the sDMA planar guanidine group by electrostatic stabilization. Furthermore, such domain achieves high affinity for the Sm proteins by binding cooperativity resulting from multiple sDMA present within the short RG domain (Tripsianes et al., 2011).

Collectively, the aforementioned evidence underline the importance of symmetric arginine dimethylation for SMN-Sm proteins interaction *in vitro*. However, they do not completely clarify the precise role that this PTM play for the snRNPs biogenesis *in vivo*.

The Matera group explored such matter in *Drosophila melanogaster* using a fly strain mutant for *dart5* (the ortholog of human PRMT5). As expected, they observed a dramatic reduction of symmetric dimethylarginine within the Sm proteins. In accordance with previous studies SMN binding to Sm proteins was reduced, and similar effects were observed in the valois (the ortholog of human MEP50) mutant flies. Surprisingly, when steady state levels of mature snRNPs were analyzed, no differences were detected (Gonsalvez et al., 2006).

Further studies in HeLa cells elucidated a critical difference between humans and *drosophila*. PRMT5 knockdown experiments showed, besides decreased Sm protein arginine methylation and the impairment of SMN-Sm proteins interaction, striking reduction in the kinetic of snRNP biogenesis similar to SMN knockdown experiments. Moreover, Cajal bodies were disrupted and Coilin was delocalized. Importantly, PRMT7 knockdown resembled the PRMT5 knockdown results, but PRMT7 overexpression did not ameliorate the effects observed in PRMT5 depleted cells, suggesting that the functions of the two type II PRMTs are not redundant in the Sm core maturation process (Gonsalvez et al., 2007). Sm protein methylation by PRMT7 was confirmed in *drosophila* where, consistently with the data collected in the *dart5* depleted flies, snRNP biogenesis was not affected. Notably, mutant flies harboring arginine to lysine substitutions in the RG domain of SmD1 did not show any defect in Sm core assembly, despite the reduced binding of SMN to the mutant SmD1, suggesting that in *Drosophila* methylation of the Sm proteins is dispensable for snRNP maturation (Gonsalvez et al., 2008).

In order to understand the downstream consequences for pre-mRNA splicing defects induced by perturbation of the key components of the snRNP core assembly pathway, I will next briefly summarize the constitutive splicing and alternative splicing mechanisms.

1.5.2 Constitutive splicing mechanism

Intron length can vary tremendously and sequence conservation is low, but some elements are indispensable to ensure correct splicing: the 5' splice junction (5'ss, donor site) and the 3' splice junction (3'ss, acceptor site), typically preceded by a string of pyrimidines (PPT) and the A branch site (Black, 2003; Chen and Manley, 2009; Pandya-Jones, 2011; Wang and Burge, 2008). Intron removal is achieved by two transesterification reactions catalyzed by the spliceosome, which assembles in a highly coordinated sequential manner. Initially the 5'ss is recognized through RNA complementarity by the U1 snRNP, whereas two subunits of the non-snRNP protein U2AF bind to the acceptor site and the PPT, while SF1 binds to the A branch point. Following the formation of this early complex (E complex), the U2 snRNP displaces SF1, associates with the branch site and then interacts with the U1 snRNP in a process that turns the intron into a loop bringing the two exons in close proximity (A complex). After the A complex is formed, three more snRNPs are recruited, U4, U5 and U6 (U4/U6.U5 tri-snRNP). This complex of five snRNPs, known as the B complex, undergoes extensive rearrangements and ultimately the U1 snRNP and the U4 snRNP are released giving rise to the active B complex. This is the complex that catalyses the first transesterification. The bond between the exon and the 5'-end of the intron at the donor site is cleaved and the 5'-end joins the A branch point by 5' to 2' phosphodiester bond. This unusual bond results in a branched lariat structure forming the C complex. The second transesterfication is catalyzed by the C complex. The C complex cleaves the bond at the 3' at the end of the intron, the acceptor site, and forms a phosphodiester bond between the two exons. The intron is released, the spliceosome disassembles and additional rounds of splicing take place **(Fig. 1.6)**.

This splicing pathway model is called the canonical cross-intron pathway, as the spliceosome particles assemble across the intron recognizing its 5'ss and 3'ss, and it is credible for introns that do not exceed the 250 bases in length. In higher metazoans introns are generally longer, and a more plausible model relies on cross exon assembly of the spliceoseome and it is therefore called the exon definition model. The entire canonical splicing process has been extensively reviewed by (Wahl et al., 2009) and (Black, 2003).

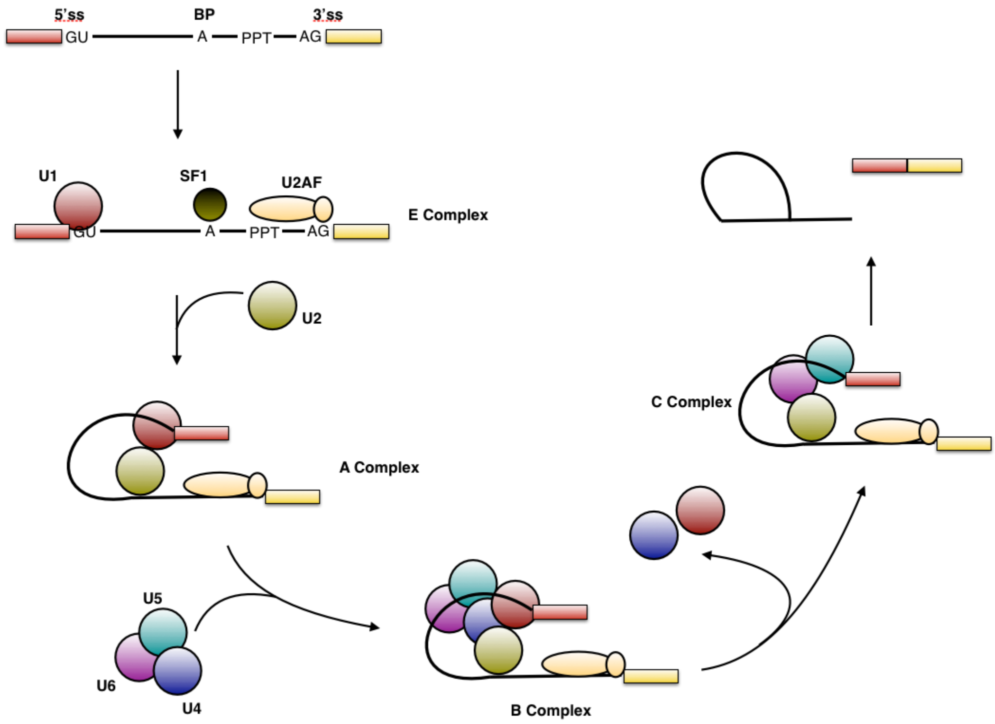

Figure 1.6: The constitutive splicing mechanism. The splicing process begins with the formation of the E complex, in which U1 snRNP binds the 5'ss, SF1 binds the A branch site (BP) and the two subunits of U2AF bind to the acceptor site and the polypyrimidine tract (PPT). Following this first step, U2 snRNP replaces SF1, associates with the A branch site and then interacts with the U1 snRNP bringing the two exons in close proximity (A complex). Three more snRNPs are then recruited, U4, U5 and U6 (U4/U6.U5 tri-snRNP) to form the B complex which undergoes extensive rearrangements and ultimately releases U1 snRNP and U4 snRNP. The resulting catalytic complex (C complex) completes the splicing process joining the two exons together and releasing the intron lariat.

1.5.3 Alternative splicing

Each exon within a transcriptional unit has the possibility of being included or excluded in the final transcript. This process of differential selection of splice site pairs is called alternative splicing and is an invaluable source of complexity which contributes to cell identity and fate. Whereas several exons are almost invariably included in a transcript (constitutive exons), others are instead selectively included or skipped (alternative exons), giving rise to multiple final mRNA products.

Unlike lower organisms, the vast majority of human genes undergoes alternative splicing and this splicing flexibility is a remarkable product of evolution. Within all human organs, the number of alternative splicing events occurring in the brain distinctively distinguishes the human species from others and such complexity overall correlates with the number of cell types and species evolution (Barbosa-Morais et al., 2012; Braunschweig et al., 2013; Dillman et al., 2013). If on one hand splicing complexity sets us apart from other species, such flexibility, granted by interconnected layer of post-transcritional regulation, is also a liability. Indeed cancer cells take advantage of alternative splicing to bypass apoptosis and cell cycle arrest, and to stimulate tumor progression and invasion (David and Manley, 2010).

Five different types of single alternative splicing events can occur within the same pre-mRNA: alternative 5' splice site, alternative 3' splice site, cassette exon, retained intron and back-splicing **(Fig. 1.7)**. Combination of multiple alternative splicing events gives rise to complex patterns, as for example mutually exclusive exons (Black, 2003; Keren et al., 2010; Memczak et al., 2013; Nilsen and Graveley, 2010). Moreover, splicing across two different pre-mRNAs (*trans*-splicing) has been described (Lasda and Blumenthal, 2011).

The intrinsic strength of the 5'ss and of the A branch point sequence are determined by their degree of complementary to the recognition sequences of the snRNAs U1 and U2, respectively, while the polypyrimidine tract has to comply with U2AF complex consensus binding site (Wu et al., 1999). Besides, a multitude of auxiliary *cis*-acting RNA motives, complement the constitutive "splicing code", functioning as exonic/intronic splicing enhancers

(ESE/ISE) or exonic/intronic silencers (ESS/ISS) (Braunschweig et al., 2013). These elements are recognized by non-snRNP RNA binding proteins which modulate alternative splicing stimulating or preventing the selection of a proximal splice site (Wang and Burge, 2008). The two most characterized families of *trans*-acting proteins are the SR proteins and the heterogeneous ribonucleoproteins (hnRNPs) **(Fig. 1.8)**. In addition the function of several other tissue-specific splicing regulatory factors such as NOVA, RBFOX and MBLN, regulatory factors has been extensively characterized (Irimia and Blencowe, 2012; Licatalosi and Darnell, 2010; Long and Caceres, 2009; Martinez-Contreras et al., 2007). Finally, an additional layer of regulation is given by RNA secondary structures which can either facilitate or hinder the interaction between splicing factors and *cis*-acting RNA elements (Jin et al., 2011).

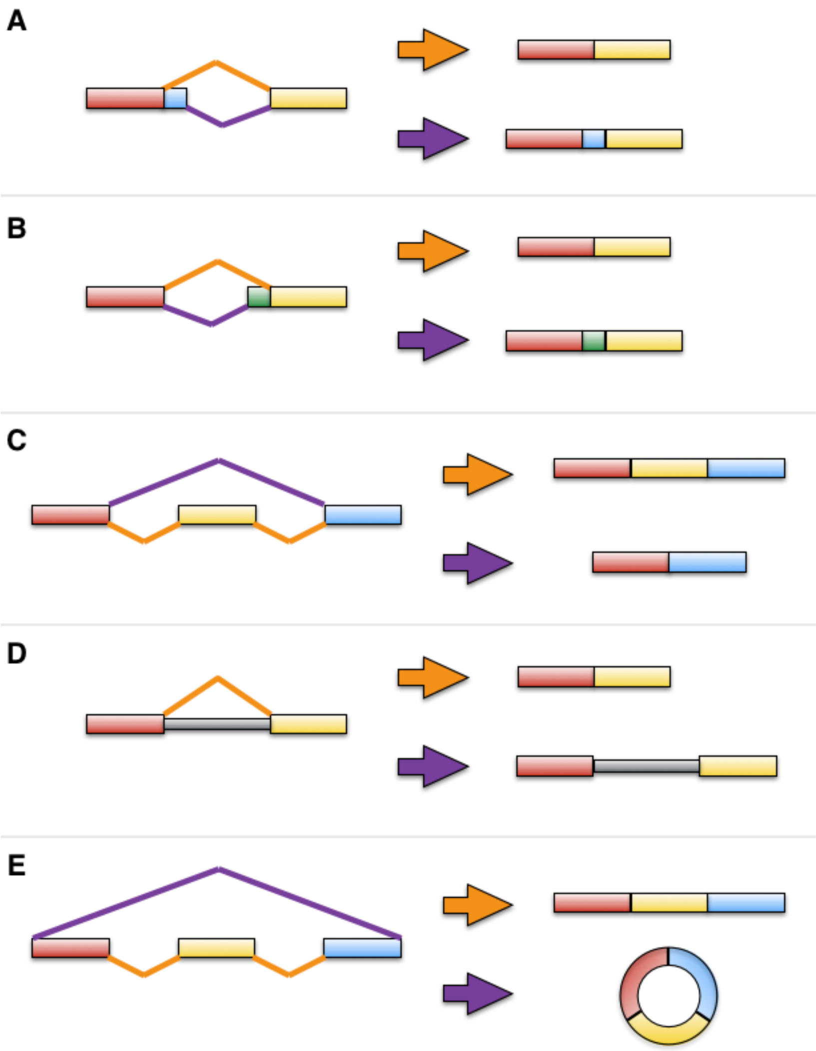

Figure 1.7: Types of alternative splicing. Schematic representation of alternative splicing events: alternative 5’ (A), alternative 3’ (B), cassette exon (C), retained intron (D) and back-splicing/circular RNA (E). Orange lines and arrows indicate the canonical splicing, whereas the purple lines and arrows indicate the alternative splicing pattern and outcome.

Another important aspect of splicing regulation is the crosstalk between transcription, chromatin landscape and splicing factors, since a large fraction of the splicing occurs co-transcriptionally (Ameur et al., 2011; Khodor et al., 2012; 2011; Tilgner et al., 2012; Vargas et al., 2011). The C-terminal domain of the RNA polymerase II (Pol II) has been shown to favor splicing and to associate with several splicing regulators (David et al., 2011; Hirose et al., 1999; Hsin and Manley, 2012). Furthermore, the recruitment of the splicing machinery has been linked to Pol II transcriptional elongation rate, which is in turn modulated by chromatin structure (Schor et al., 2013). Additionally, chromatin, in particular histone positioning, histone variants and histone modifications, have been linked to exon/intron definition and recruitment of the splicing components (Andersson et al., 2009; Huff et al., 2010; Luco et al., 2011; Schor et al., 2012; Spies et al., 2009; Tolstorukov et al., 2012) **(Fig. 1.8)**.

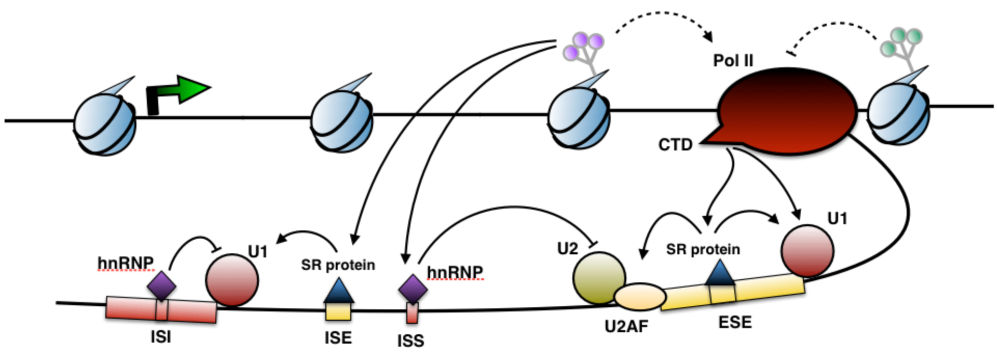

Figure 1.8: Co-transcriptional and post-transcriptional regulation of splice site selection. Schematic representation of the crosstalk between transcription, chromatin landscape and splicing factors. Auxiliary *cis*-acting RNA motives, function as exonic/intronic splicing enhancers (ESE/ISE) or exonic/intronic silencers (ESS/ISS). The *trans*-acting factors SR proteins and heterogeneous ribonucleoproteins (hnRNPs) bind to either splicing enhancers or splicing silencers respectively and stimulating or preventing spliceosome assembly. The C-terminal domain (CTD) of the RNA polymerase II (Pol II) promotes splicing recruiting several splicing regulators. The recruitment of the splicing machinery has been linked also to Pol II transcriptional elongation rate, which can be modulated by chromatin modification (dashed line). Additionally, histone modifications have been linked recruitment of the splicing components.

1.5.4 Core snRNP assembly proteins and alternative splicing

Changes in splicing patterns, due to modulation of the expression of spliceosomal components, have been observed in yeast, flies and mammals (Clark et al., 2002; Gabanella et al., 2007; Park et al., 2004; Pleiss et al., 2007; Zhang et al., 2008). However, only the recent development of genome-wide approaches, in particular exon microarrays and RNA sequencing, has shed light on the global regulation of splicing, induced by altered levels of core Sm assembly proteins.

Genetic alterations of the SMN1 gene in human result in spinal muscular atrophy (SMA). Despite the fact that SMN is widely expressed in all tissues the mechanism leading to the motor neuron-selective phenotype remains unclear. The Dreyfuss group performed a genome wide splicing analysis (exon microarray) in a mouse model of type II SMA (moderate phenotype) and made several major discoveries. Firstly, they detected tissue-specific changes in the abundance of the snRNAs and a marked decrease in snRNP assembly capacity. Secondly, they observed tissue-specific splicing defects in all the studied tissues. Hundreds of pre-mRNAs were alternatively spliced, especially those containing a large number of introns and encoding for membrane transporters and extracellular matrix proteins (Zhang et al., 2008).

Similarly, investigating the effects induced by knock-down of SmB/B' in HeLa cells, Saltzman and colleagues observed altered levels of the snRNAs (Saltzman et al., 2011). Interestingly, they discovered that SmB promotes the inclusion of a mini-exon within its own pre-mRNA. Mutations in a mini-gene resembling this exon, either strengthening the 3'ss or the 5'ss, promote the exon inclusion, but only the strong 5'ss was able to rescue the exon skipping induced by SmB downregulation. Further genome-wide experiments (RNA-sequencing) focusing on exon inclusion/exclusion events revealed the critical role played by SmB in ensuring exon inclusion of alternative cassette exons, rather than constitutive exons. Bioinformatic analysis of the skipped exons showed that these exons are shorter than average, enriched in genes involved in RNA processing and that the average strength of their 5'ss is slightly lower than average (Saltzman et al., 2011).

Despite the established biochemical role of sDMA in snRNPs biogensis, evidence for a global regulation of splicing by PRMT5 in mammals is still missing. Nevertheless interesting data have been collected studying *Arabidopsis thaliana* and *Drosophila* as model systems. Deng and colleagues identified symmetric dimethylated arginines in *Arabidopsis* Sm Proteins demonstrating conservation from plants to human (Deng et al., 2010). RNA sequencing analysis of atprmt5 (the *Arabidopsis thaliana* homolog of human PRMT5) mutant plants revealed an increased number of retained introns. Consistent with the analysis performed in the SMA mouse model (Zhang et al., 2008), pre-mRNAs with a higher number of introns were generally more affected. The alternatively spliced genes belong to several biological processes including RNA metabolism and flowering. As a result, plants lacking atprmt5 displayed pleiotropic developmental defects including growth retardation and delayed flowering time. A previous work demonstrated that the late flowering phenotype was caused by reduced levels of the Flowering locus KH domain protein (FLK), a critical inhibitor of the flowering repressor Flowering locus C (FLC) (Pei et al., 2007). Deng and colleagues discovered that such protein reduction is caused by intron retention in the *Flk* pre-mRNA. Notably, no difference in the levels of H4R3me2s was observed in plants lacking atprmt5 when compared to wild type plants (Deng et al., 2010).

A concomitant study by the Yanovsky group led to similar conclusions (Sanchez et al., 2010). Using tiling array they discovered almost 500 intron retention events in plants lacking atprmt5 when compared to wild type plants. To gain further detail they performed high-resolution RT-PCR on a panel of 288 splicing events including known alternative splicing events. They found widespread splicing changes, but mainly the switch to alternative 5'ss. Bioinformatic analysis showed that PRMT5 regulates recognition of weak 5'ss characterized by decrease frequency of the G base at the -1 position of the 5'ss and randomization at the -2, and +5 position. Analogous experiments in *Drosophila* revealed similar defects: increased intron retention and decrease in the frequency of the G in the -1 position of the 5'ss. Furthermore, the phenotype caused by lack of PRMT5 in the two model systems is related. PRMT5 depletion in *Arabidopsis thaliana* causes splicing defects in the *Pseudo response regulator 9 (Prr9)* pre-mRNA, a core clock component, resulting in impaired circadian rhythms. Similarly, in *Drosophila* alteration in splicing, induced by disruption of *dart5*, involves a subset of major component of the clock pathway, including *period*. As a consequence *dart5* mutant flies display defective circadian rhythms in locomotor activity (Sanchez et al., 2010).

1.6 PRMT5 in development

In the mentioned studies, PRMT5 has been associated with a variety of targets and biological processes, highlighting the versatility of this eclectic protein. However, none of these reports clarify the downstream effects of PRMT5 modulation *in vivo.*

The first animal model harboring PRMT5 deletion has been generated by the Matera group. Focusing on the role of symmetric arginine methylation of Sm proteins in *Drosophila*, they made the surprising discovery that PRMT5-depleted flies are viable (Gonsalvez et al., 2006). Notably, when crossed with flies either homozygous or heterozygous for a Smn hypomorphic allele, PRMT5 null flies show strong synthetic lethality (Gonsalvez et al., 2008).

1.6.1 PRMT5 in germ cells

Although PRMT5 mutants *Drosophila* are viable, male flies display dramatic defects in spermatocytes maturation, leading to absence of sperm in the seminal vesicles and consequently resulting in complete sterility. On the other hand, female flies display only minor fecundity reduction. Nonetheless, one third of the embryos suffer segmentation defects, whereas the remaining two thirds are agametic, therefore sterile. As such, PRMT5 mutation can be considered as a “grandchildless” mutation and importantly, is phenotypically similar to Valois (the *Drosophila* homolog of human MEP50). During oocytes development, the localization of specific components in the pole plasm, the cytoplasmic posterior end of the *Drosophila* oocyte, is crucial for the formation of polar granules, which are then sequestered in the pole cells. One such component is Tudor and in both PRMT5 and Valois mutant oocytes, its localization is defective. Moreover, the phenotype of Tudor mutant flies is very similar to that of PRMT5 mutant embryos. Pole cells are the precursors of *Drosophila* primordial germ cells (PGCs). During development they colonize the gonads and eventually give rise to adult germ cells. Consistent with the grandchildless classification, PRMT5 mutant embryos display lack of pole cells (Anne et al., 2007; Breitwieser et al., 1996; Findley et al., 2003; Gonsalvez et al., 2006). Additionally, the requirement of PRMT5/Valois mediated methylation of SmB, has been proved essential for pole cells development and gonad formation (Anne, 2010).

The requirement for PRMT5 in mammalian germ cells is still unexplored, but two studies suggest different nonexclusive mechanisms by which PRMT5 might play a critical role in mammalian PGCs development similar to the role PRMT5 plays in *Drosophila*. Ancelin and colleagues discovered that PRMT5 interacts with Blimp1, a DNA binding protein and major regulator of mouse PGCs specification (Ohinata et al., 2005; Vincent et al., 2005). Co-localization and chromatin immunoprecipitation experiments uncovered a dynamic regulation of the Blimp1-PRMT5 complex correlating with histone modification patterns and expression of putative Blimp1 target genes involved in germ-line development (Ancelin et al., 2006). Vagin and colleagues focused their work on the identification of the murine Piwi complexes (Vagin et al., 2009). The mouse Piwi proteins MILI, MIWI and MIWI2, belong to the Argonaute family of proteins and their expression is restricted to the germ cell lineage where their best characterized function is to suppress mobile genetic elements by two mechanisms: epigenetic transcriptional repression of transposons expression and piwi-interacting RNA (piRNA) directed cleavage of transposon mRNAs (Aravin et al., 2007a; 2007b; Brennecke et al., 2007; 2008; Kuramochi-Miyagawa et al., 2008). Mass spectrometry analysis of the PIWI complexes from germ cells of transgenic mice expressing epitope tagged MILI, MIWI and MIWI2 under their own endogenous promoter, revealed their interaction with PRMT5/MEP50 and the presence of symmetric dimethyl arginines within the RG sites at their N-termini. These methylated arginines are bound by the Tudor domain family of proteins, most of which, just like the Piwi proteins, are essential for male fertility (Chuma et al., 2006; Pan et al., 2005; Vasileva et al., 2009). These data suggest a possible role for PRMT5 in safeguarding genomic stability in germ cells (Vagin et al., 2009). Similar conclusions arise from studies in *Caenorhabditis elegans*. Both RNAi experiments and genetic depletion of the prmt-5 gene (the C. elegant homolog of mammalian PRMT5) do not cause developmental defect besides a minor reduction in growth rate. However, ɣ-irradiation and other DNA damaging agents induce strong CEP-1 (the C. elegant homolog of mammalian p53) dependent germ cell apoptosis in PRMT-5 depleted worms. Notably, PRMT-5 displays nuclear localization in the germ line, but the histone modification H4R3me2s is not reduced upon PRMT-5 inhibition and PRMT-5 is not able to methylate H3 *in vitro*. PRMT-5 interacts with, but does not methylate CEP-1. Conversely, the CEP-1 interactor CBP-1 (the C. elegant homolog of mammalian p300/CBP) forms a complex with PRMT-5 and CEP-1, contributes to the activation of the cell death pathway and is methylated by PRMT-5. As a consequence, Cbp-1 RNAi suppresses the apoptosis induced by PRMT-5 deletion in germ cells following DNA damage (Yang et al., 2009).

1.6.2 PRMT5 in pluripotent stem cells

As the number of publications demonstrate, the interest around PRMT5 has been rapidly growing in the past ten years. Developmental and cancer biologists, whose work heavily rely on mouse models, greatly contributed to uncover the role of PRMT5 in molecular pathways involved in cellular growth control and differentiation. However, only one work, by the Surani group, has so far taken advantage of mouse genetics (Tee et al., 2010). Surprisingly, different from the *Drosophila* and *C. elegans* phenotype, but similar to many mouse knockout models of proteins involved in chromatin remodeling, signaling pathways and splicing regulation, mice lacking PRMT5 are early embryonic lethal. To generate the PRMT5 knockout model, Tee and colleagues used heterozygous embryonic stem (ES) cells harboring a gene trap within the methyltransferase domain obtained from Baygenomics. PRMT5 heterozygous mice are viable and fertile, whereas PRMT5 null mice display extensive developmental defects at embryonic day (E) 6.5. Consistently, albeit E3.5 PRMT5-null blastocysts appear morphologically normal and present at the expected Mendelian ratio, their inner cell mass is not able to outgrowth when cultured *in vitro*, revealing a critical role for PRMT5 in stem cells biology. Consistently, PRMT5-null ES cells could not be obtained and studied, leaving the above mentioned observations as the only data regarding PRMT5 knock-out mice described in the literature so far. PRMT5 is maternally inherited and during mouse preimplantation development, its nuclear/cytoplasmic localization, rather than its expression, appears to be dynamically regulated. In embryonic stem cells PRMT5 is cytoplasmic and RNAi experiments resulted in upregulation of differentiation genes and loss of pluripotency. Unexpectedly, analysis of histone modifications showed selective PRMT5 dimethylation of histone H2A on the arginine 3 in the cytoplasm. Further studies using histone mutants shed light on a possible mechanism of deposition of symmetrically arginine methylated histone H2A at the promoter of differentiation genes ensuring their repression (Tee et al., 2010).

In accordance with the loss of pluripotency following PRMT5 depletion, a screening for the reprogramming activity of factors involved in PGCs development identified PRMT5 as a critical gene for the generation of induced pluripotent stem cells (iPS). When coexpressed in mouse embryonic fibroblasts (MEFs) together with KLF4 and OCT3/4, PRMT5 promoted somatic cell reprogramming into Nanog-GPF positive iPS colonies that were able to form teratomas, and exhibited germ line transmission in chimeric mice. Furthermore, PRMT5 knockdown in MEFs exogenously expressing the four canonical reprogramming factors SOX2, KLF4, OCT3/4 and MYC impaired iPS generation (Nagamatsu et al., 2011).

Additionally, work in *Planaria* has expanded our knowledge regarding the conservation of the role of PRMT5 in pluripotent cells maintenance.

Planaria is a flatworm with incredible regenerative capabilities which rely on the neoblasts, a widespread population of adult stem cells, required for tissue homeostasis and organismal growth. A unique feature of these cells is the presence of chromatoid bodies, cytoplasmic ribonucleoprotein granules. Rouhana and colleagues discovered that chromatoid bodies are enriched with symmetrically arginine dimethylated proteins methylated by the S. Mediterranea Smed-PRMT5, homolog of human PRMT5. Among the identified methylated proteins proteins they detected homologs of mammalian PIWI and Sm proteins. Smed-PRMT5 is expressed in brain, neoblasts and testis of sexual planarians. Longterm Smed-PRMT5 inhibition experiments by RNA interference resulted in size and head defects, reduction of the number of neoblasts and impaired regeneration (Rouhana et al., 2012).

1.6.3 PRMT5 in tissue-specific stem cells and differentiation

The evidence regarding PRMT5 function in germ cells specification and embryonic stem cells maintenance, point to PRMT5 as a general regulator of proliferating cells homeostasis and pluripotency, nevertheless several studies focusing on the role of PRMT5 as transcriptional co-regulator challenge this hypothesis. Investigation of tissue-specific cell proliferation and differentiation processes, combining human and mouse tissue culture approaches with localization and knockdown techniques, render a more complex picture further complicating our understanding. PRMT5 displayed an ambiguous function as both coactivator and corepressor of transcription and additionally it has been reported to participate in signal-transduction pathways, inducing or inhibiting cell differentiation.

Using cell culture model, Le Blanc and colleagues explored the role of PRMT5 during adipogenesis. Knock-down of PRMT5 in mesenchymal stem cells and preadipocytes inhibited activation of adipogenic genes, whereas PRMT5 overexpression enhanced adipogenic differentiation. In this specific case, PRMT5 acts as a transcriptional coactivator, binding multiple adipogenesis-specific promoters, and methylating arginine 8 of histone H3 (H3R8) (LeBlanc et al., 2012).

Similarly, during muscle differentiation PRMT5 promotes the expression of myogenic-specific genes and induces skeletal muscle generation. Overexpression of MyoD in the immortalized mouse fibroblast cells 3T3, leads to the transcription of the early muscle marker *Myogenin*, and of the late differentiation genes *Desmin* and *skeletal α-Actin*. PRMT5 knock-down in this cells, represses this process. Interacting with MyoD, PRMT5 binds the *Myogenin* promoter, methylates H3R8 and is required for Brg1 recruitment and *Myogenin* activation. Importantly, this observation has been confirmed in primary adult satellite cells (the quiescent muscle progenitor cells) (Dacwag et al., 2006). Also the promoters of late differentiation genes, such as MCK and Desmin, are bound by PRMT5 and methylated on H3R8 in a MyoD-dependent manner. However, when muscle differentiation is induced in 3T3 cells by overexpression of Myogenin/Mef2D1b, thus bypassing MyoD, PRMT5 methylation is not occurring and is not necessary anymore. Therefore, it is not clear to what extent PRMT5 is important for the completion of the skeletal muscle differentiation process (Dacwag et al., 2009). Notably, morpholino-mediated PRMT5 downregulation in zebrafish showed that PRMT5 regulates slow and fast fiber formation by controlling the early myogenic genes *Myod* and *Myf5* as well as *Myogenin* (Batut et al., 2011).

In a different way, PRMT5 negatively regulates keratinocytes differentiation modulating the Mitogen-activated protein kinases/Extracellular signal-regulated kinases (MAPK/ERK) signaling pathway. The balance between p38δ and ERK is of vital importance in determining keratinocytes fate. While ERK1/2 activation is necessary to sustain keratinocytes proliferation and survival, activation of p38δ by Protein kinase C δ (PKCδ)-mediated phosphorylation stimulates differentiation markers such as Involucrin and reduces the levels of ERK1/2 (Dashti et al., 2001; Eckert et al., 2003; Efimova et al., 2003; 2004). Kanade and colleagues showed that PRMT5 is part of the p38δ complex and that PRMT5 methylates one of its components. This methylation event inhibited p38δ phosphorylation, thus repressed its activation and ensured high levels of ERK1/2. Accordingly, PRMT5 knock-down induced keratinocytes differentiation, whereas PRMT5 overexpression suppressed the differentiation process (Kanade and Eckert, 2012).

This work is not the only one reporting a connection between PRMT5 and the MAPK/ERK signaling pathway. Using different cell lines Andreu-Perez and colleagues discovered that PRMT5 is able to methylate the RAF proteins CRAF and BRAF, key components of the RAS signaling cascade upstream of the MAPK kinases MEK1/2 (Hornberg et al., 2005; Lewis et al., 1998), enhancing their degradation. Thereby the amplitude and the duration of ERK1/2 activity were modulated in response to different growth factors (Andreu-Perez et al., 2011). Importantly and different from what observed in keratinocytes, in PC12 cells, a rat cell line commonly used as a model for neuronal differentiation, inhibition of PRMT5 promoted ERK1/2 activity inducing differentiation (Andreu-Perez et al., 2011).

Finally, the Nimer group, focusing on the role of the Janus kinase 2 (JAK2) mutant JAK2V617F in myeloproliferative neoplasms, unveiled a regulatory mechanism for PRMT5 activity. They showed that phosphorylation of PRMT5 by this oncogenic kinase impaired PRMT5 methyltransferase activity disrupting its association with MEP50. Surprisingly, further experiment in human hematopoietic stem/progenitor cells (HPCs), revealed that in this specific system PRMT5 negatively regulates both proliferation and erythroid differentiation (Liu et al., 2011).

1.6.4 PRMT5 in brain development

The central nervous system arises from the neural ectoderm and its proper development and functionality rely on a temporally and spatially regulated sequence of events. At embryonic day 10.5 (E10.5) of mouse gestation the neuroepithelium consists mainly of neural stem/progenitor cells (NPCs), which proliferate and maintain an undifferentiated state. This cell population progressively expands and generates all the cells that will eventually compose the brain: neurons and glial cells. In the mouse brain cortex, neurogenesis precedes gliogenesis and begins at approximately E12.5. This event is defined by multiple asymmetric divisions of NPCs which give rise to a

NPC and a post-mitotic neuron. Notably, as the differentiation process takes place in the CNS, the multipotency of the NPC population diminishes, establishing the premises for a temporally controlled development (Guillemot, 2007; Okano and Temple, 2009; Qian et al., 2000; Shen et al., 2006). At E15.5, different layers of cells are readily recognizable in the mouse cortex, where NPCs are located in the ventricular and sub-ventricular zone, while the post-mitotic neurons organize in the subplate as well as in the cortical plate (Dehay and Kennedy, 2007).

In order to gather some insight about the possible role of PRMT5 during brain development, Chittka characterized the levels of H4R3me2s and H4R3me2a in mouse cortical sections. Immunofluorescence staining revealed that H4R3me2s is the prevalent histone modification in the NPC population, whereas both H4R3me2s and H4R3me2a are associated with post-mitotic neurons and differentiating oligodendrocyte progenitor cells (Chittka, 2010).

In a separate study, Chittka and colleagues explored the possible role of the putative transcription factor Positive regulatory domain 4 (PRDM4) in mammalian brain development. PRDM4 knock-down induced neuronal differentiation of primary rat neural stem cells. Importantly, they showed that PRDM4 recruits PRMT5 to mediate histone methylation and their interaction was required to regulate the timing of neural stem cells differentiation (Chittka et al., 2012). In contrast to these data, a recent study revealed that PRDM4 knock-out mice develop normally (Bogani et al., 2013).

Huang and colleagues instead explored the function of PRMT5 in postnatal brain. They observed that PRMT5 expression increases with age and correlates with the onset of myelination. Oligodendrocytes are glial cells and they are the myelinating cells in the CNS. PRMT5 is highly expressed in oligodendrocytes as well as in neuron and astrocytes. To study the role of

PRMT5 in glial cells maturation they used the rat glioma cell line C6. These cells express oligodendrocyte markers and can be stimulated to elevate myelin gene expression levels inducing glial cells differentiation. PRMT5 knockdown increased the expression of the Inhibitor of differentiation transcription factors Id2 and Id4 leading to immature and undifferentiated proliferating cells. Consistently, in a differentiation assay performed using primary oligodendrocytes progenitor cells, PRMT5 knockdown prevented primary oligodendrocytes maturation and differentiation. Finally, they showed that PRMT5 directly binds the promoters of *Id2* and *Id4* and that lack of PRMT5 is associated with hypomethylation of the CpG regions of these promoters (Huang et al., 2011).

Chapter 2

OBJECTIVES

PRMT5 is one of the most studied protein arginine methyltransferases, yet the full repertoire of targets and regulated cellular processes remains largely unexplored. PRMT5 is currently considered the only mammalian enzyme able to generate symmetrically dimethylated arginine, and given its overexpression in multiple cancer types, it's an extremely attractive therapeutic target. However, the multitude of potentially regulated pathways and its function in vital cellular processes, such as the early steps of the spliceosome assembly, question PRMT5 druggability as a feasible strategy in chemotherapy.

Surprisingly, 15 years after its discovery and despite the rapidly expanding literature, the only notion we have regarding the role of PRMT5 in mouse development is that PRMT5 null mice are early embryonic lethal. Furthermore, contradictory evidence has been collected in tissue-culture approaches. As a result, the role of PRMT5 in mammalian development is poorly understood and its major cellular function is still unclear.

Combining the use of knock-out mouse models and next generation sequencing technologies, the objectives of this thesis are to:

- Investigate to what extent PRMT5 is required during mouse development;
- Focus on relevant organs in which PRMT5 is expressed, to further explore its physiological function;
- Elucidate the major molecular mechanism responsible for the observed phenotype;
- Link PRMT5 to cellular pathways which can be of potential interest for human pathologies.

Chapter 3

MATERIALS AND METHODS

3.1 Mouse strains

The PRMT5 KO first mice were obtained from EUCOMM (http://www.knockoutmouse.org) To generate the PRMT5 FLOX allele, the βgal-neomycin cassette was removed by crossing PRMT5 KO first mice with β-actin–Flpe transgenic mice (Rodríguez et al., 2000) [strain name: B6.Cg-Tg(ACTFLPe) 9205Dym/J; stock no.: 005703; The Jackson Laboratory]. They were then crossed to Nestin-CRE (B6.Cg-Tg(Nes-cre)1Kln/J - JAX Lab). 4-Hydroxytamoxifen (4-OHT)-inducible conditional knockouts were created by crossing $PRMT5^{F/F}$ mice with *Rosa26-CreERT2* transgenic mice (Hameyer et al., 2007) (in mixed C57BL/6 X 129S1/SvImJ background). The $p53^{+/-}$ mice (B6.129S2-$Trp53^{tm1Tyj}$/J - JAX lab), in pure C57BL/6 background, were obtained from the Tergaonkar lab (IMCB, Singapore).

Mice were housed in compliance with the Institutional Animal Care and Use Committee (IACUC) guidelines. All procedures involving the use of mice were approved by the local Institutional Animal Care and Use Committee (IACUC) and were in agreement with ASTAR ACUC standards.

3.2 Mouse genotyping

Mouse genotyping was performed on genomic DNA using a standard protocol. Briefly, mouse tail (2 mm) was lysed in 500 µL of lysis buffer (100 mM sodium chloride, 10 mM TRIS pH8.0, 25 mM EDTA, 0.5% SDS) and 2.5

µL proteinase K (Promega, V302B) overnight, shaking at 50°C in a thermomixer. Samples were spun down at 13000 rpm for 5 minutes and 500 µL of supernatant was transferred to new eppendorf tubes containing 500 µL of 2–propanol (EMSURE®, 1.09634.2500). Tubes were inverted a few times to mix well and then spun down at 13000rpm for 10 minutes. Supernatant were discarded and DNA pellets were left to dry for approximately 10 minutes at 37°C heating block. 300 µL of TRIS buffer pH 8.0 was added to the DNA pellet and samples were incubated for 30 minutes at 50°C. Embryos were genotyped using HotSHOT lysis (Truett et al., 2000).

For PCR reactions, 12.5 µL of DreamTaq Green PCR master mix 2X (Thermo Scientific (#K1082), 1.25 µL of forward and reverse primer mix (10µM), 5µL of RNAse free water and 5 µL of DNA (approximately 100ng) were used. All PCRs except those involving Rosa26-CreERT2 were performed with initial holding temperature of 95°C for 5 minutes, 35 cycles of denaturation at 95°C for 45 seconds, annealing at 60°C for 30 seconds and elonagation at 72°C for 40 seconds and a final elongation temperature of 72°C for 4 minutes and 4°C holding temperature. For Rosa26-CreERT2 primers, PCRs were performed with initial holding temperature of 95°C for 3 minutes 95°C for 30 seconds, annealing at 55°C for 30 seconds and elongation at 72°C for 30 seconds and a final elongation temperature of 72°C for 2 minutes and 4°C holding temperature. 1.5% agarose gels (agarose powder, 1st base, BIO-1000-500g, 1X TAE buffer 1st base,BUF-3000-50X4L) with 6 µL of ethidium bromide (Promega, H5041) for every 100 mL of agarose solution were prepared. PCR products were then loaded onto the gels and bands on gels were visualized using ImageQuant RT ECL imager (GE healthcare). The primers used are indicated in **Table 3.1**.

Strain	Target sequence	Forward	Reverse
NESTIN-CRE	CRE	GCCTGCATTACCGGTCGATGCAACGA	GTGGCAGATGGCGCGGCAACACCATT
p53	wt	ACAGCGTGGTGGTACCTTAT	GTAGTGGATGGTGGTATACTCAGAGCCGGCCT
	neo	ACAGCGTGGTGGTACCTTAT	GTGGCGGACCGCTATCAGGACATAGCGTTGGCT
PRMT5 KO first	b-gal	TGGTCGCTGGGGAATGAATC	CTGCTGCTGGTGTTTTGCTT
	loxP	AGCTCTTGAAATTGGAGCTGAC	TCACACCCAGTCTCTTAC
FLPE		CACTGATATTGTAAGTAGTTTGC	CTAGTGCGAAGTAGTGATCAGG
PRMT5 FLOX	frt recombination	ACACACATGGCACATATACAGA	GAAAACAGAATGGCCAGGG
ROSA26 CreERT2	CRE	GCCTGCATTACCGGTCGATGCAACGA	GTGGCAGATGGCGCGGCAACACCATT
	ROSA26wt locus	ACAGCACTGGAAATGTTACCAAGGAAC	GGCTGGCTAAACTCTGGCCCTACA

Table 3.1: Primers used for genotyping

3.3 Southern blot

PRMT5$^{+/-}$ genomic DNA was extracted from liver tissues using DNeasy blood & tissue kit (Cat#69504, Qiagen). Genomic DNA (20 µg) was digested overnight with 100 units of restriction enzyme (XhoI, Cat#R0146, NEB) in a 400 µL volume and then re-digested with 100 units of enzyme for 4 hours. Digested genomic DNA was precipitated with isopropanol and resuspended in 20 µL water. Samples were then loaded on 0.7% TBE agarose gels and run for 16 hours at 45 mA in 1x TBE buffer. The gels were then denaturated for 1 hour in 1.5 M NaCl; 0.5 M NaOH, neutralized for 1 hour in 0.5 M Tris-HCl pH 7; 3 M NaCl, washed with 2× SSC, and blotted for 24 h with 10× SSC on Hybond N^{+} membranes (Cat#RPN203B, GE Healthcare).

The membranes were then washed with 2× SSC, UV-cross-linked, and stored at 4°C. β-gal probe (510bp) was generated through PCR from the genomic

DNA of $PRMT5^{F/+}$; forward primer: TGGTCGCTGGGGAATGAATC; reverse primer: CTGCTGCTGGTGTTTTGCTT. Membranes were incubated for 2 hours at 65°C with pre-hybridization buffer that contained 6x SSPE, 5x Denhardt's reagent, 0.5% SDS and 50 µg/mL denatured salmon sperm DNA. Radioactive probes were generated using the High Prime DNA Labeling Kit (Cat#11585584001, Roche Applied Science), with ^{32}P and then purified with illustra MicroSpin G-50 Columns (Cat#27-5330-01, GE healthcare). Labeled probes were heat denatured and added to the pre-hybridization buffer for overnight incubation at 65°C in a rotating oven.

Washing steps were done as follow: 2 times with 2x SSPE, 0.1% SDS for 15 minutes each, followed by 2 times with 1x SSPE, 0.1% SDS for 30 minutes each. All washing steps was performed at 65°C with pre-warmed buffers under shaking. The membranes were then exposed to phosphor screen for few days before scanning with Molecular Imager PharosFX™ Plus System (Cat#170-9460, Bio-rad).

3.4 β-Galactosidase staining of whole organs

Adult male mice were euthanized by accepted IACUC protocol. Brain, heart, kidney liver, spleen and testis were dissected and briefly washed in PBS. The organs were next fixed in Fixative Solution (0.2% Glutaraldehyde, 2 mM $MgCl_2$, 5 mM EGTA in 0.1 M phosphate buffer pH7,3) on ice for 45 minutes. The fixed organs were rinsed 4 times for 20 minutes in Rinse Buffer (0.02% Igepal, 0.01% Sodium Deoxycholate, 2 mM $MgCl_2$ in 0.1 M phosphate buffer pH 7.3) and then stained overnight in the dark at 37°C in freshly prepared Staining Solution (0.02% Igepal, 0.01% Sodium Deoxycholate, 5mM

Potassium Ferricyanide, 5 mM Potassium Ferrocyanide, 2 mM $MgCl_2$ and 1mg/mL X-Gal in dimethylformamide [Promega] in 0.1 M phosphate buffer pH 7.3). The stained organs were extensively washed in PBS, post-fixed overnight in 4% paraformaldehyde in PBS at 4°C and again washed in PBS. Images were captured using a Stemi 200 ZEISS stereo microscope.

3.5 Tamoxifen injections

A single pulse of 2mg Tamoxifen (SIGMA, T5648) plus 1mg Progesteron (SIGMA, P8783) in mineral oil (SIGMA, M5904) was given intraperitoneally to pregnant females at E10.5. Females were euthanized by accepted IACUC protocol and the embryos were harvested and analyzed at E15.5 and E17.5.

3.6 PCR genotyping

In order to confirm the deletion of PRMT5 exon 7 upon CRE activation in mice and primary cell lines, genomic PCR were performed using the following primers:

- Forward: 5'-ACACACATGGCACATATACAGA-3'
- Reverse: 5'-TCACACCCAGTCTCTTAC-3'

Qiagen DNeasy Blood & Tissue Kit (69504) was used to extract DNA from cell pellets. DNA from different organs was extracted using the mouse genotyping protocol as mentioned above. PCR reactions and gels were prepared the same way as mentioned above. All PCRs were performed with initial holding temperature of 95°C for 5 mintues, 37 cycles of denaturation at 95°C for 45s, annealing at 60°C for 30s and elongation at 72°C for 55s and a final elongation temperature of 72°C for 4 minutes and 4°C holding temperature. 1.3% agarose gels (agarose powder, 1st base, BIO-1000-500 g, 1X TAE buffer 1st base,BUF-3000-50X4L) with 5 µL of ethidium bromide (Promega, H5041) for every 100 mL of agarose solution were prepared. PCR products were then loaded onto the gels and bands on gels were visualized using ImageQuant RT ECL imager (GE healthcare).

3.7 Histopathology and immunohistochemistry (IHC)

Haematoxylin and Eosin staining and Immunohistochemistry staining were performed in collaboration with the IMCB Histopathology Facility / Advanced Molecular Pathology Lab (AMPL).

3.7.1 Haematoxylin and eosin slide preparation

After fixation in 4% paraformaldehyde (48 hours), the tissues were trimmed at the appropriate levels to a thickness of approximately 3 mm and processed into paraffin wax using the Tissue-Tek® VIP™5 tissue processor and embedded into paraffin blocks. Sections were cut at 5 μm thickness and stained with Haematoxylin and Eosin. Brains were sectioned either midline sagittal or in cross section at the level of the mid cerebellum and the forebrain. Embryos were sectioned sagittaly close to midline.

3.7.2 Immunohistochemistry staining

Automated IHC staining and counterstaining was performed on the Leica Bond-Max™ autostainer. Slides were de-waxed and rehydrated through a descending series of alcohols. Heat-induced epitope retrieval was performed at either pH6 or pH9 followed by endogenous peroxidase blocking and washing. Slides were incubated with primary antibody at the appropriate concentration for 45 minutes. For rabbit primary antibodies, a secondary antibody polymer solution containing anti-rabbit poly-HRP-IgG in 10% animal serum was added for 10 minutes. For mouse primary antibodies, a rabbit anti-mouse IgG in 10% animal serum was added for 3 minutes followed by a polymer containing anti-rabbit poly-HRP-IgG in 10% animal serum for 3 minutes. After washing the sections, the slides were developed in DAB solution (DAKO, K3468) for 3 minutes. Hematoxylin was used as a nuclear counterstain and the sections were dehydrated and mounted in synthetic mounting media. All the microscope slide images were captured and digitalized using the Ariol high resolution brightfield scanner. The primary antibodies used are indicated in **Table 3.2**.

Detailed protocol for each marker:

PRMT5. Slides were deparaffinized in Bond™ Dewax Solution and rehydrated through 100% ethanol to 1X Bond™ Wash Solution. Heat-induced epitope retrieval was performed using Bond™ Epitope Retrieval Solution 1 (pH 6) for 40 minutes at 100°C. Slides were then cooled to room temperature with 4 washes of 1X Bond™ Wash Solution. Endogenous peroxidase blocking was performed for 15 minutes at room temperature in 3-4% (v/v) H_2O_2, followed by 3 rinses in 1X Bond™ Wash Solution. Slides were incubated with primary antibody at the appropriate concentration for 45 min. At the end of the incubation, the slides were rinsed 3 times in 1X Bond™ Wash Solution. Polymer solution containing anti-rabbit poly-HRP-IgG in 10% animal serum was then added for 10 minutes. The slides were rinsed 4 times in 1X Bond™ Wash Solution, and washed once in deionized water. Bond™ Mixed DAB Refine was applied for 3 minutes, following which the slides were rinsed in deionized water to stop the DAB reaction. Counterstaining with hematoxylin was performed for 5 minutes. After which the slides were rinsed in deionized water and 1X Bond™ Wash Solution. Slides were finally dehydrated and mounted in synthetic mounting media.

Ki67. Slides were deparaffinized in Bond™ Dewax Solution and rehydrated through 100% ethanol to 1X Bond™ Wash Solution. Heat-induced epitope retrieval was performed using Bond™ Epitope Retrieval Solution 1 (pH 6) for 40 minutes at 100°C. Slides were then cooled to room temperature with 4 washes of 1X Bond™ Wash Solution. Endogenous peroxidase blocking was performed for 30 minutes at room temperature in 3-4% (v/v) H_2O_2, followed by 3 rinses in 1X Bond™ Wash Solution. Slides were incubated with primary antibody at the appropriate concentration for 60 minutes. At the end of the incubation, the slides were rinsed 3 times in 1X Bond™ Wash Solution. Post-primary solution containing rabbit anti-mouse IgG in 10% animal serum was added for 5 minutes, followed by 3 rinses in 1X Bond™ Wash Solution. Polymer solution containing anti-rabbit poly-HRP-IgG in 10% animal serum was then added for 5 minutes. The slides were rinsed 4 times in 1X Bond™ Wash Solution, and washed once in deionized water. Bond™ Mixed DAB Refine was applied for 3 minutes, following which the slides were rinsed in deionized water to stop the DAB reaction. Counterstaining with hematoxylin was performed for 5 minutes. The slides were next rinsed in deionized water and 1X Bond™ Wash Solution. Slides were finally dehydrated and mounted in synthetic mounting media.

SOX2. Manual IHC. Slides were deparaffinized in xylene and rehydrated through descending percentages of ethanol to water. Heat-induced epitope retrieval was performed using 10 mM Citrate Buffer (Dako, S2369) for 40 min using the pressure cooker (2100 retriever, >120°C). Slides were cooled to room temperature then washed 3 x 5 minutes in TBS-T. Endogenous peroxidase blocking was performed for 15 min in 3% (v/v) H_2O_2, followed by a rinse for 5 minutes in water and a rinse in TBS-T. Serum block with 5% rabbit serum in PBS was performed for 30 minutes. Slides were incubated with primary antibody at the appropriate concentration for 60 minutes. At the end of the incubation, the slides were washed in gentle running deionized water for 10 minutes, followed by a rinse in TBS-T for 5 min. Secondary antibody incubation using rabbit anti-goat HRP (Dako, P0160, 1:100) was performed for 30 minutes. The slides were washed in gentle running deionized water for 10 min, followed by a rinse in TBS-T for 5 minutes. The slides were incubated with DAB detection reagent (DAKO, K3468) for 5 minutes, and then rinsed in deionized water for 5 minutes to stop the DAB reaction. The slides were then counterstained with hematoxylin, dehydrated, cleared and mounted in synthetic mounting media.

Cleaved Caspase 3 (CC3). Slides were deparaffinized in Bond™ Dewax Solution and rehydrated through 100% ethanol to 1X Bond™ Wash Solution. Heat-induced epitope retrieval was performed using Bond™ Epitope Retrieval Solution 1 (pH 6) for 40 minutes at 100°C. Slides were then cooled to room temperature with 4 washes of 1X Bond™ Wash Solution. Endogenous peroxidase blocking was performed for 30 minutes at room temperature in 3-4% (v/v) H_2O_2, followed by 3 rinses in 1X Bond™ Wash Solution. Serum block using 10% goat serum was performed for 30 min. Slides were then incubated with primary antibody at the appropriate concentration for 45 minutes. At the end of the incubation, the slides were rinsed 3 times in 1X Bond™ Wash Solution. Polymer solution containing anti-rabbit poly-HRP-IgG in 10% animal serum was then added for 10 minutes. The slides were rinsed 4 times in 1X Bond™ Wash Solution, and washed once in deionized water. Bond™ Mixed DAB Refine was applied for 5 minutes, following which the slides were rinsed in deionized water to stop the DAB reaction. Counterstaining with hematoxylin was performed for 5 minutes. After which the slides are rinsed in deionized water and 1X Bond™ Wash Solution. Slides were finally dehydrated and mounted in synthetic mounting media.

Immunohistochemistry staining				
Target protein	**Source**	**Cat#**	**Host**	**Conditions**
Ki67	Novocastra Leica	NCL-Ki67-MM1	Mouse	1:100 pH6
Cleaved Caspase 3	Cell Signaling Technologies	D175 #9661S	Rabbit	1:100 pH6
SOX2	Santa Cruz Biotechnology	sc-17320	Goat	1:200 pH6
PRMT5	Millipore	07-405	Rabbit	1:500 pH6

Table 3.2: Primary antibodies used for immunohistochemistry

3.8 Western blotting

Cells were lysed directly in 1X Laemmli buffer and sonicated with 3 short pulses prior to loading on SDS-Polyacrylamide Gels. Mouse tissues were lysed in RIPA buffer (50mM Tris-HCl pH7.4, 1% NP-40, 0.5% Na-deoxycholate, 0.1% SDS, 150mM NaCl, 2mM EDTA, protease inhibitors [Merck-Calbiochem, 539134-IML]) for 30 minutes on ice, and mechanically homogenized using a Polytron homogenizer (PT-MR 1600E, Kinematica AG). Protein concentration was determined using the RC DC Protein Assay (BIO-RAD). 15-50 µg of protein extract were loaded on 6-15% SDS-PAGE and subsequently transferred onto nitrocellulose membranes (Whatman PROTRAN, 10401396) using a semi-dry system.

The membranes were blocked either in 5% dry milk (SIGMA, 70133)/PBS or 5% BSA (MP Biomedicals, 0219989890)/PBS and incubated overnight with primary antibodies, followed by secondary-HRP conjugated secondary antibodies (**see Table 3.3**). The blots were developed using SuperSignal West Pico Chemiluminescent Substrate (Thermo Scientific, 34080).

Western Blot Primary antibodies				
Target protein	**Source**	**Cat#**	**Host**	**Blocking solution**
H4R3me2s	abcam	ab5823	Rabbit	5% dry milk/PBS
H3R2me2s	IMCB		Rabbit	5% dry milk/PBS
H3R8me2s	IMCB		Rabbit	5% dry milk/PBS
H2AR3me2s	IMCB		Mouse	5% dry milk/PBS
GFAP	abcam	ab53554	Goat	5% dry milk/PBS
MDM4	abcam	ab16058-100	Rabbit	5% dry milk/PBS
Smith Antigen Y12	abcam	ab3138	Mouse	5% dry milk/PBS

SNRPB	abcam	ab85534	Rabbit	5% dry milk/PBS
SNRPD1	abcam	ab50940	Rabbit	5% dry milk/PBS
SNRPD3	abcam	ab121129	Rabbit	5% dry milk/PBS
TBR1	abcam	ab31940	Rabbit	5% dry milk/PBS
TBR2	abcam	ab23345	Rabbit	5% dry milk/PBS
PARP	Cell Signaling Technologies	#9542S	Rabbit	5% dry milk/PBS
p53	Cell Signaling Technologies	(1C12) #2524S	Mouse	5% dry milk/PBS
TUJ1	Covance	MMS-435P	Mouse	5% dry milk/PBS
gammaH2AX	Millipore	JBW300 05-636	Mouse	5% dry BSA/PBS
beta-actin	Santa Cruz Biotechnology	(C4) sc-47778	Mouse	5% dry milk/PBS
p21	Santa Cruz Biotechnology	(F-5) sc-6246	Mouse	5% dry milk/PBS
P-p53	Santa Cruz Biotechnology	(FP3.2) sc-51690	Mouse	5% BSA/PBS
PRMT5	Santa Cruz Biotechnology	(C20) sc-22132	Goat	5% dry milk/PBS
SMN	Santa Cruz Biotechnology	(2B1) sc-32313	Mouse	5% dry milk/PBS
alpha-Tubulin	SIGMA	B-5-1-2 T5168	Mouse	5% dry milk/PBS
SYM10	Upstate	07-412	Rabbit	5% dry milk/PBS
Western Blot Secondary antibodies				
Target protein	**Source**	**Cat#**	**Host**	
anti-goat IgG-HRP	Santa Cruz Biotechnology	sc-2033	Donkey	
anti-mouse IgG-HRP	Santa Cruz Biotechnology	sc-2005	Goat	
anti-rabbit IgG-HRP	Santa Cruz Biotechnology	sc-2004	Goat	

Table 3.3: Antibodies used for Western blotting

3.9 Cell lines

3.9.1 Neural Stem/Progenitor Cells (NPCs)

Neurosphere cultures were established as previously described (Lim and Kaldis, 2012). Briefly, E14.5 embryos were harvested and cortices carefully dissected in ice-cold PBS and incubated in trypsin (Invitrogen, 25300120) for 10 min at 37°C. The tissue was then mechanically dissociated into single cell suspension and passed through a 40 µm cell strainer (BD Falcon, 352340) into complete NSC medium (DMEM, Life Technologies, 11965118 + 2% B-27, Life Technologies, 17504-044), 1% penicillin-streptomycin (Life Technologies, 15140122), 20 ng/mL recombinant human epidermal growth factor (EGF, Peprotech, 100-15) and 20 ng/mL recombinant human fibroblast growth factor-basic (FGF-2, Peprotech, 100-18B). Serial passages: $3x10^5$ cells were seeded at each passage in a T75 culture flask and the total number of viable cells was determined after 4 days using an automated cell counter (Z2 cell and particle counter, Beckman Coulter). $PRMT5^{F/F}$ ER day4 neurospheres were treated with either 50 nM 4-OHT (H7904; Sigma) or the equivalent volume of ethanol for 24 hours before splitting to induce PRMT5 knockout.

3.9.2 Mouse Embryonic Fibroblasts (MEFs)

Primary MEFs were prepared from E14.5 embryos as previously described (Xu, 2005). Briefly, the embryos were harvested from the uterine horns and processed separately. The head and all the tissues into the body cavity were removed and the remainder of the embryo was finely minced with a razor blade in trypsin on ice. The tissue chunks were incubates 30 minutes at 37°C in trypsin and then carefully homogenized using a syringe. The cell supention was washed twice in PBS by centrifugation for 5 minutes at 1200 rpm and then maintained in a humidified 5% CO2 atmosphere at 37°C in DMEM (Life Technologies, 11965118) supplemented with 10% fetal bovine serum (FBS, Hyclone, SH30070.03) and 1% penicillin-streptomycin (Life Technologies, 15140122).

To perform the RNA-sequencing, MEFs (passage 1) were grown to confluence in 15 cm-dishes, and treated with either 50nM 4-OHT (H7904; Sigma) or the equivalent volume of ethanol for 24 hours before splitting. $3x10^5$ cells were seeded in a 10 cm-culture dish and collected after 4 days of culture.

For the cell cycle and cell proliferation analysis, MEFs (passage 1) were grown in 15 cm-dishes and acute depletion of PRMT5 was induced in exponentially growing cells by treatment with either 50nM 4-OHT (H7904; Sigma) or the equivalent volume of ethanol for 24 hours before splitting. After the treatment $2x10^6$ cells were seeded in a 10 cm-culture dish in 0.5% FBS medium, $5x10^5$ cells were cultured in 5% FBS medium, $3x10^5$ and $1x10^6$ cells were cultured in 10% FBS and 20% FBS medium respectively to perform cell cycle analysis and RNA extraction.

3.9.3 Hematopoietic Progenitor Cells (HPCs)

Pregnant females were euthanized by accepted IACUC protocol and the embryos were harvested at E14.5 following either Tamoxifen or EtOH injection at E10.5. Fetal liver from E14.5 embryos were dissected and finely minced in Iscove's MDM medium (GIBCO). The cell suspension was homogenized using a syringe (21g needle) and washed twice in 15 mL of Iscove's MDM medium with 2% FBS by centrifugation for 10 minutes at 1200 rpm. The cell pellet was resuspended in 10 mL of Iscove's MDM medium with 2% FBS and the viable cells were counted using the automated Vi-CELL XR, Beckman Coulter to determine the fetal liver cellularity.

To perform the colony formation assay 10^5 fetal liver *Prmt5*$^{+/+}$*ER* cells, from E14.5 embryos treated with either Tamoxifen or EtOH injection at E10.5, were added to 3 mL of Methocult M3434 medium (Stem Cell Technologies) and plated into 35 mm culture dishes following the manufacturer's instruction. The culture were placed in an incubator at 37°C, 5% CO_2 and the colonies were identified and counted after 12 days.

In order to deplete PRMT5 *ex vivo*, we isolated fetal liver *Prmt5*$^{+/+}$*ER* cells from E14.5 embryos and cultured them 24 hours with either EtOH or 4-OH-Tamoxifen (OHT) 50 nM in HSC medium (80% B-cell medium [for 500 mL]: 225 mL Dulbecco's modified Eagle Medium (DMEM, Gibco), 225 mL Iscove's modified Dulbecco's Medium (IMDM, Gibco), 10% FCS, 4 mM L-glutamine, 100 µM 2-mercaptoethanol, 100 U/mL penicillin, 100 µg/mL streptomycin; 20% 5X Hematopoietic stem cell supplemement: IMDM (Gibco), 50 mL FCS, 10 mL WEHI-3B (murine myelomonocytic leukemia cell line) conditioned medium [0.45 µm filtered] as a source of IL-3, [WEHI-3B, from Warren S. Pear, MIT, were grown in IMDM, 5% FBS, 2 mM L-glutamine, 25 µM 2-mercaptoethanol], 100 U/mL penicillin,100 µg/mL streptomycin, 1 ng/mL recombinant murine IL-3 (Research Diagnostics Inc., Flanders, NJ, # RDI-2113), 10 ng/mL recombinant murine IL-6 (Research Diagnostics Inc., # RDI-2166), 100 ng/mL recombinant murine stem cell factor(Research Diagnostics Inc., # RDI-2503). After the treatment, the cells were washed in

HSC medium and the methocult assay was performed as previously described.

3.9.4 Human cell lines

HEK293T, Phoenix-Eco, A549, U87, U2OS, HCT116, were obtained from ATCC cultured in an incubator at 37°C, 5% CO_2 and propagated according to ATCC data sheets.

3.10 Vectors, transfections and infections

pMXs-IRES-Blasticidin Retroviral Vector (Cell Biolabs Inc., RTV-016) was used to overexpress PRMT5, PRMT5(AAA) and MDM4. To generate the catalytically dead PRMT5(AAA) we used pCEP4flag-PRMT5 (Wild-type) as a template and carried out side directed mutations to generate: pCEP4flag-PRMT5(R368A). This was then used as template for second SDM generating pCEP4flag-PRMT5(R368A)(G367A), which in turn was used as template for the 3rd SDM forming pCEP4flag-PRMT5 (R368A)(G367A)(G365A). The codon changes were as follows: GGA to GCA (G365A); GGA to GCA (G367A); CGG to GCG (R368A). To test the methyltransferase activity, both the WT and the triple mutant were expressed in Insect cells with flag-tags in conjunction (co-expression) with His-tagged WDR77 (MEP50). Flag purified protein preps (200nM) in 50mM Tris-Cl, pH7.5, 150mM NaCl, 10% glycerol, 1mM DTT were tested for arginine methyltransferase activity using Epigenase PRMT Methyltransferase (Type II-specific) Activity/Inhibition Assay Kit (cat # P-3088). Flag-tagged WT PRMT5 or PRMT5 (G365A;G367A;R368A) were also expressed in HEK293 cells and purified using anti-flag M2 resin.

Phoenix-Eco packaging cells were transfected with the overexpressing vectors together with VsVg expressing plasmid. Cells were incubated for 18 hours, then fresh medium was added to the cells. After 24 and 48 hours, the medium, containing the viral particles, was collected, filtered using a 0.22 µm filter, concentrated by ultracentrifugation for 2 hours at 4°C at 23000 rpm and resuspended in HBSS. The infected neural stem cells were selected using blasticidin (1µg/mL, Life Technologies, R21001) -containing medium for 6 days.

pLKO-1 Mission lentiviral vectors (Sigma) were used for PRMT5 knock-down in human cell lines and for SmB/B' knock-down in both human and mouse cells. The target sequence of the PRMT5 KD shRNA construct used was: "CCTCAAGAACTCCCTGGAATA". A scrambled shRNA (Scr) was used as a control. HEK293T cells were transfected with pLKO vector together with packaging vectors VsVg and delta8.9. Cells were incubated for 18 h, then fresh medium was added to the cells. After 24 and 48 hours, the medium, containing the viral particles, was collected, filtered using a 0.22 µm filter, concentrated by ultracentrifugation for 2 hours at 4°C at 23000 rpm and resuspended in HBSS. The concentrated virus was added to the cells supplemented with 10 µg mL^{-1} of polybrene (SIGMA, H9268). Twenty-four hours after the last infection, the medium was replaced with fresh growth medium containing puromycin (Merck-Calbiochem, 540411). Cells were selected for 4 days before harvesting.

3.11 Immunofluorescence

Whole or mechanically dissociated neurospheres (single cells) were seeded onto poly-D-lysine coated glass slides. After 4 hours incubation at 37°C, cells were fixed with 4% PFA/PBS for 15 min at room temperature, permeabilized with 0.25% Triton X-100/PBS, blocked with 1% BSA in 0.1% Triton X-100/PBS and incubated with primary antibody against Cleaved Caspase 3 (Cell Signaling Technologies, D175 #9661S, rabbit polyclonal) overnight at 4°C. Secondary antibody incubation was done for 1 hour at room temperature using anti-rabbit Alexa Fluor® 488 (Life Technologies, A212006, donkey polyclonal).

The slides were mounted with Vectashield mounting medium for fluorescence with DAPI (Vector Laboratories, Inc., H-1200). Images were captured using Lsm700 Zeiss laser scanning confocal microscope.

3.12 Microarray analysis

The cRNA for microarray analysis was prepared starting from 500 ng of total RNA, isolated as previously described, using the Illumina® TotalPrep™ RNA Amplification Kit (Ambion®). We performed the experiment at the BSF (Biopolis Shared Facilities) microarray facility using the Illumina platform. The bioinformatic analysis was performed in collaboration with J. Müller, a post doc in the lab).

The expression data from quadruplicate Illumina MouseRef-8 V2 microarrays were quantile normalized using the beadarray package v2.8.1 in R (Dunning et al., 2007) and annotated with the illuminaMousev2.db package. Probes with the label bad or no match were excluded from the analysis. p-values were multiple testing corrected using Benjamini and Hochberg (Benjamini and Yekutieli, 2001) control of the false positive rate. log2 fold changes were computed and only transcripts with an absolute fold change greater than 1.5 fold (1251 up and 2123 down) and a q-value of smaller than 0.01 were labelled as significantly differentially expressed.

3.13 Quantitative real time PCR (qRT-PCR)

Total RNA was isolated from the cells using PureLink RNA Mini Kit (Ambion, 12183-018A) and quantified using the NanoDrop 2000 (Thermo Scientific). Embryonic tissues were homogenized in 1 mL of TRIzol® Reagent (Life Technologies) and 0.2 mL of chloroform was added. Each sample was vortexed vigorously for 15 seconds, incubated at room temperature for 2 minutes and spun down at 4°C at 13200 rpm for 15 minutes. The upper phase was collected and one volume of 70% EtOH was added. RNA was then isolated using PureLink RNA Mini Kit (Ambion, 12183-018A) and quantified using the NanoDrop 2000 (Thermo Scientific).

1µg RNA was used to prepare cDNA using Vilo cDNA kit (Invitrogen). The cDNA prepared was subjected to qRT-PCR (ABI PRISM 7500), using SYBR Green PCR Supermix (Invitrogen). The final reaction volume was 20 µL: 10 µL 2X SYBR Green PCR Supermix, 4 µL forward and reverse primer mix (final concentration 200nM) and 6 µL cDNA (20 ng). The primer sequences are in **Table 3.4.** Data were expressed as relative mRNA levels normalized to housekeeper (TBP, GAPDH) expression levels in each sample.

Gene	Organism	Forward	Reverse
p53	mouse	CGCTGCTCCGATGGTGAT	TGGCGAAAAGTCTGCCTGTC
Mdm2	mouse	TGGAGTCCCGAGTTTCTCTG	AGCCACTAAATTTCTGTAGATC
Mdm4	mouse	AGTCAGGTGCGGCCAAAA	CCCAAAAGATCTCCACCACA
Ptprv	mouse	GGAGCGCTCATTTTGTCTTC	TGAGGCTAAGGCGGTAAGAA
p21	mouse	CTGGGAGGGGACAAGAG	GCTTGGAGTGATAGAAATCTG
Perp	mouse	CAGAGCCTCATGGAGTACGC	GAGAATGAAGCAGATGCACAGG
Puma	mouse	ATGGCGGACGACCTCAAC	AGTCCCATGAAGAGATTGTACATGAC
Noxa	mouse	CGGGCAGAGCTACCACCT	CGAGCGTTTCTCTCATCACA
TRP53inp1	mouse	ACCTTCTCATTGAACATCCC	TGCTTCCCCATTTCACTCT
Zmat3	mouse	CCCTGGAGGAGCTGTGTAA	CGTAGTTTCTTGCCATGGT
p19 ARF	mouse	GGGTTTTCTTGGTGAAGTTCG	TTGCCCATCATCATCACCT
Ccng1	mouse	CAGTTCTTTGGCTTTGACAC	CTTTCCTCTTCAGTCGCTTT
Gapdh	mouse	CATCTTCTTGTGCAGTGCCAG	GGCAACAATCTCCACTTTGCC
Tbp	mouse	CTGGAATTGTACCGCAGCTT	TCCTGTGCACACCATTTTTC
Prmt5	mouse	GATCCGAAGGAACTCTGAAG G	GCTGGAAGACCCAGATATGC
SmB/B'	mouse	CTTGGTCTGGTGTTGCTT	CTTCCTTGTGGGGTCATC

Table 3.4: Primers used for quantitative real time PCR

3.14 5-Bromodeoxyuridine (BrdU) labeling and flow cytometry analysis

MEFs were trypsinized and washed with PBS. Neurospheres were collected by centrifugation, washed with PBS and the cell pellet was thoroughly dissociated into single cells and passed through a 40 µm cell strainer (BD Falcon, 352340). The collected cells were fixed in 70% ice-cold ethanol overnight at -20°C. Fixed cells were subsequently stained with 20 µg/mL

Propidium Iodide, 0.1% Triton X-100/PBS, and 0.2 mg/mL RNAse A (Sigma-Aldrich, R6513) for 30 minutes at 22℃. For BrdU staining, cells were fixed after 1 hour of incubation with 100 µM BrdU. Fixed cells were then incubated for 30 minutes at room temperature in 2M Hydrochloric acid/0.1% Triton X-100 to denature the DNA, followed by neutralization with 0.1 M Sodium tetraborate, pH9.0. Cells were subsequently stained with anti-BrdU antibody conjugated with Alexa Fluor ® 488 (Cat#B35130, Life Technologies) in 0.5% Tween 20/PBS, 1% BSA for 1 hour at 22°C, followed by Propidium Iodide staining and flow cytometry analysis (Beckton & Dickson LSRII Flow Cytometry Analyser).

3.15 Nucleus and cytoplasmic fractionation

NPCs were harvested and washes twice in PBS. The cell pellet was resuspended in cold buffer A (1 mM Hepes pH 7.9, 5 mM MgCl2, 0.25 M sucrose, 100 mM NaCl, 0.1 % NP-40), passed through a 18G needle four times and incubated on ice for 10 minutes. After incubation the cell suspension was spun down at 4000 rpm for 10 minutes at 4°C. The supernatant, cytosolic fraction, was collected and 5X Laemmli buffer was added to achieve the final concentration of 1X Laemmli buffer. The pellet, nuclear fraction, was washed once in buffer A and resuspended in 1X Laemmli buffer to achieve the same total volume as the cytoplasmic fraction. 20 µL protein extract were loaded on 6-15% SDS-PAGE and western blot was performed as previously described.

3.16 Antibody purification

To generate antibodies specific for H3R8me2s and H2AR3me2s we collaborated with the IMCB antibody facility. KLH-coupled peptides mimicking the first 10 amino acids of H2A, symmetrically dimethylated on R3, were used to immunized 5 mice, while similarly designed peptides mimicking H3R8me2s were used to immunized 5 rabbits (Mimotopes, Australia). The best bleeds obtained were affinity purified using SulfoLink Coupling Resin (Thermo Scientific, 20401). Briefly, 2 mL of resin bed were equilibrated with 8 mL of Coupling buffer (50 mM Tris HCl pH 8.5, 5 mM EDTA-Na pH 8.5) using a purification column. 5 mg of cysteine-tagged peptide mimicking either H2AR3me2s or H3R8me2s (Mimotopes, Australia) were diluted in Coupling buffer, added to the column and incubated at room temperature. After 2 hour rotation the resin was washed in coupling buffer and then blocked with 50 mM L-Cysteine HCl diluted in Coupling buffer. The crude serum to be purified was next incubated with the prepared column for 2 hours at room temperature, extensively washed in Coupling buffer and finally, the purified antibody was eluted in Elution buffer (0.2 M Glycine HCL, pH 2.5) and neutralized with 50 µL/mL of Neutralization buffer (1 M Tris HCl, pH 8.5).

3.17 Peptide dot blot

Peptides mimicking the histone modification H2AR3me1, H2AR3me2a, H2AR3me2s, H4R3me1, H4R3me2a, H4R3me2s, H3R2me1, H3R2me2a, H3R2me2s, H3R8me2s, H3R17me2a, H4R26me2a, and the histone tails of histone H2A, H3 and H4 (Mimotopes, Australia) were resuspended in PBS to a final concentration of 2 mg/mL. 2 µL of a 1:10 dilution (400 ng) were spotted on PVDF membranes and dried at room temperature. The membranes were then blocked with 5% dry milk in PBS for 30 minutes at room temperature and incubated overnight with the primary antibody, followed by secondary-HRP conjugated secondary antibodies (**see Table 3.3**). The blots were developed using SuperSignal West Pico Chemiluminescent Substrate (Thermo Scientific, 34080).

3.18 Micrococcal Nuclease (MNase) assay

Nuclei from *Prmt5$^{F/F}$ER* NPCs either untreated or treated with OHT were obtained as previously described (paragraph 3.15), and resuspended in digestion buffer (0.32 M sucrose, 50 mM Tris-HCl pH7.5, 4mM $MgCl_2$, 1mM $CaCl_2$, 5mM Na butyrate, 0.1 mM PMSF). After DNA quantification the nuclei were resuspended in digestion buffer to achieve a final DNA concentration of 0.2 mg/mL. 20 µL of MNase (1U/µL Promega) was added to 500 µL of nuclei (0.1 mg DNA) and incubated at 37°C for 5, 10, 15, 20 or 40 minutes. At the end of the incubation period the digestion reactions were stopped adding 13.3 µL of 0.2 M EDTA pH 8. DNA was purified using a standard phenol extraction protocol and 8 µg of DNA were loaded onto a 2% agarose gel and bands on gel were visualized using ImageQuant RT ECL imager (GE healthcare).

3.19 Immunoprecipitation

Neurospheres were collected by centrifugation, washed once in PBS and lysed on ice in IP Lysis Buffer (300 mM NaCl, 50 mM Tris pH8, 0.4% NP-40, 10 mM $MgCl_2$, 2.5 mM $CaCl_2$) containing protease inhibitors (Merck-Calbiochem, 539134-IML) for 30 minutes. The lysate were briefly sonicated and an equal volume of IP Dilution Buffer (50 mM Tris pH8, 0.4% NP-40) was added. After incubation for 20 to 60 minutes the lysate were centrifuged for 10 minutes at 4°C at 14000 rpm. Antibodies (anti-SMN: SantaCruz Biotechnology, 2B1 sc-32313, mouse monoclonal; normal mouse IgG, SantaCruz Biotechnology, sc-2025) were added to the extract and incubated overnight on a rotating wheel at 4°C. Protein G-Sepharose beads (GE Healthcare cat#17-0618-02) were added to the mix and incubated for an additional 4 hours. The beads were pelleted, washed 5 times with IP buffer, and boiled in Laemmli buffer before loading onto SDS-PAGE.

3.20 2,2,7-Trimethylguanosine (TMG) pull down

The [^{35}S]methionine and [^{35}S]cysteine pulse-chase assay was performed as described previously (Winkler, 2005) with minor modifications. The chase time was reduced from 1 h to 45 min and NPCs were grown as described above. The newly synthesized snRNPs were purified using anti-2,2,7-Trimethylguanosine (TMG) agarose conjugate antibody (mouse, K121 NA02A Millipore) from total extract as described in the Immunoprecipitation section above.

3.21 Small nuclear RNA (snRNA) quantification by real time PCR

Neurospheres were washed twice in PBS, homogenized in 1 mL of TRIzol® Reagent (Life Technologies) and 0.2 mL of chloroform was added. Each sample was vortexed vigorously for 15 seconds, incubated at room temperature for 2 minutes and spun down at 4°C at 13200 rpm for 15 minutes. The upper phase was collected and one volume of 100% EtOH was added. RNA was then isolated using PureLink RNA Mini Kit (Ambion, 12183-018A) and quantified using the NanoDrop 2000 (Thermo Scientific). Reverse transcription and real time PCR were performed as described by (Zhang et al., 2008). Briefly, The list of primers used for qRT-PRC is in **Table 3.5** and the same reverse primers were used for the reverse transcription, which was performed using the SuperScript® II Reverse Transcriptase (Invitrogen™). For the U1, U2, U4, U5, and U6 snRNAs, and for the 5s and 5.8s rRNAs, 100 ng of total RNA was utilized as a template, whereas for the U11, U12, U4atac and U6atac reverse transcription, the starting amount of RNA was 375 ng. qRT-PCR was performed as previously described using one percent of the cDNA.

Gene	Organism	Forward	Reverse
U1 snRNA	mouse human	GATACCATGATCACGAAGGTGGTT	CACAAATTATGCAGTCGAGTTTCC
U2 snRNA	mouse human	TTTGGCTAAGATCAAGTGTAGTATCTGTTC	AATCCATTTAATATATTGTCCTCGGATAGA
U4 snRNA	mouse human	GCGCGATTATTGCTAATTGAAA	AAAAATTGCCAATGCCGACTA
U5 snRNA	mouse	TACTCTGGTTTCTCTTCAGATCGTATAAAT	AATTGGTTTAAGACTCAGAGTTGTTCCT
U6 snRNA	mouse human	GCTTCGGCAGCACATATACTAAAAT	ACGAATTTGCGTGTCATCCTT
U11 snRNA	mouse human	GTGCGGAATCGACATCAAGAG	CGCCGGGACCAACGAT
U12 snRNA	mouse	AACTTATGAGTAAGGAAAATAACGATTCG	CCGCTCAAAAATTCTTCTCACA
U4atac snRNA	mouse human	GCGCATAGTGAGGGCAGTACT	GCACCAAAATAAAGCAAAAGCTCTA

U6atac snRNA	mouse human	AGGTTAGCACTCCCCTTGACAA	TGGCAATGCCTTAACCGTATG
5 S rRNA	mouse human	CGGCCATACCACCCTGAAC	GCGGTCTCCCATCCAAGTAC
5.8 S rRNA	mouse human	CGGCTCGTGCGTCGAT	CCGCAAGTGCGTTCGAA

Table 3.5: Primers used for snRNAs quantitative real time PCR

3.22 RNA-Sequencing library preparation and splicing analysis

For RNA-Sequencing (RNA-seq) library preparation we followed the Illumina TruSeq RNA Sample Preparation Kit v2 manual. The bioinformatic analysis was performed in collaboration with J. Müller, a post doc in the lab). At least 70 million, 51bp long paired end reads were mapped to the NCBI37/mm9 version of the mouse genome per replicate using tophat 2.03 (Trapnell et al., 2009) allowing for 2 read miss matches. In total more than 40 million read could be aligned unambiguously per replicate. Differential expression analysis was performed using cuffdiff 2.01 (Trapnell et al., 2012) and only genes with a p-value of less than 0.05 and a fold change of greater than 1.5 were labelled as significantly differentially expressed.

To determine differential splicing events, MATS 3.0.6 (Shen et al., 2012) beta was used counting junction reads and reads falling into the tested region within ENSEMBL v65 gene definitions. Matching embryos were analyzed individually and only significant events occurring in at least two replicates were considered. Splicing events were labelled significant if the sum of the reads supporting a specific event exceeded 10 reads, the p-value was lower than 0.05 and the minimum inclusion level difference as determined by MATS was higher than 0.2. All other parameters were left at the default value. Shapiro scores for donor sites were calculated as stated in (Shapiro and

Senapathy, 1987). Briefly, the frequency of the first 6Bp of the Intron and the first 3Bp of the Exon were compared to reference donors. As reference donors, all canonical GT donors in the ENSEMBL v65 genome were utilized.
Intron read maps were generated on merged read counts using the package TransView 1.4.1. in R. Read maps were generated omitting overlapping known exons and converted into RPKM per intron. Only introns with a length between 0.1kBp and 10kBp and a RPKM of at least 1 were considered. All fold change values were log2 converted and log2 fold change values of the surrounding gene were subtracted to normalize for expression changes. All sequencing and microarray data have been submitted to the GEO repository and are available under accession number GSE45285.

3.23 Functional annotation

The functional annotation of the significant Microarray and RNA-Seq genes was performed with DAVID (Huang et al., 2009), using KEGG pathway (Kanehisa et al., 2012) representations.

3.24 RNA sequencing validation, splicing PCR

Primer were designed using CLC Main Workbench 5 (http://www.clcbio.com/) (**Table 3.6, 3.7 and 3.8**). All PCRs were performed with initial holding temperature of 95°C for 5 minutes, 26 cycles of denaturation at 95°C for 45 seconds, annealing at 58°C for 30 seconds and elonagation at 72°C for 40 seconds and a final elongation temperature of 72°C for 4 minutes and 4°C holding temperature. PCR products were ran in a range of 1.7% to 2.5%

agarose gels with 7 µL of ethidium bromide for every 100 mL of agarose solution prepared. PCR products were then loaded onto the gels and bands on gels were visualized using ImageQuant RT ECL imager (GE healthcare). Band intensities were quantified using ImageJ software (Schneider et al., 2012) and the percentage of exon or intron inclusion was calculated dividing the intensity value of the upper band by the sum of the intensity values of the two bands.

Gene	Forward	Reverse	Transcript accession number
Eif4e	CTACCACTAATCCCCCACC	CGTCCTCCTCGTTTGTTTT	Eif4e NM_007917
	Exon number: 5	chr3:138213227-138213290	
fibp	AGCTGACCCACAATAAGGA	CGGAGGGAGGAAGGAAAA	Fibp NM_021438
	Exon number: 9	chr19:5464334-5464431	
Epn1	GCTATGAGCAAGGAGGAGG	TCTATTGCCATCTGCAGCC	Epn1 NM_010147
	Exon number: 6	chr7:5044914-5044988	
Syce2	AGAGCATCGGCAGAGTGA	CTTTGCCATCTTCTGGGT	Syce2 NM_001168246
	Exon number: 3	chr8:87407330-87407483	
Pkd1	GCTGTCCTGTTCCTCTTCC	CACCATCTTCCTCTGAGCC	Pkd1 NM_013630
	Exon number: 31	chr17:24724124-24724237	
Bin1	CTCCCAAACACACCCCATC	AAGGTCTCCACCACCACA	Bin1 NM_001083334
	Exon number: 12	chr18:32591325-32591396	
Gphn	AGTAAAGGAGGTGCATGATGA	GGAGTAGTGCTAAGGGAGG	Gphn NM_145965.2
	Exon number: 8	chr12:79594937-79595044	
Mink1	GGAACAAAGCCAAGCCTGA	CCTTCCTCCTCCTCCTCTT	Mink1 NM_176893
	Exon number: 20	chr11:70422910-70422933	

Zfml	AGTTGGAGATGAGGAAGATGG	GTCTTGAGTCTTCCTGCGT	Zfml NM_00116637.1
	Exon number: 23	chr6:83931678-83931779	
Rnf38	CGCAGGTGAAGTGATGATGT	GGGGCTGCCTATTTGATGT	Rnf38 NM_001038993
	Exon number: 2	chr4:44171775-44171924	
Rfx3	CAACTACTCCTCTCCTCCTCC	GCACTTGCTGTACCACCT	Rfx3 NM_001166414.1
	Exon number: 2	chr19:27997698-27997756	
Nnat	CACCCACTTTCGGAACCA	TGTCGGTGCTGCTTTTCT	Nnat NM_010923.2
	Exon number: 2	chr2:157386949-157387029	
24100 04N09 Rik	TTGTGGCGTGGGATCTAGG	AGAACAGCACATCGAAGCA	2410004N09Rik NM_038151
	Exon number: 2	chr18:33955037-33955099	
Lmtk3	CGCTGCCTGATGTCTATATT	GTTCCTTCACCACCACCT	Lmtk3 NM_001005511
	Exon number: NA 5-6	chr18:53043016-53043128	
Cask	CGCTAACCAAACAGTGGA	GGGTGGTTGATGGCAAGT	Cask NM_009806
	Exon number: NA 17-18	chrX:13129499-13129567	
Isca2	CCGCTGGGAAACAACATCT	GCTGGGCTTGAGGGTTATT	Isca2 NM_028863
	Exon number: 3	chr12:86114743-86114858	
Mpdu1	CTACAGCATCACCAACAACTTC	CACCACGGCAGGTACATT	Mpdu1 NM_011900
	Exon number: 4	chr11:69471438-69471523	
Mdm4	TGTGGTGGAGATCTTTTGGG	TCAGTTCTTTTTCTGGGATTGG	Mdm4 NM_008575
	Exon number: 7	chr1:134901231-134901298	

Table 3.6: Primers used for the RNA-sequencing validation, skipped exons

Gene	Forward	Reverse	Transcript accession number
Gtf3c2	CTTCGACGACCTTATGAACCA	CGAGGTAACCGGCATCAA	Gtf3c2 NM_027901
	Exon number: 14-15	chr5:31461894-31462073	
Txlna	AACAGCATAACGAGCGAAAC	ACTCCACCGCTTCCTTCA	Txlna NM_001199695
	Exon number: 7-8	chr4:129308598-129308835	
Gdi1	AACGACGCTTCCGAAAAT	AGGCCATACAGTGGGTATAAA	Gdi1 NM_010273
	Exon number: 5-6	chrX:71553209-71553469	
Fxc1	GCGAGACTTCCTGTTGGT	GCGAGTCTCTGGTCTGTT	Fxc1 NM_019502
	Exon number: 2-3	chr7:112789371-112789542	
Setdb1	TGAATTTCTGGTTGGCTGTG	TGGCCTGGATAGTTAGCTG	Setdb1 NM_018877
	Exon number: 13-14	chr3:95141187-95142268	
Ppp1r12c	ATCACTCTGTTCCACCCT	CCACCTTTTCTGCTTCCTT	Ppp1r12c NM_029834
	Exon number: 13-14	chr7:4435159-4435245	
Gba2 (6-7)	ACGGTAACCCACACCACA	ACCGGCTTCGAGGTAACA	Gba2 NM_172692
	Exon number: 6-7	chr4:43583062-43583218	
Gba2 (8-9)	CTTTGGTTCAGATGGTGATGT	GCCCATAGTCCTGCAGAGT	Gba2 NM_172692
	Exon number: 8-9	chr4:43582533-43582702	
H2-Ke6	GTGGTTGCATTCTTGGCAT	CACCCCTGCCTTCCATATT	H2-Ke6 NM_013543
	Exon number: 8-9	chr17:34163170-34163341	
Cep110	GAACACTGGCGTGGAGAA	GGCAGACTGGGTGATGAT	Cep110 NM_12018
	Exon number: 41-42	chr2:35031120-35031648	
Ampd2	CAAAAGTGTGGTTCGGGC	TCACAGTGCTCATACGGG	Ampd2 NM_028779
	Exon number: 6-7	chr3:107882244-107882505	
Fancg	CTTCTGACTGCATTTGCCT	TCTGCTGCTCTGTCTCCT	Fancg NM_053081
	Exon number: 5-6; 6-7	chr4:43019986-43020140; chr4:43019768-43019856	

Trmt1	CGAATTCATCTTGGGGCCA	TCACAGATCTCACCCACTGC	Trmt1 NM_198020
	Exon number: 3-4	chr8:87214471-87214710	
Skiv2l	GGAGGTGACGAGGATGAAG	TGAGGTGGAGGTTTGGGAG	Skiv2l NM_021337
	Exon number: 8-9	chr17:34983940-34984088	
Ddx51	ACAGAAGTCGCTGGCTAA	ATCCTGGAGTCTGGTCAA	Ddx51 NM_027156
	Exon number: 6-7	chr5:111084432-111084584	
Prpf40b	GAGAGGGAACGGGAAAAGGA	ACTCCAGGGTGATCTGCT	Prpf40b NM_018786
	Exon number: 20-21	chr15:99145411-99145622	
Gpaa1	TCTCCCGCAAACTACCCT	GCCAACAACAACCCCACA	Gpaa1 NM_010331
	Exon number: 3-4	chr15:76162701-76162914	
Rabl2	AATCACCTATAAGAACCTGG	AGCCGAGACAAAGTACA	Rabl2 NM_026817
	Exon number: 6-7	chr15:89414438-89414710	
Phkg2	GAGCTACCGGTGATGAGTT	CGTAGGAATCGATGAGGG	Phkg2 NM_026888
	Exon number: 3-4	chr7:134721224-134721489	
Dvl1 (3-4)	GGTGGTGAAGGAGGAGAT	CGGCTACTGGCAACATTT	Dvl1 NM_010091
	Exon number: 3-4	chr4:155227867-155228092	
Dvl1 (4-5)	GGGACGGAATGGACAATGA	GATGCACTGTCTGGAGGTA	Dvl1 NM_010091
	Exon number: 4-5	chr4:155228195-155228439	

Table 3.7: Primers used for the RNA-sequencing validation, retained introns

Gene	Forward	Reverse
Human Mdm4 exon 6	TGTGGTGGAGATCTTTTGGG	GCAGTGTGGGGATATCGT
Human Gapdh	GAAGGTGAAGGTCGGAGTC	GAAGATGGTGATGGGATTTC
Mouse Gapdh	CATCTTCTTGTGCAGTGCCAG	GGCAACAATCTCCACTTTGCC
Mouse b-Actin	CAGCTTCTTTGCAGCTCCTT	CACGATGGAGGGGAATACAG

Table 3.8: Primers used for splicing PCR, human MDM4 and housekeepers

3.25 Polysome purification

The polysome purification was performed in collaboration with Leah A. Vardy (Institute of Medical Biology - IMB, A*STAR, Singapore). Polysomes were isolated and separated as previously described (Zhang et al., 2012). Briefly, 2 million cells were incubated for 10 minutes with 100 ug/mL cyclohexamide (Sigma, Cat C4859). On harvesting, the cells were resuspended in 2XRSB (20 mM Tris-HCl, pH 7.4, 20 mM NaCl, 30 mM $MgCl_2$, 200 µg/mL cycloheximide, 1000 unit/mL SUPERase•In - Ambion), and then lysed for 8 minutes on ice with 2X lysis buffer (20 mM Tris-HCl, pH 7.4, 20 mM NaCl, 300 mM $MgCl_2$, 1 % Triton X-100, 2% Tween-20, 1% deoxycholate). Following centrifugation at 12,000g for 10 minutes, cell extracts were loaded onto linear 10 – 50 % sucrose gradients (prepared in 10 mM Tris-HCl pH 7.4, 75 mM KCl and 1.5mM $MgCl_2$), and centrifuged at 36 k rpm for 70 minutes at 8°C in a SW60 rotor (Beckman Coulter). 6 fractions were collected from the top of the gradient using a piston gradient fractionator (BioComp Instruments). Following fractionation SDS was added to 1% and 5 µL of proteinase K (10 mg/mL Invitrogen) was added to each fraction, and incubated for 30 minutes at 42°C. RNA was purified by phenol-chloroform extraction followed by ethanol precipitation. cDNA was made using Superscript III with a mix of Random hexamers and Oligo dT.

3.26 Cell viability assay

Following 24 hours EtOH/OHT treatment, MEFs were plated in 96 well plates(5000 cells/well) at different serum concentrations (0.5%, 5%, 10%, 20% FBS). 4 days after plating, the cell viability assay CellTiter 96®AQueous One Solution Cell Proliferation Assay (Promega G3580) was performed according to the manufacturer's instruction.

3.27 Minigene construction

The expression constructs used for the minigene construction was kindly provided by E.Makeyev. RI (drRed2-Intron) (Makeyev et al., 2007). It contains a CMV or CAGGS promoter driving transcription of the dsRed2 fluorescent protein coding sequence interrupted by an intron. We refer to this vector as "Empty". To generate the RI-Mdm4 plasmid, a fragment containing mouse *Mdm4* exon 7 and parts of introns 6 and 7 were inserted into the intron of the RI vector at the PmeI-SpeI sites. The fragment was amplified by PCR (Platinum® Taq DNA Polymerase High Fidelity, Invitrogen) from C57BL/6 mouse genomic DNA using the following primers:

Forward: acacGTTTAAACaacatggctttgttgggtttg

Reverse: acacACTAGTAGCAAGTGACACCTCGTCATA.

We refer to this vector as "Exon 7". Primers used to check for alternative splicing were as follow:

dsRED primers

4651 CCGTGATGCAGAAGAAGAC

4630 ATTATGATCTAGAGTCGCGGC

The minigene constructs were transfected into MEFs using Lipofectamine 2000 *Invitrogen, according to the manufacturer instructions.

Chapter 4

RESULTS

4.1 A mouse model to study PRMT5 role in development

To study the role of PRMT5 in mammalian development we made use of a mouse model generated by the European Conditional Mouse Mutagenesis Program (EUCOMM). This is a conditional knock-out (KO) first mouse model (Testa et al., 2004) harboring LoxP ($^{F/F}$) sequences flanking exon 7 in the *Prmt5* gene. The KO first strategy relies on the insertion of a removable cassette (βgal cassette) within two FRT sequences, containing a strong splicing acceptor (EN2) followed by the coding sequence of the β-galactosidase gene, a selectable marker and the polyadenilation site. The β-gal cassette interrupts the transcription of the *Prmt5* gene generating a chimeric pre-mRNA, thus resulting in the depletion of PRMT5 protein expression and allowing detection of *Prmt5* transcript distribution *in vivo*. The cross of mice heterozygous for the KO first allele (*Prmt5*$^{+/-}$) with mice expressing the Flippase recombinase gene (FLP) results in the excision of the βgal cassette and the generation of heterozygous PRMT5 conditional KO mice (*Prmt5*$^{+/F}$) **(Fig. 4.1A)**.

Single site insertion of the βgal cassette in the *Prmt5*$^{+/-}$ mice was verified by Southern blotting **(Fig. 4.1B)**. As expected, the *Prmt5*$^{+/-}$ mice are viable, fertile and do not show any evident developmental defect, whereas *Prmt5*$^{-/-}$ mice are early embryonically lethal (Tee et al., 2010).

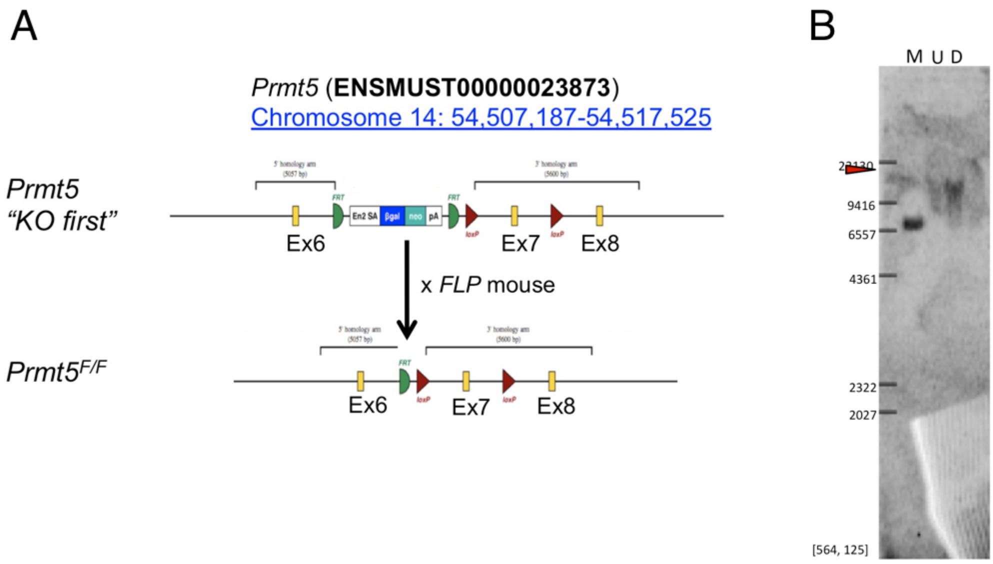

Figure 4.1: Inactivation of the *Prmt5* Gene: The PRMT5 conditional knock-out first allele. (A) Schematic representation of the EUCOMM constructs used in the study (Figure adapted from the EUCOMM website: http://www.knockoutmouse.org. **(B)** Southern Blot M: λ DNA-HindIII Digested Marker; U: Undigested *Prmt5*$^{+/-}$ genomic DNA D: XhoI-Digested *Prmt5*$^{+/-}$ genomic DNA. The red arrow indicates the band at the expected size.

4.2 PRMT5 expression in adult mouse tissues

PRMT5 expression patterns have not been studied in the mouse, thus, as a first step, we decided to characterize PRMT5 distribution in mouse adult tissues. We took advantage of the βgal cassette and performed β-galactosidase staining in adult *Prmt5* $^{+/+}$ and *Prmt5* $^{+/-}$ brain, heart, kidney, liver spleen and testis **(Fig. 4.2)**. While the wild type (wt) tissues did not show any staining (besides a minimal background staining in the testis), in *Prmt5* $^{+/-}$ tissues PRMT5 expression was seen primarily in the brain. No expression was observed in the heart and in the liver, whereas β-galactosidase staining was detected in the kidney, spleen and testis although at lower intensity compared to the brain.

To better characterize PRMT5 protein distribution and to confirm the results of the β-galactosidase staining we used an anti-PRMT5 antibody to stain an expanded panel of mouse tissues **(Fig. 4.3)**. By immunohistochemistry (IHC) we confirmed low levels of PRMT5 in the liver and in the heart. On the contrary, PRMT5 staining in testis resulted in a very strong nuclear signal. High levels of PRMT5 were also detected in the crypts of Lieberkühn and in the lining epithelium of the gatro-intestinal tract. The presence of PRMT5 protein was also confirmed in the central Nervous System (CNS), particularly in the Purkinje cells in the cerebellum, and in the nuclei of neurons populating the cerebrum and the spinal cord. Weaker PRMT5 expression was also detected in the cytoplasm of cells within the Islet of Langherans of the pancreas, and in kidney tubules. Staining was observed in the spleen, in some cells of the germinal center, in the white pulp and in the surrounding marginal zone, in the thymus medulla, and in the lung luminal bronchiolar cells.

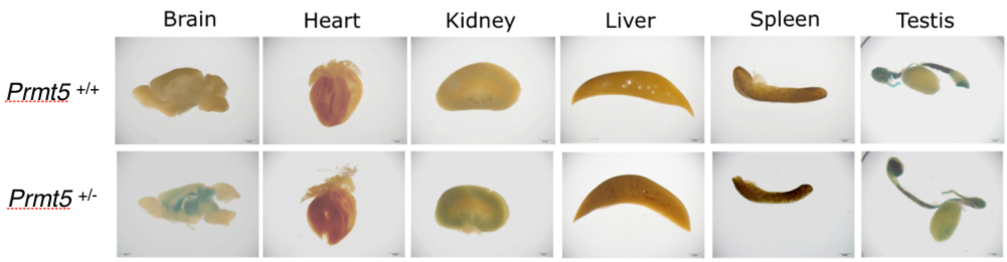

Figure 4.2: *Prmt5* Gene expression pattern in adult mouse organs. β-galactosidase staining of whole brain, heart, kidney, liver, spleen and testis from 2 month old *Prmt5* $^{+/+}$ and *Prmt5* $^{+/-}$ mice.

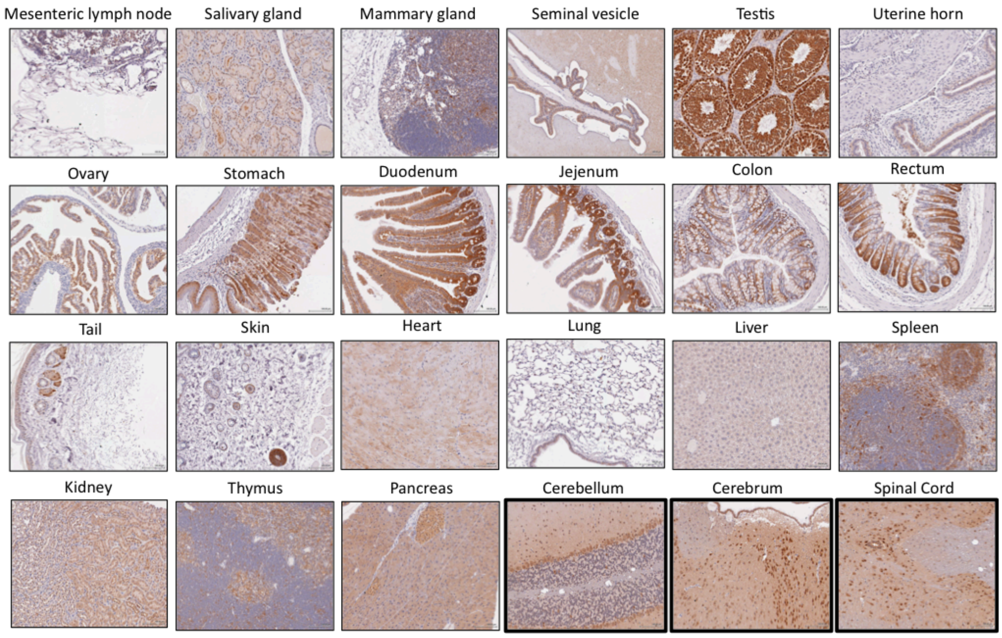

Figure 4.3: PRMT5 protein expression pattern in adult mice. PRMT5 ImmunoHistoChemistry (IHC) staining in various tissues from adult wild type mice.

4.3 PRMT5 deletion during organogenesis causes embryonic lethality

The analysis of PRMT5 distribution in multiple adult mouse organs revealed a complex expression pattern, and suggested a possible role for PRMT5 in tissues rising from different embryonic layers: ectoderm, mesoderm and endoderm. Therefore, we decided to start investigating the role of PRMT5 in mammalian development in an unbiased manner, systemically deleting PRMT5 during organogenesis. In order to achieve our goal, we generated a conditional KO strain by crossing the *Prmt5$^{F/F}$* mice to the *ROSA26:CreERt2 (ER)* mice, which allows the triggering of a recombination event in both live animals, or *ex vivo*, in primary cells, by using Tamoxifen (TAM) or 4-OH-Tamoxifen (OHT) respectively. *Prmt5* was selectively deleted in *Prmt5$^{F/F}$ER* embryos from pregnant *Prmt5*$^{F/F}$ females, crossed to *Prmt5$^{+/F}$ER* males, following Tamoxifen (TAM) injection at the stage of midgestation E10.5 **(Fig. 4.4A upper panel)**. The *Prmt5*$^{+/F}$*ER* littermates, or Ethanol (EtOH) treated *Prmt5*$^{F/F}$*ER* embryos were used as a control. CRE-ER was activated efficiently in different organs (**Fig. 4.4A lower panel**). Notably, upon TAM injection no *Prmt5*$^{F/F}$*ER* pups were born alive, thus we analyzed the embryos at E17.5 and E15.5. The mutant embryos were readily recognizable by their smaller size and pale color (**Fig. 4.4B**)**.** Instead of an organ-specific defect we observed growth retardation, suggesting a role for PRMT5 in maintaining the pool of proliferating cells, rather than driving specific differentiation programs. To test our hypothesis we examined actively proliferative organs such as lung and liver. The latter, at this stage of development, is populated by Hematopoietic Progenitor Cells (HPCs), recognizable by their dark-purple color in the H&E staining. Impairment of their homeostasis is evident in the TAM treated embryos and consistent with the pale color of the PRMT5 depleted embryos **(Fig. 4.5 top left panel)**. Phenotypically, we observed activation of the apoptotic response by staining the apoptotic marker Cleaved Caspase 3 (CC3) (Kuida et al., 1996) and dramatic exit from the cell cycle (reduced Ki67 staining) in both liver and lung **(Fig. 4.5)**.

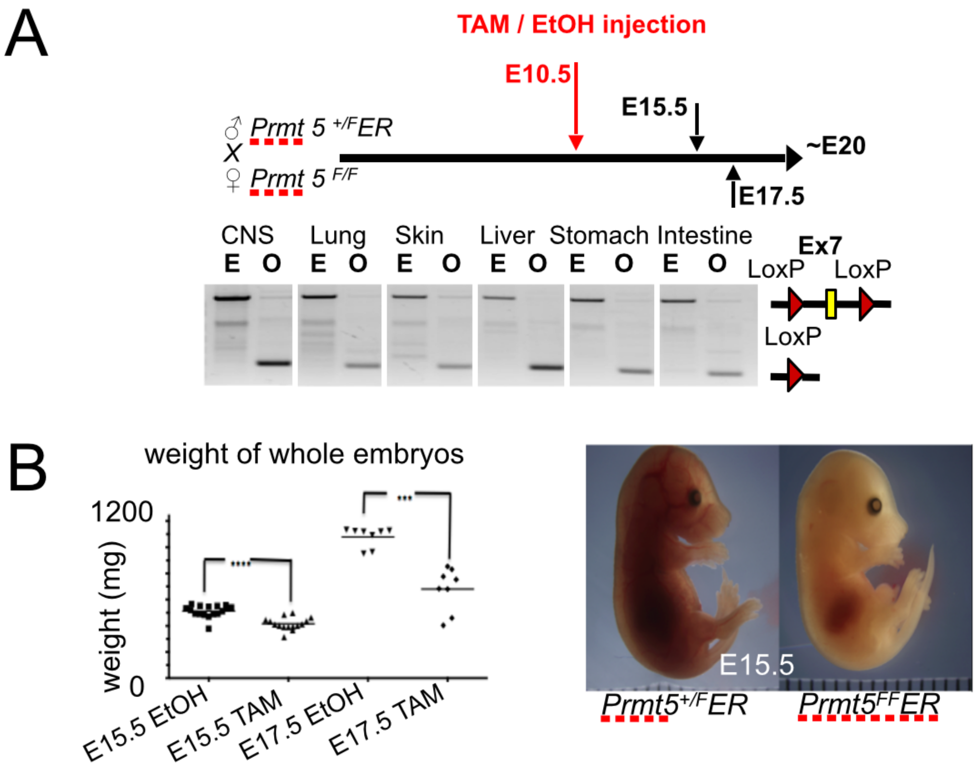

Figure 4.4: PRMT5 depletion during midgestation induces embryonic lethality. (A) Experimental strategy used to delete PRMT5 at midgestation (E10.5). Embryos were analyzed at E15.5 and E17.5. Upon TAM injection no pups were born alive. Bottom panel: Efficiency of CRE recombination taking place in different organs detected by genomic PCR. **(B)** Weight of PRMT5 wt (EtOH treated) or deleted (TAM treated) whole embryos at E15.5 and E17.5. Right panel: Representative example of E15.5 embryos with wt (left) or deleted (right) PRMT5.

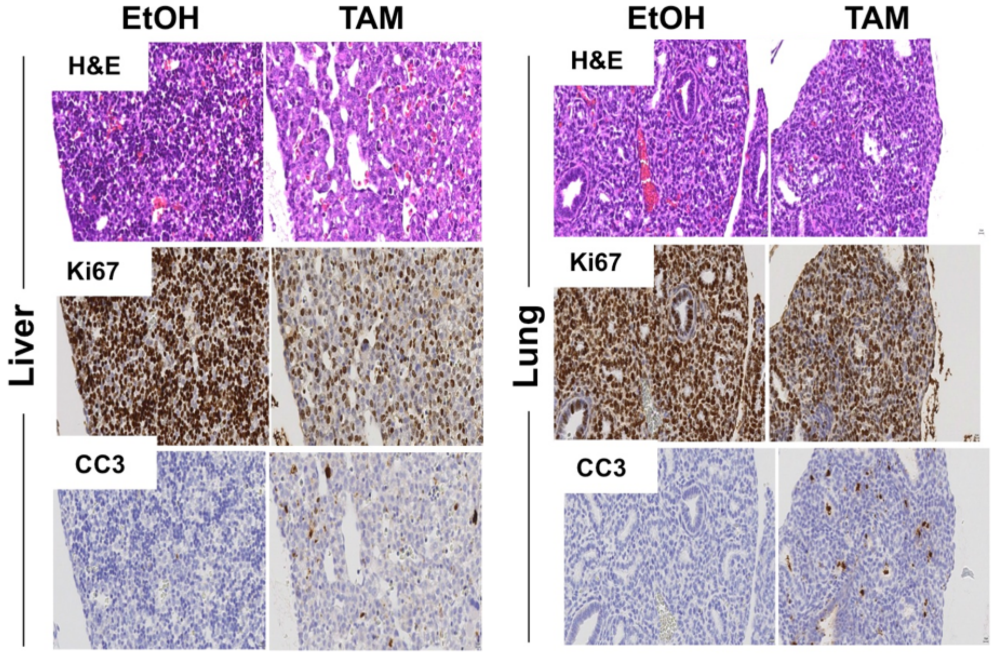

Figure 4.5: PRMT5 depletion induces cell cycle arrest and apoptosis in different tissues. Hematoxylin and eosin (H&E) staining of wild-type and knockout E15.5 lung and liver sections. In the liver light purple-stained hepatocytes and dark purple-stained hematopoietic precursor cells are easily detectable. Note the dramatic loss of the latter and the corresponding loss of ki67 staining. Below each (H&E) staining: ImmunoHistoChemistry (IHC) staining of Lung and Liver sections from a representative embryo. Cleaved Caspase 3 (CC3) is used to detect apoptotic cells and Ki67 to detect proliferating cells.

4.4 Complete PRMT5 loss impairs hematopoiesis

Since the deletion of PRMT5 in utero significantly affected the fetal liver, the site of embryonic hematopoiesis, reducing proliferation and increasing apoptosis, we decided to expand these findings inspecting E14.5 livers and testing the ability of treated and untreated HPCs to form hematopoietic colonies *in vitro*. As expected, upon TAM injection we observed striking reduction in fetal liver cellularity **(Fig. 4.6A)**. Accordingly, these cells were severely impacted in their ability to form hematopoietic colonies *in vitro* **(Fig. 4.6B left panel)**. To determine whether this phenotype was cell autonomous, we isolated E14.5 fetal liver HSCs from *Prmt5$^{F/F}$ER* embryos, grew them in EtOH or OHT containing HPC medium for 24 hours and plated them for colony formation assay. Remarkably, we observed dramatic reduction in the colony formation ability of the hematopoietic cells treated with OHT proving that PRMT5 plays a vital role for HPCs homeostasis during mouse development **(Fig. 4.6B left panel)**.

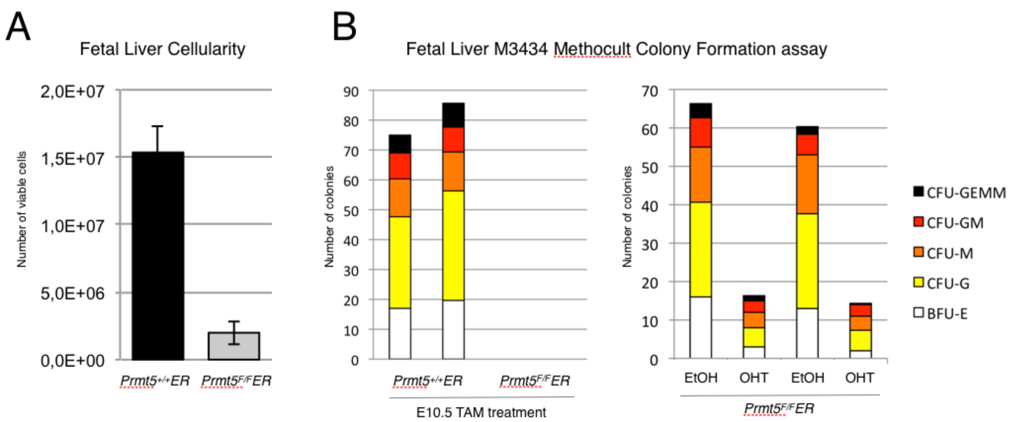

Figure 4.6: PRMT5 depletion impairs hematopoiesis. (A) Total number of live cells collected from E14.5 *Prmt5$^{+/+}$ER* and *Prmt5$^{F/F}$ER* fetal livers following TAM injection at E10.5. Each bar represents an average of at least 3 experiments. **(B)** Colony formation assay. Left panel: Liver cells as in (A) were cultured in M3434 Methocult for 11 to 14 days. Colonies were counted and classified based on they morphology. Right Panel: Liver cells from E14.5 *Prmt5$^{F/F}$ER* fetal livers were culture in HSC specific medium containing either EtOH or OHT 50nM for 24 hours. Cells were then cultured in M3434 Methocult for 11 to 14 days. Colonies were counted and classified based on they morphology. Data are as representative duplicates.

4.5 PRMT5 deficiency in the CNS results in early postnatal lethality

In order to gain further insights into the physiological and molecular basis of PRMT5 function in safeguarding proliferating cells homeostasis we next chose to focus our efforts on brain development for the following reasons:

- PRMT5 has been shown to methylate histones and core components of the spliceosomal machinery and a variety of developmental diseases of the CNS have been linked to either epigenetic or splicing defects (Castello et al., 2013; Gao and Taylor, 2012; Jakovcevski and Akbarian, 2012);
- PRMT5 is expressed in mouse brain and there is no direct evidence linking PRMT5 to either brain development or brain tumor development;
- In cancer cells PRMT5 is involved in the regulation of pathways critical for cell cycle regulation and apoptosis. Among these p53 pathway, has been extensively studied using mouse models in mouse CNS development (De Clercq et al., 2010; Doumont et al., 2005; Francoz et al., 2006; Migliorini et al., 2002; Xiong et al., 2006);
- In the developing brain, proliferating and differentiated cells are organized in a well characterized temporally and spatially ordered manner, allowing us to dissect the role of PRMT5 in both proliferation and differentiation;
- The proliferating cell population of the developing brain (Neural Stem/ Progenitor Cells) can be isolated and cultured in tissue cultured condition, expanded to high number of cells amenable for a variety of molecular biology experiments.

To specifically delete PRMT5 in the CNS we used a *Nestin-Cre (Nes)* transgenic mouse strain, which expresses Cre recombinase under a neural-specific enhancer of the *Nestin* promoter, leading to an efficient recombination event in precursors of neurons and glia, starting at embryonic day E10.5 (E10.5) (Graus-Porta et al., 2001). All the $Prmt5^{F/F}Nes$ mice were obtained from $Prmt5^{F/F}$ x $Prmt5^{+/F}Nes$ crosses and, as expected, the $Prmt5^{+/F}Nes$ mice were viable, fertile, and we could not observe any evident defects.

CNS-specific deletion of PRMT5 was confirmed by genomic PCR **(Fig. 4.7A)** and by western blotting **(Fig. 4.7B)**.

Prmt5$^{F/F}$*Nes* transgenic mice were born at the expected Mendelian frequency, but displayed smaller size **(Fig. 4.8A)**, balance disorders, tremors and akinesis. *Prmt5*$^{F/F}$*Nes* mice died within 14 days after birth, likely because of feeding problems as no milk was observed in their stomach. CNS development was impaired as evident from differences in brain size and weight, which was detectable starting at E17.5 **(Fig. 4.8B and C).**

At postnatal day 10 (P10), the external granular layer (EGL) of the cerebellum, an actively proliferating area at this age, was missing in mutant mice, as evident from both sagittal and coronal sections. The lateral ventricles were morphologically enlarged and disrupted, and the thickness of the cortex was reduced in size **(Fig. 4.9)**.

To better examine the onset of this dramatic phenotype we next focused on two earlier developmental stages. We analyzed the cellularity of the cortex of E15.5 and P0 brains. While we could not appreciate any significant differences in E15.5 brains, the cortex of P0 *Prmt5*$^{F/F}$*Nes* brains had a lower cellularity count both in the Cortical Plate (CP) and in the Ventricular/Sub Ventricular Zone (VZ/SVZ), the area populated by Neural Stem/Progenitor cells (NPCs) (**Fig. 4.10**).

To confirm the effect of PRMT5 deletion in NPCs, we performed staining of E15.5 and P0 cortexes with antibodies recognizing the Neural Stem Cell specific transcription factor SOX2 and the marker of proliferation Ki67. Consistent with data regarding the cellularity of the cortex, we did not observed an obvious reduction of SOX2/Ki67 staining in E15.5 *Prmt5*$^{F/F}$*Nes* brains (**Fig. 4.11A left panel**), whereas P0 mutant brains showed lower number of SOX2/Ki67 positive proliferating NPCs compared to controls (*PRMT5*$^{F/F}$) (**Fig. 4.11A right panel**).

Since the reduction detected in the P0 NPC population did not seem to originate from cell cycle exit of NPC at earlier stages, we decided to focus on the apoptotic response. To test the occurrence of cell death, we stained brain sections for Cleaved Caspase 3 (CC3). Despite the fact that changes in brain size and in thickness of the VZ/SVZ layer are not evident at E15.5, we did detect apoptotic death, specifically in the VZ/SVZ zone and in the ganglionic eminence, both areas containing proliferating NPCs (**Fig. 4.11B**).

The data suggested that the apoptosis induced in NPCs by the absence of PRMT5 could be the cause for the reduce brain size of *Prmt5*$^{F/F}$*Nes* animals, however we could not exclude the induction of premature differentiation, thus a combination of cell death and loss of multipotency. To test this hypothesis we extracted proteins from *Prmt5*$^{F/F}$ and *Prmt5*$^{F/F}$*Nes* P0 and P10 brains and tested the expression of NPCs markers (SOX2), intermediate progenitor markers (TBR2), as well as neuronal and glia marker (TBR1/TuJ and GFAP respectively). We did observe a significant decrease of SOX2 and TBR2 levels upon PRMT5 deletion, while the levels of differentiated neurons and glia markers were similar in both control and mutant brains (**Fig. 4.12**) suggesting a role for PRMT5 as inhibitor of apoptosis rather than regulator of stem cell identity in NPCs.

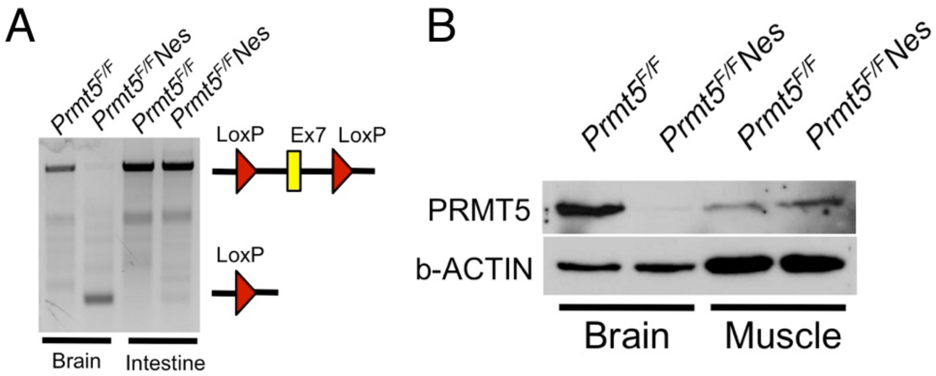

Figure 4.7: PRMT5 depletion in the brain. (**A**) PCR showing the efficiency of CRE recombination taking place specifically in the Brain. Intestine is used as a negative control. **(B)** PRMT5 protein levels in the CNS of *Prmt5*$^{F/F}$ and *Prmt5*$^{F/F}$*Nes* 10 days old mice. Protein extracts from muscles were used as controls.

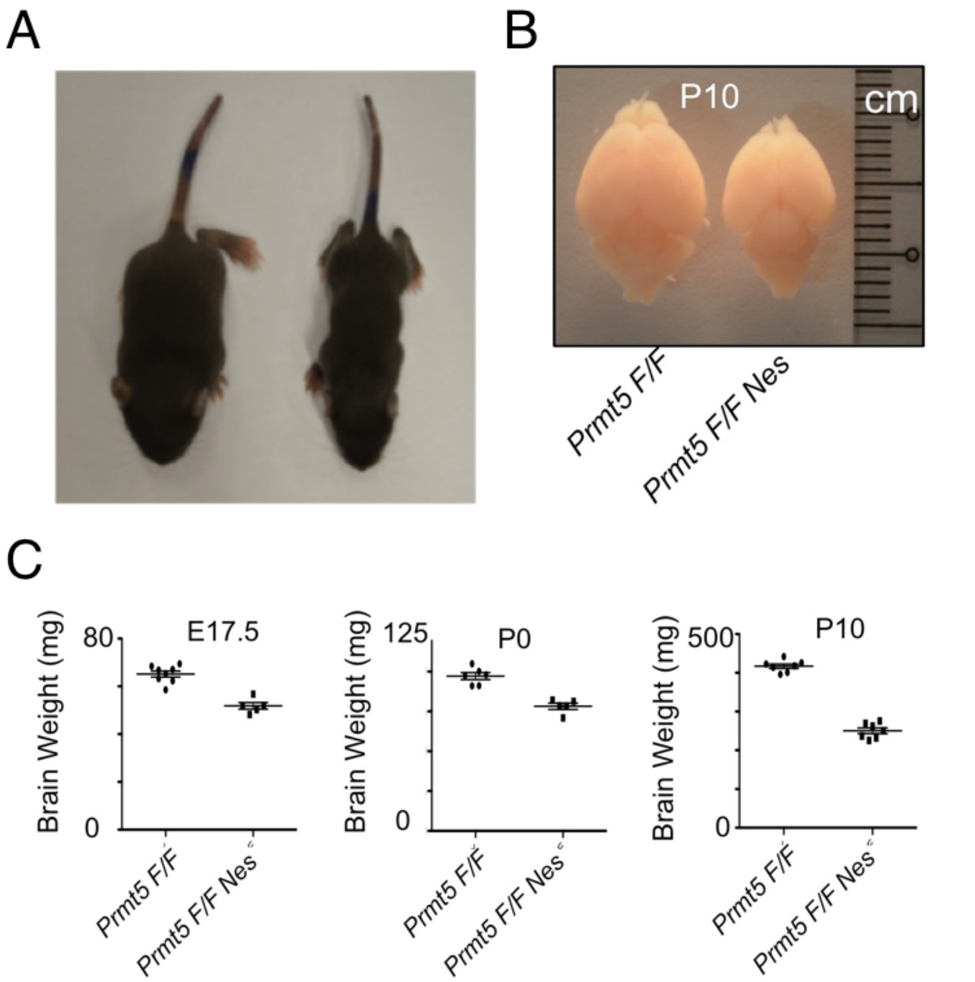

Figure 4.8: PRMT5 deficiency in the CNS results in early postnatal lethality. *Nestin-Cre*-induced deletion of the *PRMT5* gene in the CNS: **(A)** Post natal day 10 (P10) *Prmt5*$^{F/F}$ (on the left) and *Prmt5*$^{F/F}$ *Nes* mice (on the right). **(B)** Brain size of P10 *Prmt5*$^{F/F}$ and *Prmt5*$^{F/F}$ *Nes* mice are shown as an example. (**C**) Weight in mg of wild type (*Prmt5*$^{F/F}$) and *Prmt5* deleted (*Prmt5*$^{F/F}$ *Nes*) brains at three different time points (E17.5, P0 and P10).

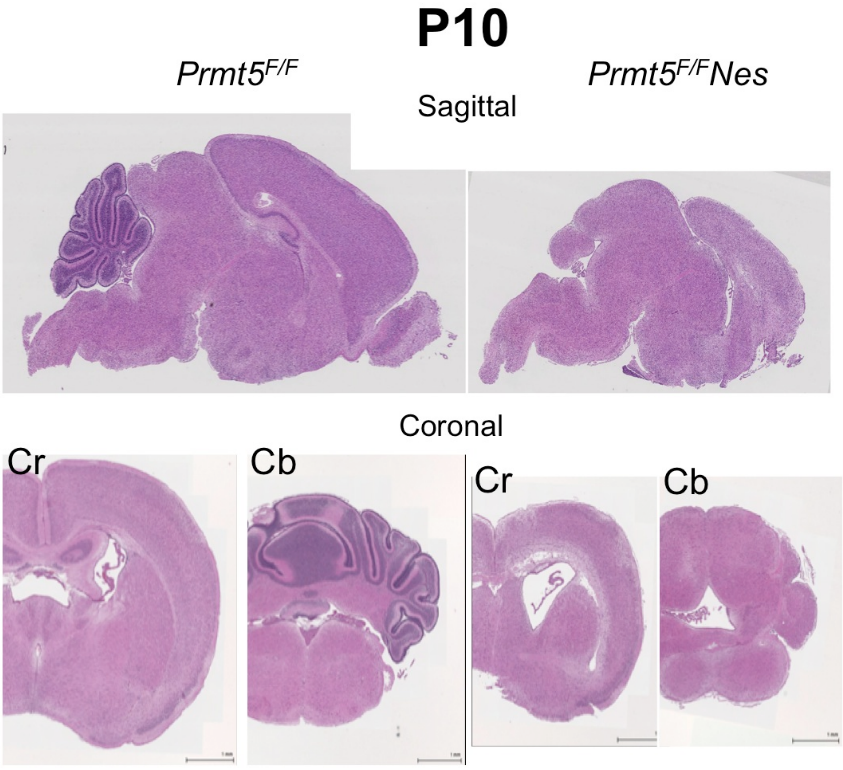

Figure 4.9: PRMT5 deficiency in the CNS results in widespread brain defects. Hematoxylin and Eosin (H&E)-stained Sagittal and Coronal sections of P10 Cerebrum (Cr), and the Cerebellum (Cb) from *Prmt5$^{F/F}$* (right) and *Prmt5$^{F/F}$ Nes* (left).

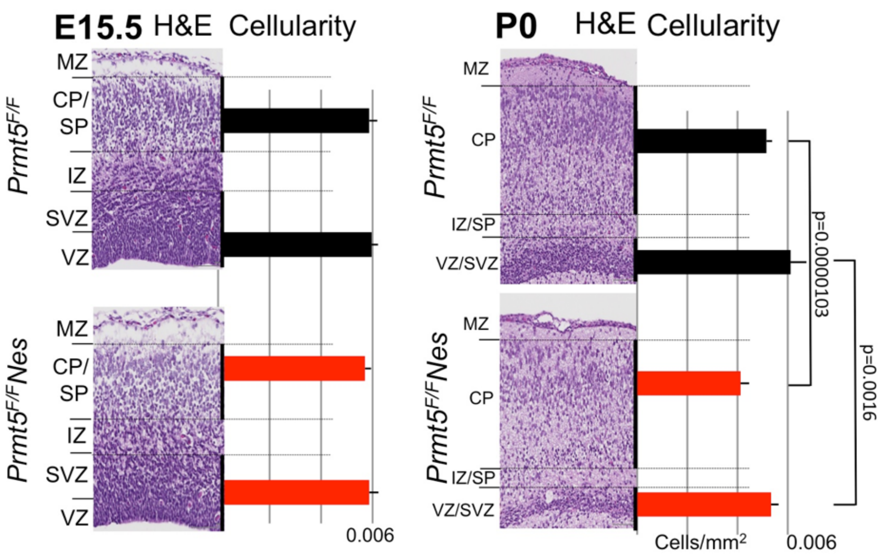

Figure 4.10: PRMT5 deficiency in the CNS results in reduced cellularity in neonatal brain. H&E coronal sections of *Prmt5$^{F/F}$* and *Prmt5$^{F/F}$Nes* E15.5 and P0 brains. Cellularity of CP/SP and VZ/SVZ zones are indicated in wt (black) and mutant (red) brains. MZ=Marginal Zone, CP=Cortical Plate, SP=Subplate, IZ=Intermediate Zone, SVZ=Sub Ventricular Zone, VZ=Ventricular Zone. Each bar represents an average of at least 3 experiments.

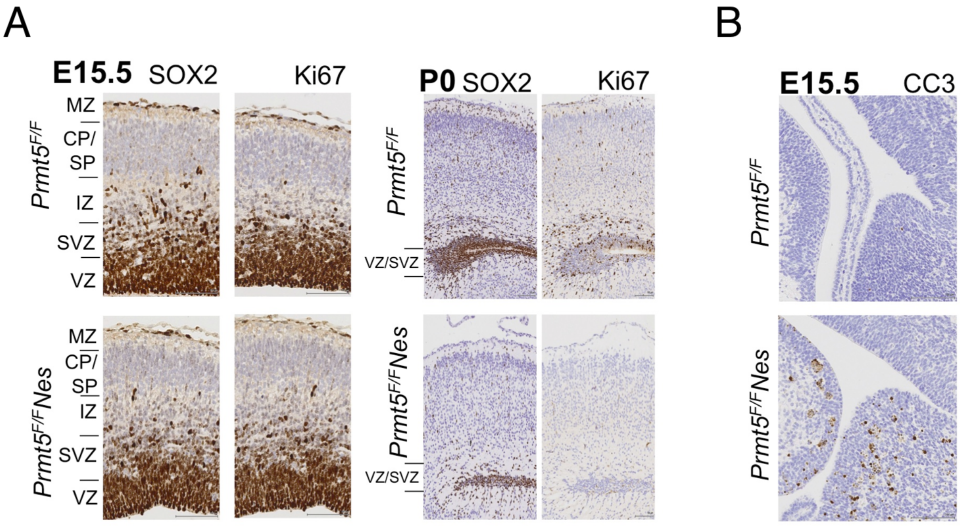

Figure 4.11: PRMT5 deficiency in the CNS results in depletion of the NPC population. (A) SOX2 and Ki67 IHC staining in coronal sections of E15.5 and P0 brains. (**B**) Cleaved Caspase 3 (CC3) staining is shown in both the cortex and the Gangliomic Eminence. MZ=Marginal Zone, CP=Cortical Plate, SP=Subplate, IZ=Intermediate Zone, SVZ=Sub Ventricular Zone, VZ=Ventricular Zone.

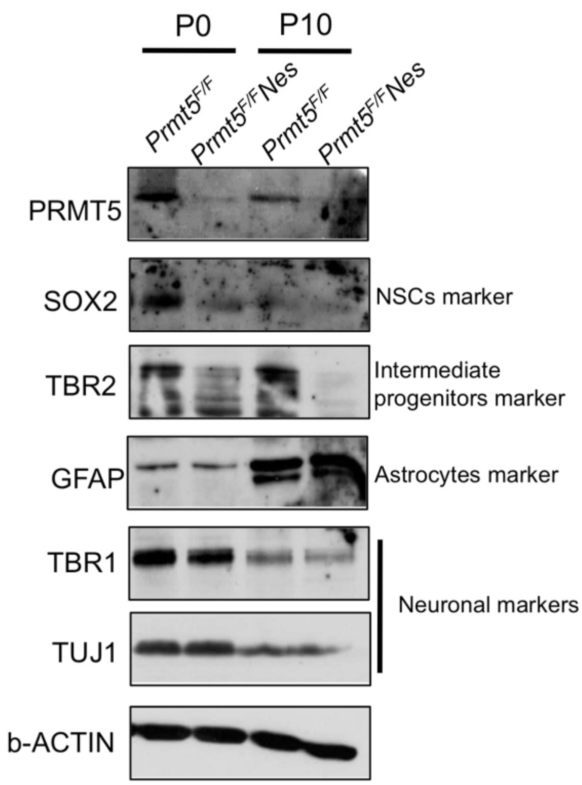

Figure 4.12: PRMT5 deficiency in the CNS does not alter the levels of neuronal and astrocyte markers. Protein levels (Antibodies used are indicated on the left of each panel) in the CNS (whole brain) of P0 and P10 *Prmt5*$^{F/F}$ and *Prmt5*$^{F/F}$*Nes* mice.

4.6 PRMT5 is required for Neural Stem/Progenitor Cell homeostasis

To further define whether PRMT5 is required for normal cell cycle regulation and survival and to protect cells from apoptosis, we derived NPCs from the dorsal telencephalon of E14.5 mice. NPCs can be efficiently grown *in vitro* as neurospheres and their self-renewal capacity can be assessed by sequential passaging. The number of primary spheres was significantly reduced in *Prmt5$^{F/F}$Nes* as opposed to controls. Furthermore, the number of cells in *Prmt5$^{F/F}$Nes* spheres was markedly reduced (**Fig. 4.13A**) and, importantly, their self renewal potential was impaired as highlighted by the fact that, following replating, virtually no secondary spheres could be derived (**Fig. 4.13B**). To confirm the results obtained *in vivo*, we first counted the percentage of pyknotic nuclei, typical feature of cells undergoing either necrosis or apoptosis, and next stained *Prmt5$^{F/F}$Nes* derived NPCs for Cleaved Caspase 3, to verify that they were undergoing apoptosis. As expected, we detected a dramatic increase of pyknotic nuclei in *Prmt5$^{F/F}$Nes* derived NPCs and the majority of the the cells forming the small primary mutant spheres were positive for CC3, confirming the requirement for PRMT5 to suppress cell death (**Fig. 4.13C**).

To test whether PRMT5 catalytic activity was necessary for the observed phenotype we infected primary NPCs derived from *Prmt5$^{F/F}$Nes* mice with wild-type human PRMT5 (hPRMT5), or a catalytically inactive mutant (hPRMT5AAA) and passaged them to derive secondary spheres. PRMT5 levels of expression were confirmed by western blot (**Fig. 4.14A**) and notably. only cells infected with hPRMT5 were able to grow and could be propagated into secondary spheres. When expanded into tertiary spheres cells expressing hPRMT5 grew as efficiently as NPCs derived from *Prmt5$^{F/F}$* control litters (**Fig. 4.14B**).

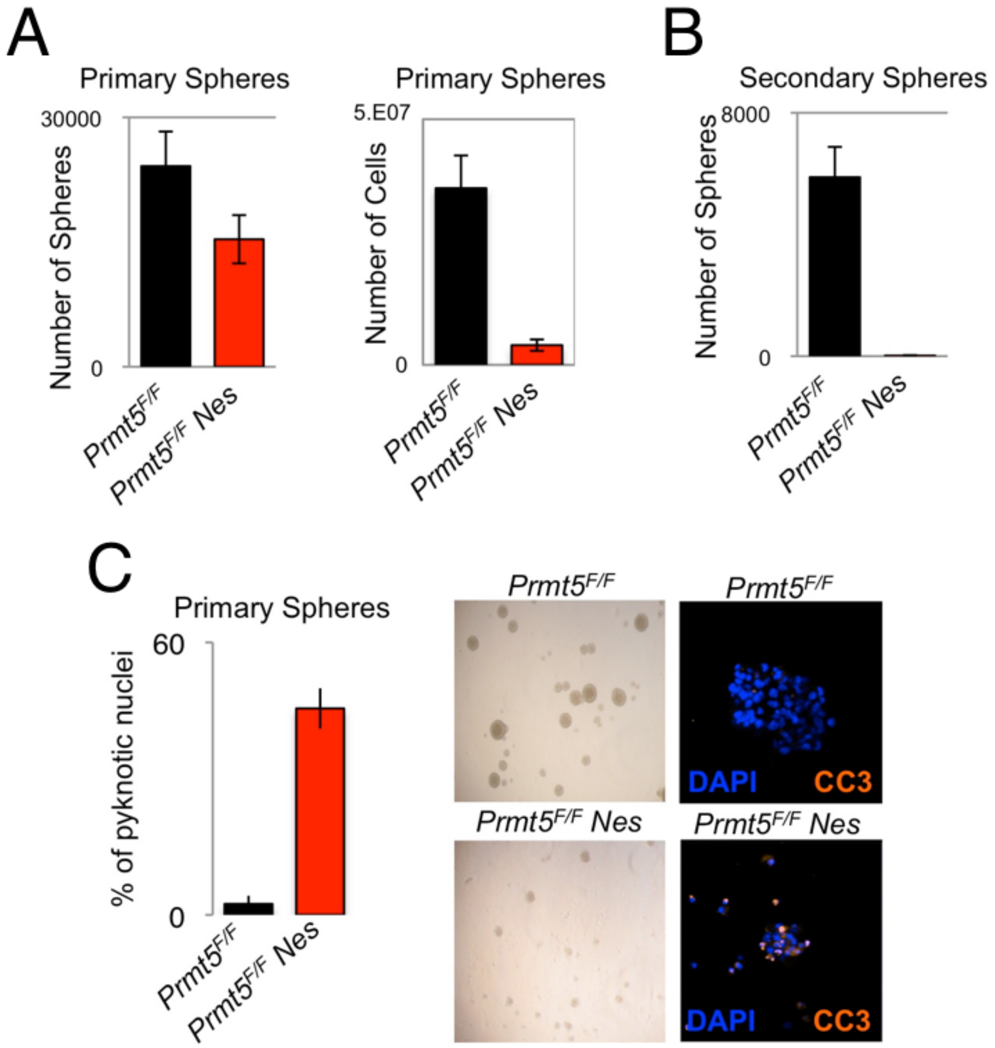

Figure 4.13: PRMT5 is required for Neural Stem/Progenitor Cell homeostasis. (**A**) Number of Primary Neurosphere and total number of cells from cultures of E14.5 dorsal telencephalon NPCs derived from *Prmt5$^{F/F}$* and *Prmt5$^{F/F}$ Nes* embryos. Each bar represents an average of at least 3 experiments. (**B**) Number of secondary Neurosphere as in A. **(C)** Neurospheres derived from *Prmt5$^{F/F}$* or *Prmt5$^{F/F}$ Nes* NPCs were stained with DAPI and CC3 and the percentage of pyknotic nuclei was counted.

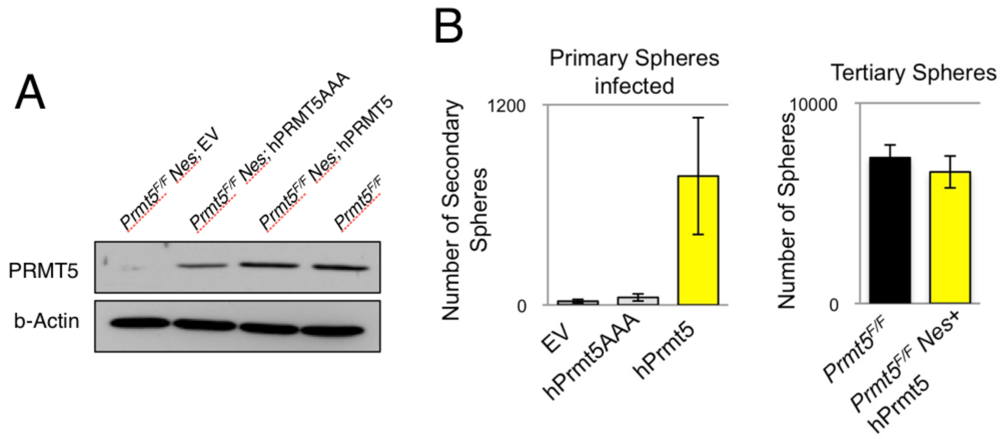

Figure 4.14: PRMT5 catalytic activity is essential to rescue the growth defect phenotype in NPCs. **(A)** Primary Neurospheres from *Prmt5$^{F/F}$ Nes* mice were infected with Empty Vector (EV), wild-type PRMT5 (hPRMT5), or a catalytically inactive PRMT5 mutant (hPRMT5AAA) and PRMT5 protein levels were measured by western blot. **(B)** Number of secondary neurospheres formed by cells infected as in A (left panel) and number of tertiary neurospheres formed by *Prmt5$^{F/F}$ Nes* NPCs infected with human PRMT5 passaged to derive Tertiary Neurospheres compared with tertiary neurospheres formed by *Prmt5$^{F/F}$* NPCs. Each bar represents an average of at least 3 experiments.

4.7 Depletion of PRMT5 in Neural Stem/Progenitor Cell activates the p53 response

To understand the molecular mechanism underpinning the observed apoptotic phenotype we next performed a gene expression analysis of *Prmt5$^{F/F}$Nes* NPCs using the Illumina microarray platform. Primary spheres were cultured for four days post-isolation and cRNA libraries from total RNA were prepared following the manufacturer instructions. Approximately 2500 genes were differentially expressed when compared to control. Functional annotation of differentially expressed genes showed downregulation of genes involved in cell cycle progression and replication, consistent with the observed phenotype. On the other hand, among others, the p53 signaling pathway was one of the most significantly upregulated (**Fig. 4.15A**)

(Appendix B) (Bezzi et al., 2013).

p53 is a transcription factor that drives the expression of several downstream targets involved in cell cycle arrest and apoptosis, in response to a variety of stimuli, including activation of the DNA damage response (DDR) (Lane, 1992). Much is known about the regulation of p53 by post-translational modifications and many of them, including phosphorylation and acetylation, are known to regulate its protein stability, leading to transcriptional activation. As mentioned in the introduction, also PRMT5 has been shown to modulate p53 transcriptional activity skewing the p53 response towards activation of apoptotic genes (Jansson et al., 2008). However, quantitative real time PCR validation of the activated of p53 target genes revealed that besides upregulation of known apoptotic genes such as *Puma*, *Noxa*, *TRP53inp1* and *Perp*, the cell cycle regulator genes *p21* and *Ccng1* were equally upregulated (**Fig. 4.15B**). Moreover, the La Thangue group demonstrated that the PRMT5-p53 connection was restricted to the DNA damage induced response (Jansson et al., 2008), suggesting that the phenotype we observed might be a consequence of the hypothetical dual function of PRMT5 in ensuring genome stability and in directly modulating p53 itself. Therefore, we switched to the *Prmt5* $^{F/F}$*ER* system for three main reasons: firstly it allowed us to look at cell-autonomous defects, secondly we could derive a much larger number of cells amenable for further mechanistic studies, and thirdly it allowed us to focus on early time points after PRMT5 depletion, in order to detect causal defects. In all experiments described hereafter, in which *Prmt5*$^{F/F}$*ER* derived cells were analyzed, we have always used the *ROSA26:CreERt2 (ER)* counterparts as negative controls, making sure that the addition of OHT or Tamoxifen was not toxic.

We first checked whether upon PRMT5 deletion, *Prmt5*$^{F/F}$*ER* NPCs responded similarly to the *Prmt5*$^{F/F}$*Nes* NPCs. This was indeed the case, as primary spheres formed after 24 hours treatment with OHT were not reduce in number, but they were smaller and contained a significantly lower number of cells. Accordingly, their capacity to form secondary spheres was dramatically impaired (**Fig. 4.16A**).

Secondly, we wanted to check whether we could detect DDR activation and whether p53 would be stabilized. We did observe a modest p53 protein stabilization and p53 phosphorylation (P-p53) and basal levels of H2AX phosphorylation (γH2AX). As a positive control we used a DNA damaging agent (Etoposide), which as expected, greatly stabilized p53 and increased the levels of γH2AX. Notably, despite a minor activation of the DDR response, the absence of PRMT5 caused an even greater induction of the p53 target gene p21, if compared to Etoposide (**Fig. 4.16B**). This is in contrast to what has previously been observed using siRNA/shRNA strategies to reduce the levels of PRMT5 in human cancer lines (Allende-Vega et al., 2013; Scoumanne et al., 2009). Moreover, it is in contrast with the observation of the La Thangue group (Jansson et al., 2008), suggesting that we might have discovered and alternative pathway linking p53 and PRMT5.

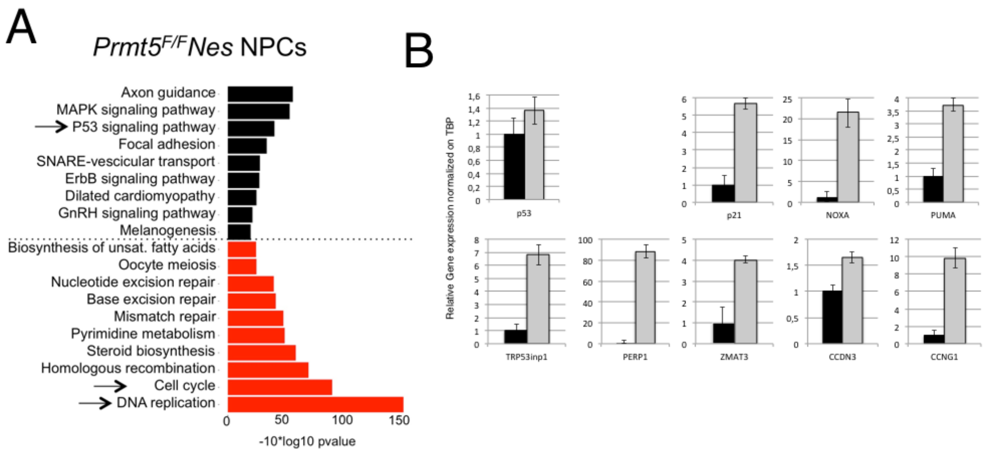

Figure 4.15: Microarray analysis of *Prmt5F/FNes* NPCs. (A) Functional annotation of differentially expressed genes. Clusters based on significantly up and down regulated genes in *Prmt5F/FNes* NPCs compared to *Prmt5F/F* are indicated as black and red bars respectively. Upregulation of the p53-signaling and down regulation of cell cycle and DNA replication genes are indicated by arrows. **(B)** Quantitative Real Time PCR validation of the activation of some gene involved in the p53 response activated in *Prmt5F/F Nes* NPCs (grey) normalized on the Ct values obtained from *Prmt5F/F* NPCs and on the housekeeper gene TBP. Each bar represents an average of at least 3 experiments. The bioinformatic analysis was performed in collaboration with J. Müller.

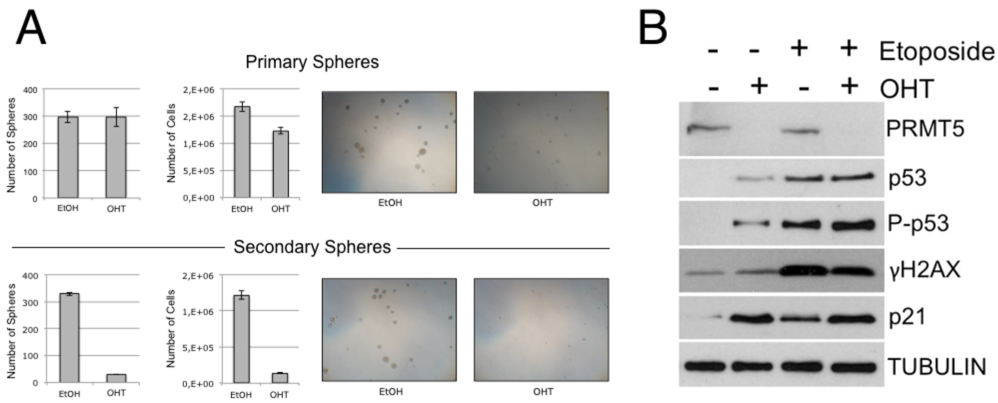

Figure 4.16: Activation of the p53 response in *Prmt5F/FER* NPCs treated with OHT. (A) Number of Primary and Secondary Neurosphere and total number of cells from cultures of E14.5 dorsal telencephalon NPCs derived from *Prmt5F/FER* embryos. The cells were treated with either OHT or EtOH for 24 hours and then plated for sphere formation assay. Each bar represents an average of at least 3 experiments. Representative images of the spheres are shown. (**B**) Protein levels upon treatment with OHT and subsequent PRMT5 depletion for 4 days. Antibodies used are indicated on the right of each panel. As a positive control p53 and the DDR response were induced by treating cells with Etoposide 10 µM for 2h.

4.8 p53 deletion partially rescues *Prmt5$^{F/F}$Nes* developmental defects

The data indicated that PRMT5 deficiency triggered a p53 response and that the phenotypic outcome in NPCs led to cell death. To formally prove this conclusion we crossed *Prmt5$^{F/F}$Nes* mice into a *p53* null background. *Prmt5$^{F/F}$Nes*;*p53-/-* mice displayed improved balance, increase in size **(Fig. 4.17A)** and milder tremors and akinesis when compared to *Prmt5$^{F/F}$Nes* mice. Accordingly, *Prmt5 $^{F/F}$Nes*;*p53-/-* mice survived on average one week longer than *Prmt5 $^{F/F}$Nes*;*p53wt*, while mice heterozygous for *p53* (*Prmt5 $^{F/F}$Nes*;*p53+/-)* displayed an intermediate phenotype (**Fig. 4.17B**).

Analysis of P10 brains showed a partial rescue of the developmental defects. EGL morphogenesis in the cerebellum improved dramatically, the same was true for the thickness of the cortex and the overall size of the brain was increased compared to *Prmt5$^{F/F}$Nes* brains (**Fig. 4.18A**).

When stained for activated Caspase 3, E15.5 *Prmt5$^{F/F}$Nes*;*p53-/-* embryos showed a complete rescue of the apoptotic response, with levels of staining similar to wild type (**Fig. 4.18B compare to FIg. 4.11B**). Importantly the number of SOX2 positive cells in the VZ/SVZ zone of *Prmt5$^{F/F}$Nes*;*p53-/-* embryos was increased when compared to *Prmt5$^{F/F}$Nes*;*p53wt* brains **(Fig. 4.18C compare to Fig. 4.11A)**. However, we did not observe a significant rescue of proliferating Ki67 positive cells, suggesting a p53-independent impairment in cell cycle progression, which most likely accounts for the lethality of the animals 20-22 days after birth (**Fig. 4.18C**).

This results demonstrate that p53 plays an important role in regulating the apoptotic response in *Prmt5$^{F/F}$Nes* brains. The fact that we still observed death of the animals, although significantly delayed, however pointed at additional proliferative defects in targeted cells. To gain further insight we first checked by RT-qPCR the level of transcriptional upregulation of p53 targets in both *Prmt5* $^{F/F}$*Nes* and *Prmt5* $^{F/F}$*ER* NPCs in a *p53*$^{-/-}$ background.

When we derived NPCs from *Prmt5*$^{F/F}$*Nes* mice with different p53 backgrounds and cultured them as neurospheres, p53 deficiency led to a significant, but not complete rescue in the number of proliferating cells, consistent with the evidence collected *in vivo* (**Fig. 4.19A**). Activation of cell cycle inhibitor *p21*, pro-apoptotic *Noxa*, *Puma* (Akhtar et al., 2006) and several other target genes was completely muted in the absence of p53, excluding compensation by other transcription factors, such as p53 family members p63 and p73 (Levrero et al., 2000) (**Fig. 4.19B). ** Moreover, flow cytometry analysis in *Prmt5* $^{F/F}$*ER* NPCs further confirmed that PRMT5 depletion in the absence of p53 led to a striking reduction in the number of apoptotic cells (**Fig. 4.19C**) and that the activation of p53 target genes was completely p53-dependent (**Fig. 4.19C**).

Propidium iodide (PI) staining followed by flow cytometry analysis revealed the almost complete rescue of the apoptotic response upon p53 deletion (**Fig. 4.20A**). In order to gain a better picture of the cell cycle profile, we next treated the different NPCs population with 5-Bromodeoxyuridine (BrdU), which is incorporated only by the replicating cells. Flow cytometry analysis carried out following PI/anti-BrdU staining showed significant reduction of the number of BrdU positive cells, suggesting defects in the DNA replication process and explaining the modality of their exit from the cell cycle (**Fig. 4.20B).** These data confirm that, despite inactivation of the p53 response, a second mechanism prevents these cells from proliferating. To mechanistically understand what causes the observed phenotype and to clarify whether PRMT5 acts on the p53 signaling or on the cell cycle regulation through different pathways, we next decided to focus on its molecular function.

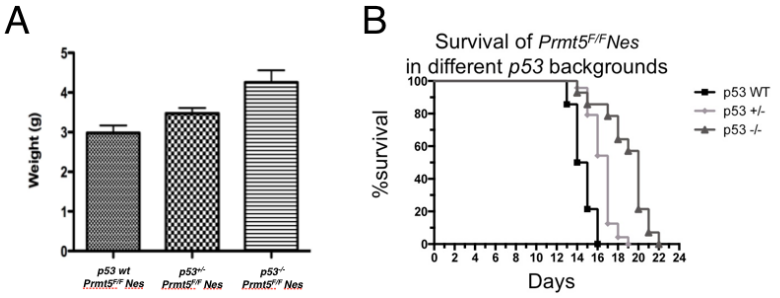

Figure 4.17: p53 deletion increases the survival of *Prmt5$^{F/F}$Nes* mice. (A) Weight in mg of 14 days old *Prmt5$^{F/F}$ Nes* mice in *p53 wt: n = 8*, *het (+/-): n = 8* or *null (-/-): n= 8* background. (**B**) Kaplan-Meier survival analysis of *Prmt5$^{F/F}$Nes* mice in *p53 wt: n = 14*, *het (+/-): n = 24* or *null (-/-): n= 14* background.

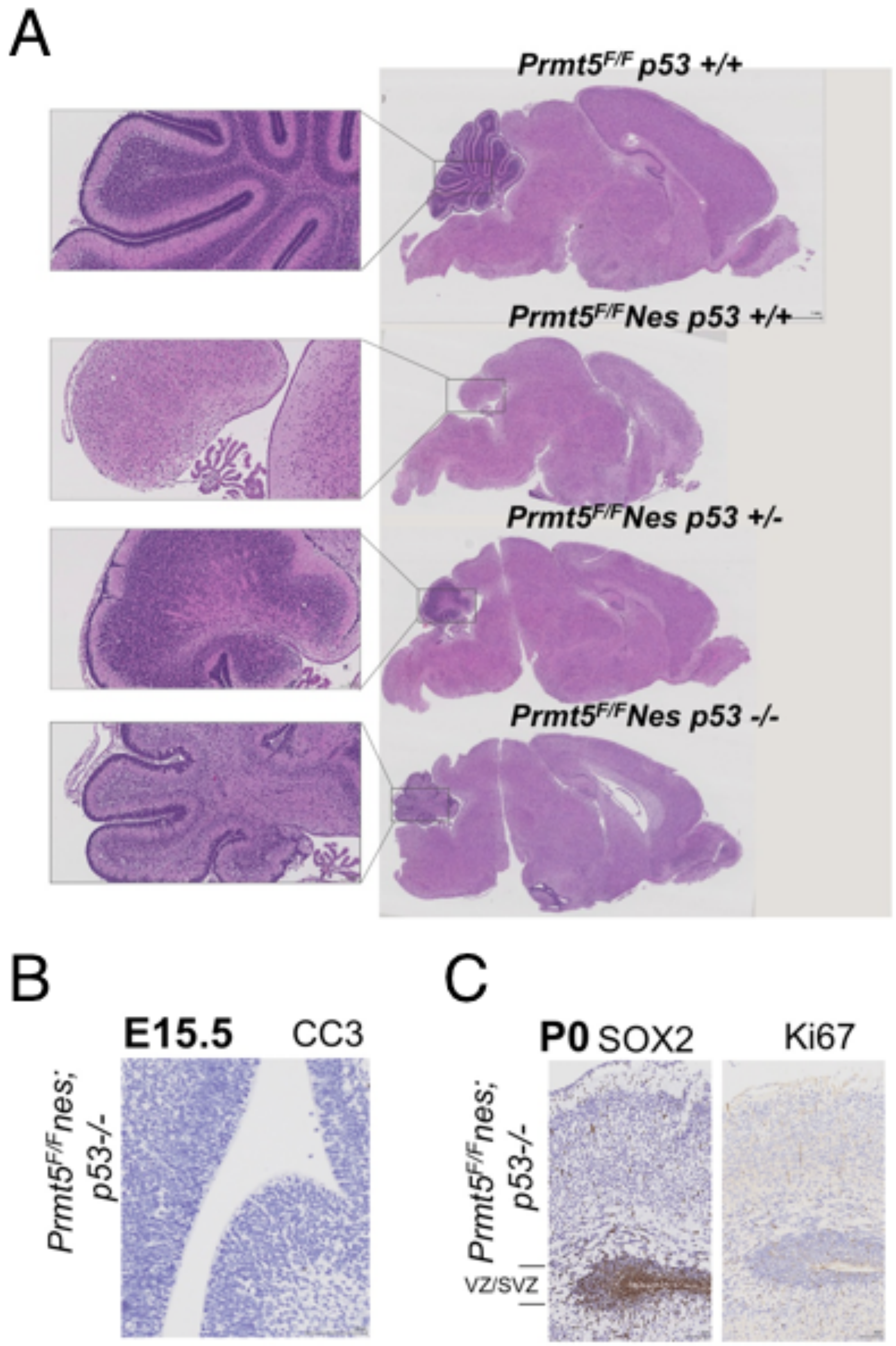

Figure 4.18: p53 deletion partially rescues *Prmt5*$^{F/F}$Nes developmental defects. (A) Hematoxylin and Eosin (H&E)-stained coronal brain sections of *Prmt5*$^{F/F}$Nes mice with different *p53* backgrounds. The cerebellum is shown at higher magnification in the inset. (**B**) Coronal sections of E15.5 brains stained for Cleaved Caspase 3 (CC3) and **(C)** and P0 brains stained for SOX2 and Ki67 to identify stem cells and assess their proliferation status. Antibodies used are indicated for each panel.

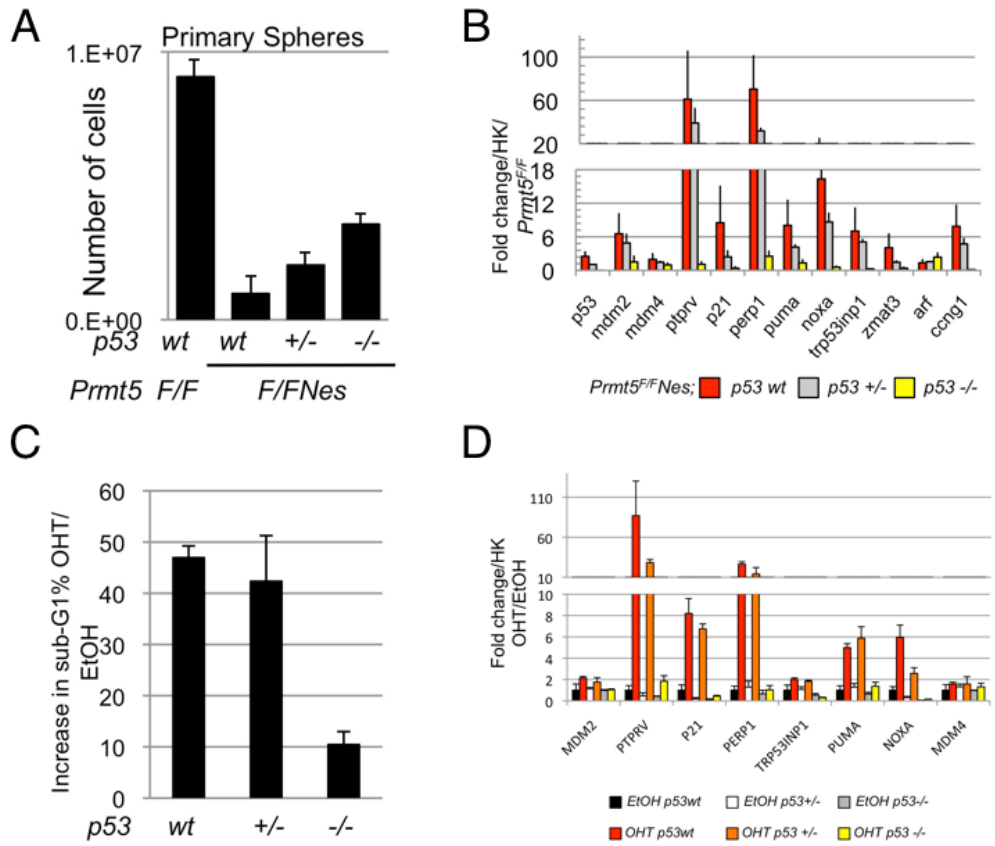

Figure 4.19: p53 deletion fully rescues the activation of p53 target genes. (A) Total number of NPC cells grown as Primary Neurospheres derived from $Prmt5^{F/F}Nes;p53^{wt}$, $Prmt5^{F/F}Nes;p53^{+/-}$ and $Prmt5^{F/F}Nes;p53^{-/-}$ as indicated. (**B**) Expression of p53 upregulated target genes in NPCs from different genotypes as indicated. The activation of the genes is expressed as the average fold change of 3 embryos/NPCs, normalized against $Prmt5^{F/F}Nes;p53^{wt}$ and HK. **(C)** $Prmt5^{F/F}ER$ NPCs treated with OHT to delete PRMT5 were stained with propidium iodide and subjected to flow cytometry analysis. Bars indicate the increase in sub-G1/apoptotic cell populations, normalized to EtOH treated cells. P53 genotypes are indicated. **(D)** Expression of p53 upregulated target gens in NPCs (EtOH/OHT) from $Prmt5^{F/F}ER;p53^{wt}$ (black/red), $Prmt5^{F/F}ER;p53^{+/-}$ (white/orange). $Prmt5^{F/F}ER;p53^{-/-}$ (grey/yellow). The activation of the genes is expressed as the average fold change of at least 3 embryos/NPCs, normalized against $Prmt5^{F/F};p53^{wt}$ and HK. Each bar represents an average of at least 3 experiments

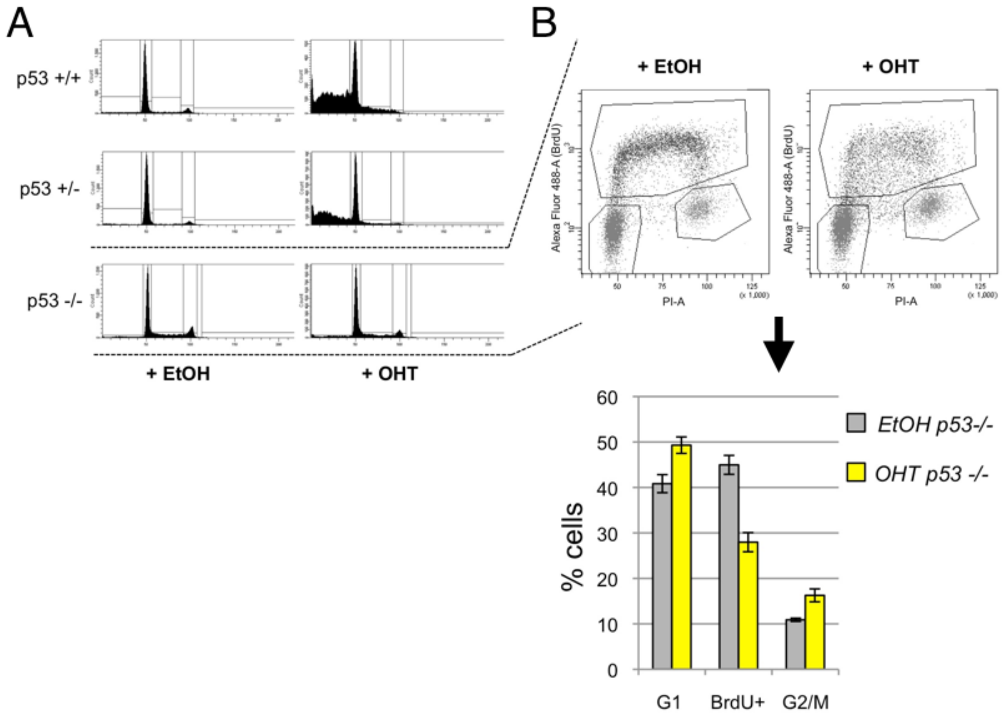

Figure 4.20: PRMT5 deletion induces cell cycle exit in p53 null NPCs. (A) Flow cytometry analysis on *Prmt5*$^{F/F}$*ER* (EtOH/OHT) in the indicated p53 genetic backgrounds. (**B**) Cells were stained with BrdU and the percentage of cells that are actively replicating (BrdU+) or not (in the G1 or G2/M phase of the cell cycle) is indicated by the bar plot. Each bar is the average of three independent experiments.

4.9 PRMT5 deletion in the brain reduces the levels of H2AR3me2s

PRMT5 has been shown to function in both the nucleus and the cytoplasm, methylating histones and non-histone proteins. We performed nuclear/ cytoplasmic fractionation in NPCs, and observed high levels of PRMT5 in the cytoplasm and lower amounts in the nucleus **(Fig. 4.21A)**. To confirm this localization pattern *in vivo*, we stained for PRMT5 in E15.5 brains. In the NPCs of the ventricular and subventricular zone PRMT5 was strongly present in the cytoplasm and localized also in the nucleus, whereas in the post mitotic neurons populating the intermediate zone, the cortical plate and the subplate it mainly localized in the nucleus **(Fig. 4.21B)**, suggesting a possible function for PRMT5-mediated histone modifications in brain development.

To assess PRMT5 role as histone methyltransferase in the mouse brain we decided to check the levels of the histone modifications H3R2me2s, H3R8me2s, H4R3me2s and H2AR3me2s. In order to perform this experiment we sought to raise specific H3R8me2s and H2AR3me2s antibodies, as we did for H3R2me2s (Migliori et al., 2012). In collaboration with the IMCB antibody facility, 5 mice were immunized with KLH-coupled peptides mimicking H2AR3me2s, as well as 5 rabbits were immunized with KLH-coupled peptides mimicking H3R8me2s. The bleeds obtained were tested by peptide blots and the most promising sera were affinity purified and further tested performing peptide blots, competition assays and western blots on cellular nuclear extracts. Peptide blots for the two best antibodies against H2AR3me2s and H3R8me2s are displayed in **Fig. 4.22A**. Surprisingly, when we checked the levels of these PRMT5-mediated histone methylation events *in vivo*, the only modification significantly reduced in the PRMT5 depleted mouse brain was H2AR3me2s **(Fig. 4.22B)**. Notably, albeit the anti-H2AR3me2s antibody was cross-reacting with the H4R3me2s peptide **(Fig. 4.22A)**, it did not recognize histone H4 in total or nuclear cellular extract. Therefore, we decided to study the role of H2AR3me2s in chromatin regulation as we did for H3R2me2s (Migliori et al., 2012), by performing ChIP-sequencing in NPCs and peptide pull down assays from total NPCs lysate labelled with stable isotopes (SILAC) couple to mass spectrometry. Unfortunately, the ChIP-sequencing analysis (performed by J. Müller, a post doc in the lab) did not show any particular enrichment of H2AR3me2s in the promoter, intragenic or enhancer regions, and there was no correlation with the transcriptional changes observed in the *Prmt5 $^{F/F}$Nes* NPCs. Moreover, the peptide pull down assays coupled to mass spectrometry (the analysis was performed by the IMCB Quantitative Proteomics Facility) did not detect any specific H2AR3me2s binding partner. Since H2AR3me2s has been shown to be catalyzed in the cytoplasm (Tee et al., 2010), thus methylation precedes deposition into chromatin, we decided to investigate whether this post translational modification plays any role in chromatin assembly. Micrococcal nuclease assay in wt or depleted PRMT5 NPCs was performed and it did not show any significant difference in the digestion patterns suggesting that the absence of PRMT5, and as a consequence of H2AR3me2s, does not impact chromatin assembly **(Fig. 4.22C)**. Our data were therefore inconclusive and we decided to look at other possible methylated targets that could be linked to the observed phenotype.

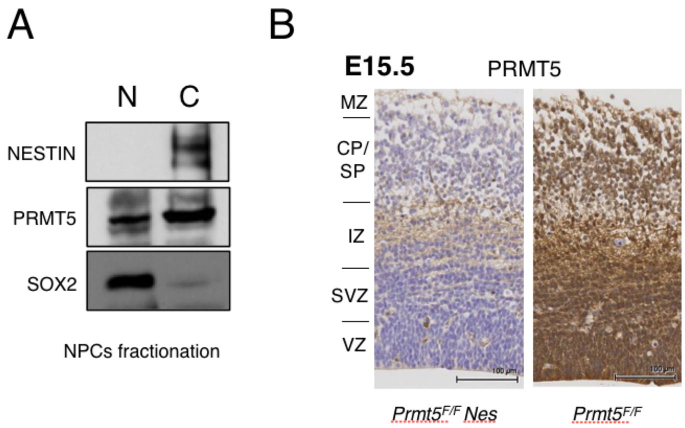

Figure 4.21: PRMT5 cellular localization in NPCs. (A) Nuclear/cytoplasmic fractionation of NPCs. PRMT5 protein levels are shown. SOX2 has been used as a control for the Nuclear fraction (N), while Nestin has been used as a control for the Cytosolic fraction (C). (**B**) PRMT5 IHC staining in coronal sections of *Prmt5*$^{F/F}$ and *Prmt5*$^{F/F}$*Nes* E15.5 brains. MZ=Marginal Zone, CP=Cortical Plate, SP=Subplate, IZ=Intermediate Zone, SVZ=Sub Ventricular Zone, VZ=Ventricular Zone.

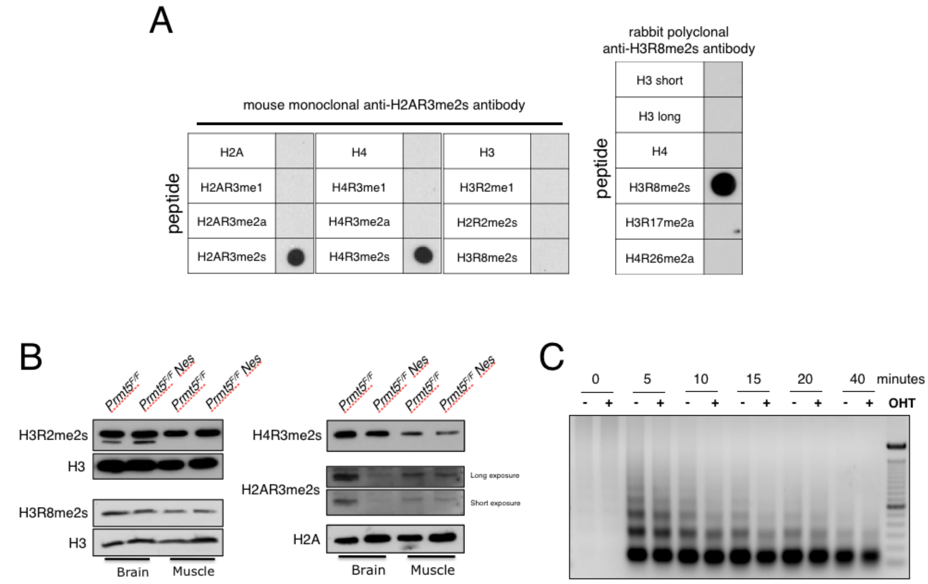

Figure 4.22: PRMT5 depletion in NPCs has minor effects on chromatin dynamics. (A) Characterization of the H2AR3me2s and the H3R8me2s antibodies by peptide dot blot analysis. Synthetic peptides mimicking previously identified histone arginine methylated sites (indicated on the left) were spotted on PVDF membrane and incubated with the indicated antibody. (**B**) Histone modification levels (antibodies used are indicated on the left of each panel) in the brain and in the muscle (used as a control) of P10 *Prmt5*$^{F/F}$ and *Prmt5*$^{F/F}$*Nes* mice. **(C)** Micrococcal Nuclease (MNase) assay. Nuclei from *Prmt5*$^{F/F}$*ER* NPCs either untreated or treated with OHT to delete PRMT5, where incubated with MNase (20U/0.1mg of DNA) for the time indicated. MNase digests the DNA within nucleosome linker regions and the bands are approximately the size of the DNA wrapped around one (lower band) or more (upper bands) nucleosomes.

4.10 PRMT5 depletion in NPCs affects snRNP assembly

Looking for defects that could mechanistically underpin both the activation of the p53 pathway and the additional proliferation defects we sought to examine the putative role of PRMT5 in mammalian pre-mRNA splicing. In plants, *Drosophila* and HeLa cells, PRMT5 was known to symmetrically dimethylate Sm proteins (Deng et al., 2010; Gonsalvez et al., 2006; 2007; Sanchez et al., 2010). We first tested whether this was also relevant during mammalian development. We treated *Prmt5*$^{F/F}$*ER* NPCs with either EtOH or OHT and observed that despite constant levels of SmD1 and D3 proteins, there was a reduction in the levels of symmetric arginine dimethylation by day 4, as detectable by two well characterized independent antibodies (SYM10 and Y12), which detect the symmetrically arginine dimethylated Sm proteins B/B', D1 and D3 **(Fig. 4.23A).**

Consistent with the fact that the SMN1 Tudor Domain binds arginine-methylated SmB/B', D1 and D3, 4 days after the OHT treatment (*Prmt5* deletion) we observed a reduced binding of SMN1 to SmD1 and SmD3 **(Fig. 4.23B)**, suggesting that PRMT5-depleted NPCs would have suboptimal snRNP maturation. To test this hypothesis we replicated in *Prmt5* $^{F/F}$*ER* NPCs the TMG pulldown experiment, following pulse-chaise protein radioactive labeling, performed by the Matera group in HeLa cells treated with PRMT5 siRNA (Gonsalvez et al., 2007). Our data confirmed that in mammalian cells the absence of PRMT5 reduces the kinetic of snRNP assembly as evident from the marked reduction of the bands in the OHT treated NPCs **(Fig. 4.23C)**.

Notably, in both a SMA mouse model, in which SMN levels are dramatically reduced (Zhang et al., 2008), and in SmB/B' knock down studies (Saltzman et al., 2011) the levels of the snRNAs were significantly altered compared to the respective controls. Thus, we quantified the amount of the snRNAs in NPCs after 2 and 4 days of PRMT5 depletion and we did not observed significant changes **(Fig. 4.23D)**. This result confirmed that the reduced amount of assembled snRNPs were not a cause of lower levels of snRNAs, but rather impairment of the snRNP assembly and maturation process. Moreover, this relatively early time point, 4 days, was suitable to investigate direct defects induced by PRMT5 deletion in the splicing pattern ruling out indirect effects caused by altered levels of the snRNAs. Therefore, we selected cells at 4 days post OHT treatment, for further experiments.

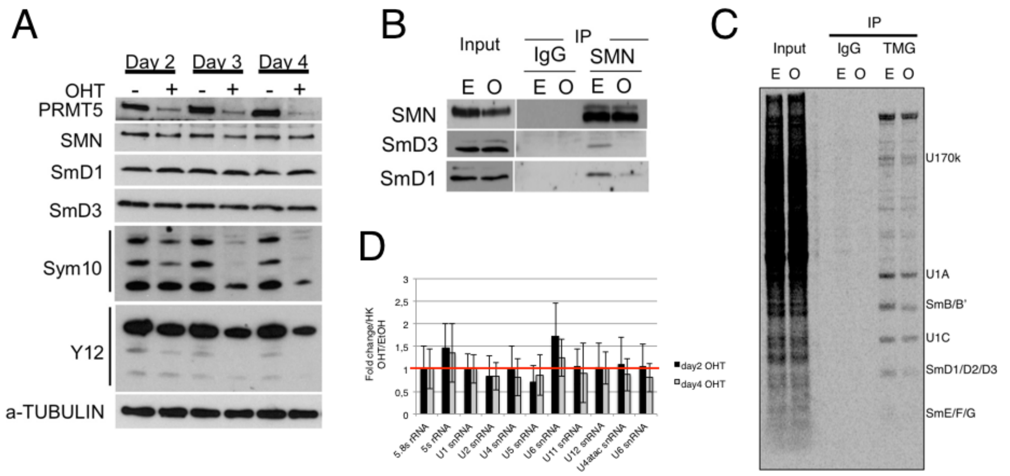

Figure 4.23: PRMT5 depletion in NPCs affects snRNP assembly. (A) PRMT5, SmD1, SmD3 and SMN1 levels were assessed in *Prmt5$^{F/F}$ER* NPC cells depleted of PRMT5 after 2, 3 and 4 days post OHT treatment. Levels of Symmetric Arginine Dimethylation was assessed by staining SmB/B', SmD1 and SmD3 with SYM10 and Y12 antibodies. **(B)** Co-ImmunoPrecipitation between SMN and SmD3 and SmD1, as indicated, in the presence (E: Ethanol) or absence of PRMT5 (O: OHT). **(C)** *Prmt5$^{F/F}$ER* NPCs were treated for 24 h with either Ethanol (E) or OHT (O) and cultured for 4 days before ^{35}S pulse-chase assay. The cells were harvested and the snRNPs from total lysate were immunoprecipitated using anti-TMG antibody–coated beads or control IgG. **(D)** Expression of snRNAs in NPCs *Prmt5$^{F/F}$ER*, 2 (black) and 4 days (grey) post OHT treatment. The amount of the genes is expressed as the average fold change of at least 3 embryos/NPCs, normalized against *Prmt5$^{F/F}$ER* EtOH treated NPCs and 5.8s rRNA. Each bar represents an average of at least 3 experiments.

4.11 PRMT5 loss leads to malfunction of the constitutive splicing machinery and to Alternative Splicing events

In order to mechanistically understand what could link the snRNP assembly defects to apoptosis, we generated libraries for Pair End RNA-sequencing from samples treated with either EtOH or OHT. We identified 2416 genes being differentially expressed between the two conditions **(Appendix C)** (Bezzi et al., 2013). Consistently, the functional annotation of the up- and downregulated genes were similar to the one from *Prmt5$^{F/F}$Nes* cells and showed the activation of the p53 pathway as the top upregulated category **(Fig. 4.24).** Notably, samples submitted for RNA-sequencing, were collected at an earlier time point, compared to the *Prmt5$^{F/F}$Nes* NPCs, in which PRMT5 deletion occurred in utero at approximately E10.5. In latter dataset, we observed upregulation of important developmental pathways, such as the MAPK signaling pathway, and genes involved in NPC differentiation (i.e. axon guidance), which were not detected by RNA-seq, suggesting either a late activation of these pathways, an indirect activation caused by the onset of phenotype or a non cell autonomous effect.

In contrast to what reported in plants and *drosophila*, where PRMT5 regulates splice site selection without greatly affecting constitutive pre-mRNA splicing (Sanchez et al., 2010), we observed that the compiled number of reads in introns was elevated in the absence of PRMT5, with 1682 introns being significantly affected **(Fig. 4.25A).** We then proceeded to characterize in more detail the splicing defects, using Multivariate Analysis of Transcript Splicing (MATS) (Shen et al., 2012) **(Appendix A)** (Bezzi et al., 2013)**.** *Prmt5$^{F/F}$ER* mice are not on pure C57BL/*6* genetic background, hence we sequenced three independent NPC populations, and first checked the variability in splicing among embryos. In the absence of PRMT5 we observed an overlap of 320 genes affected by Alternative Splicing in 2/3 embryos **(Fig. 4.25B)**. PRMT5 depletion triggered a majority of Retained Introns (RI) and Skipped Exons (SE) events in all 3 embryos **(Fig. 4.25C)**, and we could validate 18/20 SE events **(Fig. 4.26)** and 21/21 RI events **(Fig. 4.27)**, confirming that despite the observed embryo to embryo variability, we identified a robust set of conserved alternatively spliced events. Importantly, all the alternative splicing events validated by real time PCR occurred also in *Prmt5$^{F/F}$ER;p53-/-* NPCs post OHT treatment, which do not undergo apoptosis, ruling out the possibility that these splicing defects were indirectly induced by the cell death.

Both the RI **(Fig. 4.28A left panel)** and SE **(Fig. 4.28A right panel)** events detected in the absence of PRMT5 are characterized by a weak 5’-donor site, as quantified by their low CV score (Shapiro score) (Shapiro and Senapathy, 1987), their low MaxEntScan (Yeo and Burge, 2004) **(Fig. 4.28B)** and H-Bond (Freund et al., 2003) **(Fig. 4.28C)** scores, and an overall randomization of the key bases at position -1, -2, +4 and +5.

What distinguishes SE from RI events is the length of the affected intron, which is significantly shorter in the case of RI events **(Fig. 4.28D)**. Hence, absence of PRMT5 leads to selective retention of introns and skipping of exons with weak donor sites.

These Alternatively Spliced genes are not random, but belonged to specific biological pathways. Importantly, network analysis revealed that these genes are involved in post-transcriptional RNA processing, membrane organization and negative regulation of cell cycle processes **(Fig. 4.29A)**. The latter included transduction of the p53 signaling pathway, suggesting that early problems with the core splicing machinery can be sensed by key alternatively spliced mRNAs to instruct cell cycle arrest or apoptosis **(Fig. 4.29B)**.

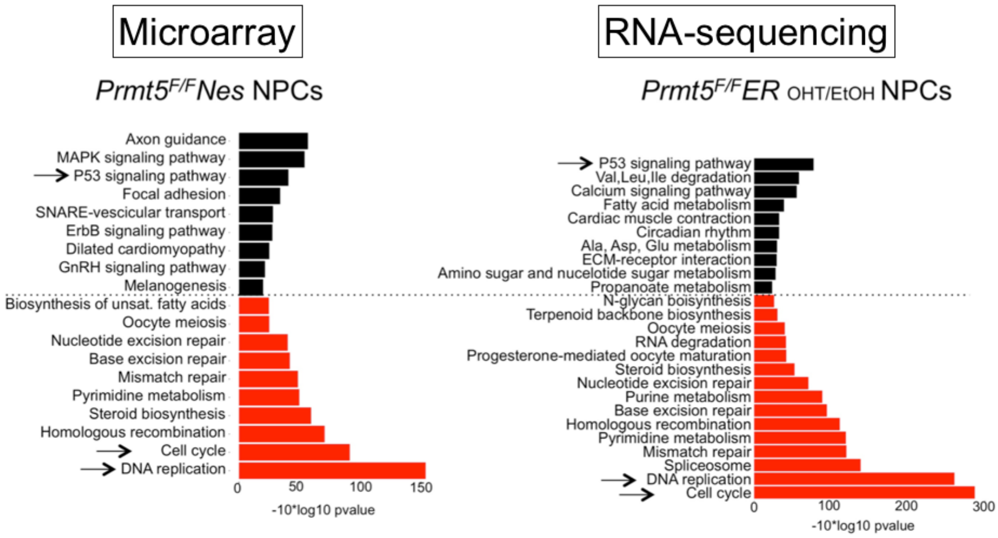

Figure 4.24: RNA-sequencing analysis of differentially expressed genes in *Prmt5$^{F/F}$ER* NPCs. Functional annotation of differentially expressed genes from Fig. 4.15A (left panel) compared to gene expression analysis and functional annotation (RNA-seq data) of *Prmt5$^{F/F}$ER* NPCs 4 days post treatment with either EtOH or OHT to delete *Prmt5*. The bioinformatic analysis was performed in collaboration with J. Müller.

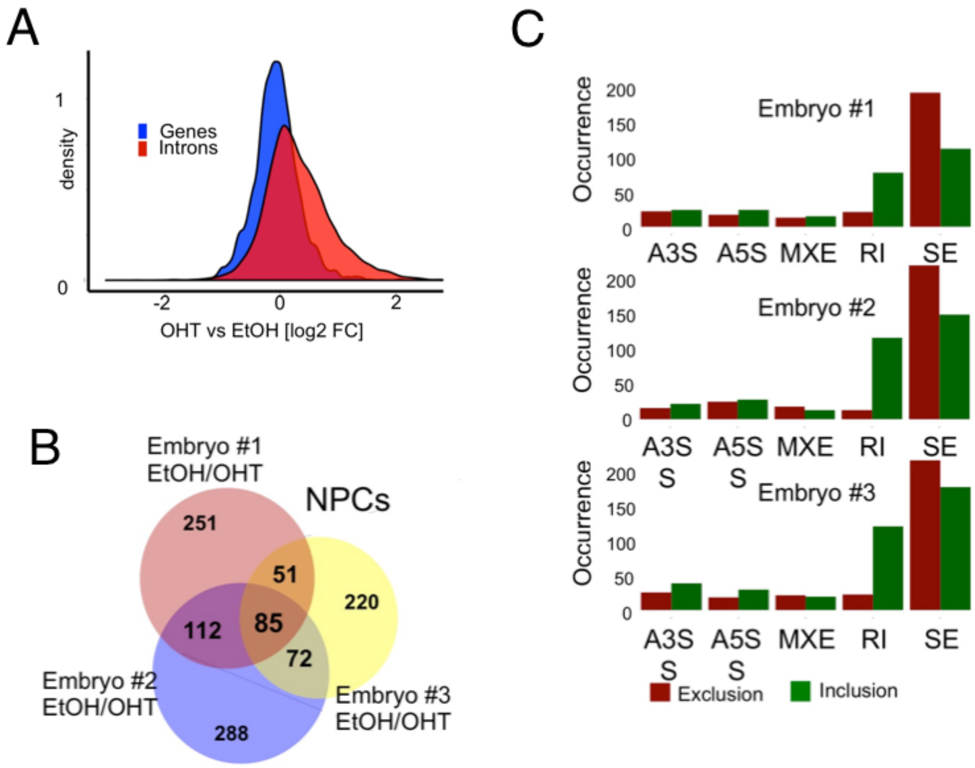

Figure 4.25: PRMT5 loss leads to malfunction of the constitutive splicing machinery and to alternative splicing events. (A) Total number of reads in introns (red) or genes (blue) expressed as fold change of the events in NPCs lacking PRMT5 over control (wild- type PRMT5). A smooth density estimate is drawn as calculated by a Gaussian kernel. **(B)** Number of genes affected by alternative splicing events in each NPC population (derived from independent embryos). **(C)** Quantification of the Alternative Splicing defects observed in wt (EtOH) vs mutant (OHT) NPCs. The specific Alternative Splicing events, as classified by MATS, are indicated by the bar plots, for each embryo. In red are the number of Excluded/Skipped events upon PRMT5 deletion, while green indicates the included events (less abundant in PRMT5 wt conditions). A3S: alternative 3' splice site; A5S: alternative 5' splice site; MXE: mutually exclusive exon; RI: retained intron; SE: skipped exon. The bioinformatic analysis was performed in collaboration with J. Müller.

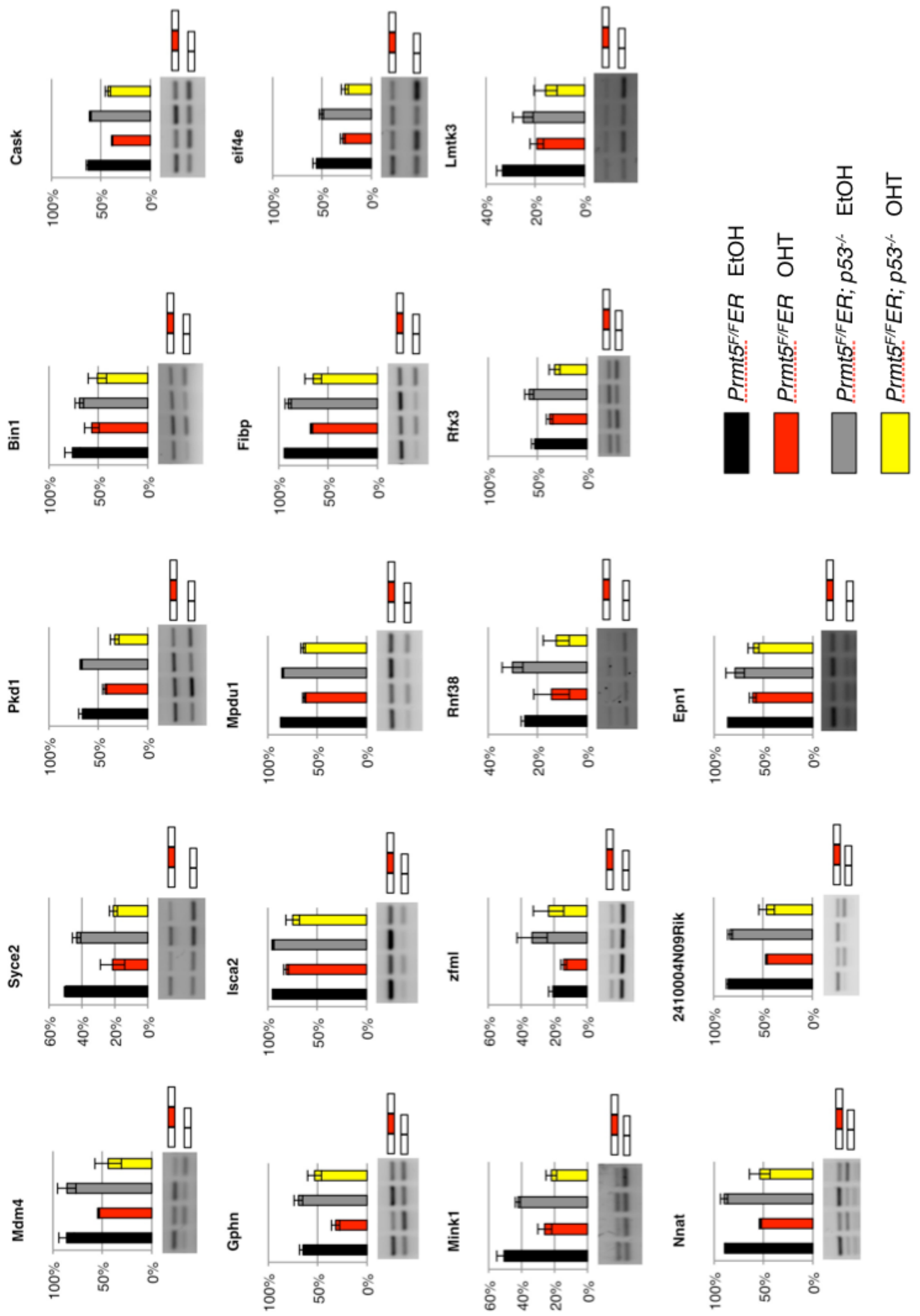

Figure 4.26: PCR validation of the Skipped Exon events. PCR validation and relative quantification of the Skipped Exon (SE) events taking place on the indicated genes (classified by MATS as SE events), upon *Prmt5* deletion (E: Ethanol; O: OHT). Black/Red: p53 wt; Grey/Yellow: p53-/- background. The affected exons/introns number and genomic coordinates are indicated in Appendix A and Table 3.6

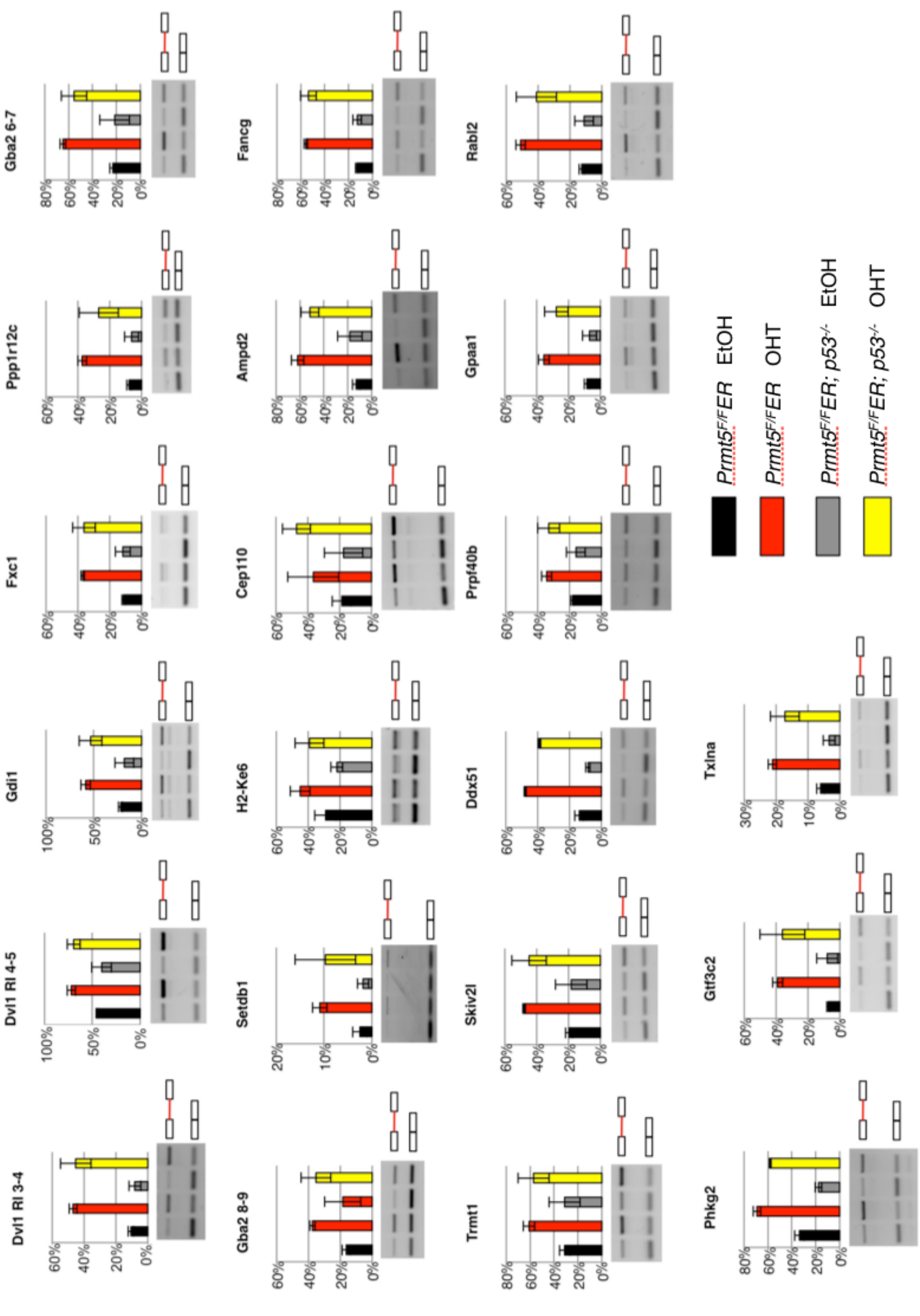

Figure 4.27: PCR validation of the Retained Intron events. PCR validation and relative quantification of the Retained Intron (RI) events taking place on the indicated genes (classified by MATS as RI events), upon *Prmt5* deletion (E: Ethanol; O: OHT). Black/Red: p53 wt; Grey/Yellow: p53-/- background. The affected exons/introns number and genomic coordinates are indicated in Appendix A and Table 3.7.

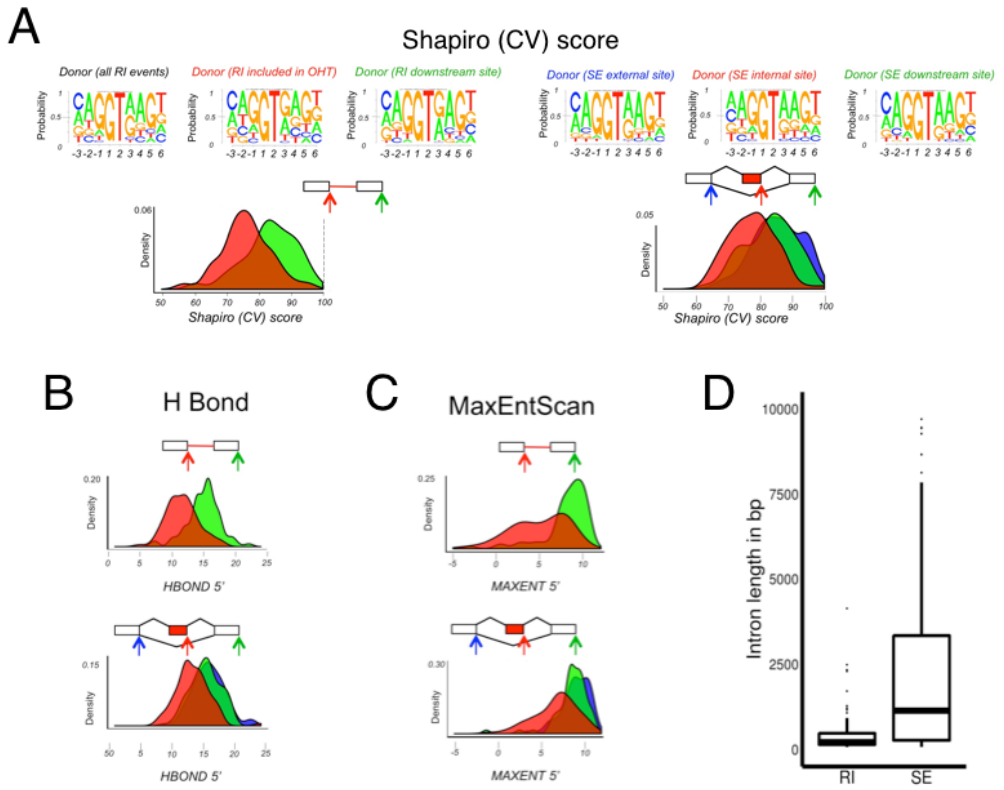

Figure 4.28: PRMT5 depletion impairs the correct splicing of alternative exons with weak 5' donor site. (A) Left panel: Shapiro (CV) score of 59 donor sites of the RI events in NPCs identified by MATS. A smooth density estimate is drawn as calculated by a Gaussian kernel. The top panels depict the sequence logo of the 59 donor of all RI events (left) and the 59 donor of the RI events detected upon PRMT5 deletion (right, indicated by the red arrow). The CV score of the downstream donor site is displayed for direct comparison. Right panel: same as in the left panel. Shapiro (CV) score of 59 donor sites of the SE events (in red). The CV scores of the exclusion site (left, indicated by the blue arrow) and the downstream donor site (right, indicated by the green arrow) are displayed for direct comparison. **(B)** H-Bond score (indicator for the capability to form H-bonds with U1 snRNA) of RI and SE events in the upper and lower panel respectively. At each splice site (with a significant splicing event upon Prmt5 depletion) we scored for the 3Bp within the exon and 8Bp within the intron. The result is drawn as calculated by a Gaussian kernel. In **(C)**, MaxEntScan was used for scoring, comparing the altered splice sites upon Prmt5 depletion to a model based on all human canonical splice sites (3Bp in the exon direction and 6Bp in the intron direction were used for scoring). **(D)** Boxplot of intron lengths of the intron included in OHT RI splicing events and of the two introns excluded in OHT SE splicing events. The bioinformatic analysis was performed in collaboration with J. Müller.

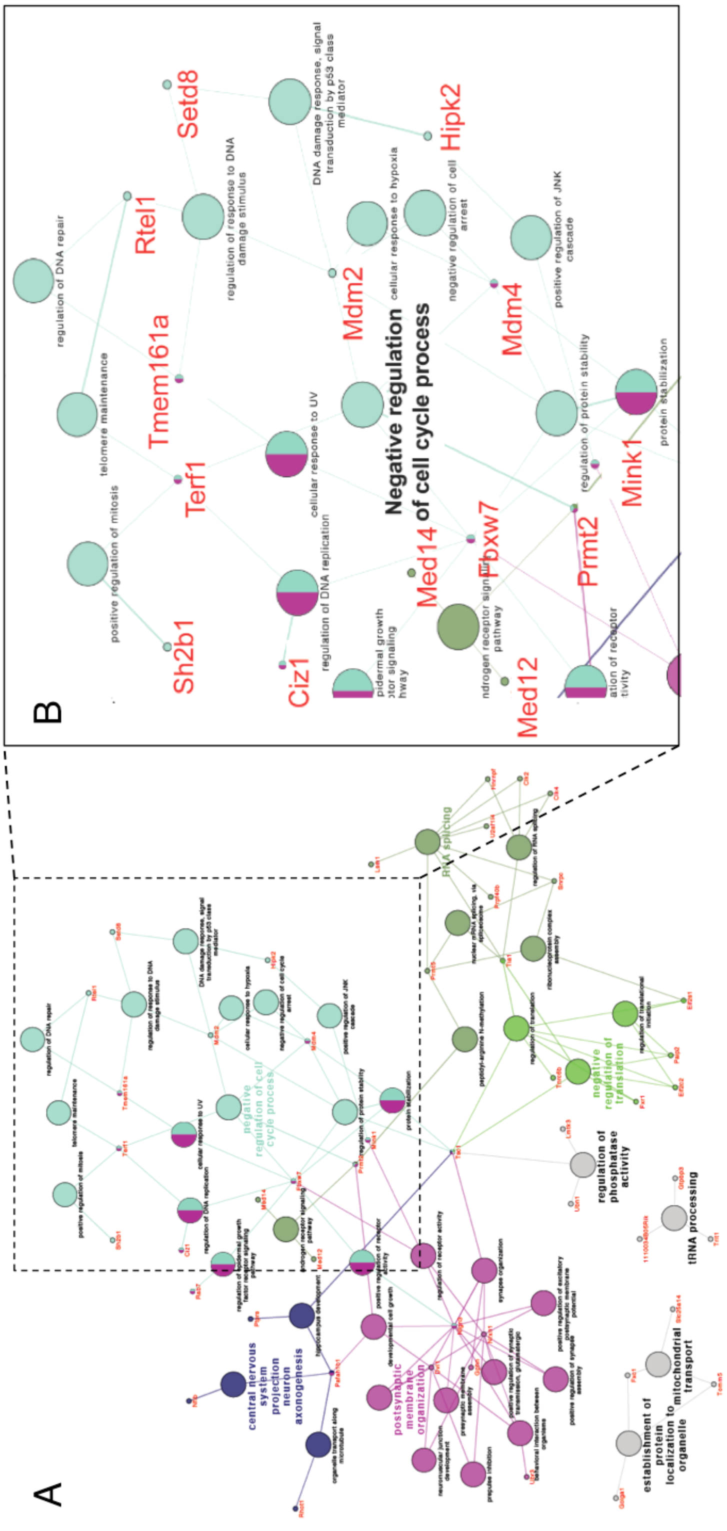

Fig 4.29: PRMT5 deletion induces alternative splicing events in genes involved in negative regulation of the cell cycle. (A) Network representation of the differentially spliced genes upon Prmt5 deletion in NPCs. The Gene Ontology terms are represented as nodes based on their kappa score. The edges represent the relationships between the GO terms and the shared genes (**B**) Enlargement of the network showing the genes involved in negative regulation of the cycle. The bioinformatic analysis was performed in collaboration with J. Müller.

4.12 *Mdm4* AS event is a sensor of PRMT5 depletion and of defects in the constitutive splicing machinery

MDM4 (also known as MDMX) has been reported to be downregulated upon direct depletion of spliceosome components (Allende-Vega et al., 2013) and perturbation of its levels stood out as potentially recapitulating the activation of the p53 response that we observed *in vivo.* Importantly, the phenotype of the *Mdm4*-/- conditional CNS deletion is remarkably similar to what was observed for *Prmt5*$^{F/F}$*Nes*, and the most upregulated gene in the absence of PRMT5 is *Ptprv* (**Appendix C**), which was originally identified as deregulated in *Mdm4*-/- embryos (Doumont et al., 2005).

We thus decided to focus our attention on the Alternative Splicing of *Mdm4* **(Fig. 4.26)** for the rest of the study. MDM4 is a direct regulator of p53-activity, it binds to p53 and inhibits its function by blocking its transactivation capabilities (Francoz et al., 2006; Xiong et al., 2006). *Mdm4* undergoes alternative splicing at exon 7, in *Prmt5*$^{F/F}$*ER* OHT-treated cells, resulting in the production of a shorter MDM4 isoform that has been previously described in the literature as MDM4S (Lenos and Jochemsen, 2011; Rallapalli et al., 2003) **(Fig. 4.30A upper panel)**. Importantly, the *Mdm4 Exon 7* skipping results in a frame-shift which encodes for a Premature Termination Codon (PTC) within *Mdm4 Exon 8. Mdm4 Exon 7* is located within a 1kb genomic region that is highly conserved in vertebrates (as assessed by PhyloP) **(Fig. 4.30A lower panel)**, suggesting a common mechanism to regulate the abundance of the differentially spliced isoform.

To verify that the Alternative Splicing event of *Mdm4/Mdm4s* was also occurring *in vivo* we derived *Prmt5*$^{F/F}$*Nes* NPCs with different *p53* backgrounds. Reassuringly, the exon skipping was induced in *Prmt5*$^{F/F}$*Nes*

NPCs and the degree of alternative splicing was even greater in *p53-/-* cells **(Fig. 4.30B)**. A possible explanation for this observation is that the cells in which *Mdm4* AS takes place are rapidly eliminated due to p53 activation.

The literature on the MDM4S protein isoform is quite controversial (Lenos and Jochemsen, 2011; Rallapalli et al., 2003), with reports suggesting its possible role as a potent p53 inhibitor, and others stating that the MDM4S product is unstable. Notably, all the data is based on forced overexpression experiments and negative results (failure to detect the endogenous protein product). We thus decided to address this issue by looking at the *Mdm4s* mRNA stability. We performed polysome profiling of cells upon PRMT5 deletion and noted that the full length *Mdm4* product was present in the polysome fractions (F4-5)*,* while the *Mdm4s* mRNA was associated with fractions containing significantly fewer polysomes (F3-4) **(Fig. 4.30C)**.

This result suggested two possibilities: either a low level of translation of the *Mdm4s* RNA, or the fact that this RNA would be targeted for Nonsense Mediated Decay (NMD), the typical fate for isoforms with a PTC (Lareau et al., 2007; Lewis et al., 2003). To test the latter possibility we treated cells with Cyclohexamide (CHX), an inhibitor of protein synthesis, known to block NMD-mediated mRNA degradation, and later with Actinomycin D, which blocks RNA Pol II transcription. The data in **(Fig. 4.30D)**, demonstrates that the *Mdm4s* isoform is less stable than the full-length product and it is targeted for NMD.

Our data suggests that upon PRMT5 depletion, the *Mdm4* mRNA undergoes Alternative Splicing, giving rise to the unstable *Mdm4s* product. Indeed this leads to the reduction of the full length MDM4 protein **(Fig. 4.31A)**. To extend our findings beyond perturbation of the splicing machinery through PRMT5, we treated NPCs with well-characterized splicing inhibitors (TG003 and Spliceostatin A) (Kaida et al., 2007; Muraki et al., 2004), and consistently observed *Mdm4*/Mdm4s alternatively splicing. As controls, neither p53-activation by Nutlin, nor the induction of DNA damage by Etoposide generated similar results **(Fig. 4.31B)**. These results are in contrast with previous literature (Allende-Vega et al., 2013) and provide a direct mechanistic link between perturbation of the splicing machinery and downstream activation of p53.

To further confirm our hypothesis we demonstrated that the p53 transcriptional response **(Fig. 4.31C),** and the induction of apoptosis **(Fig. 4.31D),** caused by PRMT5 deletion, could be rescued by re-introducing full length MDM4 into NPCs. Not surprisingly, the rescue was only partial due to other AS events induced by the absence of PRMT5 **(Fig. 4.29B)**.

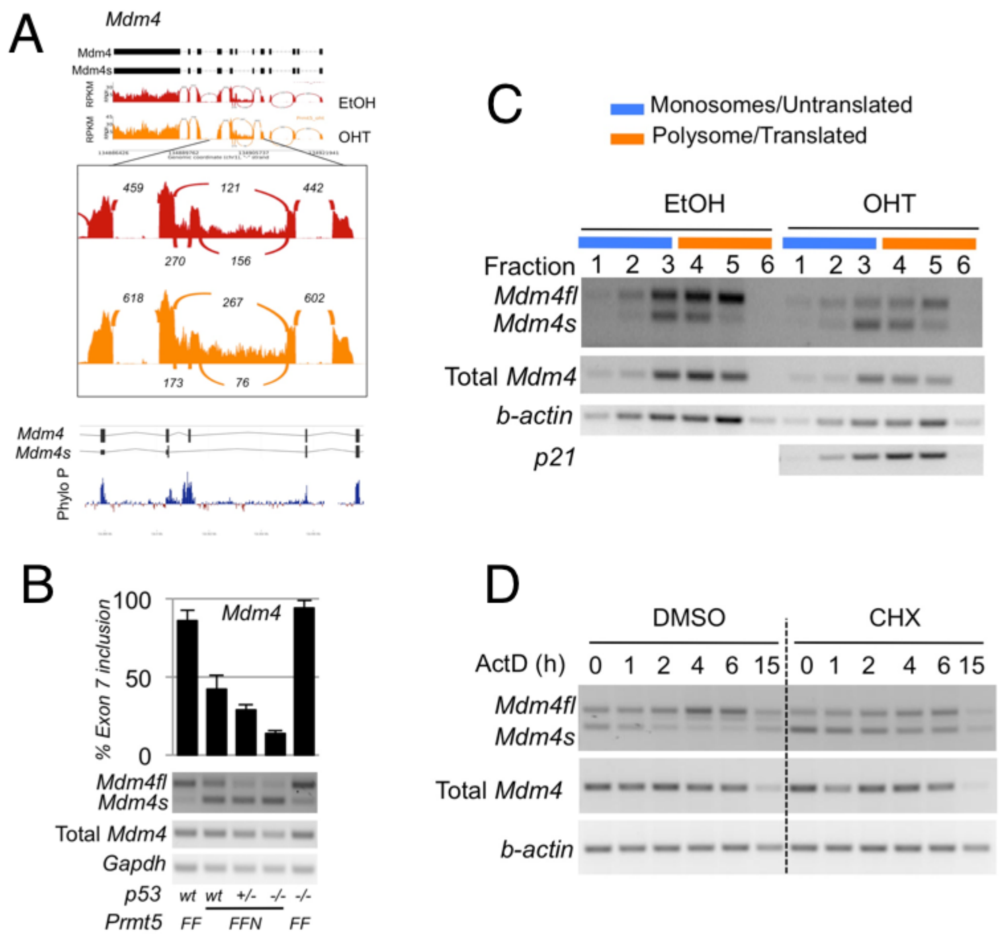

Figure 4.30: *Mdm4* alternative splicing event is a sensor of PRMT5 deletion and *Mdm4s* is targeted by the NMD pathway. (A) Upper panel: Representative example using MATS analysis and Sashimi plots (for visualization) of *Mdm4* gene alternatively spliced in *Prmt5$^{F/F}$ER* derived NPCs with wt (Red) or deleted (Yellow) *Prmt5*. Lower panel: Degree of sequence conservation across species of the indicated genomic region surrounding *Mdm4 Exon7.* **(B)** PCR validation and relative quantification of the alternative splicing event taking place on the Mdm4 mRNA upon PRMT5 deletion in different p53 genetic backgrounds. (**C**) Polysome profiling of cells upon PRMT5 deletion (OHT). RNA is detected by semiquantitative PCR. *p21*, a short gene, was used as a control to exclude the possibility of a length bias between the *Mdm4* and *Mdm4s* distribution. **(D)** Semiquantitative PCR of the indicated transcripts upon CHX (100 mg/mL) treatment to block NMD. Cells were pretreated for 3 h and then for the indicated time with 5 mg/mL Actinomycin D to block transcription. The polysome purification was performed in collaboration with Leah A. Vardy.

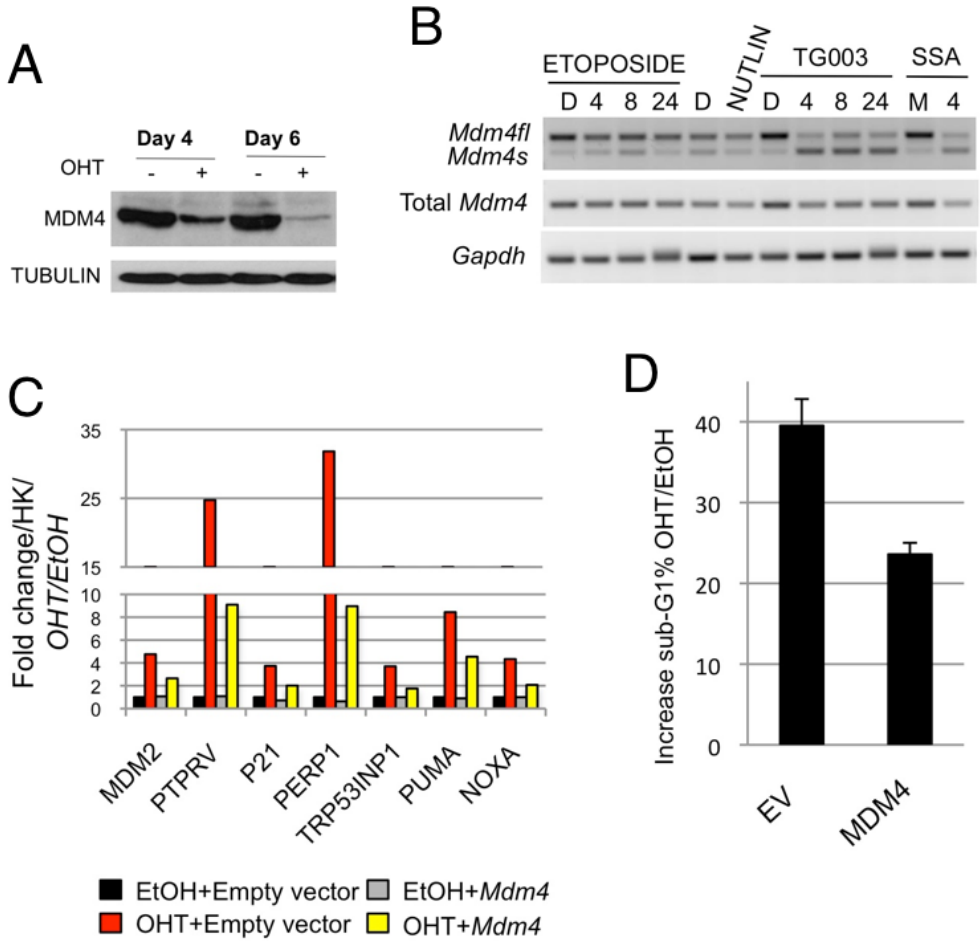

Figure 4.31: *Mdm4* pre-mRNA is a sensor of defects in the splicing machinery. (A) MDM4 full-length protein levels are reduced upon PRMT5 deletion. (O) OHT. Tubulin was used as a loading control. **(B)** PCR detecting both Mdm4 and Mdm4s in wild-type (wt) and mutant NPCs upon inhibition of the splicing machinery, 100 mM TG003, and 30 ng/mL Spliceostatin A (SSA), or p53 stabilization (Nutlin and 5 mM etoposide). (D) DMSO; (M) MetOH. **(C)** Full-length Mdm4, re-expressed in PRMT5-depleted NPCs, is able to partially rescue the activation of the p53 response. PCR quantification of p53 target genes upon PRMT5 deletion in cells re-expressing full-length Mdm4 (gray and blue bars) or negative control, empty vector plasmid (black and red bars). A representative experiment of three is shown as an example. **(D)** NPCs infected with a retroviral vector stably expressing MDM4 or empty vector (EV) control. PRMT5 was deleted (OHT), and cells were stained with propidium iodide and subjected to flow cytometry analysis. Bars indicate the increase in sub-G1/apoptotic cell populations, normalized to EtOH-treated cells.

4.13 PRMT5 depletion triggers Mdm4 AS and p53 activation in multiple tissues

So far we have dissected the role of PRMT5 in the developing CNS, and showed that it plays a key role in ensuring the proper splicing of *Mdm4*, in proliferating NPCs. The phenotype observed in other organs, such as lung and liver **(Fig.4.5)**, upon PRMT5 deletion during organogenesis, was remarkably similar to what we observed in the brain, in terms of apoptosis and cell cycle arrest. Thus, we next asked what would be the effect of deleting PRMT5 on the p53 pathway and on Mdm4 splicing in different organs in the mouse embryo.

Comparing different organs from E15.5 *Prmt5*$^{F/F}$*ER* embryos, following either EtOH or Tamoxifen injection at E10.5, we did observe a switch in the ratio of the full length over the *Mdm4s* isoform in most samples **(Fig. 4.32 bottom panel)**. Importantly, the degree of *Mdm4* Alternative Splicing, upon PRMT5 deletion, correlates with upregulation of p53 targets **(Fig. 4.32 top panel)**.

Consistent with the phenotype described in **Fig.4.5**, the effect was more pronounced in actively proliferative organs such as lung and liver. Notably, in the brain the *Mdm4* isoform switch was not so obvious. These data suggested that the splicing defects were specifically occurring in replicating cells. Therefore, we hypothesized that when analyzed using RNA from total tissue the *Mdm4* isoform switch was clear in organs with abundant pool of proliferating cells, and instead masked by the RNA of non proliferating cells in tissues where the pool of growing cells was smaller (e.g. in brain). Moreover, elimination of the cells in which the *Mdm4* isoform switch occurred, through p53 activation, and the constant degradation of the *Mdm4s* isoform (NMD) might contribute to hinder the detection of the *Mdm4s* isoform by PCR form total tissues.

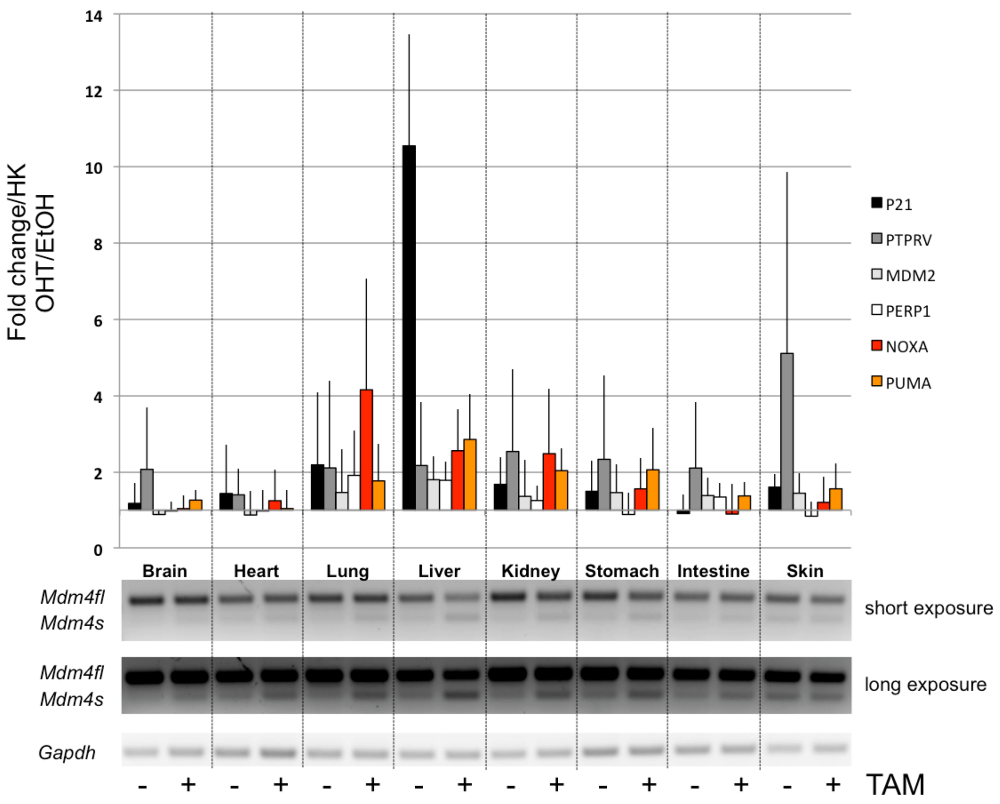

Figure 4.32: PRMT5 depletion triggers *Mdm4* AS and p53 activation in multiple tissues. Quantitative PCR (qPCR) quantification of p53 targets in the indicated organs upon PRMT5 deletion. (Bottom panel) PCR validation of the alternative splicing event taking place on the Mdm4 mRNA upon PRMT5 deletion in the same organs.

4.14 The severity of PRMT5 depletion-induced splicing defects correlates with the cell proliferation rate.

In order to gain further insights regarding the mechanism linking splicing defect to the severity of the phenotype observed in proliferating cells, we used Mouse Embryonic Fibroblasts (MEFs) to determine whether cells with different growth rates would be differentially affected by loss of PRMT5.

First we could confirm in MEFs most of what observed in NPCs **(Fig. 4.33)**. Methylation of the Sm proteins was dramatically reduced 4 days post OHT treatment **(Fig. 4.33A)** and the compiled number of reads in introns increased in the absence of PRMT5 **(Fig. 4.33B**). The most notable difference was that MEFs displayed less splicing defects when compared to NPCs. Despite this difference the overlap of genes with increased intronic reads was remarkable (57%) **(Fig. 4.33C and) (Appendix D) (Appendix E)** (Bezzi et al., 2013). Similar to what observed in NPCs, both the RI **(Fig. 4.33D left panel)** and SE **(Fig. 4.33D right panel)** events detected using Multivariate Analysis of Transcript Splicing (MATS) (Shen et al., 2012) are characterized by a weak 5'-donor site, as quantified by their low CV score (Shapiro score) (Shapiro and Senapathy, 1987) scores, and an overall randomization of the key bases at position -1, -2, +4 and +5.

We next grew MEFs in four different serum (FBS) conditions (0.5%, 5%, 10%, 20%) to regulate their growth rate. We initially decided to focus on one specific event, the alternative splicing of *Mdm4*, in order to elucidate the extent of p53 dependency of the response. Cells that exit the cell cycle (0.5%) did not express high levels of *Mdm4*, but cells that were serum-stimulated (0.5%-20%), increased the *Mdm4fl* isoform **(Fig. 4.34A upper panel**), which corresponded to an increase in MDM4 protein levels **(Fig. 4.34A lower panel**). In the absence of PRMT5, MDM4 upregulation was absent and p53 target genes were activated in a p53-dependent manner in normal growth condition (10% FBS) **(Fig. 4.34B)**.

MEFs underwent G1 arrest and apoptosis and the effect of PRMT5 depletion was more severe in growing cells, whereas it had no effect in resting cells. To study the p53-dependency of this response, we repeated these experiments in *p53*$^{-/-}$ MEFs. PRMT5 depletion in *p53*$^{-/-}$ MEFs caused a less severe change in cell cycle profile **(Fig. 4.34C)**. Consistently, cell growth was also reduced in p53 wt cells, and to a lesser extent in p53$^{-/-}$ cells. In both cases (p53 wt or p53$^{-/-}$ MEFs), the reduction in cell growth was proportional to serum levels **(Fig. 4.34D)**.

Given that in p53 null background, PRMT5 depletion in NPCs induced cell cycle arrest, we assessed the alternative splicing of several genes with weak 5'-Donor in both p53 wt and p53$^{-/-}$ cells, which likely contribute to the p53-independent effects observed in different growing condition. Notably the splicing efficiency of the majority of these genes was improved upon serum stimulation **(Fig. 4.35** green line**)**, while PRMT5 depletion **(Fig. 4.35** red line**)** increased exon skipping and intron inclusion in both p53 wt and p53$^{-/-}$ cells in a serum-dependent manner. Thus, similar to the phenotype, the splicing defects observed upon PRMT5 depletion are more severe in actively growing cells and they are likely the cause, either due to activation of the MDM4-p53 axis or to p53-independent perturbation of several other pathways, rather than the consequence of the observed growth defects.

Finally, we decided to use MEFs to prove that the *Mdm4* splice switch observed at endogenous level was a direct effect of splicing defects. Minigene constructs are crucial tools for the analysis of splicing regulatory factors that control splicing efficiency and alternative splicing. Therefore, we generated a minigene carrying just exon 7 of *Mmd4* and the region surrounding it **(Fig. 4.36A)**. Reassuringly, exon 7 was skipped upon PRMT5 depletion (OHT) in MEFs, confirming the specific alternative splicing event observed at the endogenous level **(Fig. 4.36B)**.

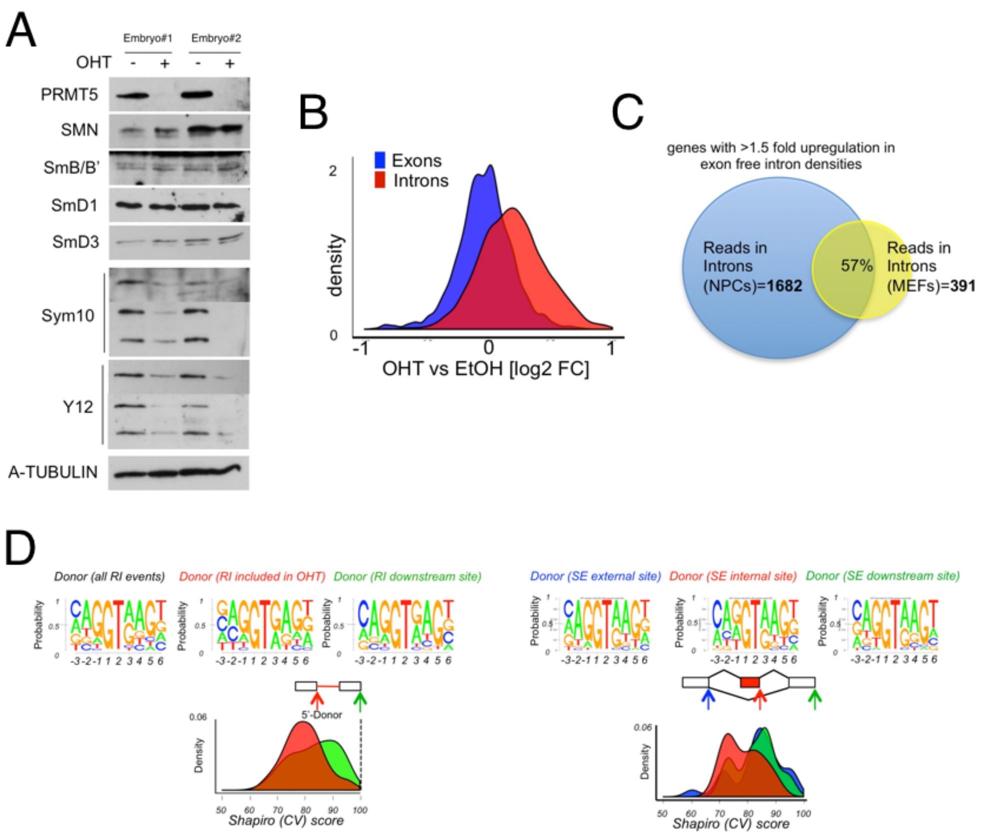

Figure 4.33: PRMT5 depletion induces splicing defects in MEFs. (A) PRMT5, SMN1, SmB/B', SmD1 and SmD3 levels were assessed in MEFs depleted of PRMT5 (OHT). Levels of Symmetric Arginine Dimethylation were assessed by staining SmB, SmD1 and SmD3 with SYM10 and Y12 antibodies. MEFs isolated from two different embryos are shown, **(B)** Total number of reads in genes (blue) or introns (red), expressed as fold change of the events in MEFs lacking PRMT5 over control (wt PRMT5). A smooth density estimate is drawn as calculated by a Gaussian kernel. **(C)** Venn diagram: Overlap between the affected genes in NPCs (total of 1682) vs MEFs (total of 391). (**D)** Shapiro (CV) score of 5' donor sites of the RI (left) and SE (right) events in MEFs, identified by MATS. A smooth density estimate is drawn as calculated by a Gaussian kernel. The top panels depict the sequence logo of the 5'donor sites as indicated by the arrows. The bioinformatic analysis was performed in collaboration with J. Müller.

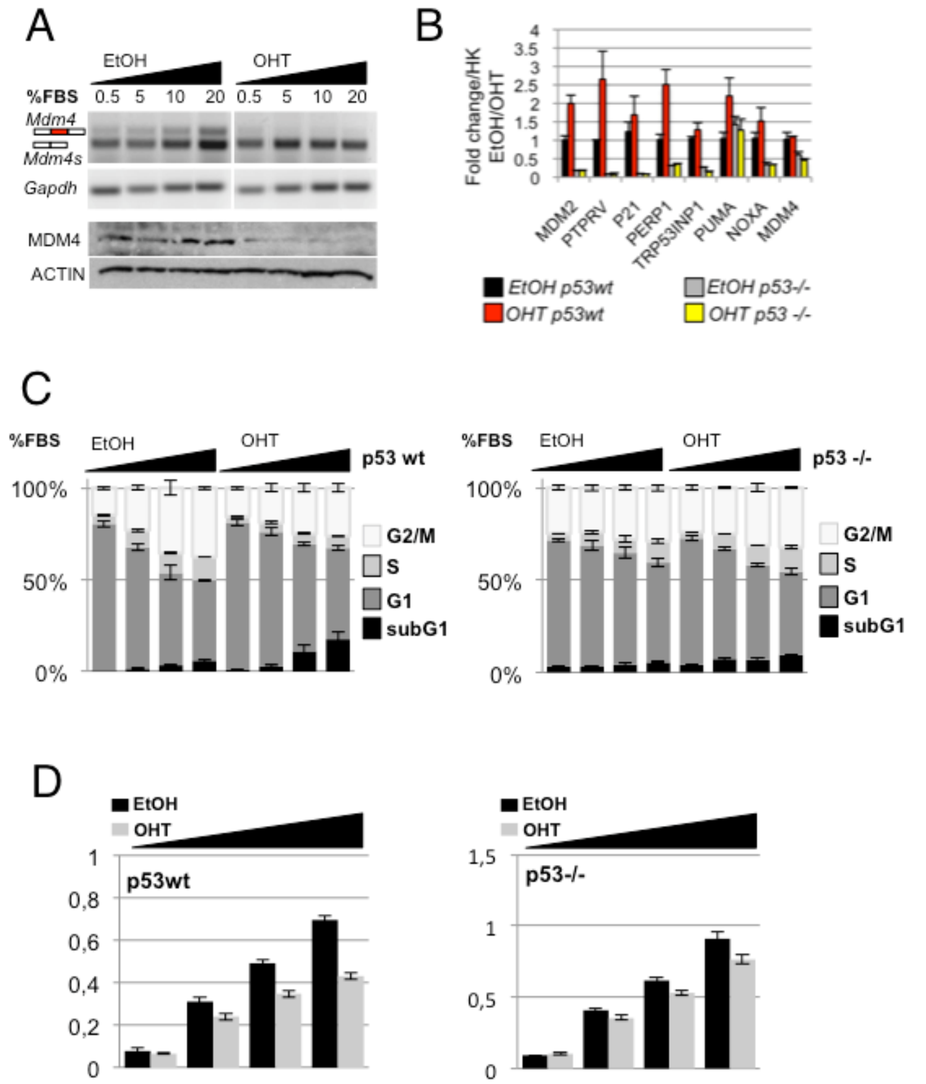

Figure 4.34: PRMT5 depletion results in a more severe phenotype in actively growing MEFs. (**A**) Gel electrophoresis images showing *Mdm4* splice isoforms in *Prmt5$^{F/F}$ER* MEFs cultured under varying serum concentrations following PRMT5 deletion (upper panel) and immunoblots showing a corresponding decrease in MDM4 protein levels (lower panel). (**B**) Expression of p53 upregulated target gens in MEFs growing in 10% FBS medium, from *Prmt5$^{F/F}$ER;p53^{wt}* treated with EtOH/OHT (black/red) or *Prmt5$^{F/F}$ER;p53$^{-/-}$* (grey/yellow). The activation of the genes is expressed as the average fold change of at least 3 embryos/MEFs, normalized against HK and to the EtOH levels. **(C).** Cell cycle analysis of *p53^{wt}* (left panel) and *p53$^{-/-}$* (right panel), *Prmt5$^{F/F}$ER* MEFs under varying serum concentrations following PRMT5 deletion. **(D)** Cell viability of *p53^{wt}*, *Prmt5$^{F/F}$ER* MEFs (left panel) and *p53$^{-/-}$*, *Prmt5$^{F/F}$ER* MEFs (right panel) following OHT treatment.

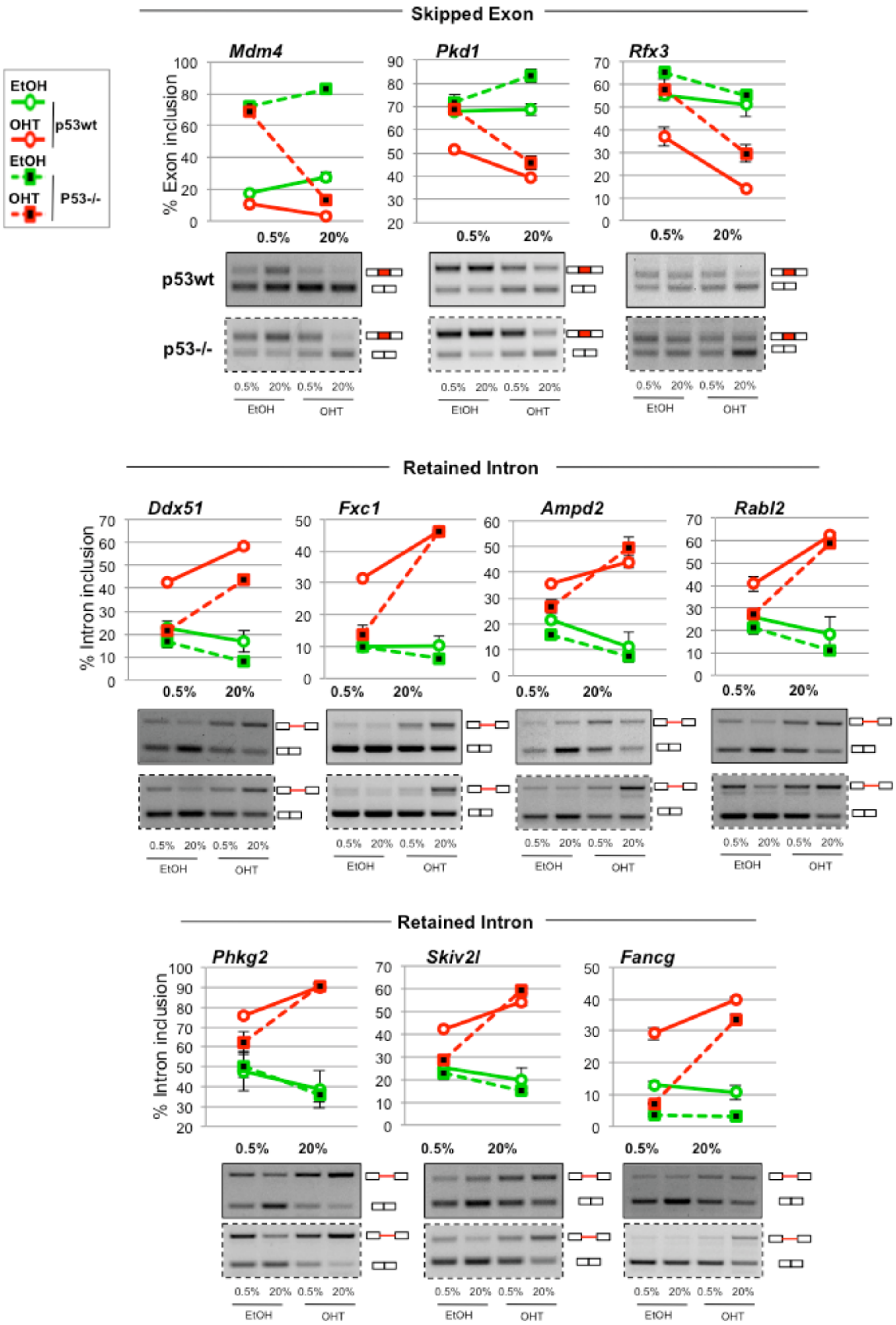

Figure 4.35: PRMT5 depletion results in more severe splicing defects in actively growing MEFs. Gel electrophoresis images (lower panels) and quantification (upper panels) showing aberrant splicing patterns in several genes in *Prmt5$^{F/F}$CreER* MEFs with different p53 background, cultured under varying serum concentrations following PRMT5 depletion.

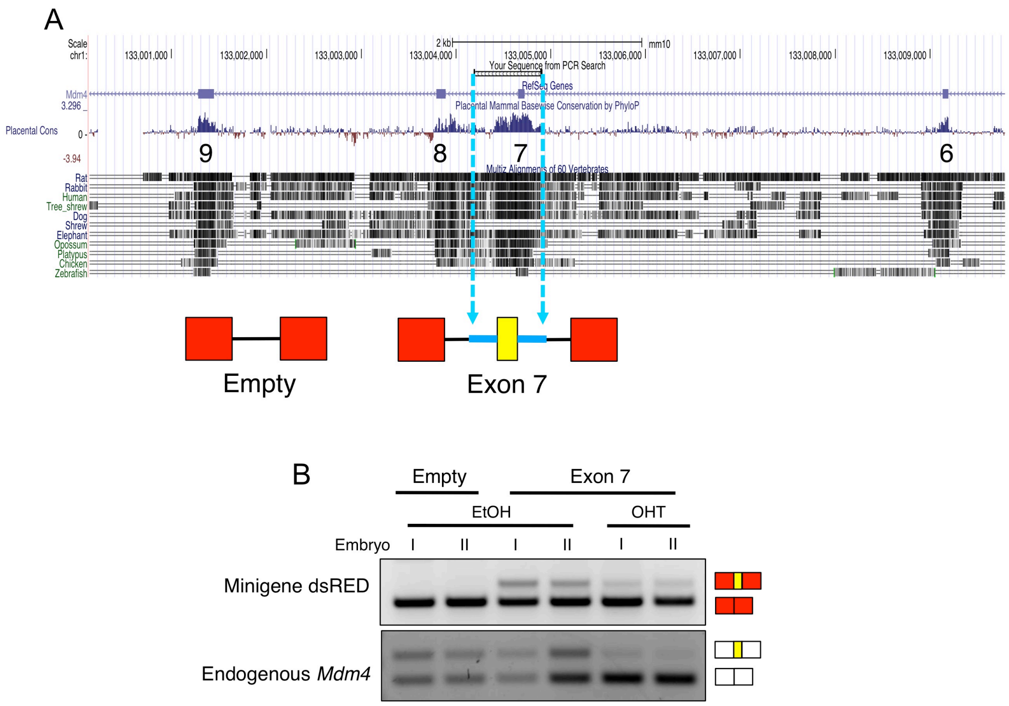

Figure 4.36: A minigene carrying *Mdm4* exon7 recapitulates the splice switch occurring at the level of endogenous *Mdm4* pre-mRNA. (**A**) Diagram of the Mdm4 minigenes. **(B)** MEFs cells (isolated from embryos I and II) transfected with the indicated constructs. Cells were treated with either EtOH or OHT and the total RNAs were analyzed by PCR to examine the transgenic Exon 7 inclusion. Endogenous *Mdm4* splicing is shown in the bottom panel.

4.15 *Mdm4* pre-mRNA senses defects in the spliceosomal machinery in cancer lines.

Activation of the p53 pathway is important in cell homeostasis, as well as in development, but it is certainly best known for its aberrant deregulation in human cancer. PRMT5 has been described as a potential oncogene in human malignancies (Karkhanis et al., 2011). Given the high degree of conservation of the region around the AS exon 7 on mouse *Mdm4*, we tested whether the orthologous human exon 6 conserved a similar sensing mechanism. Upon PRMT5 knock down, and treatment with the splicing inhibitor TG003, we observed a similar AS event occurring on the human

Mdm4 transcript in cancer cell lines derived from different tissues (osteosarcoma, gastric, breast and glioma) **(Fig. 4.37A)**.

Notably, perturbation of the splicing machinery by knockdown of SmB/B', a target of PRMT5 and component of the core snRNP, led to Mdm4 alternative splicing in both U2OS and NPCs **(Fig. 4.37B-D)**. Further investigation of the phenotype induced in NPCs by downregulation of SmB/B' revealed high similarity with the phenotype observed in PRMT5 null NPCs. Several p53 target genes were upregulated **(Fig. 4.36E)** and the number of apoptotic cells increased significantly **(Fig. 4.36F)**.

Overall we believe our data uncover a key mechanism of PRMT5 function that is conserved in mammalian cells during development and relevant to human cancer.

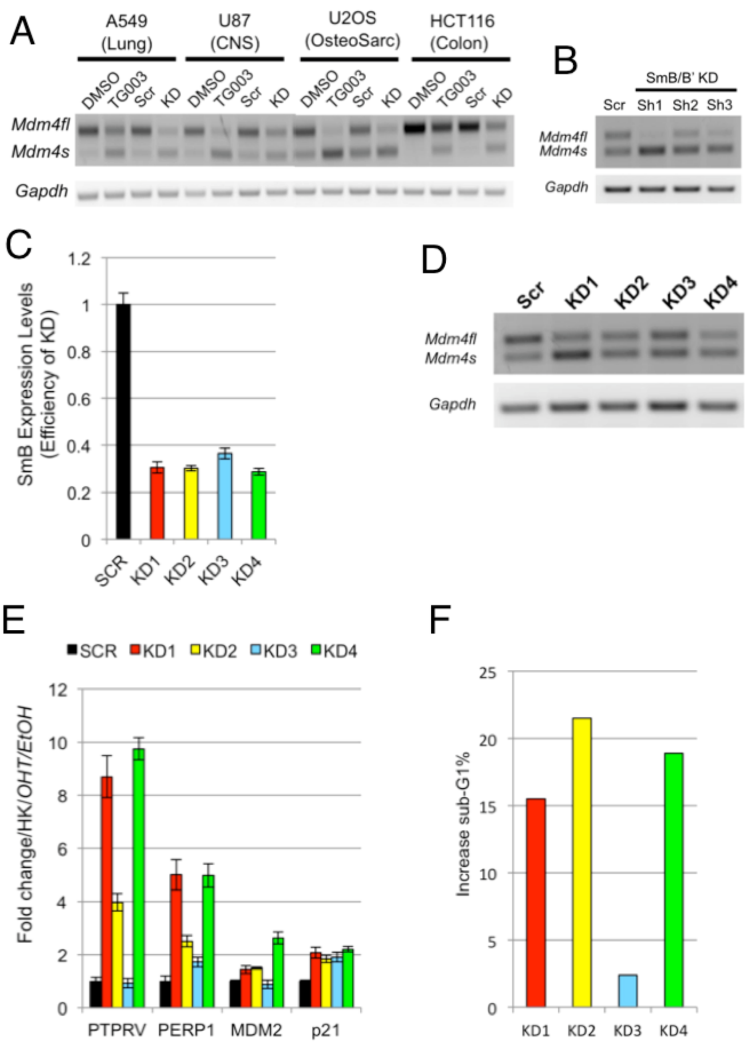

Figure 4.37: PRMT5 depletion triggers Mdm4 AS and p53 activation in multiple tissues. (A) PCR quantification of the alternative splicing event taking place on the *Mdm4* mRNA upon PRMT5 knockdown (KD). Scramble shRNA was used as a control (Scr). Treatment with the splicing inhibitor TG003 (or with DMSO vehicle control) was used as an alternative way of perturbing the splicing machinery. The experiments were performed in the indicated human cancer cells (shown at the top). GAPDH was used as a loading control. **(B)** Quantification of *Mdm4fl/ Mdm4s* splicing levels 4 d after infection and 2-d selection in 1 mg/mL puromycin upon knockdown with three different shRNA lentiviral constructs (Sh1–Sh3) in U2OS cells. (Scr) Scrambled control shRNA.(**C**) SmB/B' expression levels in NPCs as quantified by Real Time PCR 4 days post-infection and 2 days selection in puromycin (0.2mg/mL) upon Knock Down with 4 different sh-RNA lentiviral constructs (KD1-4). Scr = Scrambled control sh-RNA. In the same experiment we have (**D**) Quantified Mdm4fl/Mdm4s splicing, (**E**) the expression levels of p53 targets and (**F**) the increase in SubG1 population in infected cells relative to scramble using PI staining and flow cytometry.

Chapter 5

DISCUSSION

5.1 Role of PRMT5 in development

The role of PRMT5 *in vivo* has been studied in *Planaria*, *C. elegans*, *Drosophila* and plants. However, the lack of PRMT5, results in distinct phenotypes in different systems. In *Planaria*, PRMT5 depletion results in defects in homeostasis, growth and regeneration (Rouhana et al., 2012). In *C. elegans* PRMT5 prevents DNA damage-induced apoptosis, and its inactivation leads to apoptosis in the germline, following ionizing radiation (Yang et al., 2009). In flies, it leads to problems in germ cell specification and circadian rhythm (Gonsalvez et al., 2006; Sanchez et al., 2010), while in plants to defects in flowering and circadian rhythm (Deng et al., 2010; Sanchez et al., 2010). Similarly, in mammalian cell lines, modulation of the expression of PRMT5 in tissue-specific cell proliferation and differentiation experiments, resulted in apparently contradictory phenotypes. PRMT5 has been shown to be required for adipogenesis (LeBlanc et al., 2012), myogenesis (Dacwag et al., 2009) and oligodendrocyte maturation and differentiation (Huang et al., 2011), whereas in keratinocytes (Kanade and Eckert, 2012) and in mouse embryonic stem cells (Tee et al., 2010), PRMT5 is crucial for the maintenance of the undifferentiated state. Conversely, in the hematopoietic system PRMT5 appears to be a negative regulator of hematopoietic stem/progenitor cell proliferation and erythroid differentiation (Liu et al., 2011).

We show for the first time data on a PRMT5 conditional KO-mouse model. We performed acute depletion of PRMT5 during organogenesis, tissue-specific depletion in the CNS, and *ex vivo* depletion in neural stem/progenitor cells, hematopoietic stem/progenitor cells and mouse embryonic fibroblasts. Our studies demonstrate that PRMT5 safeguards the homeostasis of proliferating cells, rather than controlling tissue-specific stem cell multipotency and differentiation, inhibiting both apoptosis and the activation of negative regulators of the cell cycle.

The discrepancy between our results and previous observations can be reconciled by two considerations. Firstly, PRMT5 could be differentially required in different organisms and to some extent the putative type II PRMT, PRMT7, or other unknown PRMTs, might compensate the loss of PRMT5. PRMT7 is an essential gene in *drosophila* (unlike PRMT5) (Gonsalvez et al., 2008), while in HeLa cells it has been shown to be important for the methylation of Sm proteins and to have non-redundant functions in cytoplasmic snRNP biogenesis (Gonsalvez et al., 2007). Our data suggest that, at least in mouse development, PRMT7 is not compensating for the absence of PRMT5, but to which extent, if any, PRMT7 plays a role in mammalian splicing *in vivo* remains to be addressed.

Secondly, we are looking at a full deletion of PRMT5, as opposed to the knock-down studies reported so far. Albeit modest alteration of the relative stoichiometry of splicing regulatory proteins leads to alternative splicing patterns (Black, 2003; Hou et al., 2002; Licatalosi and Darnell, 2006; Martinez-Contreras et al., 2006; Paradis et al., 2007), the KO-mouse models of some of these proteins have shown a more dramatic phenotype. Particularly, full SMN KO has an early embryonic phenotype similar to the PRMT5 full KO (Hsieh-Li et al., 2000; Tee et al., 2010). In contrast hypomorphic mouse models expressing different levels of SMN display spinal muscular atrophy (SMA) with different degrees of severity and neurospheres derived from the these mice did not differ in number when compared to wild type (Shafey et al., 2008). This threshold effect is confirmed in tissue culture where a dramatic reduction of SMN (>85%) is required to observe cell death (Zhang et al., 2008).

5.2 Role of PRMT5 in stem cell biology

A previous publication has reported the constitutive KO of PRMT5 using a gene trap model (Tee et al., 2010). Phenotypically, lack of PRMT5 leads to de-repression of differentiation genes in mouse Embryonic Stem cells (mES) due, at least in part, to the lack of symmetric arginine 3 methylation on histone H2A (H2AR3me2s). However, because of the early embryonic lethality, the authors were not able to perform large-scale molecular experiments, and thus whether PRMT5 plays any role in controlling splicing in mES remained to be explored. It is of note that PRMT5 has been used to improve iPS derivation in combination with klf4 and Oct3/4 (Nagamatsu et al., 2011). Reducing p53 activity is known to be very important to enhance iPS derivation (Hong et al., 2009; Kawamura et al., 2009). We thus believe that our data, which link PRMT5 methyltransferase activity to the regulation of MDM4 abundance, by controlling its alternative splicing, will provide new insights to this expanding field of research. Furthermore, recent studies highlight the decisive function of splicing regulatory protein, such as SON and MBNL, and the importance of alternative splicing programs in pluripotency and reprogramming (Gabut et al., 2011; Han et al., 2013; Lu et al., 2013).

5.3 Role of PRMT5 in histone modifications

PRMT5 has shown a remarkable versatility towards histone substrates *in vitro*, and gene expression regulatory properties have been investigated for four PRMT5-mediated histone modifications: H4R3me2s, H3R8me2s, H2AR3me2s and H3R2me2s (Bedford and Clarke, 2009; Karkhanis et al., 2011). Surprisingly, analysis of the bulk levels of these histone modifications in PRMT5 null brain revealed the reduction of only one of them, H2AR3me2s. This data suggest that PRMT5 is not the only type II symmetric arginine methyltransferase in higher eukaryotes. Further studies are needed in order to clearly define the catalytic nature of PRMT7 and PRMT9 and likely other type II PRMTs are yet to be discovered. An alternative explanation for the stability of these PTMs is that there are no existing arginine demethylases and thus erasure occurs upon histone exchange or protein degradation. The fact that in the absence of PRMT5 the overall levels of H4R3me2s, H3R8me2s and H3R2me2s do not change, does not exclude the fact that these histone modifications play a critical role in transcriptional regulation. Moreover, we cannot rule out the possibility that PRMT5 methylates histones of a subset of specific genes. In this case more work needs to be done to find specific PRMT5 target genes and to identify chromatin binding partners which restrict PRMT5 activity toward these promoters.

We were not able to link H2AR3me2s to either transcriptional regulation or chromatin assembly. Moreover, we did not investigate the H2AR3me2s methylation event in other chromatin related processes such as replication, mitosis, and in chromatin configuration in the nucleus. Therefore, we believe that the role of H2AR3me2s is yet to be discovered and the fact that this histone modification has been shown to be catalyzed in the cytoplasm (Tee et al., 2010) expand the prospect of potential functions.

Our data do not exclude a role for PRMT5 in transcriptional regulation, however its function as a chromatin remodeler might be more restricted, but at the same time more complex than expected.

5.4 Role of PRMT5 in splicing regulation

Despite the discovery of PRMT5 involvement in the methylation of the Sm core is one of the first evidence collected regarding its activity, most of the following studies ignored the potential function of PRMT5 in splicing regulation, and confirmation in mammals of this anticipated role has been lacking so far.

We have shown, by using a conditional KO-mouse-model and a combination of *in vitro* and *in vivo* approaches that PRMT5 is an essential regulator of splicing in mammals. The first key finding is that shortly after the dramatic reduction of the levels of symmetric arginine dimethylated Sm proteins, caused by lack of PRMT5, an increase of intron reads was readily detected by RNA-sequencing, suggesting a primary function in ensuring correct constitutive splicing. In accordance with previous studies, our data place PRMT5 upstream of SMN in the maturation cycle of Sm proteins *in vivo*. Unfortunately, neither the Dreyfuss group, which performed splicing analysis in tissues from a SMA mouse model (Zhang et al., 2008), nor the Blencowe group, which analyzed the transcriptome-wide effects of a SmB/B' knock-down in HeLa cells (Saltzman et al., 2011), focused their attention on retained introns. Therefore we could not cross-compare our results. Reassuringly, increased intronic retention upon PRMT5 depletion was observed in both plants and *Drosophila* (Deng et al., 2010; Sanchez et al., 2010).

The second key finding is that besides safeguarding constitutive splicing, PRMT5 promotes the inclusion of exons, as well as the exclusion of introns, characterized by weak 5‘ donor site. Importantly, this PRMT5 function is not restricted to the CNS, as in the absence of PRMT5 we could validate the skipping of some of these exons and the inclusion of some of these introns in other tissues. Although SMA is often referred to as a motor neuron disease, recent evidence suggest that the splicing defects are present in multiple organs (Zhang et al., 2008) and this can lead to disease-relevant phenotypes in cells other than motor neurons (Hayhurst et al., 2012). However, the aforementioned study by the Dreyfuss group did not uncover any specific feature of the splicing sites of alternative spliced exons (Zhang et al., 2008). A possible explanation is that while we inspected a specific cell population shortly after PRMT5 depletion, they analyzed the splicing patterns using RNA extracted from whole mouse tissues, therefore making the comparison between the two dataset difficult. On the other hand, our data are consistent with the splicing defects observed in exons with weak 5’ donor site, rather than weak 3’ acceptor site, upon SmB/B’ knock-down in HeLa cells and PRMT5 depletion in plants and *Drosophila* (Deng et al., 2010; Saltzman et al., 2011; Sanchez et al., 2010).

Although accumulation of introns in the transcriptome, and skipping of exons with weak 5’ donor site are in accordance with the idea of on an overall reduction of splicing efficiency due to problems in the snRNPs maturation process, an alternative and non exclusive hypothesis which could explain the data we collected comes to mind: PRMT5 might control splicing more broadly than simply through regulating the maturation of snRNPs. In this respect the splicing regulator CA150 (Cheng et al., 2007) has been identified as a PRMT5 target, and this could be the case for other splicing proteins, which are known to be arginine methylated (Boisvert et al., 2003; Bremang et al., 2013; Ong et al., 2004). Another intriguing hypothesis is that PRMT5-mediated methylation of the Sm proteins directly modulates the weak 5' splice site recognition promoting RNA-RNA interactions. In yeast, SmB, SmD1 and SmD3 has been shown to directly bind the pre-mRNA in proximity of the donor site, stabilizing its interaction with the U1snRNA (Zhang et al., 2001).

Finally, considering the fact that we were not able to elucidate the role of H2AR3me2s in transcriptional regulation, we cannot exclude that this histone modification is involved indirectly in splicing regulation by affecting chromatin structure at specific loci.

5.5 Role of PRMT5 in regulating cell cycle progression and cell death

We have here described how cells can sense general defects in the core splicing machinery, such as the one caused by PRMT5 depletion, by regulating the alternative splicing of a key p53 activator such as *Mdm4*. This alternative splicing event reduces the full length MDM4 protein and gives rise to the unstable MDM4S product (Lenos and Jochemsen, 2011), thus activating the p53 transcriptional program. Our findings describe for the first time the link between the methylosome (Friesen et al., 2001b), the core splicing machinery, alternative splicing and activation of a p53 response in mammalian development.

What we have uncovered here is, indeed, a much broader picture, of how cells can activate the alternative splicing of sensor mRNAs (eg. *Mdm4*), at key exons, characterized by weak 5' donor sites. This occurs upon perturbation of the general splicing machinery, whether because of PRMT5 deletion, or chemical inhibition (**Figure 4.31B**), to arrest growth and/or induce apoptosis. Besides *Mdm4* there are other mRNAs that can potentially play a similar role. To mention a few, the SE event observed in the mRNA of 5' cap-binding protein eIF4E, which is a rate limiting component in the translation process, could affect genes involved in apoptosis and cell cycle arrest (Mamane et al., 2004) (**Figure 4.26**), while the RI events observed in Dvl1 might lead to the inactivation of the Wnt/Dvl1/b-catenin signaling pathway which is known to support NPCs growth and self-renewal potential (Faigle and Song, 2013) (**Figure 4.27**). It would be equally interesting to explore whether the modulation of the splicing of some of the identified genes suffering aberrant splicing results in functional consequences to splicing related diseases.

We have described that the complete deletion of PRMT5 in mouse cells leads to a minor induction of γH2AX, but to a strong activation of p53 target genes, such as p21, even when compared to Etoposide. This is in contrast to what has previously been observed using siRNA/shRNA strategies to reduce the levels of PRMT5 in human cancer lines (Jansson et al., 2008; Scoumanne et al., 2009). This discrepancy could be due to differences between mouse and human cells, between primary cells and cancer cells and to the fact that PRMT5 levels have to fall below a certain threshold in order to observe an activation of the p53 pathway. The latter concept has already been observed for other splicing regulators such as SMN (Zhang et al., 2008). Both the concept that perturbation of the core splicing machinery can lead to regulation of alternative splicing (Saltzman et al., 2011) and that apoptosis is regulated by alternative splicing (Moore et al., 2010; Schwerk and Schulze-Osthoff, 2005) have previously been described. The fundamental advance we described here is that the two pathways are directly linked because *Mdm4*, the target of alternative splicing, unlike Bcl2-like factors, caspases, death receptors and proapoptotic ligands, is as a direct upstream regulator of p53.

Splicing disorders have been estimated to occur in 50% of tumors (David and Manley, 2010; Ritchie et al., 2008; Ward and Cooper, 2010). These can contribute to tumor progression by giving rise to alternative isoforms of oncogenes or tumor suppressors. At the same time, while the perturbation of the splicing machinery was known to activate the p53 pathway, the underlying mechanisms by which this occurred were unknown (Allende-Vega et al., 2013). Our data uncover the mechanism of p53 activation by identifying *Mdm4* as a key sensor mRNA. We believe this data to be extremely relevant for the entire p53 field. Mdm4 is indeed upregulated in several p53wt tumors (Gembarska et al., 2012), and our findings provide new therapeutic avenues to alter its protein levels by affecting its splicing pattern.

Chapter 6

CONCLUSIONS

We were able to show, by combining *in vivo* studies in conditional mouse models and high-throughput techniques, that PRMT5 is essential for proliferating cells homeostasis rather than pluripotency, mostly by ensuring correct pre-mRNA processing. Moreover, we discovered a noncanonical, DNA damage-independent, splicing efficiency-dependent mechanism of p53 response activation. This mechanism relies on the alternative splicing of the *Mdm4* pre-mRNA, which shortly after PRMT5 deletion senses the reduction in splicing efficiency **(Fig. 6.1)**. This work expands our understanding of the complex network regulating correct splicing and cell fate decisions in mammalian development, as well as in human cancer lines, providing new possibilities to target the arginine methyltransferase family to treat neurodegenerative diseases (Dredge et al., 2001; Tollervey et al., 2011) and cancer (David and Manley, 2010; Ritchie et al., 2008; Ward and Cooper, 2010). Recent GWAS studies have uncovered a high rate of mutations in splicing regulators (Damm et al., 2012; Papaemmanuil et al., 2011; Yoshida et al., 2012), pinpointing their potential involvement as driver oncogenes. As a consequence there has been growing interest in drugging the spliceosome machinery for anti cancer therapy (Bonnal et al., 2012). Our results shed light on the possible reason why PRMT5 is required by cancer cells, and at the same time they warn that targeting PRMT5 might induce undesirable side effects linked to adult stem cells homeostasis. Therefore, further studies are needed in order to find a therapeutic window of opportunity.

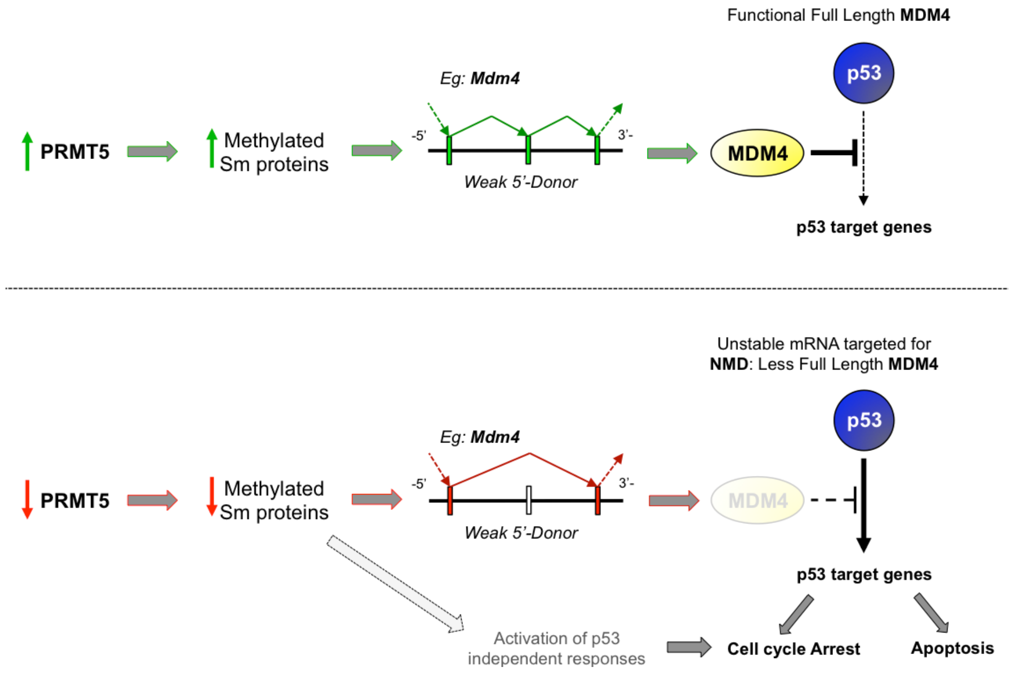

Figure 6.1. Schematic model of the data presented in the study: Upon PRMT5 deletion (or reduction), we observed a loss of symmetric arginine dimethylation at key components of the splicing machinery (SmB/B', SmD1, SmD3, and possibly others). This leads to aberrant snRNP maturation. The consequence is the activation of a sensing mechanism, which is linked to alternative splicing of key mRNAs (mainly RIs and SEs). As an example, we show Mdm4, which induces a potent p53 transcriptional activation. (Bottom) Other alternative splicing events might be equally important and will ultimately result in a p53-independent cell cycle arrest.

BIBLIOGRAPHY

Aggarwal, P., Vaites, L.P., Kim, J.K., Mellert, H., Gurung, B., Nakagawa, H., Herlyn, M., Hua, X., Rustgi, A.K., McMahon, S.B., et al. (2010). Nuclear Cyclin D1/CDK4 Kinase Regulates CUL4 Expression and Triggers Neoplastic Growth via Activation of the PRMT5 Methyltransferase. Cancer Cell *18*, 329–340.

Akhtar, R.S., Geng, Y., Klocke, B.J., Latham, C.B., Villunger, A., Michalak, E.M., Strasser, A., Carroll, S.L., and Roth, K.A. (2006). BH3-only proapoptotic Bcl-2 family members Noxa and Puma mediate neural precursor cell death. J. Neurosci. *26*, 7257–7264.

Allende-Vega, N., Dayal, S., Agarwala, U., Sparks, A., Bourdon, J.-C., and Saville, M.K. (2013). p53 is activated in response to disruption of the pre-mRNA splicing machinery. Oncogene *32*, 1–14.

Ameur, A., Zaghlool, A., Halvardson, J., Wetterbom, A., Gyllensten, U., Cavelier, L., and Feuk, L. (2011). Total RNA sequencing reveals nascent transcription and widespread co-transcriptional splicing in the human brain. Nat. Struct. Mol. Biol. *18*, 1435–1440.

Ancelin, K., Lange, U.C., Hajkova, P., Schneider, R., Bannister, A.J., Kouzarides, T., and Surani, M.A. (2006). Blimp1 associates with Prmt5 and directs histone arginine methylation in mouse germ cells. Nat. Cell Biol. *8*, 623–630.

Andersson, R., Enroth, S., Rada-Iglesias, A., Wadelius, C., and Komorowski, J. (2009). Nucleosomes are well positioned in exons and carry characteristic histone modifications. Genome Research *19*, 1732–1741.

Andreu-Perez, P., Esteve-Puig, R., de Torre-Minguela, C., Lopez-Fauqued, M., Bech-Serra, J.J., Tenbaum, S., Garcia-Trevijano, E.R., Canals, F., Merlino, G., Avila, M.A., et al. (2011). Protein Arginine Methyltransferase 5 Regulates ERK1/2 Signal Transduction Amplitude and Cell Fate Through CRAF. Science Signaling *4*, ra58–ra58.

Anne, J. (2010). Arginine methylation of SmB is required for Drosophila germ cell development. Development *137*, 2819–2828.

Anne, J., Ollo, R., Ephrussi, A., and Mechler, B.M. (2007). Arginine methyltransferase Capsuleen is essential for methylation of spliceosomal Sm proteins and germ cell formation in Drosophila. Development *134*, 137–146.

Antonysamy, S., Bonday, Z., Campbell, R.M., Doyle, B., Druzina, Z., Gheyi, T., Han, B., Jungheim, L.N., Qian, Y., Rauch, C., et al. (2012). Crystal structure of the human PRMT5:MEP50 complex. Proc. Natl. Acad. Sci. U.S.a. *109*, 17960–17965.

Aravin, A.A., Hannon, G.J., and Brennecke, J. (2007a). The Piwi-piRNA pathway provides an adaptive defense in the transposon arms race. Science *318*, 761–764.

Aravin, A.A., Sachidanandam, R., Girard, A., Fejes-Toth, K., and Hannon, G.J. (2007b). Developmentally regulated piRNA clusters implicate MILI in transposon control. Science *316*, 744–747.

Bandyopadhyay, S., Harris, D.P., Adams, G.N., Lause, G.E., McHugh, A., Tillmaand, E.G., Money, A., Willard, B., Fox, P.L., and DiCorleto, P.E. (2012). HOXA9 Methylation by PRMT5 Is Essential for Endothelial Cell Expression of Leukocyte Adhesion Molecules. Mol. Cell. Biol. *32*, 1202–1213.

Barbosa-Morais, N.L., Irimia, M., Pan, Q., Xiong, H.Y., Gueroussov, S., Lee, L.J., Slobodeniuc, V., Kutter, C., Watt, S., Colak, R., et al. (2012). The evolutionary landscape of alternative splicing in vertebrate species. Science *338*, 1587–1593.

Battle, D.J., Lau, C.-K., Wan, L., Deng, H., Lotti, F., and Dreyfuss, G. (2006). The Gemin5 protein of the SMN complex identifies snRNAs. Mol. Cell *23*, 273–279.

Batut, J., Duboé, C., and Vandel, L. (2011). The Methyltransferases PRMT4/CARM1 and PRMT5 Control Differentially Myogenesis in Zebrafish. PLoS ONE *6*, e25427.

Bedford, M.T., and Clarke, S.G. (2009). Protein arginine methylation in mammals: who, what, and why. Mol. Cell *33*, 1–13.

Benjamini, Y., and Yekutieli, D. (2001). The control of the false discovery rate in multiple testing under dependency. Annals of Statistics.

Bezzi, M., Teo, S.X., Muller, J., Mok, W.C., Sahu, S.K., Vardy, L.A., Bonday, Z.Q., and Guccione, E. (2013). Regulation of constitutive and alternative splicing by PRMT5 reveals a role for Mdm4 pre-mRNA in sensing defects in the spliceosomal machinery. Genes Dev. *27*, 1903–1916.

Black, D.L. (2003). Mechanisms of alternative pre-messenger RNA splicing. Annu. Rev. Biochem. *72*, 291–336.

Boffa, L.C., Karn, J., Vidali, G., and Allfrey, V.G. (1977). Distribution of NG, NG,-dimethylarginine in nuclear protein fractions. Biochemical and Biophysical Research Communications *74*, 969–976.

Bogani, D., Morgan, M.A.J., Nelson, A.C., Costello, I., McGouran, J.F., Kessler, B.M., Robertson, E.J., and Bikoff, E.K. (2013). The PR/SET domain zinc finger protein Prdm4 regulates gene expression in embryonic stem cells but plays a nonessential role in the developing mouse embryo. Mol. Cell. Biol. *33*, 3936–3950.

Boisvert, F.M. (2002). Symmetrical dimethylarginine methylation is required for the localization of SMN in Cajal bodies and pre-mRNA splicing. J. Cell Biol. *159*, 957–969.

Boisvert, F.-M., Côté, J., Boulanger, M.-C., and Richard, S. (2003). A proteomic analysis of arginine-methylated protein complexes. Mol. Cell Proteomics *2*, 1319–1330.

Bonnal, S., Vigevani, L., and Valcárcel, J. (2012). The spliceosome as a target of novel antitumour drugs. Nat Rev Drug Discov *11*, 847–859.

Brahms, H., Meheus, L., de Brabandere, V., Fischer, U., and Lührmann, R. (2001). Symmetrical dimethylation of arginine residues in spliceosomal Sm protein B/B' and the Sm-like protein LSm4, and their interaction with the SMN protein. Rna *7*, 1531–1542.

Brahms, H., Raymackers, J., Union, A., de Keyser, F., Meheus, L., and Lührmann, R. (2000). The C-terminal RG dipeptide repeats of the spliceosomal Sm proteins D1 and D3 contain symmetrical dimethylarginines, which form a major B-cell epitope for anti-Sm autoantibodies. J. Biol. Chem. *275*, 17122–17129.

Branscombe, T.L., Frankel, A., Lee, J.H., Cook, J.R., Yang, Z., Pestka, S., and Clarke, S. (2001). PRMT5 (Janus kinase-binding protein 1) catalyzes the formation of symmetric dimethylarginine residues in proteins. J. Biol. Chem. *276*, 32971–32976.

Braunschweig, U., Gueroussov, S., Plocik, A.M., Graveley, B.R., and Blencowe, B.J. (2013). Dynamic integration of splicing within gene regulatory pathways. Cell *152*, 1252–1269.

Breitwieser, W., Markussen, F.H., Horstmann, H., and Ephrussi, A. (1996). Oskar protein interaction with Vasa represents an essential step in polar granule assembly. Genes Dev. *10*, 2179–2188.

Bremang, M., Cuomo, A., Agresta, A.M., Stugiewicz, M., Spadotto, V., and Bonaldi, T. (2013). Mass spectrometry-based identification and characterisation of lysine and arginine methylation in the human proteome. Mol Biosyst *9*, 2231–2247.

Brennecke, J., Aravin, A.A., Stark, A., Dus, M., Kellis, M., Sachidanandam, R., and Hannon, G.J. (2007). Discrete small RNA-generating loci as master regulators of transposon activity in Drosophila. Cell *128*, 1089–1103.

Brennecke, J., Malone, C.D., Aravin, A.A., Sachidanandam, R., Stark, A., and Hannon, G.J. (2008). An epigenetic role for maternally inherited piRNAs in transposon silencing. Science *322*, 1387–1392.

Castello, A., Fischer, B., Hentze, M.W., and Preiss, T. (2013). RNA-binding proteins in Mendelian disease. Trends in Genetics *29*, 318–327.

Chen, M., and Manley, J.L. (2009). Mechanisms of alternative splicing regulation: insights from molecular and genomics approaches. Nat. Rev. Mol. Cell Biol. *10*, 741–754.

Cheng, D., Côté, J., Shaaban, S., and Bedford, M.T. (2007). The arginine methyltransferase CARM1 regulates the coupling of transcription and mRNA processing. Mol. Cell *25*, 71–83.

Chittka, A. (2010). Dynamic Distribution of Histone H4 Arginine 3 Methylation Marks in the Developing Murine Cortex. PLoS ONE *5*, e13807.

Chittka, A., Nitarska, J., Grazini, U., and Richardson, W.D. (2012). Transcription factor positive regulatory domain 4 (PRDM4) recruits protein arginine methyltransferase 5 (PRMT5) to mediate histone arginine methylation and control neural stem cell proliferation and differentiation. Journal of Biological Chemistry *287*, 42995–43006.

Cho, E.-C., Zheng, S., Munro, S., Liu, G., Carr, S.M., Moehlenbrink, J., Lu, Y.-C., Stimson, L., Khan, O., Konietzny, R., et al. (2012). Arginine methylation controls growth regulation by E2F-1. Embo J. 1–13.

Chuma, S., Hosokawa, M., Kitamura, K., Kasai, S., Fujioka, M., Hiyoshi, M., Takamune, K., Noce, T., and Nakatsuji, N. (2006). Tdrd1/Mtr-1, a tudor-related gene, is essential for male germ-cell differentiation and nuage/germinal granule formation in mice. Proc. Natl. Acad. Sci. U.S.a. *103*, 15894–15899.

Clark, T.A., Sugnet, C.W., and Ares, M. (2002). Genomewide analysis of mRNA processing in yeast using splicing-specific microarrays. Science *296*, 907–910.

Côté, J., and Richard, S. (2005). Tudor domains bind symmetrical dimethylated arginines. J. Biol. Chem. *280*, 28476–28483.

Da Cruz, S., and Cleveland, D.W. (2011). Understanding the role of TDP-43 and FUS/TLS in ALS and beyond. Curr. Opin. Neurobiol. *21*, 904–919.

Dacwag, C.S., Bedford, M.T., Sif, S., and Imbalzano, A.N. (2009). Distinct Protein Arginine Methyltransferases Promote ATP-Dependent Chromatin Remodeling Function at Different Stages of Skeletal Muscle Differentiation. Mol. Cell. Biol. *29*, 1909–1921.

Dacwag, C.S., Ohkawa, Y., Pal, S., Sif, S., and Imbalzano, A.N. (2006). The Protein Arginine Methyltransferase Prmt5 Is Required for Myogenesis because It Facilitates ATP-Dependent Chromatin Remodeling. Mol. Cell. Biol. *27*, 384–394.

Damm, F., Kosmider, O., Gelsi-Boyer, V., Renneville, A., Carbuccia, N., Hidalgo-Curtis, C., Valle, Della, V., Couronné, L., Scourzic, L., Chesnais, V., et al. (2012). Mutations affecting mRNA splicing define distinct clinical phenotypes and correlate with patient outcome in myelodysplastic syndromes. Blood *119*, 3211–3218.

Dashti, S.R., Efimova, T., and Eckert, R.L. (2001). MEK7-dependent activation of p38 MAP kinase in keratinocytes. J. Biol. Chem. *276*, 8059–8063.

David, C.J., and Manley, J.L. (2010). Alternative pre-mRNA splicing regulation in cancer: pathways and programs unhinged. Genes Dev. *24*, 2343–2364.

David, C.J., Boyne, A.R., Millhouse, S.R., and Manley, J.L. (2011). The RNA polymerase II C-terminal domain promotes splicing activation through recruitment of a U2AF65-Prp19 complex. Genes Dev. *25*, 972–983.

De Clercq, S., Gembarska, A., Denecker, G., Maetens, M., Naessens, M., Haigh, K., Haigh, J.J., and Marine, J.-C. (2010). Widespread Overexpression of Epitope-Tagged Mdm4 Does Not Accelerate Tumor Formation In Vivo. Mol. Cell. Biol. *30*, 5394–5405.

Dehay, C., and Kennedy, H. (2007). Cell-cycle control and cortical development. Nat. Rev. Neurosci. *8*, 438–450.

Deng, X., Gu, L., Liu, C., Lu, T., Lu, F., Lu, Z., Cui, P., Pei, Y., Wang, B., Hu, S., et al. (2010). Arginine methylation mediated by the Arabidopsis homolog of PRMT5 is essential for proper pre-mRNA splicing. Proc. Natl. Acad. Sci. U.S.a. *107*, 19114–19119.

Dillman, A.A., Hauser, D.N., Gibbs, J.R., Nalls, M.A., McCoy, M.K., Rudenko, I.N., Galter, D., and Cookson, M.R. (2013). mRNA expression, splicing and editing in the embryonic and adult mouse cerebral cortex. Nat. Neurosci. *16*, 499–506.

Doumont, G., Martoriati, A., Beekman, C., Bogaerts, S., Mee, P.J., Bureau, F., Colombo, E., Alcalay, M., Bellefroid, E., Marchesi, F., et al. (2005). G1 checkpoint failure and increased tumor susceptibility in mice lacking the novel p53 target Ptprv. Embo J. *24*, 3093–3103.

Dredge, B.K., Polydorides, A.D., and Darnell, R.B. (2001). The splice of life: alternative splicing and neurological disease. Nat. Rev. Neurosci. *2*, 43–50.

Dunning, M.J., Smith, M.L., Ritchie, M.E., and Tavaré, S. (2007). beadarray: R classes and methods for Illumina bead-based data. Bioinformatics *23*, 2183–2184.

Eckert, R.L., Efimova, T., Balasubramanian, S., Crish, J.F., Bone, F., and Dashti, S. (2003). p38 Mitogen-activated protein kinases on the body surface--a function for p38 delta. J. Invest. Dermatol. *120*, 823–828.

Efimova, T., Broome, A.-M., and Eckert, R.L. (2003). A regulatory role for p38 delta MAPK in keratinocyte differentiation. Evidence for p38 delta-ERK1/2 complex formation. J. Biol. Chem. *278*, 34277–34285.

Efimova, T., Broome, A.-M., and Eckert, R.L. (2004). Protein kinase Cdelta regulates keratinocyte death and survival by regulating activity and subcellular localization of a p38delta-extracellular signal-regulated kinase 1/2 complex. Mol. Cell. Biol. *24*, 8167–8183.

Fabbrizio, E., Messaoudi, El, S., Polanowska, J., Paul, C., Cook, J.R., Lee, J.-H., Negre, V., Rousset, M., Pestka, S., Le Cam, A., et al. (2002). Negative regulation of transcription by the type II arginine methyltransferase PRMT5. EMBO Rep. *3*, 641–645.

Faigle, R., and Song, H. (2013). Signaling mechanisms regulating adult neural stem cells and neurogenesis. Biochim. Biophys. Acta *1830*, 2435–2448.

Findley, S.D., Tamanaha, M., Clegg, N.J., and Ruohola-Baker, H. (2003). Maelstrom, a Drosophila spindle-class gene, encodes a protein that colocalizes with Vasa and RDE1/AGO1 homolog, Aubergine, in nuage.

Development *130*, 859–871.

Fischer, et al. (2008). An Assembly Chaperone Collaborates with the SMN Complex to Generate Spliceosomal SnRNPs. Cell *135*, 497–509.

Francoz, S., Froment, P., Bogaerts, S., De Clercq, S., Maetens, M., Doumont, G., Bellefroid, E., and Marine, J.-C. (2006). Mdm4 and Mdm2 cooperate to inhibit p53 activity in proliferating and quiescent cells in vivo. Proc. Natl. Acad. Sci. U.S.a. *103*, 3232–3237.

Freund, M., Asang, C., Kammler, S., Konermann, C., Krummheuer, J., Hipp, M., Meyer, I., Gierling, W., Theiss, S., Preuss, T., et al. (2003). A novel approach to describe a U1 snRNA binding site. Nucleic Acids Res. *31*, 6963–6975.

Friesen, W.J., and Dreyfuss, G. (2000). Specific sequences of the Sm and Sm-like (Lsm) proteins mediate their interaction with the spinal muscular atrophy disease gene product (SMN). J. Biol. Chem. *275*, 26370–26375.

Friesen, W.J., Massenet, S., Paushkin, S., Wyce, A., and Dreyfuss, G. (2001a). SMN, the product of the spinal muscular atrophy gene, binds preferentially to dimethylarginine-containing protein targets. Mol. Cell *7*, 1111–1117.

Friesen, W.J., Paushkin, S., Wyce, A., Massenet, S., Pesiridis, G.S., Van Duyne, G., Rappsilber, J., Mann, M., and Dreyfuss, G. (2001b). The methylosome, a 20S complex containing JBP1 and pICln, produces dimethylarginine-modified Sm proteins. Mol. Cell. Biol. *21*, 8289–8300.

Friesen, W.J., Wyce, A., Paushkin, S., Abel, L., Rappsilber, J., Mann, M., and Dreyfuss, G. (2002). A novel WD repeat protein component of the methylosome binds Sm proteins. J. Biol. Chem. *277*, 8243–8247.

Gabanella, F., Butchbach, M.E.R., Saieva, L., Carissimi, C., Burghes, A.H.M., and Pellizzoni, L. (2007). Ribonucleoprotein assembly defects correlate with spinal muscular atrophy severity and preferentially affect a subset of spliceosomal snRNPs. PLoS ONE *2*, e921.

Gabut, M., Samavarchi-Tehrani, P., Wang, X., Slobodeniuc, V., O'Hanlon, D., Sung, H.-K., Alvarez, M., Talukder, S., Pan, Q., Mazzoni, E.O., et al. (2011). An Alternative Splicing Switch Regulates Embryonic Stem Cell Pluripotency and Reprogramming. Cell *147*, 132–146.

Gao, F.-B., and Taylor, J.P. (2012). RNA-binding proteins in neurological disease. Brain Research *1462*, 1–2.

Gembarska, A., Luciani, F., Fedele, C., Russell, E.A., Dewaele, M., Villar, S., Zwolinska, A., Haupt, S., de Lange, J., Yip, D., et al. (2012). MDM4 is a key therapeutic target in cutaneous melanoma. Nat. Med.

Girardot, M., Hirasawa, R., Kacem, S., Fritsch, L., Pontis, J., Kota, S.K., Filipponi, D., Fabbrizio, E., Sardet, C., Lohmann, F., et al. (2014). PRMT5-mediated histone H4 arginine-3 symmetrical dimethylation marks chromatin at G + C-rich regions of the mouse genome. Nucleic Acids Res. *42*, 235–248.

Gonsalvez, G.B., Praveen, K., Hicks, A.J., Tian, L., and Matera, A.G. (2008). Sm protein methylation is dispensable for snRNP assembly in Drosophila melanogaster. Rna *14*, 878–887.

Gonsalvez, G.B., Rajendra, T.K., Tian, L., and Matera, A.G. (2006). The Sm-protein methyltransferase, dart5, is essential for germ-cell specification and maintenance. Curr. Biol. *16*, 1077–1089.

Gonsalvez, G.B., Tian, L., Ospina, J.K., Boisvert, F.-M., Lamond, A.I., and Matera, A.G. (2007). Two distinct arginine methyltransferases are required for biogenesis of Sm-class ribonucleoproteins. J. Cell Biol. *178*, 733–740.

Graus-Porta, D., Blaess, S., Senften, M., Littlewood-Evans, A., Damsky, C., Huang, Z., Orban, P., Klein, R., Schittny, J.C., and Müller, U. (2001). Beta1-class integrins regulate the development of laminae and folia in the cerebral and cerebellar cortex. Neuron *31*, 367–379.

Grimm, C., Chari, A., Pelz, J.-P., Kuper, J., Kisker, C., Diederichs, K., Stark, H., Schindelin, H., and Fischer, U. (2013). Structural basis of assembly chaperone- mediated snRNP formation. Mol. Cell *49*, 692–703.

Gubitz, A.K., Feng, W., and Dreyfuss, G. (2004). The SMN complex. Experimental Cell Research *296*, 51–56.

Guderian, G., Peter, C., Wiesner, J., Sickmann, A., Schulze-Osthoff, K., Fischer, U., and Grimmler, M. (2011). RioK1, a new interactor of protein arginine methyltransferase 5 (PRMT5), competes with pICln for binding and modulates PRMT5 complex composition and substrate specificity. Journal of Biological Chemistry *286*, 1976–1986.

Guillemot, F. (2007). Cell fate specification in the mammalian telencephalon. Prog. Neurobiol. *83*, 37–52.

Gurung, B., Feng, Z., and Hua, X. (2013). Menin directly represses Gli1 expression independent of canonical Hedgehog signaling. Molecular Cancer Research *11*, 1215–1222.

Hameyer, D., Loonstra, A., Eshkind, L., Schmitt, S., Antunes, C., Groen, A., Bindels, E., Jonkers, J., Krimpenfort, P., Meuwissen, R., et al. (2007). Toxicity of ligand-dependent Cre recombinases and generation of a conditional Cre deleter mouse allowing mosaic recombination in peripheral tissues. Physiol. Genomics *31*, 32–41.

Han, H., Irimia, M., Ross, P.J., Sung, H.-K., Alipanahi, B., David, L., Golipour, A., Gabut, M., Michael, I.P., Nachman, E.N., et al. (2013). MBNL proteins repress ES-cell-specific alternative splicing and reprogramming. Nature *498*, 241–245.

Hayhurst, M., Wagner, A.K., Cerletti, M., Wagers, A.J., and Rubin, L.L. (2012). A cell-autonomous defect in skeletal muscle satellite cells expressing low levels of survival of motor neuron protein. Developmental Biology *368*, 323–334.

Hebert, M.D., Shpargel, K.B., Ospina, J.K., Tucker, K.E., and Matera, A.G.

(2002). Coilin methylation regulates nuclear body formation. Dev. Cell *3*, 329–337.

Hirose, Y., Tacke, R., and Manley, J.L. (1999). Phosphorylated RNA polymerase II stimulates pre-mRNA splicing. Genes Dev. *13*, 1234–1239.

Ho, M.-C., Wilczek, C., Bonanno, J.B., Xing, L., Seznec, J., Matsui, T., Carter, L.G., Onikubo, T., Kumar, P.R., Chan, M.K., et al. (2013). Structure of the arginine methyltransferase PRMT5-MEP50 reveals a mechanism for substrate specificity. PLoS ONE *8*, e57008.

Hong, H., Takahashi, K., Ichisaka, T., Aoi, T., Kanagawa, O., Nakagawa, M., Okita, K., and Yamanaka, S. (2009). Suppression of induced pluripotent stem cell generation by the p53-p21 pathway. Nature *460*, 1132–1135.

Hornberg, J.J., Binder, B., Bruggeman, F.J., Schoeberl, B., Heinrich, R., and Westerhoff, H.V. (2005). Control of MAPK signalling: from complexity to what really matters. Oncogene *24*, 5533–5542.

Hou, V.C., Lersch, R., Gee, S.L., Ponthier, J.L., Lo, A.J., Wu, M., Turck, C.W., Koury, M., Krainer, A.R., Mayeda, A., et al. (2002). Decrease in hnRNP A/B expression during erythropoiesis mediates a pre-mRNA splicing switch. Embo J. *21*, 6195–6204.

Hsieh-Li, H.M., Chang, J.G., Jong, Y.J., Wu, M.H., Wang, N.M., Tsai, C.H., and Li, H. (2000). A mouse model for spinal muscular atrophy. Nat. Genet. *24*, 66–70.

Hsin, J.-P., and Manley, J.L. (2012). The RNA polymerase II CTD coordinates transcription and RNA processing. Genes Dev. *26*, 2119–2137.

Huang, D.W., Sherman, B.T., and Lempicki, R.A. (2009). Systematic and integrative analysis of large gene lists using DAVID bioinformatics resources. Nat Protoc *4*, 44–57.

Huang, J., Vogel, G., Yu, Z., Almazan, G., and Richard, S. (2011). Type II Arginine Methyltransferase PRMT5 Regulates Gene Expression of Inhibitors of Differentiation/DNA Binding Id2 and Id4 during Glial Cell Differentiation. Journal of Biological Chemistry *286*, 44424–44432.

Huff, J.T., Plocik, A.M., Guthrie, C., and Yamamoto, K.R. (2010). Reciprocal intronic and exonic histone modification regions in humans. Nat. Struct. Mol. Biol. *17*, 1495–1499.

Hughes, R.M., and Waters, M.L. (2006). Arginine methylation in a beta-hairpin peptide: implications for Arg-pi interactions, DeltaCp(o), and the cold denatured state. J. Am. Chem. Soc. *128*, 12735–12742.

Hyllus, D., Stein, C., Schnabel, K., Schiltz, E., Imhof, A., Dou, Y., Hsieh, J., and Bauer, U.-M. (2007). PRMT6-mediated methylation of R2 in histone H3 antagonizes H3 K4 trimethylation. Genes Dev. *21*, 3369–3380.

Irimia, M., and Blencowe, B.J. (2012). Alternative splicing: decoding an expansive regulatory layer. Current Opinion in Cell Biology *24*, 323–332.

Jacobs, S.A., and Khorasanizadeh, S. (2002). Structure of HP1 chromodomain bound to a lysine 9-methylated histone H3 tail. Science *295*, 2080–2083.

Jakovcevski, M., and Akbarian, S. (2012). Epigenetic mechanisms in neurological disease. Nat. Med. *18*, 1194–1204.

Jansson, M., Durant, S.T., Cho, E.-C., Sheahan, S., Edelmann, M., Kessler, B., and La Thangue, N.B. (2008). Arginine methylation regulates the p53 response. Nat. Cell Biol. *10*, 1431–1439.

Jiang, W., Roemer, M.E., and Newsham, I.F. (2005). The tumor suppressor DAL-1/4.1B modulates protein arginine N-methyltransferase 5 activity in a substrate-specific manner. Biochemical and Biophysical Research Communications *329*, 522–530.

Jin, Y., Yang, Y., and Zhang, P. (2011). New insights into RNA secondary structure in the alternative splicing of pre-mRNAs. RNA Biol *8*, 450–457.

Kaida, D., Motoyoshi, H., Tashiro, E., Nojima, T., Hagiwara, M., Ishigami, K., Watanabe, H., Kitahara, T., Yoshida, T., Nakajima, H., et al. (2007). Spliceostatin A targets SF3b and inhibits both splicing and nuclear retention of pre-mRNA. Nature Chemical Biology *3*, 576–583.

Kanade, S.R., and Eckert, R.L. (2012). Protein Arginine Methyltransferase 5 (PRMT5) Signaling Suppresses Protein Kinase C - and p38 -dependent Signaling and Keratinocyte Differentiation. Journal of Biological Chemistry *287*, 7313–7323.

Kanehisa, M., Goto, S., Sato, Y., Furumichi, M., and Tanabe, M. (2012). KEGG for integration and interpretation of large-scale molecular data sets. Nucleic Acids Res. *40*, D109–D114.

Karkhanis, V., Hu, Y.-J., Baiocchi, R.A., Imbalzano, A.N., and Sif, S. (2011). Versatility of PRMT5-induced methylation in growth control and development. Trends Biochem. Sci. *36*, 633–641.

Katz, J.E., Dlakić, M., and Clarke, S. (2003). Automated identification of putative methyltransferases from genomic open reading frames. Mol. Cell Proteomics *2*, 525–540.

Kawamura, T., Suzuki, J., Wang, Y.V., Ménendez, S., Morera, L.B., Raya, A., Wahl, G.M., and Izpisúa Belmonte, J.C. (2009). Linking the p53 tumour suppressor pathway to somatic cell reprogramming. Nature *460*, 1140–1144.

Keren, H., Lev-Maor, G., and Ast, G. (2010). Alternative splicing and evolution: diversification, exon definition and function. Nat. Rev. Genet. *11*, 345–355.

Khodor, Y.L., Menet, J.S., Tolan, M., and Rosbash, M. (2012). Cotranscriptional splicing efficiency differs dramatically between Drosophila and mouse. Rna *18*, 2174–2186.

Khodor, Y.L., Rodriguez, J., Abruzzi, K.C., Tang, C.-H.A., Marr, M.T., and

Rosbash, M. (2011). Nascent-seq indicates widespread cotranscriptional pre-mRNA splicing in Drosophila. Genes Dev. *25*, 2502–2512.

Kornberg, R.D., and Lorch, Y. (1999). Twenty-five years of the nucleosome, fundamental particle of the eukaryote chromosome. Cell *98*, 285–294.

Kuida, K., Zheng, T.S., Na, S., Kuan, C., Yang, D., Karasuyama, H., Rakic, P., and Flavell, R.A. (1996). Decreased apoptosis in the brain and premature lethality in CPP32-deficient mice. Nature *384*, 368–372.

Kuramochi-Miyagawa, S., Watanabe, T., Gotoh, K., Totoki, Y., Toyoda, A., Ikawa, M., Asada, N., Kojima, K., Yamaguchi, Y., Ijiri, T.W., et al. (2008). DNA methylation of retrotransposon genes is regulated by Piwi family members MILI and MIWI2 in murine fetal testes. Genes Dev. *22*, 908–917.

Lacroix, M., Messaoudi, El, S., Rodier, G., Le Cam, A., Sardet, C., and Fabbrizio, E. (2008). The histone-binding protein COPR5 is required for nuclear functions of the protein arginine methyltransferase PRMT5. EMBO Rep. *9*, 452–458.

Lane, D.P. (1992). Cancer. p53, guardian of the genome. Nature *358*, 15–16.

Lareau, L.F., Brooks, A.N., Soergel, D.A.W., Meng, Q., and Brenner, S.E. (2007). The coupling of alternative splicing and nonsense-mediated mRNA decay. Adv. Exp. Med. Biol. *623*, 190–211.

Lasda, E.L., and Blumenthal, T. (2011). Trans-splicing. Wiley Interdiscip Rev RNA *2*, 417–434.

LeBlanc, S.E., Konda, S., Wu, Q., Hu, Y.J., Oslowski, C.M., Sif, S., and Imbalzano, A.N. (2012). Protein Arginine Methyltransferase 5 (Prmt5) Promotes Gene Expression of Peroxisome Proliferator-Activated Receptor 2 (PPAR 2) and Its Target Genes during Adipogenesis. Molecular Endocrinology *26*, 583–597.

Lee, J., Sayegh, J., Daniel, J., Clarke, S., and Bedford, M.T. (2005). PRMT8, a new membrane-bound tissue-specific member of the protein arginine methyltransferase family. J. Biol. Chem. *280*, 32890–32896.

Lenos, K., and Jochemsen, A.G. (2011). Functions of MDMX in the Modulation of the p53-Response. Journal of Biomedicine and Biotechnology *2011*, 1–14.

Levrero, M., De Laurenzi, V., Costanzo, A., Gong, J., Wang, J.Y., and Melino, G. (2000). The p53/p63/p73 family of transcription factors: overlapping and distinct functions. Journal of Cell Science *113 (Pt 10)*, 1661–1670.

Lewis, B.P., Green, R.E., and Brenner, S.E. (2003). Evidence for the widespread coupling of alternative splicing and nonsense-mediated mRNA decay in humans. Proc. Natl. Acad. Sci. U.S.a. *100*, 189–192.

Lewis, T.S., Shapiro, P.S., and Ahn, N.G. (1998). Signal transduction through MAP kinase cascades. Adv. Cancer Res. *74*, 49–139.

Licatalosi, D.D., and Darnell, R.B. (2006). Splicing regulation in neurologic disease. Neuron *52*, 93–101.

Licatalosi, D.D., and Darnell, R.B. (2010). RNA processing and its regulation: global insights into biological networks. Nat. Rev. Genet. *11*, 75–87.

Lim, S., and Kaldis, P. (2012). Loss of Cdk2 and Cdk4 Induces a Switch from Proliferation to Differentiation in Neural Stem Cells. Stem Cells *30*, 1509–1520.

Liu, F., Zhao, X., Perna, F., Wang, L., Koppikar, P., Abdel-Wahab, O., Harr, M.W., Levine, R.L., Xu, H., Tefferi, A., et al. (2011). JAK2V617F-Mediated Phosphorylation of PRMT5 Downregulates Its Methyltransferase Activity and Promotes Myeloproliferation. Cancer Cell *19*, 283–294.

Long, J.C., and Caceres, J.F. (2009). The SR protein family of splicing factors: master regulators of gene expression. Biochem. J. *417*, 15–27.

Lu, X., Göke, J., Sachs, F., Jacques, P.-É., Liang, H., Feng, B., Bourque, G., Bubulya, P.A., and Ng, H.-H. (2013). SON connects the splicing-regulatory network with pluripotency in human embryonic stem cells. Nat. Cell Biol. *15*, 1141–1152.

Luco, R.F., Allo, M., Schor, I.E., Kornblihtt, A.R., and Misteli, T. (2011). Epigenetics in alternative pre-mRNA splicing. Cell *144*, 16–26.

Luger, K., Mäder, A.W., Richmond, R.K., Sargent, D.F., and Richmond, T.J. (1997). Crystal structure of the nucleosome core particle at 2.8 A resolution. Nature *389*, 251–260.

Luscombe, N.M., Laskowski, R.A., and Thornton, J.M. (2001). Amino acid-base interactions: a three-dimensional analysis of protein-DNA interactions at an atomic level. Nucleic Acids Res. *29*, 2860–2874.

Makeyev, E.V., Zhang, J., Carrasco, M.A., and Maniatis, T. (2007). The MicroRNA miR-124 promotes neuronal differentiation by triggering brain-specific alternative pre-mRNA splicing. Mol. Cell *27*, 435–448.

Mamane, Y., Petroulakis, E., Rong, L., Yoshida, K., Ler, L.W., and Sonenberg, N. (2004). eIF4E--from translation to transformation. Oncogene *23*, 3172–3179.

Martinez-Contreras, R., Cloutier, P., Shkreta, L., Fisette, J.-F., Revil, T., and Chabot, B. (2007). hnRNP proteins and splicing control. Adv. Exp. Med. Biol. *623*, 123–147.

Martinez-Contreras, R., Fisette, J.-F., Nasim, F.-U.H., Madden, R., Cordeau, M., and Chabot, B. (2006). Intronic binding sites for hnRNP A/B and hnRNP F/H proteins stimulate pre-mRNA splicing. Plos Biol *4*, e21.

Matera, A.G., Terns, R.M., and Terns, M.P. (2007). Non-coding RNAs: lessons from the small nuclear and small nucleolar RNAs. Nat. Rev. Mol. Cell Biol. *8*, 209–220.

Meister, G., Eggert, C., Bühler, D., Brahms, H., Kambach, C., and Fischer, U. (2001). Methylation of Sm proteins by a complex containing PRMT5 and the putative U snRNP assembly factor pICln. Curr. Biol. *11*, 1990–1994.

Meister, G., and Fischer, U. (2002). Assisted RNP assembly: SMN and PRMT5 complexes cooperate in the formation of spliceosomal UsnRNPs. Embo J. *21*, 5853–5863.

Memczak, S., Jens, M., Elefsinioti, A., Torti, F., Krueger, J., Rybak, A., Maier, L., Mackowiak, S.D., Gregersen, L.H., Munschauer, M., et al. (2013). Circular RNAs are a large class of animal RNAs with regulatory potency. Nature *495*, 333–338.

Migliori, V., Müller, J., Phalke, S., Low, D., Bezzi, M., Mok, W.C., Sahu, S.K., Gunaratne, J., Capasso, P., Bassi, C., et al. (2012). Symmetric dimethylation of H3R2 is a newly identified histone mark that supports euchromatin maintenance. Nat. Struct. Mol. Biol. *19*, 136–144.

Migliorini, D., Lazzerini Denchi, E., Danovi, D., Jochemsen, A., Capillo, M., Gobbi, A., Helin, K., Pelicci, P.G., and Marine, J.-C. (2002). Mdm4 (Mdmx) regulates p53-induced growth arrest and neuronal cell death during early embryonic mouse development. Mol. Cell. Biol. *22*, 5527–5538.

Moore, M.J., Wang, Q., Kennedy, C.J., and Silver, P.A. (2010). An Alternative Splicing Network Links Cell-Cycle Control to Apoptosis. Cell *142*, 625–636.

Muraki, M., Ohkawara, B., Hosoya, T., Onogi, H., Koizumi, J., Koizumi, T., Sumi, K., Yomoda, J.-I., Murray, M.V., Kimura, H., et al. (2004). Manipulation of alternative splicing by a newly developed inhibitor of Clks. J. Biol. Chem. *279*, 24246–24254.

Nagamatsu, G., Kosaka, T., Kawasumi, M., Kinoshita, T., Takubo, K., Akiyama, H., Sudo, T., Kobayashi, T., Oya, M., and Suda, T. (2011). A Germ Cell-specific Gene, Prmt5, Works in Somatic Cell Reprogramming. Journal of Biological Chemistry *286*, 10641–10648.

Nielsen, P.R., Nietlispach, D., Mott, H.R., Callaghan, J., Bannister, A., Kouzarides, T., Murzin, A.G., Murzina, N.V., and Laue, E.D. (2002). Structure of the HP1 chromodomain bound to histone H3 methylated at lysine 9. Nature *416*, 103–107.

Nilsen, T.W., and Graveley, B.R. (2010). Expansion of the eukaryotic proteome by alternative splicing. Nature *463*, 457–463.

Nishioka, K., and Reinberg, D. (2003). Methods and tips for the purification of human histone methyltransferases. Methods *31*, 49–58.

Novoyatleva, T., Tang, Y., Rafalska, I., and Stamm, S. (2006). Pre-mRNA missplicing as a cause of human disease. Prog. Mol. Subcell. Biol. *44*, 27–46.

Ohinata, Y., Payer, B., O'Carroll, D., Ancelin, K., Ono, Y., Sano, M., Barton, S.C., Obukhanych, T., Nussenzweig, M., Tarakhovsky, A., et al. (2005). Blimp1 is a critical determinant of the germ cell lineage in mice. Nature *436*, 207–213.

Okano, H., and Temple, S. (2009). Cell types to order: temporal specification of CNS stem cells. Curr. Opin. Neurobiol. *19*, 112–119.

Ong, S.-E., Mittler, G., and Mann, M. (2004). Identifying and quantifying in vivo methylation sites by heavy methyl SILAC. Nat Meth *1*, 119–126.

Pal, S., Baiocchi, R.A., Byrd, J.C., Grever, M.R., Jacob, S.T., and Sif, S. (2007). Low levels of miR-92b/96 induce PRMT5 translation and H3R8/H4R3 methylation in mantle cell lymphoma. Embo J. *26*, 3558–3569.

Pal, S., Vishwanath, S.N., Erdjument-Bromage, H., Tempst, P., and Sif, S. (2004). Human SWI/SNF-associated PRMT5 methylates histone H3 arginine 8 and negatively regulates expression of ST7 and NM23 tumor suppressor genes. Mol. Cell. Biol. *24*, 9630–9645.

Pal, S., Yun, R., Datta, A., Lacomis, L., Erdjument-Bromage, H., Kumar, J., Tempst, P., and Sif, S. (2003). mSin3A/histone deacetylase 2- and PRMT5-containing Brg1 complex is involved in transcriptional repression of the Myc target gene cad. Mol. Cell. Biol. *23*, 7475–7487.

Pan, J., Goodheart, M., Chuma, S., Nakatsuji, N., Page, D.C., and Wang, P.J. (2005). RNF17, a component of the mammalian germ cell nuage, is essential for spermiogenesis. Development *132*, 4029–4039.

Pandya-Jones, A. (2011). Pre-mRNA splicing during transcription in the mammalian system. Wiley Interdiscip Rev RNA *2*, 700–717.

Papaemmanuil, E., Cazzola, M., Boultwood, J., Malcovati, L., Vyas, P., Bowen, D., Pellagatti, A., Wainscoat, J.S., Hellstrom-Lindberg, E., Gambacorti-Passerini, C., et al. (2011). Somatic SF3B1 mutation in myelodysplasia with ring sideroblasts. N. Engl. J. Med. *365*, 1384–1395.

Paradis, C., Cloutier, P., Shkreta, L., Toutant, J., Klarskov, K., and Chabot, B. (2007). hnRNP I/PTB can antagonize the splicing repressor activity of SRp30c. Rna *13*, 1287–1300.

Park, J.W., Parisky, K., Celotto, A.M., Reenan, R.A., and Graveley, B.R. (2004). Identification of alternative splicing regulators by RNA interference in Drosophila. Proc. Natl. Acad. Sci. U.S.a. *101*, 15974–15979.

Patel, S.R., Bhumbra, S.S., Paknikar, R.S., and Dressler, G.R. (2011). Epigenetic Mechanisms of Groucho/Grg/TLE Mediated Transcriptional Repression. Mol. Cell 1–11.

Pei, Y., Niu, L., Lu, F., Liu, C., Zhai, J., Kong, X., and Cao, X. (2007). Mutations in the Type II protein arginine methyltransferase AtPRMT5 result in pleiotropic developmental defects in Arabidopsis. Plant Physiol. *144*, 1913–1923.

Pesiridis, G.S., Diamond, E., and Van Duyne, G.D. (2009). Role of pICLn in methylation of Sm proteins by PRMT5. J. Biol. Chem. *284*, 21347–21359.

Petrossian, T., and Clarke, S. (2009). Bioinformatic Identification of Novel Methyltransferases. Epigenomics *1*, 163–175.

Petrossian, T.C., and Clarke, S.G. (2011). Uncovering the human methyltransferasome. Molecular & Cellular Proteomics *10*, M110.000976.

Pleiss, J.A., Whitworth, G.B., Bergkessel, M., and Guthrie, C. (2007). Transcript specificity in yeast pre-mRNA splicing revealed by mutations in core spliceosomal components. Plos Biol *5*, e90.

Pollack, B.P., Kotenko, S.V., He, W., Izotova, L.S., Barnoski, B.L., and Pestka, S. (1999). The human homologue of the yeast proteins Skb1 and Hsl7p interacts with Jak kinases and contains protein methyltransferase activity. J. Biol. Chem. *274*, 31531–31542.

Qian, X., Shen, Q., Goderie, S.K., He, W., Capela, A., Davis, A.A., and Temple, S. (2000). Timing of CNS cell generation: a programmed sequence of neuron and glial cell production from isolated murine cortical stem cells. Neuron *28*, 69–80.

Rallapalli, R., Strachan, G., Tuan, R.S., and Hall, D.J. (2003). Identification of a domain within MDMX-S that is responsible for its high affinity interaction with p53 and high-level expression in mammalian cells. J. Cell. Biochem. *89*, 563–575.

Rank, G., Cerruti, L., Simpson, R.J., Moritz, R.L., Jane, S.M., and Zhao, Q. (2010). Identification of a PRMT5-dependent repressor complex linked to silencing of human fetal globin gene expression. Blood *116*, 1585–1592.

Rathert, P., Dhayalan, A., Murakami, M., Zhang, X., Tamas, R., Jurkowska, R., Komatsu, Y., Shinkai, Y., Cheng, X., and Jeltsch, A. (2008). Protein lysine methyltransferase G9a acts on non-histone targets. Nature Chemical Biology *4*, 344–346.

Rho, J., Choi, S., Seong, Y.R., Cho, W.K., Kim, S.H., and Im, D.S. (2001). Prmt5, which forms distinct homo-oligomers, is a member of the protein-arginine methyltransferase family. J. Biol. Chem. *276*, 11393–11401.

Ritchie, W., Granjeaud, S., Puthier, D., and Gautheret, D. (2008). Entropy measures quantify global splicing disorders in cancer. PLoS Comput. Biol. *4*, e1000011.

Rodríguez, C.I., Buchholz, F., Galloway, J., Sequerra, R., Kasper, J., Ayala, R., Stewart, A.F., and Dymecki, S.M. (2000). High-efficiency deleter mice show that FLPe is an alternative to Cre-loxP. Nat. Genet. *25*, 139–140.

Rouhana, L., Vieira, A.P., Roberts-Galbraith, R.H., and Newmark, P.A. (2012). PRMT5 and the role of symmetrical dimethylarginine in chromatoid bodies of planarian stem cells. Development *139*, 1083–1094.

Saltzman, A.L., Pan, Q., and Blencowe, B.J. (2011). Regulation of alternative splicing by the core spliceosomal machinery. Genes Dev. *25*, 373–384.

Sanchez, S.E., Petrillo, E., Beckwith, E.J., Zhang, X., Rugnone, M.L., Hernando, C.E., Cuevas, J.C., Herz, M.A.G., Depetris-Chauvin, A., Simpson, C.G., et al. (2010). A methyl transferase links the circadian clock to the regulation of alternative splicing. Nature *468*, 112–116.

Schneider, C.A., Rasband, W.S., and Eliceiri, K.W. (2012). NIH Image to ImageJ: 25 years of image analysis. Nat Meth *9*, 671–675.

Schor, I.E., Gómez Acuña, L.I., and Kornblihtt, A.R. (2013). Coupling between transcription and alternative splicing. Cancer Treat. Res. *158*, 1–24.

Schor, I.E., Llères, D., Risso, G.J., Pawellek, A., Ule, J., Lamond, A.I., and Kornblihtt, A.R. (2012). Perturbation of chromatin structure globally affects localization and recruitment of splicing factors. PLoS ONE *7*, e48084.

Schwerk, C., and Schulze-Osthoff, K. (2005). Regulation of Apoptosis by Alternative Pre-mRNA Splicing. Mol. Cell *19*, 1–13.

Scoumanne, A., Zhang, J., and Chen, X. (2009). PRMT5 is required for cell-cycle progression and p53 tumor suppressor function. Nucleic Acids Res. *37*, 4965–4976.

Selenko, P., Sprangers, R., Stier, G., Bühler, D., Fischer, U., and Sattler, M. (2001). SMN tudor domain structure and its interaction with the Sm proteins. Nat. Struct. Biol. *8*, 27–31.

Shafey, D., MacKenzie, A.E., and Kothary, R. (2008). Neurodevelopmental abnormalities in neurosphere-derived neural stem cells from SMN-depleted mice. J. Neurosci. Res. *86*, 2839–2847.

Shapiro, M.B., and Senapathy, P. (1987). RNA splice junctions of different classes of eukaryotes: sequence statistics and functional implications in gene expression. Nucleic Acids Res. *15*, 7155–7174.

Shen, Q., Wang, Y., Dimos, J.T., Fasano, C.A., Phoenix, T.N., Lemischka, I.R., Ivanova, N.B., Stifani, S., Morrisey, E.E., and Temple, S. (2006). The timing of cortical neurogenesis is encoded within lineages of individual progenitor cells. Nat. Neurosci. *9*, 743–751.

Shen, S., Park, J.W., Huang, J., Dittmar, K.A., Lu, Z.-X., Zhou, Q., Carstens, R.P., and Xing, Y. (2012). MATS: a Bayesian framework for flexible detection of differential alternative splicing from RNA-Seq data. Nucleic Acids Res. *40*, e61.

Spies, N., Nielsen, C.B., Padgett, R.A., and Burge, C.B. (2009). Biased chromatin signatures around polyadenylation sites and exons. Mol. Cell *36*, 245–254.

Stetler, A., Winograd, C., Sayegh, J., Cheever, A., Patton, E., Zhang, X., Clarke, S., and Ceman, S. (2006). Identification and characterization of the methyl arginines in the fragile X mental retardation protein Fmrp. Hum. Mol. Genet. *15*, 87–96.

Strahl, B.D., and Allis, C.D. (2000). The language of covalent histone modifications. Nature *403*, 41–45.

Sun, L., Wang, M., Lv, Z., Yang, N., Liu, Y., Bao, S., Gong, W., and Xu, R.-M. (2011). Structural insights into protein arginine symmetric dimethylation by PRMT5. Proc. Natl. Acad. Sci. U.S.a. *108*, 20538–20543.

Swiercz, R., Cheng, D., Kim, D., and Bedford, M.T. (2007). Ribosomal protein rpS2 is hypomethylated in PRMT3-deficient mice. J. Biol. Chem. *282*, 16917–16923.

Tabata, T., Kokura, K., Dijke, Ten, P., and Ishii, S. (2009). Ski co-repressor complexes maintain the basal repressed state of the TGF-beta target gene, SMAD7, via HDAC3 and PRMT5. Genes Cells *14*, 17–28.

Tee, W.W., Pardo, M., Theunissen, T.W., Yu, L., Choudhary, J.S., Hajkova, P., and Surani, M.A. (2010). Prmt5 is essential for early mouse development and acts in the cytoplasm to maintain ES cell pluripotency. Genes Dev. *24*, 2772–2777.

Testa, G., Schaft, J., van der Hoeven, F., Glaser, S., Anastassiadis, K., Zhang, Y., Hermann, T., Stremmel, W., and Stewart, A.F. (2004). A reliable lacZ expression reporter cassette for multipurpose, knockout-first alleles. Genesis *38*, 151–158.

Tilgner, H., Knowles, D.G., Johnson, R., Davis, C.A., Chakrabortty, S., Djebali, S., Curado, J., Snyder, M., Gingeras, T.R., and Guigó, R. (2012). Deep sequencing of subcellular RNA fractions shows splicing to be predominantly co-transcriptional in the human genome but inefficient for lncRNAs. Genome Research *22*, 1616–1625.

Tollervey, J.R., Wang, Z., Hortobágyi, T., Witten, J.T., Zarnack, K., Kayikci, M., Clark, T.A., Schweitzer, A.C., Rot, G., Curk, T., et al. (2011). Analysis of alternative splicing associated with aging and neurodegeneration in the human brain. Genome Research *21*, 1572–1582.

Tolstorukov, M.Y., Goldman, J.A., Gilbert, C., Ogryzko, V., Kingston, R.E., and Park, P.J. (2012). Histone variant H2A.Bbd is associated with active transcription and mRNA processing in human cells. Mol. Cell *47*, 596–607.

Trapnell, C., Pachter, L., and Salzberg, S.L. (2009). TopHat: discovering splice junctions with RNA-Seq. Bioinformatics *25*, 1105–1111.

Trapnell, C., Roberts, A., Goff, L., Pertea, G., Kim, D., Kelley, D.R., Pimentel, H., Salzberg, S.L., Rinn, J.L., and Pachter, L. (2012). Differential gene and transcript expression analysis of RNA-seq experiments with TopHat and Cufflinks. Nat Protoc *7*, 562–578.

Tripsianes, K., Madl, T., Machyna, M., Fessas, D., Englbrecht, C., Fischer, U., Neugebauer, K.M., and Sattler, M. (2011). Structural basis for dimethylarginine recognition by the Tudor domains of human SMN and SPF30 proteins. Nat. Struct. Mol. Biol. *18*, 1414–1420.

Vagin, V.V., Wohlschlegel, J., Qu, J., Jonsson, Z., Huang, X., Chuma, S., Girard, A., Sachidanandam, R., Hannon, G.J., and Aravin, A.A. (2009). Proteomic analysis of murine Piwi proteins reveals a role for arginine methylation in specifying interaction with Tudor family members. Genes Dev. *23*, 1749–1762.

Vance, C., Rogelj, B., Hortobágyi, T., De Vos, K.J., Nishimura, A.L., Sreedharan, J., Hu, X., Smith, B., Ruddy, D., Wright, P., et al. (2009). Mutations in FUS, an RNA processing protein, cause familial amyotrophic lateral sclerosis type 6. Science *323*, 1208–1211.

Vargas, D.Y., Shah, K., Batish, M., Levandoski, M., Sinha, S., Marras, S.A.E., Schedl, P., and Tyagi, S. (2011). Single-molecule imaging of transcriptionally coupled and uncoupled splicing. Cell *147*, 1054–1065.

Vasileva, A., Tiedau, D., Firooznia, A., Müller-Reichert, T., and Jessberger, R. (2009). Tdrd6 is required for spermiogenesis, chromatoid body architecture, and regulation of miRNA expression. Curr. Biol. *19*, 630–639.

Vincent, S.D., Dunn, N.R., Sciammas, R., Shapiro-Shalef, M., Davis, M.M., Calame, K., Bikoff, E.K., and Robertson, E.J. (2005). The zinc finger transcriptional repressor Blimp1/Prdm1 is dispensable for early axis formation but is required for specification of primordial germ cells in the mouse. Development *132*, 1315–1325.

Wade, M., Wang, Y.V., and Wahl, G.M. (2010). The p53 orchestra: Mdm2 and Mdmx set the tone. Trends Cell Biol. *20*, 299–309.

Wahl, M.C., Will, C.L., and Lührmann, R. (2009). The Spliceosome: Design Principles of a Dynamic RNP Machine. Cell *136*, 701–718.

Wang, L., Pal, S., and Sif, S. (2008). Protein arginine methyltransferase 5 suppresses the transcription of the RB family of tumor suppressors in leukemia and lymphoma cells. Mol. Cell. Biol. *28*, 6262–6277.

Wang, M., Xu, R.-M., and Thompson, P.R. (2013). Substrate specificity, processivity, and kinetic mechanism of protein arginine methyltransferase 5. Biochemistry *52*, 5430–5440.

Wang, Y.-C., and Li, C. (2012). Evolutionarily conserved protein arginine methyltransferases in non-mammalian animal systems. Febs J *279*, 932–945.

Wang, Z., and Burge, C.B. (2008). Splicing regulation: from a parts list of regulatory elements to an integrated splicing code. Rna *14*, 802–813.

Ward, A.J., and Cooper, T.A. (2010). The pathobiology of splicing. J. Pathol. *220*, 152–163.

Wei, H., Wang, B., Miyagi, M., She, Y., Gopalan, B., Huang, D.-B., Ghosh, G., Stark, G.R., and Lu, T. (2013). PRMT5 dimethylates R30 of the p65 subunit to activate NF-κB. Proc. Natl. Acad. Sci. U.S.a. *110*, 13516–13521.

Winkler, C. (2005). Reduced U snRNP assembly causes motor axon degeneration in an animal model for spinal muscular atrophy. Genes Dev. *19*, 2320–2330.

Wlodarski, T., Kutner, J., Towpik, J., Knizewski, L., Rychlewski, L., Kudlicki, A., Rowicka, M., Dziembowski, A., and Ginalski, K. (2011). Comprehensive structural and substrate specificity classification of the Saccharomyces cerevisiae methyltransferome. PLoS ONE *6*, e23168.

Workman, J.L., and Kingston, R.E. (1998). Alteration of nucleosome structure as a mechanism of transcriptional regulation. Annu. Rev. Biochem. *67*, 545–579.

Wu, S., Romfo, C.M., Nilsen, T.W., and Green, M.R. (1999). Functional recognition of the 3' splice site AG by the splicing factor U2AF35. Nature *402*, 832–835.

Xiong, S., Van Pelt, C.S., Elizondo-Fraire, A.C., Liu, G., and Lozano, G. (2006). Synergistic roles of Mdm2 and Mdm4 for p53 inhibition in central nervous system development. Proc. Natl. Acad. Sci. U.S.a. *103*, 3226–3231.

Xu, J. (2005). Preparation, culture, and immortalization of mouse embryonic fibroblasts. Curr Protoc Mol Biol *Chapter 28*, Unit28.1.

Yadav, N., Lee, J., Kim, J., Shen, J., Hu, M.C.-T., Aldaz, C.M., and Bedford, M.T. (2003). Specific protein methylation defects and gene expression perturbations in coactivator-associated arginine methyltransferase 1-deficient mice. Proc. Natl. Acad. Sci. U.S.a. *100*, 6464–6468.

Yang, M., Sun, J., Sun, X., Shen, Q., Gao, Z., and Yang, C. (2009). Caenorhabditis elegans Protein Arginine Methyltransferase PRMT-5 Negatively Regulates DNA Damage-Induced Apoptosis. PLoS Genet *5*, e1000514.

Yang, Y., and Bedford, M.T. (2013). Protein arginine methyltransferases and cancer. Nat Rev Cancer *13*, 37–50.

Yeo, G., and Burge, C.B. (2004). Maximum entropy modeling of short sequence motifs with applications to RNA splicing signals. J. Comput. Biol. *11*, 377–394.

Yoshida, K., Sanada, M., Shiraishi, Y., Nowak, D., Nagata, Y., Yamamoto, R., Sato, Y., Sato-Otsubo, A., Kon, A., Nagasaki, M., et al. (2012). Frequent pathway mutations of splicing machinery in myelodysplasia. Nature *478*, 64–69.

Yu, Z., Chen, T., Hébert, J., Li, E., and Richard, S. (2009). A mouse PRMT1 null allele defines an essential role for arginine methylation in genome maintenance and cell proliferation. Mol. Cell. Biol. *29*, 2982–2996.

Yuan, C.-C., Matthews, A.G.W., Jin, Y., Chen, C.F., Chapman, B.A., Ohsumi, T.K., Glass, K.C., Kutateladze, T.G., Borowsky, M.L., Struhl, K., et al. (2012). Histone H3R2 symmetric dimethylation and histone H3K4 trimethylation are tightly correlated in eukaryotic genomes. Cell Rep *1*, 83–90.

Zhang, D., Abovich, N., and Rosbash, M. (2001). A biochemical function for the Sm complex. Mol. Cell *7*, 319–329.

Zhang, D., Zhao, T., Ang, H.S., Chong, P., Saiki, R., Igarashi, K., Yang, H., and Vardy, L.A. (2012). AMD1 is essential for ESC self-renewal and is translationally down-regulated on differentiation to neural precursor cells. Genes Dev. *26*, 461–473.

Zhang, Z., Lotti, F., Dittmar, K., Younis, I., Wan, L., Kasim, M., and Dreyfuss, G. (2008). SMN Deficiency Causes Tissue-Specific Perturbations in the Repertoire of snRNAs and Widespread Defects in Splicing. Cell *133*, 585–600.

Zhao, Q., Rank, G., Tan, Y.T., Li, H., Moritz, R.L., Simpson, R.J., Cerruti, L., Curtis, D.J., Patel, D.J., Allis, C.D., et al. (2009). PRMT5-mediated methylation of histone H4R3 recruits DNMT3A, coupling histone and DNA methylation in gene silencing. Nat. Struct. Mol. Biol. *16*, 304–311.

Zheng, S., Moehlenbrink, J., Lu, Y.-C., Zalmas, L.-P., Sagum, C.A., Carr, S., McGouran, J.F., Alexander, L., Fedorov, O., Munro, S., et al. (2013). Arginine Methylation-Dependent Reader-Writer Interplay Governs Growth Control by E2F-1. Mol. Cell.

Zurita-Lopez, C.I., Sandberg, T., Kelly, R., and Clarke, S.G. (2012). Human Protein Arginine Methyltransferase 7 (PRMT7) Is a Type III Enzyme Forming -NG-Monomethylated Arginine Residues. Journal of Biological Chemistry *287*, 7859–7870.

APPENDICES

Table of contents:

APPENDIX A - RNA-sequencing MATS analysis in NPCs

Event	Gene Name	ExonID	IncLevEtOH	IncLevOHT	IncLevDifference	PValue	Direction	Replicate
A3SS	2500003M10Rik	ENSMUSG00000001017#chr3#-#90310029l90311180l 90310029l90310183l90311466l90311548#I#A3SS	0.705	1	-0.295	0	Inclusion	26
A3SS	2500003M10Rik	ENSMUSG00000001017#chr3#-#90310029l90311180l 90310029l90310183l90311466l90311548#I#A3SS	0.748	1	-0.252	3.45156E-11	Inclusion	28
A3SS	Gtpbp3	ENSMUSG00000007610#chr8#+#74014553l74014866l 74014793l74014866l74014233l74014436#I#A3SS	0.239	0.478	-0.239	0.048924486	Inclusion	24
A3SS	Gtpbp3	ENSMUSG00000007610#chr8#+#74014553l74014866l 74014793l74014866l74014233l74014436#I#A3SS	0.189	0.439	-0.25	0.007787578	Inclusion	28
A3SS	Prmt2	ENSMUSG00000020230#chr10#-#75699456l75699569l 75699456l75699566l75700494l75700610#I#A3SS	0	0.429	-0.429	1.11183E-06	Inclusion	26
A3SS	Prmt2	ENSMUSG00000020230#chr10#-#75699456l75699569l 75699456l75699566l75700494l75700610#I#A3SS	0	0.24	-0.24	0.013528117	Inclusion	28
A3SS	Tsc1	ENSMUSG00000026812#chr2#+#28534471l28534638l 28534486l28534638l28533681l28533725#E#A3SS	0.908	0.29	0.618	0.010743791	Exclusion	24
A3SS	Tsc1	ENSMUSG00000026812#chr2#+#28534471l28534638l 28534486l28534638l28533681l28533725#E#A3SS	0.732	0.235	0.497	0.000678307	Exclusion	26
A3SS	Ccnl2	ENSMUSG00000029068#chr4#+#155192647l155194537l 155194437l155194537l155192031l155192096#I#A3SS	0.502	0.771	-0.269	4.81117E-07	Inclusion	26
A3SS	Ccnl2	ENSMUSG00000029068#chr4#+#155192647l155194537l 155194437l155194537l155192031l155192096#I#A3SS	0.523	0.854	-0.331	2.49465E-07	Inclusion	28
A3SS	Cdv3	ENSMUSG00000032803#chr9#-#103255432l103258359l 103255432l103257643l103258609l103258769#I#A3SS	0.701	1	-0.299	1.40337E-08	Inclusion	26
A3SS	Cdv3	ENSMUSG00000032803#chr9#-#103255432l103258359l 103255432l103257643l103258609l103258769#I#A3SS	0.715	1	-0.285	1.21879E-05	Inclusion	28
A3SS	Iffo1	ENSMUSG00000038271#chr6#+#125101812l125102789l 125102631l125102789l125101402l125101543#I#A3SS	0.208	0.512	-0.304	0.000466979	Inclusion	26
A3SS	Iffo1	ENSMUSG00000038271#chr6#+#125101812l125102789l 125102631l125102789l125101402l125101543#I#A3SS	0.243	0.531	-0.288	0.010925383	Inclusion	28
A3SS	Iffo1	ENSMUSG00000038271#chr6#+#125102461l125102789l 125102631l125102789l125101402l125101543#I#A3SS	0.236	0.488	-0.252	0.013796421	Inclusion	26
A3SS	Iffo1	ENSMUSG00000038271#chr6#+#125102461l125102789l 125102631l125102789l125101402l125101543#I#A3SS	0.179	0.478	-0.299	0.012152286	Inclusion	28
A3SS	Arfrp1	ENSMUSG00000038671#chr2#-#181098718l181098900l 181098718l181098801l181099015l181099103#I#A3SS	0.13	0.332	-0.202	1.00544E-05	Inclusion	26
A3SS	Arfrp1	ENSMUSG00000038671#chr2#-#181098718l181098900l 181098718l181098801l181099015l181099103#I#A3SS	0.119	0.357	-0.238	1.83922E-05	Inclusion	28
A3SS	Usp48	ENSMUSG00000043411#chr4#+#137193674l137193805l 137193679l137193805l137190812l137190923#E#A3SS	1	0.756	0.244	6.70433E-05	Exclusion	26
A3SS	Usp48	ENSMUSG00000043411#chr4#+#137193674l137193805l 137193679l137193805l137190812l137190923#E#A3SS	1	0.789	0.211	0.003416318	Exclusion	28
A3SS	Hipk2	ENSMUSG00000061436#chr6#-#38671453l38671596l 38671453l38671593l38679919l38680041#I#A3SS	0.773	1	-0.227	0.029242637	Inclusion	26
A3SS	Hipk2	ENSMUSG00000061436#chr6#-#38671453l38671596l 38671453l38671593l38679919l38680041#I#A3SS	0.75	1	-0.25	0.021380028	Inclusion	28
A3SS	Sox13	ENSMUSG00000070643#chr1#-#135285025l135285140l 135285025l135285137l135285505l135285574#I#A3SS	0	0.571	-0.571	0.038784838	Inclusion	24
A3SS	Sox13	ENSMUSG00000070643#chr1#-#135285025l135285140l 135285025l135285137l135285505l135285574#I#A3SS	0.267	0.813	-0.546	0.006586536	Inclusion	28
A5SS	Mettl17	ENSMUSG00000004561#chr14#+#52508821l52509072l 52508821l52508892l52509202l52509310#I#A5SS	0.267	0.495	-0.228	0.033699469	Inclusion	26
A5SS	Mettl17	ENSMUSG00000004561#chr14#+#52508821l52509072l 52508821l52508892l52509202l52509310#I#A5SS	0.245	0.579	-0.334	0.012564765	Inclusion	28

A5SS	Ggnbp2	ENSMUSG00000020530#chr11#-#84654916l84655126l84654922l84655126l84653762l84653937#I#A5SS	0.58	0.819	-0.239	0.003961512	Inclusion	24
A5SS	Ggnbp2	ENSMUSG00000020530#chr11#-#84654916l84655126l84654922l84655126l84653762l84653937#I#A5SS	0.635	0.838	-0.203	0.000162959	Inclusion	26
A5SS	Mtch1	ENSMUSG00000024012#chr17#-#29473111l29473256l29473162l29473256l29470902l29470950#I#A5SS	0.356	0.56	-0.204	4.50307E-08	Inclusion	26
A5SS	Mtch1	ENSMUSG00000024012#chr17#-#29473111l29473256l29473162l29473256l29470902l29470950#I#A5SS	0.377	0.602	-0.225	8.61798E-07	Inclusion	28
A5SS	Nrxn1	ENSMUSG00000024109#chr17#-#90458815l90458903l90458824l90458903l90436416l90436724#E#A5SS	0.43	0.226	0.204	0.033077991	Exclusion	26
A5SS	Nrxn1	ENSMUSG00000024109#chr17#-#90458815l90458903l90458824l90458903l90436416l90436724#E#A5SS	0.424	0.131	0.293	0.002307033	Exclusion	28
A5SS	Luc7l	ENSMUSG00000024188#chr17#+#26389910l26391333l26389910l26390036l26391975l26392070#I#A5SS	0.434	0.85	-0.416	0.001348594	Inclusion	24
A5SS	Luc7l	ENSMUSG00000024188#chr17#+#26389910l26391333l26389910l26390036l26391975l26392070#I#A5SS	0.311	0.804	-0.493	2.43203E-11	Inclusion	26
A5SS	Luc7l	ENSMUSG00000024188#chr17#+#26389910l26391333l26389910l26390036l26391975l26392070#I#A5SS	0.512	0.817	-0.305	0.007846918	Inclusion	28
A5SS	Ccnt2	ENSMUSG00000026349#chr1#+#129694417l129694773l129694417l129694463l129695966l129696130#I#A5SS	0.46	0.741	-0.281	0.001295887	Inclusion	26
A5SS	Ccnt2	ENSMUSG00000026349#chr1#+#129694417l129694773l129694417l129694463l129695966l129696130#I#A5SS	0.435	0.71	-0.275	0.004054835	Inclusion	28
A5SS	Ccnl1	ENSMUSG00000027829#chr3#-#65759051l65759198l65759125l65759198l65755355l65755476#I#A5SS	0.273	0.606	-0.333	0.00548507	Inclusion	26
A5SS	Ccnl1	ENSMUSG00000027829#chr3#-#65759051l65759198l65759125l65759198l65755355l65755476#I#A5SS	0.18	0.472	-0.292	0.009124999	Inclusion	28
A5SS	Trim24	ENSMUSG00000029833#chr6#+#37895520l37895789l37895520l37895687l37899221l37899398#I#A5SS	0.376	0.583	-0.207	0.000441244	Inclusion	26
A5SS	Trim24	ENSMUSG00000029833#chr6#+#37895520l37895789l37895520l37895687l37899221l37899398#I#A5SS	0.344	0.553	-0.209	0.002603105	Inclusion	28
A5SS	Sorbs2	ENSMUSG00000031626#chr8#+#46885063l46885155l46885063l46885152l46886318l46886365#I#A5SS	0	0.909	-0.909	0.013934306	Inclusion	24
A5SS	Sorbs2	ENSMUSG00000031626#chr8#+#46885063l46885155l46885063l46885152l46886318l46886365#I#A5SS	0	0.409	-0.409	0.0229736	Inclusion	28
A5SS	Tecr	ENSMUSG00000031708#chr8#-#86097607l86097821l86097769l86097821l86097309l86097354#I#A5SS	0.074	0.312	-0.238	5.02177E-05	Inclusion	24
A5SS	Tecr	ENSMUSG00000031708#chr8#-#86097607l86097821l86097769l86097821l86097309l86097354#I#A5SS	0.039	0.423	-0.384	0	Inclusion	26
A5SS	Mrps17	ENSMUSG00000034211#chr5#+#130221558l130221816l130221558l130221785l130222601l130222741#I#A5SS	0.389	0.645	-0.256	0.003450069	Inclusion	26
A5SS	Mrps17	ENSMUSG00000034211#chr5#+#130221558l130221816l130221558l130221785l130222601l130222741#I#A5SS	0.351	0.595	-0.244	0.03908612	Inclusion	28
A5SS	Neto2	ENSMUSG00000036902#chr8#-#88187285l88187330l88187306l88187330l88187077l88187205#E#A5SS	0.649	0.36	0.289	0.014808359	Exclusion	24
A5SS	Neto2	ENSMUSG00000036902#chr8#-#88187285l88187330l88187306l88187330l88187077l88187205#E#A5SS	0.55	0.284	0.266	0.00195195	Exclusion	26
A5SS	Neto2	ENSMUSG00000036902#chr8#-#88187285l88187330l88187306l88187330l88187077l88187205#E#A5SS	0.687	0.257	0.43	6.24506E-06	Exclusion	28
A5SS	Rps16	ENSMUSG00000037563#chr7#+#29137195l29137429l29137195l29137292l29137512l29137715#I#A5SS	0.397	1	-0.603	0.012595136	Inclusion	26
A5SS	Rps16	ENSMUSG00000037563#chr7#+#29137195l29137429l29137195l29137292l29137512l29137715#I#A5SS	0.244	1	-0.756	0.012599165	Inclusion	28
A5SS	Hnrnpf	ENSMUSG00000042079#chr6#+#117856799l117857226l117856799l117856857l117867487l117867616#I#A5SS	0.544	1	-0.456	2.32439E-05	Inclusion	24
A5SS	Hnrnpf	ENSMUSG00000042079#chr6#+#117856799l117857226l117856799l117856857l117867487l117867616#I#A5SS	0.603	1	-0.397	9.05509E-10	Inclusion	26
A5SS	Ubr3	ENSMUSG00000044308#chr2#+#69829481l69829694l69829481l69829682l69831732l69831869#E#A5SS	0.655	0.369	0.286	0.022560573	Exclusion	26
A5SS	Ubr3	ENSMUSG00000044308#chr2#+#69829481l69829694l69829481l69829682l69831732l69831869#E#A5SS	0.584	0.312	0.272	0.044252472	Exclusion	28

A5SS	Mapk10	ENSMUSG00000046709#chr5#-#103487312|103487411|103487339|103487411|103467537|103467707#E#A5SS	0.529	0	0.529	0.000184592	Exclusion	26
A5SS	Mapk10	ENSMUSG00000046709#chr5#-#103487312|103487411|103487339|103487411|103467537|103467707#E#A5SS	1	0.146	0.854	0.011660447	Exclusion	28
A5SS	Ankrd16	ENSMUSG00000047909#chr2#+#11701303|11701524|11701303|11701450|11703103|11705383#I#A5SS	0.474	0.84	-0.366	0.0024282	Inclusion	26
A5SS	Ankrd16	ENSMUSG00000047909#chr2#+#11701303|11701524|11701303|11701450|11703103|11705383#I#A5SS	0.477	0.833	-0.356	0.024281553	Inclusion	28
A5SS	Ldlrad3	ENSMUSG00000048058#chr2#-#101953689|101953836|101953785|101953836|101910089|101910215#E#A5SS	1	0.604	0.396	0.005974263	Exclusion	24
A5SS	Ldlrad3	ENSMUSG00000048058#chr2#-#101953689|101953836|101953785|101953836|101910089|101910215#E#A5SS	0.911	0.639	0.272	0.006398212	Exclusion	26
A5SS	Bdp1	ENSMUSG00000049658#chr13#-#100819590|100819984|100819814|100819984|100816680|100816794#E#A5SS	0.659	0.391	0.268	0.009530614	Exclusion	26
A5SS	Bdp1	ENSMUSG00000049658#chr13#-#100819590|100819984|100819814|100819984|100816680|100816794#E#A5SS	0.784	0.344	0.44	0.00031667	Exclusion	28
A5SS	Tia1	ENSMUSG00000071337#chr6#+#86374955|86375197|86374955|86375064|86375443|86375539#I#A5SS	0.131	0.353	-0.222	3.27486E-05	Inclusion	24
A5SS	Tia1	ENSMUSG00000071337#chr6#+#86374955|86375197|86374955|86375064|86375443|86375539#I#A5SS	0.151	0.38	-0.229	2.25907E-09	Inclusion	26
A5SS	Tia1	ENSMUSG00000071337#chr6#+#86374955|86375197|86374955|86375064|86375443|86375539#I#A5SS	0.178	0.488	-0.31	2.27829E-11	Inclusion	28
MXE	Dnm1l	ENSMUSG00000022789#chr16#-#16318537|16318570|16318856|16318934|16316694|16316871|16319544|16319601#I#MXE	0.253	0.457	-0.204	0.021503723	Inclusion	24
MXE	Dnm1l	ENSMUSG00000022789#chr16#-#16318537|16318570|16318856|16318934|16316694|16316871|16319544|16319601#I#MXE	0.275	0.537	-0.262	0.00014655	Inclusion	28
MXE	Brwd1	ENSMUSG00000022914#chr16#-#96225466|96226315|96230326|96231175|96224040|96224961|96231426|96231594#E#MXE	0.889	0.454	0.435	0.023229596	Exclusion	24
MXE	Brwd1	ENSMUSG00000022914#chr16#-#96225466|96226315|96230326|96231175|96224040|96224961|96231426|96231594#E#MXE	0.75	0.4	0.35	0.030111452	Exclusion	26
MXE	Brwd1	ENSMUSG00000022914#chr16#-#96225466|96226315|96230326|96231175|96224040|96224961|96231426|96231594#E#MXE	0.706	0.255	0.451	0.004950118	Exclusion	28
MXE	Tmem234	ENSMUSG00000028797#chr4#+#129278650|129278777|129279113|129279205|129278226|129278487|129279438|129279505#I#MXE	0.184	0.485	-0.301	0.001017308	Inclusion	24
MXE	Tmem234	ENSMUSG00000028797#chr4#+#129278650|129278777|129279113|129279205|129278226|129278487|129279438|129279505#I#MXE	0.285	0.497	-0.212	0.027849154	Inclusion	28
MXE	Tmem234	ENSMUSG00000028797#chr4#+#129278650|129278869|129279113|129279205|129278226|129278378|129279438|129279505#I#MXE	0.264	0.512	-0.248	0.003870566	Inclusion	24
MXE	Tmem234	ENSMUSG00000028797#chr4#+#129278650|129278869|129279113|129279205|129278226|129278378|129279438|129279505#I#MXE	0.299	0.519	-0.22	0.010606737	Inclusion	28
MXE	Tmem234	ENSMUSG00000028797#chr4#+#129278650|129278869|129279113|129279205|129278226|129278487|129279438|129279505#I#MXE	0.246	0.53	-0.284	0.00057778	Inclusion	24
MXE	Tmem234	ENSMUSG00000028797#chr4#+#129278650|129278869|129279113|129279205|129278226|129278487|129279438|129279505#I#MXE	0.265	0.502	-0.237	0.000120263	Inclusion	26
MXE	Tmem234	ENSMUSG00000028797#chr4#+#129278650|129278869|129279113|129279205|129278226|129278487|129279438|129279505#I#MXE	0.265	0.527	-0.262	0.000945151	Inclusion	28
MXE	Tia1	ENSMUSG00000071337#chr6#+#86369094|86369127|86369687|86369806|86368871|86368926|86370317|86370405#E#MXE	0.811	0.523	0.288	4.42721E-05	Exclusion	24
MXE	Tia1	ENSMUSG00000071337#chr6#+#86369094|86369127|86369687|86369806|86368871|86368926|86370317|86370405#E#MXE	0.8	0.53	0.27	3.44417E-06	Exclusion	28
RI	2500003M10Rik	ENSMUSG00000001017#chr3#-#90310029|90311548|90310029|90310183|90311466|90311548#I#RI	0.696	1	-0.304	0	Inclusion	26

RI	2500003M10Rik	ENSMUSG00000001017#chr3#-#90310029l90311548l90310029l90310183l90311466l90311548#l#RI	0.734	1	-0.266	2.03005E-11	Inclusion	28
RI	Trmt1	ENSMUSG00000001909#chr8#+#87214415l87214846l87214415l87214471l87214709l87214846#l#RI	0.207	0.451	-0.244	0.000468471	Inclusion	24
RI	Trmt1	ENSMUSG00000001909#chr8#+#87214415l87214846l87214415l87214471l87214709l87214846#l#RI	0.177	0.39	-0.213	3.0974E-06	Inclusion	26
RI	Trmt1	ENSMUSG00000001909#chr8#+#87214415l87214846l87214415l87214471l87214709l87214846#l#RI	0.226	0.431	-0.205	0.002336542	Inclusion	28
RI	Slc1a5	ENSMUSG00000001918#chr7#+#17381106l17381507l17381106l17381301l17381372l17381507#l#RI	0.337	1	-0.663	0.001728613	Inclusion	24
RI	Slc1a5	ENSMUSG00000001918#chr7#+#17381106l17381507l17381106l17381301l17381372l17381507#l#RI	0.353	1	-0.647	0.000982165	Inclusion	28
RI	Tmem161a	ENSMUSG00000002342#chr8#+#72704604l72704948l72704604l72704748l72704834l72704948#l#RI	0.112	0.69	-0.578	3.82649E-05	Inclusion	24
RI	Tmem161a	ENSMUSG00000002342#chr8#+#72704604l72704948l72704604l72704748l72704834l72704948#l#RI	0.167	0.4	-0.233	0.001799367	Inclusion	26
RI	Tpra1	ENSMUSG00000002871#chr6#+#88860144l88860395l88860144l88860255l88860334l88860395#l#RI	0.178	0.416	-0.238	0.046319457	Inclusion	26
RI	Tpra1	ENSMUSG00000002871#chr6#+#88860144l88860395l88860144l88860255l88860334l88860395#l#RI	0.077	0.588	-0.511	5.10148E-05	Inclusion	28
RI	Dgkq	ENSMUSG00000004815#chr5#-#109078843l109079398l109078843l109078944l109079219l109079398#l#RI	0.177	0.665	-0.488	2.61763E-07	Inclusion	26
RI	Dgkq	ENSMUSG00000004815#chr5#-#109078843l109079398l109078843l109078944l109079219l109079398#l#RI	0.212	0.473	-0.261	0.029575559	Inclusion	28
RI	Plod3	ENSMUSG00000004846#chr5#+#137466020l137466409l137466020l137466146l137466287l137466409#l#RI	0.012	0.23	-0.218	0	Inclusion	26
RI	Plod3	ENSMUSG00000004846#chr5#+#137466020l137466409l137466020l137466146l137466287l137466409#l#RI	0.029	0.292	-0.263	9.33298E-12	Inclusion	28
RI	Rrnad1	ENSMUSG00000004896#chr3#-#87728265l87729353l87728265l87728450l87728868l87729353#l#RI	0.634	1	-0.366	0.003329894	Inclusion	24
RI	Rrnad1	ENSMUSG00000004896#chr3#-#87728265l87729353l87728265l87728450l87728868l87729353#l#RI	0.556	0.911	-0.355	0.000107141	Inclusion	26
RI	Rrnad1	ENSMUSG00000004896#chr3#-#87728265l87729353l87728265l87728450l87728868l87729353#l#RI	0.626	1	-0.374	0.000314529	Inclusion	28
RI	Wdr83	ENSMUSG00000005150#chr8#-#87603687l87604124l87603687l87603736l87604018l87604124#l#RI	0.258	0.591	-0.333	6.5912E-07	Inclusion	26
RI	Wdr83	ENSMUSG00000005150#chr8#-#87603687l87604124l87603687l87603736l87604018l87604124#l#RI	0.215	0.563	-0.348	2.2863E-05	Inclusion	28
RI	Neu1	ENSMUSG00000007038#chr17#+#35069510l35071130l35069510l35069773l35070947l35071130#l#RI	0.135	0.453	-0.318	0.00078676	Inclusion	24
RI	Neu1	ENSMUSG00000007038#chr17#+#35069510l35071130l35069510l35069773l35070947l35071130#l#RI	0.124	0.49	-0.366	4.79213E-11	Inclusion	26
RI	Neu1	ENSMUSG00000007038#chr17#+#35069510l35071130l35069510l35069773l35070947l35071130#l#RI	0.267	0.529	-0.262	0.0310446	Inclusion	28
RI	Hps5	ENSMUSG00000014418#chr7#-#54030183l54031321l54030183l54030307l54031134l54031321#l#RI	0.092	1	-0.908	6.25679E-06	Inclusion	24
RI	Hps5	ENSMUSG00000014418#chr7#-#54030183l54031321l54030183l54030307l54031134l54031321#l#RI	0.16	0.367	-0.207	0.04764147	Inclusion	28
RI	Gdi1	ENSMUSG00000015291#chrX#+#71553010l71553600l71553010l71553209l71553468l71553600#l#RI	0.281	0.562	-0.281	2.0953E-08	Inclusion	24
RI	Gdi1	ENSMUSG00000015291#chrX#+#71553010l71553600l71553010l71553209l71553468l71553600#l#RI	0.317	0.564	-0.247	2.30815E-13	Inclusion	26
RI	Gdi1	ENSMUSG00000015291#chrX#+#71553010l71553600l71553010l71553209l71553468l71553600#l#RI	0.233	0.651	-0.418	0	Inclusion	28
RI	Setdb1	ENSMUSG00000015697#chr3#-#95141070l95142954l95141070l95141187l95142267l95142954#l#RI	0.177	0.516	-0.339	1.40394E-07	Inclusion	24
RI	Setdb1	ENSMUSG00000015697#chr3#-#95141070l95142954l95141070l95141187l95142267l95142954#l#RI	0.229	0.527	-0.298	4.05789E-09	Inclusion	26

RI	Setdb1	ENSMUSG00000015697#chr3#-#95141070l95142954l 95141070l95141187l95142267l95142954#l#RI	0.203	0.5	-0.297	2.23738E-08	Inclusion	28
RI	Surf1	ENSMUSG00000015790#chr2#-#26768902l26769178l 26768902l26769025l26769096l26769178#l#RI	0.084	0.464	-0.38	6.46128E-08	Inclusion	26
RI	Surf1	ENSMUSG00000015790#chr2#-#26768902l26769178l 26768902l26769025l26769096l26769178#l#RI	0.076	0.436	-0.36	7.03042E-05	Inclusion	28
RI	Ctsa	ENSMUSG00000017760#chr2#+#164659529l164659931l 164659529l164659708l164659819l164659931#l#RI	0.031	0.33	-0.299	1.3179E-09	Inclusion	24
RI	Ctsa	ENSMUSG00000017760#chr2#+#164659529l164659931l 164659529l164659708l164659819l164659931#l#RI	0.01	0.283	-0.273	6.66134E-16	Inclusion	28
RI	Ppp1r1 2c	ENSMUSG00000019254#chr7#-#4435075l4435335l4435075l 4435159l4435244l4435335#l#RI	0.108	0.373	-0.265	1.41617E-05	Inclusion	24
RI	Ppp1r1 2c	ENSMUSG00000019254#chr7#-#4435075l4435335l4435075l 4435159l4435244l4435335#l#RI	0.077	0.297	-0.22	8.90199E-11	Inclusion	26
RI	Ppp1r1 2c	ENSMUSG00000019254#chr7#-#4435075l4435335l4435075l 4435159l4435244l4435335#l#RI	0.085	0.335	-0.25	2.06208E-07	Inclusion	28
RI	Pafah1 b1	ENSMUSG00000020745#chr11#-#74487451l74493116l 74487451l74491244l74492959l74493116#l#RI	0.045	1	-0.955	0	Inclusion	24
RI	Pafah1 b1	ENSMUSG00000020745#chr11#-#74487451l74493116l 74487451l74491244l74492959l74493116#l#RI	0.029	1	-0.971	0	Inclusion	26
RI	Tmem 44	ENSMUSG00000022537#chr16#-#30540824l30543574l 30540824l30540995l30543487l30543574#l#RI	0.22	0.519	-0.299	2.099E-06	Inclusion	24
RI	Tmem 44	ENSMUSG00000022537#chr16#-#30540824l30543574l 30540824l30540995l30543487l30543574#l#RI	0.189	0.558	-0.369	0	Inclusion	26
RI	Tmem 44	ENSMUSG00000022537#chr16#-#30540824l30543574l 30540824l30540995l30543487l30543574#l#RI	0.162	0.533	-0.371	0	Inclusion	28
RI	Adck5	ENSMUSG00000022550#chr15#+#76424582l76424877l 76424582l76424714l76424793l76424877#l#RI	0.038	0.74	-0.702	0.00192554	Inclusion	24
RI	Adck5	ENSMUSG00000022550#chr15#+#76424582l76424877l 76424582l76424714l76424793l76424877#l#RI	0.125	0.426	-0.301	0.009885559	Inclusion	26
RI	Adck5	ENSMUSG00000022550#chr15#+#76424582l76424877l 76424582l76424714l76424793l76424877#l#RI	0	0.533	-0.533	1.05755E-05	Inclusion	28
RI	Gpaa1	ENSMUSG00000022561#chr15#+#76162589l76163061l 76162589l76162701l76162913l76163061#l#RI	0.192	0.426	-0.234	0.002959909	Inclusion	24
RI	Gpaa1	ENSMUSG00000022561#chr15#+#76162589l76163061l 76162589l76162701l76162913l76163061#l#RI	0.181	0.447	-0.266	4.2544E-08	Inclusion	26
RI	Gpaa1	ENSMUSG00000022561#chr15#+#76162589l76163061l 76162589l76162701l76162913l76163061#l#RI	0.164	0.46	-0.296	2.09818E-06	Inclusion	28
RI	Rabl2	ENSMUSG00000022621#chr15#-#89414340l89414821l 89414340l89414438l89414709l89414821#l#RI	0.191	0.424	-0.233	0.018711761	Inclusion	24
RI	Rabl2	ENSMUSG00000022621#chr15#-#89414340l89414821l 89414340l89414438l89414709l89414821#l#RI	0.204	0.732	-0.528	1.65253E-11	Inclusion	26
RI	Rabl2	ENSMUSG00000022621#chr15#-#89414340l89414821l 89414340l89414438l89414709l89414821#l#RI	0.215	0.782	-0.567	5.81561E-09	Inclusion	28
RI	Lmbr1l	ENSMUSG00000022999#chr15#-#98738950l98739190l 98738950l98739027l98739106l98739190#l#RI	0.085	0.457	-0.372	0.000230104	Inclusion	26
RI	Lmbr1l	ENSMUSG00000022999#chr15#-#98738950l98739190l 98738950l98739027l98739106l98739190#l#RI	0	0.433	-0.433	0.000240227	Inclusion	28
RI	Prpf40 b	ENSMUSG00000023007#chr15#+#99145273l99145717l 99145273l99145411l99145621l99145717#l#RI	0.105	0.389	-0.284	0.002555533	Inclusion	24
RI	Prpf40 b	ENSMUSG00000023007#chr15#+#99145273l99145717l 99145273l99145411l99145621l99145717#l#RI	0.141	0.349	-0.208	0.000732996	Inclusion	26
RI	Prpf40 b	ENSMUSG00000023007#chr15#+#99145273l99145717l 99145273l99145411l99145621l99145717#l#RI	0.155	0.466	-0.311	0.000407326	Inclusion	28
RI	Prmt5	ENSMUSG00000023110#chr14#-#55134942l55135452l 55134942l55135028l55135333l55135452#l#RI	0.034	0.384	-0.35	7.68439E-07	Inclusion	24
RI	Prmt5	ENSMUSG00000023110#chr14#-#55134942l55135452l 55134942l55135028l55135333l55135452#l#RI	0.037	0.442	-0.405	1.27676E-14	Inclusion	26
RI	Prmt5	ENSMUSG00000023110#chr14#-#55134942l55135452l 55134942l55135028l55135333l55135452#l#RI	0.05	0.468	-0.418	4.4077E-10	Inclusion	28

RI	1600002H07Rik	ENSMUSG00000024118#chr17#-#24356675l24357255l24356675l24357078l24357196l24357255#I#RI	0.134	0.55	-0.416	0.006693103	Inclusion	24
RI	1600002H07Rik	ENSMUSG00000024118#chr17#-#24356675l24357255l24356675l24357078l24357196l24357255#I#RI	0.138	0.34	-0.202	0.018796977	Inclusion	26
RI	1600002H07Rik	ENSMUSG00000024118#chr17#-#24356675l24357255l24356675l24357078l24357196l24357255#I#RI	0.152	0.414	-0.262	0.010115438	Inclusion	28
RI	1600002H07Rik	ENSMUSG00000024118#chr17#-#24357196l24357560l24357196l24357255l24357461l24357560#I#RI	0.078	1	-0.922	0.000187266	Inclusion	24
RI	1600002H07Rik	ENSMUSG00000024118#chr17#-#24357196l24357560l24357196l24357255l24357461l24357560#I#RI	0.063	0.312	-0.249	0.014849602	Inclusion	28
RI	Snrpc	ENSMUSG00000024217#chr17#+#27977408l27979323l27977408l27977451l27979214l27979323#E#RI	1	0.026	0.974	0.000615055	Exclusion	26
RI	Snrpc	ENSMUSG00000024217#chr17#+#27977408l27979323l27977408l27977451l27979214l27979323#E#RI	1	0.015	0.985	0.000923936	Exclusion	28
RI	Zfp523	ENSMUSG00000024220#chr17#+#28338205l28339293l28338205l28338385l28339059l28339293#I#RI	0.278	0.525	-0.247	0.007628416	Inclusion	26
RI	Zfp523	ENSMUSG00000024220#chr17#+#28338205l28339293l28338205l28338385l28339059l28339293#I#RI	0.271	0.66	-0.389	0.001086391	Inclusion	28
RI	Adamts10	ENSMUSG00000024299#chr17#+#33675012l33675355l33675012l33675118l33675208l33675355#I#RI	0.491	1	-0.509	4.79708E-08	Inclusion	26
RI	Adamts10	ENSMUSG00000024299#chr17#+#33675012l33675355l33675012l33675118l33675208l33675355#I#RI	0.48	1	-0.52	8.35715E-05	Inclusion	28
RI	Mus81	ENSMUSG00000024906#chr19#-#5483454l5483665l5483454l5483558l5483634l5483665#I#RI	0.183	0.456	-0.273	0.003465341	Inclusion	26
RI	Mus81	ENSMUSG00000024906#chr19#-#5483454l5483665l5483454l5483558l5483634l5483665#I#RI	0.154	0.486	-0.332	0.001790184	Inclusion	28
RI	Mbd6	ENSMUSG00000025409#chr10#-#126724451l126724746l126724451l126724594l126724682l126724746#I#RI	0.167	0.506	-0.339	0.011542965	Inclusion	26
RI	Mbd6	ENSMUSG00000025409#chr10#-#126724451l126724746l126724451l126724594l126724682l126724746#I#RI	0.141	0.621	-0.48	0.002576984	Inclusion	28
RI	Wdr73	ENSMUSG00000025722#chr7#-#88045529l88046120l88045529l88045597l88046070l88046120#I#RI	0.35	0.686	-0.336	0.044659849	Inclusion	24
RI	Wdr73	ENSMUSG00000025722#chr7#-#88045529l88046120l88045529l88045597l88046070l88046120#I#RI	0.41	0.776	-0.366	0.014673202	Inclusion	28
RI	0610011F06Rik	ENSMUSG00000025731#chr17#+#26013605l26014114l26013605l26013684l26013894l26014114#I#RI	0.513	0.745	-0.232	0.019025644	Inclusion	26
RI	0610011F06Rik	ENSMUSG00000025731#chr17#+#26013605l26014114l26013605l26013684l26013894l26014114#I#RI	0.497	0.759	-0.262	0.025727393	Inclusion	28
RI	Wdr75	ENSMUSG00000025995#chr1#+#45874107l45875109l45874107l45874288l45875014l45875109#I#RI	0.039	1	-0.961	4.81837E-14	Inclusion	26
RI	Wdr75	ENSMUSG00000025995#chr1#+#45874107l45875109l45874107l45874288l45875014l45875109#I#RI	0.033	1	-0.967	1.57697E-11	Inclusion	28
RI	Glb1l	ENSMUSG00000026200#chr1#-#75205261l75205797l75205261l75205412l75205630l75205797#I#RI	0.259	1	-0.741	0.005249216	Inclusion	24
RI	Glb1l	ENSMUSG00000026200#chr1#-#75205261l75205797l75205261l75205412l75205630l75205797#I#RI	0.273	1	-0.727	0.001045687	Inclusion	26
RI	Golga1	ENSMUSG00000026754#chr2#-#38902542l38903286l38902542l38902654l38903116l38903286#I#RI	0.086	0.304	-0.218	3.5293E-06	Inclusion	26
RI	Golga1	ENSMUSG00000026754#chr2#-#38902542l38903286l38902542l38902654l38903116l38903286#I#RI	0.147	0.366	-0.219	0.002931971	Inclusion	28
RI	Fxr1	ENSMUSG00000027680#chr3#+#33956945l33957153l33956945l33957003l33957090l33957153#E#RI	1	0.392	0.608	1.19604E-08	Exclusion	24
RI	Fxr1	ENSMUSG00000027680#chr3#+#33956945l33957153l33956945l33957003l33957090l33957153#E#RI	1	0.351	0.649	2.55351E-15	Exclusion	28
RI	Ampd2	ENSMUSG00000027889#chr3#-#107882102l107882691l107882102l107882244l107882504l107882691#I#RI	0.238	0.606	-0.368	0.000189937	Inclusion	24

RI	Ampd2	ENSMUSG00000027889#chr3#-#107882102l107882691l 107882102l107882244l107882504l107882691#l#RI	0.249	0.616	-0.367	1.12607E-10	Inclusion	26
RI	Ampd2	ENSMUSG00000027889#chr3#-#107882102l107882691l 107882102l107882244l107882504l107882691#l#RI	0.223	0.528	-0.305	1.12186E-05	Inclusion	28
RI	Fancg	ENSMUSG00000028453#chr4#-#43019855l43020275l 43019855l43019986l43020139l43020275#l#RI	0.072	1	-0.928	0.000454379	Inclusion	24
RI	Fancg	ENSMUSG00000028453#chr4#-#43019855l43020275l 43019855l43019986l43020139l43020275#l#RI	0.081	0.749	-0.668	1.76959E-06	Inclusion	26
RI	Fancg	ENSMUSG00000028453#chr4#-#43019855l43020275l 43019855l43019986l43020139l43020275#l#RI	0.13	0.68	-0.55	0.000661507	Inclusion	28
RI	Gba2	ENSMUSG00000028467#chr4#-#43582360l43582827l 43582360l43582533l43582701l43582827#l#RI	0.069	0.383	-0.314	5.86329E-05	Inclusion	24
RI	Gba2	ENSMUSG00000028467#chr4#-#43582360l43582827l 43582360l43582533l43582701l43582827#l#RI	0.089	0.309	-0.22	0.000565167	Inclusion	28
RI	Gba2	ENSMUSG00000028467#chr4#-#43582908l43583320l 43582908l43583062l43583217l43583320#l#RI	0.15	0.47	-0.32	0.000140603	Inclusion	24
RI	Gba2	ENSMUSG00000028467#chr4#-#43582908l43583320l 43582908l43583062l43583217l43583320#l#RI	0.09	0.393	-0.303	3.78697E-13	Inclusion	26
RI	Gba2	ENSMUSG00000028467#chr4#-#43582908l43583320l 43582908l43583062l43583217l43583320#l#RI	0.061	0.464	-0.403	6.10623E-15	Inclusion	28
RI	Mutyh	ENSMUSG00000028687#chr4#+#116490492l116490887l 116490492l116490642l116490845l116490887#l#RI	0.396	0.816	-0.42	0.003751198	Inclusion	26
RI	Mutyh	ENSMUSG00000028687#chr4#+#116490492l116490887l 116490492l116490642l116490845l116490887#l#RI	0.287	0.853	-0.566	0.009732033	Inclusion	28
RI	Ccnl2	ENSMUSG00000029068#chr4#+#155192031l155194537l 155192031l155192096l155194437l155194537#l#RI	0.459	0.731	-0.272	1.0907E-06	Inclusion	26
RI	Ccnl2	ENSMUSG00000029068#chr4#+#155192031l155194537l 155192031l155192096l155194437l155194537#l#RI	0.483	0.827	-0.344	3.42264E-07	Inclusion	28
RI	Dvl1	ENSMUSG00000029071#chr4#+#155227745l155228195l 155227745l155227867l155228091l155228195#l#RI	0.128	0.628	-0.5	1.66278E-09	Inclusion	24
RI	Dvl1	ENSMUSG00000029071#chr4#+#155227745l155228195l 155227745l155227867l155228091l155228195#l#RI	0.174	0.644	-0.47	5.55112E-16	Inclusion	26
RI	Dvl1	ENSMUSG00000029071#chr4#+#155227745l155228195l 155227745l155227867l155228091l155228195#l#RI	0.161	0.592	-0.431	1.95475E-10	Inclusion	28
RI	Gtf3c2	ENSMUSG00000029144#chr5#-#31461806l31462234l 31461806l31461894l31462072l31462234#l#RI	0.07	0.355	-0.285	1.29751E-11	Inclusion	24
RI	Gtf3c2	ENSMUSG00000029144#chr5#-#31461806l31462234l 31461806l31461894l31462072l31462234#l#RI	0.107	0.391	-0.284	1.11022E-16	Inclusion	26
RI	Gtf3c2	ENSMUSG00000029144#chr5#-#31461806l31462234l 31461806l31461894l31462072l31462234#l#RI	0.079	0.398	-0.319	0	Inclusion	28
RI	Slc30a 9	ENSMUSG00000029221#chr5#+#67733332l67735808l 67733332l67733468l67735768l67735808#l#RI	0.103	0.305	-0.202	0.000453577	Inclusion	24
RI	Slc30a 9	ENSMUSG00000029221#chr5#+#67733332l67735808l 67733332l67733468l67735768l67735808#l#RI	0.08	0.3	-0.22	3.07688E-11	Inclusion	26
RI	Slc30a 9	ENSMUSG00000029221#chr5#+#67733332l67735808l 67733332l67733468l67735768l67735808#l#RI	0.08	0.364	-0.284	2.13227E-11	Inclusion	28
RI	Ddx51	ENSMUSG00000029504#chr5#+#111084325l111084692l 111084325l111084432l111084583l111084692#l#RI	0.069	0.333	-0.264	0.002567733	Inclusion	24
RI	Ddx51	ENSMUSG00000029504#chr5#+#111084325l111084692l 111084325l111084432l111084583l111084692#l#RI	0.052	0.305	-0.253	3.24941E-05	Inclusion	26
RI	Ddx51	ENSMUSG00000029504#chr5#+#111084325l111084692l 111084325l111084432l111084583l111084692#l#RI	0.042	0.352	-0.31	1.73311E-05	Inclusion	28
RI	Wbp1	ENSMUSG00000030035#chr6#-#83070178l83070870l 83070178l83070281l83070765l83070870#l#RI	0.097	0.299	-0.202	4.2517E-05	Inclusion	24
RI	Wbp1	ENSMUSG00000030035#chr6#-#83070178l83070870l 83070178l83070281l83070765l83070870#l#RI	0.091	0.372	-0.281	9.12381E-13	Inclusion	28
RI	Fam98 c	ENSMUSG00000030590#chr7#-#29938340l29939554l 29938340l29938508l29939437l29939554#l#RI	0.17	0.543	-0.373	9.09503E-06	Inclusion	26
RI	Fam98 c	ENSMUSG00000030590#chr7#-#29938340l29939554l 29938340l29938508l29939437l29939554#l#RI	0.229	0.752	-0.523	0.000248088	Inclusion	28

RI	Phkg2	ENSMUSG00000030815#chr7#+#134721048l134721543l134721048l134721224l134721488l134721543#I#RI	0.267	0.596	-0.329	3.50088E-05	Inclusion	26
RI	Phkg2	ENSMUSG00000030815#chr7#+#134721048l134721543l134721048l134721224l134721488l134721543#I#RI	0.268	0.533	-0.265	0.00803002	Inclusion	28
RI	Renbp	ENSMUSG00000031387#chrX#-#71174454l71175856l71174454l71175601l71175746l71175856#I#RI	0	0.251	-0.251	0.011750228	Inclusion	24
RI	Renbp	ENSMUSG00000031387#chrX#-#71174454l71175856l71174454l71175601l71175746l71175856#I#RI	0	0.207	-0.207	0.000326781	Inclusion	26
RI	Adamts7	ENSMUSG00000032363#chr9#+#90087862l90089107l90087862l90088703l90088880l90089107#I#RI	0.331	0.583	-0.252	0.002253733	Inclusion	26
RI	Adamts7	ENSMUSG00000032363#chr9#+#90087862l90089107l90087862l90088703l90088880l90089107#I#RI	0.408	0.678	-0.27	0.003870919	Inclusion	28
RI	Parl	ENSMUSG00000033918#chr16#-#20285837l20287142l20285837l20285908l20286992l20287142#I#RI	0.034	1	-0.966	1.99549E-08	Inclusion	24
RI	Parl	ENSMUSG00000033918#chr16#-#20285837l20287142l20285837l20285908l20286992l20287142#I#RI	0.039	1	-0.961	3.33067E-16	Inclusion	26
RI	Mrps17	ENSMUSG00000034211#chr5#+#130221558l130222741l130221558l130221785l130222601l130222741#I#RI	0.377	0.678	-0.301	0.005040861	Inclusion	24
RI	Mrps17	ENSMUSG00000034211#chr5#+#130221558l130222741l130221558l130221785l130222601l130222741#I#RI	0.354	0.672	-0.318	2.02017E-06	Inclusion	26
RI	Mrps17	ENSMUSG00000034211#chr5#+#130221558l130222741l130221558l130221785l130222601l130222741#I#RI	0.359	0.659	-0.3	0.000559077	Inclusion	28
RI	Ccdc106	ENSMUSG00000035228#chr7#+#5011097l5012387l5011097l5011307l5011808l5012387#E#RI	1	0.175	0.825	0.000584666	Exclusion	24
RI	Ccdc106	ENSMUSG00000035228#chr7#+#5011097l5012387l5011097l5011307l5011808l5012387#E#RI	0.47	0.113	0.357	1.58035E-05	Exclusion	26
RI	Ccdc106	ENSMUSG00000035228#chr7#+#5011097l5012387l5011097l5011307l5011808l5012387#E#RI	0.52	0.204	0.316	0.032997048	Exclusion	28
RI	Ankrd13b	ENSMUSG00000037907#chr11#-#77285950l77286379l77285950l77286114l77286226l77286379#I#RI	0.12	0.454	-0.334	5.62411E-08	Inclusion	26
RI	Ankrd13b	ENSMUSG00000037907#chr11#-#77285950l77286379l77285950l77286114l77286226l77286379#I#RI	0.152	0.573	-0.421	3.50351E-05	Inclusion	28
RI	Arfrp1	ENSMUSG00000038671#chr2#-#181098718l181099103l181098718l181098801l181099015l181099103#I#RI	0.136	0.368	-0.232	2.82471E-09	Inclusion	26
RI	Arfrp1	ENSMUSG00000038671#chr2#-#181098718l181099103l181098718l181098801l181099015l181099103#I#RI	0.14	0.403	-0.263	1.01031E-07	Inclusion	28
RI	Rtel1	ENSMUSG00000038685#chr2#+#181086280l181086658l181086280l181086404l181086507l181086658#I#RI	0.089	0.579	-0.49	6.60605E-12	Inclusion	26
RI	Rtel1	ENSMUSG00000038685#chr2#+#181086280l181086658l181086280l181086404l181086507l181086658#I#RI	0.117	0.519	-0.402	2.7993E-06	Inclusion	28
RI	Rccd1	ENSMUSG00000038930#chr7#-#87465187l87466067l87465187l87465584l87465747l87466067#I#RI	0.642	1	-0.358	0.038897274	Inclusion	26
RI	Rccd1	ENSMUSG00000038930#chr7#-#87465187l87466067l87465187l87465584l87465747l87466067#I#RI	0.4	1	-0.6	0.002898018	Inclusion	28
RI	Ciz1	ENSMUSG00000039205#chr2#+#32226383l32226928l32226383l32226621l32226768l32226928#I#RI	0.435	0.693	-0.258	0.032505825	Inclusion	24
RI	Ciz1	ENSMUSG00000039205#chr2#+#32226383l32226928l32226383l32226621l32226768l32226928#I#RI	0.412	0.782	-0.37	4.09865E-05	Inclusion	28
RI	D2Wsu81e	ENSMUSG00000039660#chr2#-#30033112l30033485l30033112l30033241l30033439l30033485#I#RI	0.141	0.348	-0.207	0.009211287	Inclusion	24
RI	D2Wsu81e	ENSMUSG00000039660#chr2#-#30033112l30033485l30033112l30033241l30033439l30033485#I#RI	0.066	0.374	-0.308	1.35579E-11	Inclusion	28
RI	Skiv2l	ENSMUSG00000040356#chr17#-#34983811l34984269l34983811l34983940l34984087l34984269#I#RI	0.088	0.328	-0.24	0.001183662	Inclusion	24
RI	Skiv2l	ENSMUSG00000040356#chr17#-#34983811l34984269l34983811l34983940l34984087l34984269#I#RI	0.118	0.392	-0.274	6.19612E-07	Inclusion	26
RI	Skiv2l	ENSMUSG00000040356#chr17#-#34983811l34984269l34983811l34983940l34984087l34984269#I#RI	0.078	0.371	-0.293	6.28835E-08	Inclusion	28
RI	Ankle1	ENSMUSG00000046295#chr8#+#73930760l73931648l73930760l73930872l73931111l73931648#I#RI	0.563	1	-0.437	0.034193751	Inclusion	24

RI	Ankle1	ENSMUSG00000046295#chr8#+#73930760l73931648l73930760l73930872l73931111l73931648#I#RI	0.321	0.637	-0.316	0.029089012	Inclusion	26
RI	Zfp672	ENSMUSG00000049755#chr11#-#58132825l58133456l58132825l58133092l58133368l58133456#I#RI	0.339	1	-0.661	0.001541971	Inclusion	26
RI	Zfp672	ENSMUSG00000049755#chr11#-#58132825l58133456l58132825l58133092l58133368l58133456#I#RI	0.446	1	-0.554	0.044427403	Inclusion	28
RI	Pddc1	ENSMUSG00000051007#chr7#-#148595744l148596784l148595744l148595839l148596676l148596784#I#RI	0.095	0.346	-0.251	0.001822531	Inclusion	24
RI	Pddc1	ENSMUSG00000051007#chr7#-#148595744l148596784l148595744l148595839l148596676l148596784#I#RI	0.07	0.493	-0.423	1.11022E-16	Inclusion	26
RI	Pddc1	ENSMUSG00000051007#chr7#-#148595744l148596784l148595744l148595839l148596676l148596784#I#RI	0.094	0.376	-0.282	2.68946E-05	Inclusion	28
RI	E130306D19Rik	ENSMUSG00000051517#chr4#-#43511767l43512209l43511767l43511888l43512114l43512209#I#RI	0.104	0.308	-0.204	0.009968156	Inclusion	24
RI	E130306D19Rik	ENSMUSG00000051517#chr4#-#43511767l43512209l43511767l43511888l43512114l43512209#I#RI	0.101	0.317	-0.216	0.002051484	Inclusion	28
RI	Txlna	ENSMUSG00000053841#chr4#-#129308523l129308954l129308523l129308598l129308834l129308954#I#RI	0.052	0.26	-0.208	1.22741E-10	Inclusion	24
RI	Txlna	ENSMUSG00000053841#chr4#-#129308523l129308954l129308523l129308598l129308834l129308954#I#RI	0.058	0.28	-0.222	0	Inclusion	26
RI	Txlna	ENSMUSG00000053841#chr4#-#129308523l129308954l129308523l129308598l129308834l129308954#I#RI	0.051	0.311	-0.26	0	Inclusion	28
RI	Tmem191c	ENSMUSG00000055692#chr16#+#17277054l17277343l17277054l17277132l17277286l17277343#I#RI	0.391	1	-0.609	0.019734821	Inclusion	24
RI	Tmem191c	ENSMUSG00000055692#chr16#+#17277054l17277343l17277054l17277132l17277286l17277343#I#RI	0.353	1	-0.647	0.000681756	Inclusion	28
RI	4933421E11Rik	ENSMUSG00000056260#chr3#+#106534580l106537536l106534580l106536060l106537275l106537536#I#RI	0.117	1	-0.883	0.003275867	Inclusion	24
RI	4933421E11Rik	ENSMUSG00000056260#chr3#+#106534580l106537536l106534580l106536060l106537275l106537536#I#RI	0.089	1	-0.911	1.33509E-05	Inclusion	28
RI	Cep110	ENSMUSG00000057110#chr2#+#35031057l35031842l35031057l35031120l35031647l35031842#I#RI	0.199	0.592	-0.393	0.000112248	Inclusion	24
RI	Cep110	ENSMUSG00000057110#chr2#+#35031057l35031842l35031057l35031120l35031647l35031842#I#RI	0.205	0.598	-0.393	1.87152E-08	Inclusion	26
RI	Cep110	ENSMUSG00000057110#chr2#+#35031057l35031842l35031057l35031120l35031647l35031842#I#RI	0.209	0.743	-0.534	1.70719E-08	Inclusion	28
RI	Mtfmt	ENSMUSG00000059183#chr9#+#65288152l65289495l65288152l65288255l65289419l65289495#I#RI	0.278	0.67	-0.392	0.001966768	Inclusion	26
RI	Mtfmt	ENSMUSG00000059183#chr9#+#65288152l65289495l65288152l65288255l65289419l65289495#I#RI	0.175	0.58	-0.405	0.004284988	Inclusion	28
RI	Slx1b	ENSMUSG00000059772#chr7#-#133835252l133835569l133835252l133835337l133835441l133835569#I#RI	0.072	1	-0.928	0.002142478	Inclusion	24
RI	Slx1b	ENSMUSG00000059772#chr7#-#133835252l133835569l133835252l133835337l133835441l133835569#I#RI	0.087	0.347	-0.26	0.033585697	Inclusion	26
RI	Ppox	ENSMUSG00000062729#chr1#-#173209560l173210132l173209560l173209705l173209999l173210132#I#RI	0.551	0.883	-0.332	0.000410621	Inclusion	26
RI	Ppox	ENSMUSG00000062729#chr1#-#173209560l173210132l173209560l173209705l173209999l173210132#I#RI	0.576	0.825	-0.249	0.035772614	Inclusion	28
RI	Hdac10	ENSMUSG00000062906#chr15#-#88958023l88958448l88958023l88958121l88958351l88958448#I#RI	0.182	0.632	-0.45	0.005854858	Inclusion	26
RI	Hdac10	ENSMUSG00000062906#chr15#-#88958023l88958448l88958023l88958121l88958351l88958448#I#RI	0.058	0.741	-0.683	7.6248E-05	Inclusion	28
RI	Suds3	ENSMUSG00000066900#chr5#-#117541690l117543040l117541690l117542865l117542954l117543040#I#RI	0.667	0.942	-0.275	0.003483469	Inclusion	24
RI	Suds3	ENSMUSG00000066900#chr5#-#117541690l117543040l117541690l117542865l117542954l117543040#I#RI	0.698	0.914	-0.216	0.000223925	Inclusion	26

RI	Clk2	ENSMUSG00000068917#chr3#+#88973536l88974037l 88973536l88973624l88973970l88974037#I#RI	0.199	0.421	-0.222	1.3907E-06	Inclusion	26
RI	Clk2	ENSMUSG00000068917#chr3#+#88973536l88974037l 88973536l88973624l88973970l88974037#I#RI	0.212	0.493	-0.281	5.30586E-07	Inclusion	28
RI	H2-Ke6	ENSMUSG00000073422#chr17#-#34164350l34164785l 34164350l34164467l34164567l34164785#I#RI	0.129	0.406	-0.277	0.000886798	Inclusion	26
RI	H2-Ke6	ENSMUSG00000073422#chr17#-#34164350l34164785l 34164350l34164467l34164567l34164785#I#RI	0.18	0.697	-0.517	7.724E-06	Inclusion	28
RI	Fnbp1	ENSMUSG00000075415#chr2#-#30881725l30888708l 30881725l30884403l30888549l30888708#I#RI	0.168	0.395	-0.227	2.84155E-10	Inclusion	26
RI	Fnbp1	ENSMUSG00000075415#chr2#-#30881725l30888708l 30881725l30884403l30888549l30888708#I#RI	0.168	0.385	-0.217	1.5108E-06	Inclusion	28
RI	U2af1l4	ENSMUSG00000078765#chr7#+#31351767l31352519l 31351767l31351955l31352161l31352519#I#RI	0.661	1	-0.339	0.045409142	Inclusion	24
RI	U2af1l4	ENSMUSG00000078765#chr7#+#31351767l31352519l 31351767l31351955l31352161l31352519#I#RI	0.562	0.885	-0.323	0.015834381	Inclusion	26
RI	Pms2	ENSMUSG00000079109#chr5#+#144688967l144689911l 144688967l144689135l144689810l144689911#I#RI	0.105	0.424	-0.319	0.007555295	Inclusion	24
RI	Pms2	ENSMUSG00000079109#chr5#+#144688967l144689911l 144688967l144689135l144689810l144689911#I#RI	0.104	0.342	-0.238	0.000893702	Inclusion	26
RI	Pms2	ENSMUSG00000079109#chr5#+#144688967l144689911l 144688967l144689135l144689810l144689911#I#RI	0.071	0.45	-0.379	1.43581E-05	Inclusion	28
RI	Med12	ENSMUSG00000079487#chrX#+#98489296l98489514l 98489296l98489351l98489426l98489514#I#RI	0.645	0.924	-0.279	0.001485339	Inclusion	26
RI	Med12	ENSMUSG00000079487#chrX#+#98489296l98489514l 98489296l98489351l98489426l98489514#I#RI	0.638	0.909	-0.271	0.006853576	Inclusion	28
RI	Fxc1	ENSMUSG00000089847#chr7#+#112789275l112789742l 112789275l112789371l112789541l112789742#I#RI	0.109	0.441	-0.332	3.83637E-08	Inclusion	24
RI	Fxc1	ENSMUSG00000089847#chr7#+#112789275l112789742l 112789275l112789371l112789541l112789742#I#RI	0.125	0.488	-0.363	0	Inclusion	26
SE	Dazap2	ENSMUSG00000000346#chr15#+#100447343l100447462l 100446068l100446155l100448355l100448601#E#SE	1	0.782	0.218	2.25247E-06	Exclusion	24
SE	Dazap2	ENSMUSG00000000346#chr15#+#100447343l100447462l 100446068l100446155l100448355l100448601#E#SE	1	0.694	0.306	2.22045E-16	Exclusion	28
SE	Epn2	ENSMUSG00000001036#chr11#-#61361509l61361544l 61360193l61360413l61367011l61367081#E#SE	0.566	0.255	0.311	0.018567268	Exclusion	26
SE	Epn2	ENSMUSG00000001036#chr11#-#61361509l61361544l 61360193l61360413l61367011l61367081#E#SE	0.771	0.429	0.342	0.020723293	Exclusion	28
SE	Epn2	ENSMUSG00000001036#chr11#-#61361509l61361544l 61360193l61360413l61379323l61379396#E#SE	0.897	0.536	0.361	0.034887346	Exclusion	26
SE	Epn2	ENSMUSG00000001036#chr11#-#61361509l61361544l 61360193l61360413l61379323l61379396#E#SE	0.861	0.469	0.392	0.023004204	Exclusion	28
SE	Sec24b	ENSMUSG00000001052#chr3#-#129723455l129723560l 129714709l129714790l129736748l129736892#E#SE	0.362	0.118	0.244	0.001674111	Exclusion	24
SE	Sec24b	ENSMUSG00000001052#chr3#-#129723455l129723560l 129714709l129714790l129736748l129736892#E#SE	0.389	0.159	0.23	0.001185177	Exclusion	28
SE	Zdhhc4	ENSMUSG00000001844#chr5#-#144090356l144090576l 144090069l144090249l144090844l144090907#I#SE	0.229	0.55	-0.321	0.046075977	Inclusion	24
SE	Zdhhc4	ENSMUSG00000001844#chr5#-#144090356l144090576l 144090069l144090249l144090844l144090907#I#SE	0.365	0.641	-0.276	0.049496165	Inclusion	26
SE	Ap4e1	ENSMUSG00000001998#chr2#+#126835406l126835611l 126834487l126834636l126837526l126837598#I#SE	0.069	0.35	-0.281	0.017315841	Inclusion	24
SE	Ap4e1	ENSMUSG00000001998#chr2#+#126835406l126835611l 126834487l126834636l126837526l126837598#I#SE	0.031	0.373	-0.342	6.91713E-06	Inclusion	26
SE	Syce2	ENSMUSG00000003824#chr8#+#87407329l87407483l 87396618l87396731l87409833l87410022#E#SE	0.582	0.254	0.328	0.001435977	Exclusion	24
SE	Syce2	ENSMUSG00000003824#chr8#+#87407329l87407483l 87396618l87396731l87409833l87410022#E#SE	0.561	0.207	0.354	2.62207E-06	Exclusion	26
SE	Syce2	ENSMUSG00000003824#chr8#+#87407329l87407483l 87396618l87396731l87409833l87410022#E#SE	0.479	0.149	0.33	2.94951E-05	Exclusion	28

SE	Slc2a9	ENSMUSG00000005107#chr5#-#38808413l38808546l38782952l38783063l38827778l38827924#I#SE	0	1	-1	0.000396184	Inclusion	24
SE	Slc2a9	ENSMUSG00000005107#chr5#-#38808413l38808546l38782952l38783063l38827778l38827924#I#SE	0.258	0.903	-0.645	0.04680775	Inclusion	28
SE	Eps15l1	ENSMUSG00000006276#chr8#-#74882211l74882344l74869864l74870070l74891802l74891885#E#SE	0.568	0.326	0.242	0.004258673	Exclusion	26
SE	Eps15l1	ENSMUSG00000006276#chr8#-#74882211l74882344l74869864l74870070l74891802l74891885#E#SE	0.767	0.464	0.303	0.017718588	Exclusion	28
SE	Nfib	ENSMUSG00000008575#chr4#-#81956206l81956295l81941984l81942715l81966377l81966460#E#SE	0.443	0	0.443	0.000248746	Exclusion	24
SE	Nfib	ENSMUSG00000008575#chr4#-#81956206l81956295l81941984l81942715l81966377l81966460#E#SE	0.478	0.098	0.38	0.003478256	Exclusion	28
SE	Ptprs	ENSMUSG00000013236#chr17#-#56568521l56568580l56564302l56564400l56573875l56574020#E#SE	1	0.509	0.491	0.008377683	Exclusion	24
SE	Ptprs	ENSMUSG00000013236#chr17#-#56568521l56568580l56564302l56564400l56573875l56574020#E#SE	0.706	0.269	0.437	0.002241568	Exclusion	26
SE	5033414D02Rik	ENSMUSG00000016495#chr19#-#29424849l29424959l29423194l29423495l29432806l29432893#E#SE	0.814	0.566	0.248	0.024898043	Exclusion	24
SE	5033414D02Rik	ENSMUSG00000016495#chr19#-#29424849l29424959l29423194l29423495l29432806l29432893#E#SE	0.851	0.616	0.235	0.010462864	Exclusion	28
SE	Rhot1	ENSMUSG00000017686#chr11#+#80071015l80071138l80069363l80069459l80079243l80080246#I#SE	0.504	1	-0.496	0.010992788	Inclusion	24
SE	Rhot1	ENSMUSG00000017686#chr11#+#80071015l80071138l80069363l80069459l80079243l80080246#I#SE	0.402	0.665	-0.263	0.025142356	Inclusion	26
SE	Rhot1	ENSMUSG00000017686#chr11#+#80071015l80071138l80069363l80069459l80079243l80080246#I#SE	0.332	0.635	-0.303	0.018163417	Inclusion	28
SE	Kif3a	ENSMUSG00000018395#chr11#+#53404218l53404227l53400336l53400432l53406875l53407032#E#SE	0.968	0	0.968	1.94435E-07	Exclusion	26
SE	Kif3a	ENSMUSG00000018395#chr11#+#53404218l53404227l53400336l53400432l53406875l53407032#E#SE	0.9	0	0.9	0.000632293	Exclusion	28
SE	Mpdu1	ENSMUSG00000018761#chr11#-#69471437l69471523l69471226l69471345l69472067l69472200#E#SE	0.87	0.54	0.33	0	Exclusion	26
SE	Mpdu1	ENSMUSG00000018761#chr11#-#69471437l69471523l69471226l69471345l69472067l69472200#E#SE	0.864	0.547	0.317	1.41398E-10	Exclusion	28
SE	Mpdu1	ENSMUSG00000018761#chr11#-#69471437l69471558l69471226l69471345l69472067l69472200#E#SE	0.709	0.497	0.212	0.017321821	Exclusion	24
SE	Mpdu1	ENSMUSG00000018761#chr11#-#69471437l69471558l69471226l69471345l69472067l69472200#E#SE	0.774	0.393	0.381	0	Exclusion	26
SE	Mpdu1	ENSMUSG00000018761#chr11#-#69471437l69471558l69471226l69471345l69472067l69472200#E#SE	0.771	0.4	0.371	2.89501E-10	Exclusion	28
SE	Cep57l1	ENSMUSG00000019813#chr10#-#41448433l41448520l41443666l41443744l41449136l41449214#E#SE	0.408	0.099	0.309	0.001155744	Exclusion	26
SE	Cep57l1	ENSMUSG00000019813#chr10#-#41448433l41448520l41443666l41443744l41449136l41449214#E#SE	0.376	0.081	0.295	0.006486405	Exclusion	28
SE	Tmpo	ENSMUSG00000019961#chr10#-#90616022l90616142l90615829l90615925l90621492l90621590#E#SE	0.86	0.496	0.364	6.99441E-15	Exclusion	24
SE	Tmpo	ENSMUSG00000019961#chr10#-#90616022l90616142l90615829l90615925l90621492l90621590#E#SE	0.845	0.509	0.336	0	Exclusion	26
SE	Tmpo	ENSMUSG00000019961#chr10#-#90616022l90616142l90615829l90615925l90621492l90621590#E#SE	0.855	0.466	0.389	0	Exclusion	28
SE	Mdm2	ENSMUSG00000020184#chr10#-#117146709l117146840l117142210l117142285l117147001l117147084#E#SE	0.919	0.473	0.446	0.004113587	Exclusion	24
SE	Mdm2	ENSMUSG00000020184#chr10#-#117146709l117146840l117142210l117142285l117147001l117147084#E#SE	0.84	0.454	0.386	0.00167448	Exclusion	28
SE	Mdm2	ENSMUSG00000020184#chr10#-#117146755l117146840l117142210l117142285l117147001l117147078#E#SE	0.959	0.692	0.267	0.012711912	Exclusion	24
SE	Mdm2	ENSMUSG00000020184#chr10#-#117146755l117146840l117142210l117142285l117147001l117147078#E#SE	0.913	0.621	0.292	0.001732291	Exclusion	28

SE	Clk4	ENSMUSG00000020385#chr11#+#51082270l51082348l51081666l51081733l51084038l51084097#I#SE	0.442	1	-0.558	0.022919972	Inclusion	24
SE	Clk4	ENSMUSG00000020385#chr11#+#51082270l51082348l51081666l51081733l51084038l51084097#I#SE	0.539	1	-0.461	0.034313222	Inclusion	26
SE	Clk4	ENSMUSG00000020385#chr11#+#51082270l51082348l51081666l51081733l51084038l51084097#I#SE	0.474	1	-0.526	0.022633817	Inclusion	28
SE	Eif4enif1	ENSMUSG00000020454#chr11#+#3133990l3134062l3129871l3130104l3134464l3134648#E#SE	0.72	0.453	0.267	0.002850471	Exclusion	26
SE	Eif4enif1	ENSMUSG00000020454#chr11#+#3133990l3134062l3129871l3130104l3134464l3134648#E#SE	0.759	0.387	0.372	0.000251809	Exclusion	28
SE	Rnf144a	ENSMUSG00000020642#chr12#-#27090183l27090257l27074258l27074440l27099965l27100121#E#SE	0.325	0	0.325	0.000778227	Exclusion	26
SE	Rnf144a	ENSMUSG00000020642#chr12#-#27090183l27090257l27074258l27074440l27099965l27100121#E#SE	0.504	0.179	0.325	0.045154512	Exclusion	28
SE	Mink1	ENSMUSG00000020827#chr11#+#70422909l70422933l70422667l70422756l70423055l70423219#E#SE	0.585	0.124	0.461	0.006442368	Exclusion	24
SE	Mink1	ENSMUSG00000020827#chr11#+#70422909l70422933l70422667l70422756l70423055l70423219#E#SE	0.395	0.088	0.307	0.000687888	Exclusion	26
SE	Mink1	ENSMUSG00000020827#chr11#+#70422909l70422933l70422667l70422756l70423055l70423219#E#SE	0.574	0.241	0.333	0.019414666	Exclusion	28
SE	Luc7l3	ENSMUSG00000020863#chr11#-#94153707l94153786l94152642l94152892l94154240l94154346#I#SE	0.499	1	-0.501	5.96026E-06	Inclusion	26
SE	Luc7l3	ENSMUSG00000020863#chr11#-#94153707l94153786l94152642l94152892l94154240l94154346#I#SE	0.652	0.945	-0.293	0.041321073	Inclusion	28
SE	Lsm12	ENSMUSG00000020922#chr11#-#102025857l102025950l102025265l102025481l102026673l102026800#I#SE	0.03	1	-0.97	0.001238511	Inclusion	24
SE	Lsm12	ENSMUSG00000020922#chr11#-#102025857l102025950l102025265l102025481l102026673l102026800#I#SE	0	1	-1	8.75084E-05	Inclusion	28
SE	Eif2s1	ENSMUSG00000021116#chr12#+#79980937l79981044l79978078l79978230l79982118l79982216#I#SE	0.338	1	-0.662	7.28297E-06	Inclusion	24
SE	Eif2s1	ENSMUSG00000021116#chr12#+#79980937l79981044l79978078l79978230l79982118l79982216#I#SE	0.435	1	-0.565	2.95404E-05	Inclusion	26
SE	Erh	ENSMUSG00000021131#chr12#-#81738476l81738597l81735008l81735514l81741943l81742031#E#SE	0.872	0.453	0.419	0.000329504	Exclusion	26
SE	Erh	ENSMUSG00000021131#chr12#-#81738476l81738597l81735008l81735514l81741943l81742031#E#SE	0.876	0.201	0.675	0.001112057	Exclusion	28
SE	Isca2	ENSMUSG00000021241#chr12#+#86114742l86114858l86114524l86114627l86115492l86116039#E#SE	0.858	0.607	0.251	0.00315283	Exclusion	24
SE	Isca2	ENSMUSG00000021241#chr12#+#86114742l86114858l86114524l86114627l86115492l86116039#E#SE	0.778	0.467	0.311	3.39383E-08	Exclusion	26
SE	Isca2	ENSMUSG00000021241#chr12#+#86114742l86114858l86114524l86114627l86115492l86116039#E#SE	0.783	0.576	0.207	0.00805817	Exclusion	28
SE	Ylpm1	ENSMUSG00000021244#chr12#+#86369719l86371837l86355650l86356543l86374866l86374984#E#SE	1	0.778	0.222	0.013352701	Exclusion	24
SE	Ylpm1	ENSMUSG00000021244#chr12#+#86369719l86371837l86355650l86356543l86374866l86374984#E#SE	1	0.785	0.215	0.000282666	Exclusion	26
SE	Fam193b	ENSMUSG00000021495#chr13#-#55665880l55665941l55657343l55657586l55671065l55672481#I#SE	0.722	1	-0.278	0.030234593	Inclusion	24
SE	Fam193b	ENSMUSG00000021495#chr13#-#55665880l55665941l55657343l55657586l55671065l55672481#I#SE	0.74	1	-0.26	0.001644235	Inclusion	26
SE	Erbb2ip	ENSMUSG00000021709#chr13#-#104617986l104618103l104614799l104615006l104623577l104625108#E#SE	0.929	0.514	0.415	0.000568275	Exclusion	24
SE	Erbb2ip	ENSMUSG00000021709#chr13#-#104617986l104618103l104614799l104615006l104623577l104625108#E#SE	0.843	0.568	0.275	0.000961604	Exclusion	26
SE	Brd1	ENSMUSG00000022387#chr15#-#88526790l88527104l88522178l88522314l88531202l88531307#E#SE	1	0.039	0.961	0.00111092	Exclusion	24
SE	Brd1	ENSMUSG00000022387#chr15#-#88526790l88527104l88522178l88522314l88531202l88531307#E#SE	1	0.019	0.981	0.012520089	Exclusion	28
SE	Tmem44	ENSMUSG00000022537#chr16#-#30549478l30549543l30547428l30547555l30550448l30550656#I#SE	0.351	0.661	-0.31	4.90804E-05	Inclusion	26

SE	Tmem 44	ENSMUSG00000022537#chr16#-#30549478l30549543l 30547428l30547555l30550448l30550656#I#SE	0.432	0.739	-0.307	0.000795269	Inclusion	28
SE	Fam86	ENSMUSG00000022544#chr16#-#5249004l5249138l5248657l 5248923l5249439l5249541#E#SE	1	0.77	0.23	0.024958539	Exclusion	26
SE	Fam86	ENSMUSG00000022544#chr16#-#5249004l5249138l5248657l 5248923l5249439l5249541#E#SE	1	0.675	0.325	0.015627113	Exclusion	28
SE	Ntan1	ENSMUSG00000022681#chr16#+#13826975l13827078l 13819417l13819529l13827152l13827218#E#SE	0.552	0.32	0.232	0.03901906	Exclusion	24
SE	Ntan1	ENSMUSG00000022681#chr16#+#13826975l13827078l 13819417l13819529l13827152l13827218#E#SE	0.503	0.265	0.238	8.09534E-05	Exclusion	26
SE	Top3b	ENSMUSG00000022779#chr16#+#16875161l16875248l 16870866l16870922l16877924l16878109#E#SE	1	0	1	0.001490057	Exclusion	24
SE	Top3b	ENSMUSG00000022779#chr16#+#16875161l16875248l 16870866l16870922l16877924l16878109#E#SE	0.398	0.042	0.356	0.007582168	Exclusion	28
SE	Top3b	ENSMUSG00000022779#chr16#+#16875164l16875248l 16870849l16870922l16877924l16878109#E#SE	1	0	1	0.00147932	Exclusion	24
SE	Top3b	ENSMUSG00000022779#chr16#+#16875164l16875248l 16870849l16870922l16877924l16878109#E#SE	0.449	0.043	0.406	0.002518242	Exclusion	28
SE	Tmbim 6	ENSMUSG00000023010#chr15#+#99230087l99230302l 99223416l99223471l99232010l99232094#E#SE	1	0.09	0.91	5.85925E-07	Exclusion	24
SE	Tmbim 6	ENSMUSG00000023010#chr15#+#99230087l99230302l 99223416l99223471l99232010l99232094#E#SE	1	0.064	0.936	1.45328E-13	Exclusion	28
SE	Tmbim 6	ENSMUSG00000023010#chr15#+#99230491l99230638l 99223452l99223471l99232010l99232094#E#SE	1	0.014	0.986	0.001893811	Exclusion	24
SE	Tmbim 6	ENSMUSG00000023010#chr15#+#99230491l99230638l 99223452l99223471l99232010l99232094#E#SE	1	0.018	0.982	0.021217638	Exclusion	28
SE	Csad	ENSMUSG00000023044#chr15#-#102010259l102010324l 102009951l102010033l102010401l102010518#E#SE	0.918	0.623	0.295	0.000710629	Exclusion	26
SE	Csad	ENSMUSG00000023044#chr15#-#102010259l102010324l 102009951l102010033l102010401l102010518#E#SE	1	0.731	0.269	0.002475197	Exclusion	28
SE	Prmt5	ENSMUSG00000023110#chr14#-#55132127l55132291l 55130829l55130991l55133433l55133483#E#SE	0.966	0.016	0.95	0	Exclusion	24
SE	Prmt5	ENSMUSG00000023110#chr14#-#55132127l55132291l 55130829l55130991l55133433l55133483#E#SE	0.859	0.005	0.854	0	Exclusion	26
SE	Prmt5	ENSMUSG00000023110#chr14#-#55132127l55132291l 55130829l55130991l55133433l55133483#E#SE	0.82	0	0.82	0	Exclusion	28
SE	Luc7l	ENSMUSG00000024188#chr17#+#26390918l26390989l 26389943l26390036l26391975l26392070#I#SE	0.236	0.819	-0.583	0.000123979	Inclusion	24
SE	Luc7l	ENSMUSG00000024188#chr17#+#26390918l26390989l 26389943l26390036l26391975l26392070#I#SE	0.303	0.823	-0.52	2.63809E-10	Inclusion	26
SE	Svil	ENSMUSG00000024236#chr18#+#5060512l5060608l5059227l 5059367l5062159l5062403#I#SE	0.092	0.362	-0.27	0.036996887	Inclusion	24
SE	Svil	ENSMUSG00000024236#chr18#+#5060512l5060608l5059227l 5059367l5062159l5062403#I#SE	0.034	0.293	-0.259	0.00019242	Inclusion	28
SE	Bin1	ENSMUSG00000024381#chr18#+#32585877l32586006l 32584473l32584621l32591324l32591396#I#SE	0.59	0.883	-0.293	5.57088E-06	Inclusion	26
SE	Bin1	ENSMUSG00000024381#chr18#+#32585877l32586006l 32584473l32584621l32591324l32591396#I#SE	0.592	0.842	-0.25	0.007655949	Inclusion	28
SE	Bin1	ENSMUSG00000024381#chr18#+#32591324l32591396l 32585877l32586006l32591636l32591747#E#SE	1	0.6	0.4	0.000249166	Exclusion	24
SE	Bin1	ENSMUSG00000024381#chr18#+#32591324l32591396l 32585877l32586006l32591636l32591747#E#SE	0.913	0.551	0.362	9.27806E-05	Exclusion	28
SE	Tcof1	ENSMUSG00000024613#chr18#-#60991819l60991963l 60991427l60991649l60992080l60992278#E#SE	0.869	0.471	0.398	0.005701241	Exclusion	24
SE	Tcof1	ENSMUSG00000024613#chr18#-#60991819l60991963l 60991427l60991649l60992080l60992278#E#SE	0.863	0.637	0.226	0.033056066	Exclusion	26
SE	Fibp	ENSMUSG00000024911#chr19#+#5464333l5464431l5464128l 5464215l5464924l5465051#E#SE	0.883	0.45	0.433	2.10032E-07	Exclusion	24
SE	Fibp	ENSMUSG00000024911#chr19#+#5464333l5464431l5464128l 5464215l5464924l5465051#E#SE	0.823	0.416	0.407	3.33067E-16	Exclusion	26

SE	Fibp	ENSMUSG00000024911#chr19#+#5464333l5464431l5464128l5464215l5464924l5465051#E#SE	0.844	0.444	0.4	7.96306E-09	Exclusion	28
SE	Terf1	ENSMUSG00000025925#chr1#+#15823481l15823570l15821587l15821647l15828262l15828369#E#SE	0.847	0.625	0.222	0.040552446	Exclusion	24
SE	Terf1	ENSMUSG00000025925#chr1#+#15823481l15823570l15821587l15821647l15828262l15828369#E#SE	0.882	0.509	0.373	9.54958E-06	Exclusion	28
SE	Pnkd	ENSMUSG00000026179#chr1#+#74333665l74333782l74332415l74332584l74393958l74394074#E#SE	0.771	0.516	0.255	0.009396736	Exclusion	24
SE	Pnkd	ENSMUSG00000026179#chr1#+#74333665l74333782l74332415l74332584l74393958l74394074#E#SE	0.804	0.527	0.277	1.63575E-07	Exclusion	26
SE	Rgs7	ENSMUSG00000026527#chr1#-#177006954l177007008l176989866l176989925l177008319l177008409#E#SE	0.48	0.242	0.238	0.02904557	Exclusion	24
SE	Rgs7	ENSMUSG00000026527#chr1#-#177006954l177007008l176989866l176989925l177008319l177008409#E#SE	0.41	0.182	0.228	0.000336875	Exclusion	26
SE	Atf2	ENSMUSG00000027104#chr2#-#73691851l73691948l73688920l73689039l73701225l73701356#E#SE	0.801	0.359	0.442	6.20958E-05	Exclusion	24
SE	Atf2	ENSMUSG00000027104#chr2#-#73691851l73691948l73688920l73689039l73701225l73701356#E#SE	0.787	0.486	0.301	0.002253783	Exclusion	28
SE	Stx16	ENSMUSG00000027522#chr2#+#173917902l173918068l173916982l173917123l173918934l173919026#E#SE	0.404	0.175	0.229	0.027725214	Exclusion	24
SE	Stx16	ENSMUSG00000027522#chr2#+#173917902l173918068l173916982l173917123l173918934l173919026#E#SE	0.468	0.188	0.28	5.11219E-06	Exclusion	26
SE	Crtc2	ENSMUSG00000027936#chr3#+#90063075l90063144l90062386l90062448l90063307l90063414#E#SE	1	0.613	0.387	0.039061297	Exclusion	24
SE	Crtc2	ENSMUSG00000027936#chr3#+#90063075l90063144l90062386l90062448l90063307l90063414#E#SE	1	0.603	0.397	0.023554589	Exclusion	28
SE	Fbxw7	ENSMUSG00000028086#chr3#+#84668058l84668122l84667885l84667933l84707422l84708001#I#SE	0.025	1	-0.975	2.24471E-06	Inclusion	26
SE	Fbxw7	ENSMUSG00000028086#chr3#+#84668058l84668122l84667885l84667933l84707422l84708001#I#SE	0.095	0.511	-0.416	0.020386824	Inclusion	28
SE	Trit1	ENSMUSG00000028653#chr4#+#122726394l122726507l122726011l122726123l122726719l122726797#E#SE	0.672	0.378	0.294	0.02021758	Exclusion	26
SE	Trit1	ENSMUSG00000028653#chr4#+#122726394l122726507l122726011l122726123l122726719l122726797#E#SE	0.634	0.316	0.318	0.024689211	Exclusion	28
SE	Ccdc163	ENSMUSG00000028689#chr4#+#116381844l116381878l116381113l116381699l116382042l116382224#E#SE	0.854	0.229	0.625	0.00031372	Exclusion	26
SE	Ccdc163	ENSMUSG00000028689#chr4#+#116381844l116381878l116381113l116381699l116382042l116382224#E#SE	1	0.308	0.692	0.021875984	Exclusion	28
SE	Tmem234	ENSMUSG00000028797#chr4#+#129278650l129278777l129278226l129278487l129279113l129279205#I#SE	0.354	0.675	-0.321	0.027544706	Inclusion	26
SE	Tmem234	ENSMUSG00000028797#chr4#+#129278650l129278777l129278226l129278487l129279113l129279205#I#SE	0.396	0.891	-0.495	0.00584456	Inclusion	28
SE	Tmem234	ENSMUSG00000028797#chr4#+#129278650l129278869l129278226l129278487l129279113l129279174#I#SE	0.397	0.755	-0.358	0.041648936	Inclusion	24
SE	Tmem234	ENSMUSG00000028797#chr4#+#129278650l129278869l129278226l129278487l129279113l129279174#I#SE	0.397	0.77	-0.373	0.002564988	Inclusion	26
SE	Tmem234	ENSMUSG00000028797#chr4#+#129278650l129278869l129278226l129278487l129279113l129279174#I#SE	0.366	0.914	-0.548	0.000533567	Inclusion	28
SE	Rer1	ENSMUSG00000029048#chr4#-#154457217l154457345l154456796l154456863l154460313l154460491#I#SE	0.248	0.479	-0.231	1.33497E-08	Inclusion	26
SE	Rer1	ENSMUSG00000029048#chr4#-#154457217l154457345l154456796l154456863l154460313l154460491#I#SE	0.275	0.526	-0.251	3.25526E-06	Inclusion	28
SE	Rer1	ENSMUSG00000029048#chr4#-#154457217l154457426l154456775l154456863l154460313l154460480#I#SE	0.241	0.465	-0.224	5.74452E-09	Inclusion	26
SE	Rer1	ENSMUSG00000029048#chr4#-#154457217l154457426l154456775l154456863l154460313l154460480#I#SE	0.259	0.507	-0.248	1.21406E-06	Inclusion	28
SE	Ccnl2	ENSMUSG00000029068#chr4#+#155192647l155192773l155192031l155192096l155194437l155194537#I#SE	0.45	0.706	-0.256	3.96673E-05	Inclusion	26
SE	Ccnl2	ENSMUSG00000029068#chr4#+#155192647l155192773l155192031l155192096l155194437l155194537#I#SE	0.404	0.803	-0.399	1.0497E-07	Inclusion	28

SE	Calu	ENSMUSG00000029767#chr6#+#29311293l29311487l29306476l29306697l29311559l29311753#I#SE	0.457	0.732	-0.275	1.91513E-13	Inclusion	24
SE	Calu	ENSMUSG00000029767#chr6#+#29311293l29311487l29306476l29306697l29311559l29311753#I#SE	0.467	0.736	-0.269	0	Inclusion	26
SE	Calu	ENSMUSG00000029767#chr6#+#29311293l29311487l29306476l29306697l29311559l29311753#I#SE	0.456	0.666	-0.21	5.42701E-11	Inclusion	28
SE	Zfml	ENSMUSG00000030016#chr6#+#83931677l83931779l83926195l83926344l83933969l83934068#E#SE	1	0.416	0.584	0.000494583	Exclusion	24
SE	Zfml	ENSMUSG00000030016#chr6#+#83931677l83931779l83926195l83926344l83933969l83934068#E#SE	0.757	0.364	0.393	0.000173552	Exclusion	26
SE	Sh2b1	ENSMUSG00000030733#chr7#-#133611463l133611563l133610507l133611287l133611933l133612155#E#SE	0.795	0.358	0.437	3.56301E-07	Exclusion	26
SE	Sh2b1	ENSMUSG00000030733#chr7#-#133611463l133611563l133610507l133611287l133611933l133612155#E#SE	0.726	0.322	0.404	0.001793049	Exclusion	28
SE	Eri2	ENSMUSG00000030929#chr7#-#126930917l126930999l126930252l126930341l126931247l126931348#E#SE	0.766	0.472	0.294	0.002314365	Exclusion	26
SE	Eri2	ENSMUSG00000030929#chr7#-#126930917l126930999l126930252l126930341l126931247l126931348#E#SE	0.789	0.548	0.241	0.039420566	Exclusion	28
SE	Cask	ENSMUSG00000031012#chrX#-#13129498l13129567l13128072l13128108l13132003l13132072#E#SE	0.607	0.302	0.305	0.000427601	Exclusion	24
SE	Cask	ENSMUSG00000031012#chrX#-#13129498l13129567l13128072l13128108l13132003l13132072#E#SE	0.549	0.251	0.298	3.72937E-08	Exclusion	26
SE	Cask	ENSMUSG00000031012#chrX#-#13129498l13129567l13128072l13128108l13132003l13132072#E#SE	0.614	0.28	0.334	3.99186E-06	Exclusion	28
SE	Rbm10	ENSMUSG00000031060#chrX#+#20214551l20214782l20212856l20213040l20216558l20216628#I#SE	0.066	1	-0.934	0.002132515	Inclusion	24
SE	Rbm10	ENSMUSG00000031060#chrX#+#20214551l20214782l20212856l20213040l20216558l20216628#I#SE	0.153	1	-0.847	0.000687283	Inclusion	26
SE	Slc25a14	ENSMUSG00000031105#chrX#+#45977138l45977374l45976754l45977005l45982428l45982522#I#SE	0.411	1	-0.589	0.002304089	Inclusion	24
SE	Slc25a14	ENSMUSG00000031105#chrX#+#45977138l45977374l45976754l45977005l45982428l45982522#I#SE	0.393	0.696	-0.303	0.028214158	Inclusion	26
SE	Slc25a14	ENSMUSG00000031105#chrX#+#45977138l45977383l45976754l45977005l45982428l45982522#I#SE	0.408	1	-0.592	0.002913385	Inclusion	24
SE	Slc25a14	ENSMUSG00000031105#chrX#+#45977138l45977383l45976754l45977005l45982428l45982522#I#SE	0.399	0.683	-0.284	0.043809774	Inclusion	26
SE	Cenpi	ENSMUSG00000031262#chrX#+#130843104l130843172l130842622l130842767l130843265l130843386#E#SE	0.914	0.5	0.414	0.003726632	Exclusion	24
SE	Cenpi	ENSMUSG00000031262#chrX#+#130843104l130843172l130842622l130842767l130843265l130843386#E#SE	0.848	0.526	0.322	0.024749559	Exclusion	28
SE	Nlgn3	ENSMUSG00000031302#chrX#+#98502413l98502473l98497626l98497770l98504095l98504245#E#SE	0.81	0.55	0.26	2.72058E-05	Exclusion	26
SE	Nlgn3	ENSMUSG00000031302#chrX#+#98502413l98502473l98497626l98497770l98504095l98504245#E#SE	1	0.632	0.368	1.43885E-12	Exclusion	28
SE	Vps37a	ENSMUSG00000031600#chr8#+#41626378l41626447l41626242l41626301l41629163l41629307#E#SE	1	0.688	0.312	0.00482157	Exclusion	24
SE	Vps37a	ENSMUSG00000031600#chr8#+#41626378l41626447l41626242l41626301l41629163l41629307#E#SE	1	0.676	0.324	0.000919464	Exclusion	28
SE	Pkd1	ENSMUSG00000032855#chr17#+#24724123l24724237l24723406l24723533l24724344l24724394#E#SE	0.601	0.323	0.278	0.014405591	Exclusion	24
SE	Pkd1	ENSMUSG00000032855#chr17#+#24724123l24724237l24723406l24723533l24724344l24724394#E#SE	0.682	0.372	0.31	3.7366E-06	Exclusion	26
SE	Pkd1	ENSMUSG00000032855#chr17#+#24724123l24724237l24723406l24723533l24724344l24724394#E#SE	0.724	0.386	0.338	0.000511508	Exclusion	28
SE	Kctd17	ENSMUSG00000033287#chr15#+#78267330l78267424l78266014l78266140l78267587l78268009#E#SE	0.642	0.423	0.219	0.007782032	Exclusion	26
SE	Kctd17	ENSMUSG00000033287#chr15#+#78267330l78267424l78266014l78266140l78267587l78268009#E#SE	0.592	0.376	0.216	0.039570667	Exclusion	28
SE	Pla2g4b	ENSMUSG00000033852#chr2#+#119857042l119857138l119856551l119856608l119857310l119857387#E#SE	0.81	0.244	0.566	1.63537E-05	Exclusion	26

SE	Pla2g4b	ENSMUSG00000033852#chr2#+#119857042l119857138l119856551l119856608l119857310l119857387#E#SE	1	0.478	0.522	0.013242958	Exclusion	28
SE	Epn1	ENSMUSG00000035203#chr7#+#5044913l5044988l5044442l5044567l5045500l5045584#E#SE	0.724	0.374	0.35	3.36202E-05	Exclusion	24
SE	Epn1	ENSMUSG00000035203#chr7#+#5044913l5044988l5044442l5044567l5045500l5045584#E#SE	0.675	0.413	0.262	9.47728E-07	Exclusion	26
SE	Epn1	ENSMUSG00000035203#chr7#+#5044913l5044988l5044442l5044567l5045500l5045584#E#SE	0.714	0.366	0.348	4.81459E-07	Exclusion	28
SE	Rnf38	ENSMUSG00000035696#chr4#-#44171774l44171924l44165231l44165425l44200320l44200391#E#SE	0.501	0.077	0.424	0.00275754	Exclusion	24
SE	Rnf38	ENSMUSG00000035696#chr4#-#44171774l44171924l44165231l44165425l44200320l44200391#E#SE	0.578	0.222	0.356	0.002243747	Exclusion	26
SE	Tbc1d24	ENSMUSG00000036473#chr17#-#24319730l24319794l24319394l24319490l24320638l24320797#E#SE	1	0.456	0.544	0.010399451	Exclusion	24
SE	Tbc1d24	ENSMUSG00000036473#chr17#-#24319730l24319794l24319394l24319490l24320638l24320797#E#SE	1	0.709	0.291	0.03972514	Exclusion	28
SE	Eif2c2	ENSMUSG00000036698#chr15#-#72956876l72956964l72955593l72955741l72957383l72957518#E#SE	1	0.495	0.505	0.003196351	Exclusion	26
SE	Eif2c2	ENSMUSG00000036698#chr15#-#72956876l72956964l72955593l72955741l72957383l72957518#E#SE	1	0.46	0.54	0.005919959	Exclusion	28
SE	Cuedc2	ENSMUSG00000036748#chr19#-#46412802l46412901l46407107l46407191l46413058l46413150#E#SE	0.459	0.211	0.248	0.004152205	Exclusion	24
SE	Cuedc2	ENSMUSG00000036748#chr19#-#46412802l46412901l46407107l46407191l46413058l46413150#E#SE	0.413	0.198	0.215	5.2422E-05	Exclusion	26
SE	Cuedc2	ENSMUSG00000036748#chr19#-#46412802l46412910l46407107l46407191l46413058l46413150#E#SE	0.427	0.181	0.246	0.003048638	Exclusion	24
SE	Cuedc2	ENSMUSG00000036748#chr19#-#46412802l46412910l46407107l46407191l46413058l46413150#E#SE	0.384	0.183	0.201	0.000131361	Exclusion	26
SE	Tubb4b	ENSMUSG00000036752#chr2#-#25079453l25079564l25077679l25078888l25079643l25079752#E#SE	1	0.719	0.281	4.03703E-07	Exclusion	26
SE	Tubb4b	ENSMUSG00000036752#chr2#-#25079453l25079564l25077679l25078888l25079643l25079752#E#SE	1	0.788	0.212	0.018871108	Exclusion	28
SE	Zfp280c	ENSMUSG00000036916#chrX#-#45946690l45946775l45944849l45944938l45947540l45947681#I#SE	0.428	1	-0.572	0.001621777	Inclusion	26
SE	Zfp280c	ENSMUSG00000036916#chrX#-#45946690l45946775l45944849l45944938l45947540l45947681#I#SE	0.447	0.926	-0.479	0.01732084	Inclusion	28
SE	Paip2	ENSMUSG00000037058#chr18#+#35759698l35759771l35758294l35758413l35772976l35773156#I#SE	0.132	1	-0.868	0.002484313	Inclusion	24
SE	Paip2	ENSMUSG00000037058#chr18#+#35759698l35759771l35758294l35758413l35772976l35773156#I#SE	0.321	1	-0.679	0.004300401	Inclusion	28
SE	Lsm1	ENSMUSG00000037296#chr8#+#26904148l26904264l26902628l26902697l26912399l26914447#E#SE	0.927	0.148	0.779	1.18291E-05	Exclusion	24
SE	Lsm1	ENSMUSG00000037296#chr8#+#26904148l26904264l26902628l26902697l26912399l26914447#E#SE	1	0.695	0.305	0.007335843	Exclusion	28
SE	Rps16	ENSMUSG00000037563#chr7#+#29137381l29137429l29137195l29137292l29137512l29137715#I#SE	0.214	1	-0.786	0.01217122	Inclusion	26
SE	Rps16	ENSMUSG00000037563#chr7#+#29137381l29137429l29137195l29137292l29137512l29137715#I#SE	0.222	1	-0.778	0.012684275	Inclusion	28
SE	Parp11	ENSMUSG00000037997#chr6#+#127421565l127421686l127420719l127420848l127424253l127424329#I#SE	0.473	0.812	-0.339	0.010664565	Inclusion	26
SE	Parp11	ENSMUSG00000037997#chr6#+#127421565l127421686l127420719l127420848l127424253l127424329#I#SE	0.43	0.86	-0.43	0.007376735	Inclusion	28
SE	Josd2	ENSMUSG00000038695#chr7#+#51723675l51723787l51723445l51723529l51724176l51724339#I#SE	0.38	1	-0.62	0.000230076	Inclusion	26
SE	Josd2	ENSMUSG00000038695#chr7#+#51723675l51723787l51723445l51723529l51724176l51724339#I#SE	0.49	1	-0.51	0.032054394	Inclusion	28
SE	Atp5l	ENSMUSG00000038717#chr9#-#44722733l44722894l44721332l44721549l44728692l44728825#E#SE	0.902	0.487	0.415	0.000191441	Exclusion	26
SE	Atp5l	ENSMUSG00000038717#chr9#-#44722733l44722894l44721332l44721549l44728692l44728825#E#SE	1	0.344	0.656	0.034160602	Exclusion	28

SE	Rpl12	ENSMUSG00000038900#chr2#+#32819016l32819103l32818504l32818586l32819260l32819373#I#SE	0.49	0.834	-0.344	0.018101149	Inclusion	24
SE	Rpl12	ENSMUSG00000038900#chr2#+#32819016l32819103l32818504l32818586l32819260l32819373#I#SE	0.7	0.911	-0.211	0.008595347	Inclusion	26
SE	Rpl12	ENSMUSG00000038900#chr2#+#32819016l32819103l32818504l32818586l32819260l32819373#I#SE	0.508	0.876	-0.368	4.69947E-05	Inclusion	28
SE	Hexdc	ENSMUSG00000039307#chr11#+#121078206l121078390l121076484l121076649l121079401l121079473#I#SE	0.268	1	-0.732	0.0064838	Inclusion	26
SE	Hexdc	ENSMUSG00000039307#chr11#+#121078206l121078390l121076484l121076649l121079401l121079473#I#SE	0.357	1	-0.643	0.004875086	Inclusion	28
SE	Ubn1	ENSMUSG00000039473#chr16#+#5081986l5082076l5081510l5081754l5084148l5086378#E#SE	0.347	0.062	0.285	0.000132041	Exclusion	24
SE	Ubn1	ENSMUSG00000039473#chr16#+#5081986l5082076l5081510l5081754l5084148l5086378#E#SE	0.353	0.129	0.224	0.001131072	Exclusion	28
SE	Alkbh3	ENSMUSG00000040174#chr2#-#93850419l93850565l93848580l93848749l93850839l93850911#I#SE	0.447	0.785	-0.338	0.040995042	Inclusion	24
SE	Alkbh3	ENSMUSG00000040174#chr2#-#93850419l93850565l93848580l93848749l93850839l93850911#I#SE	0.422	0.695	-0.273	0.013274552	Inclusion	26
SE	Pitpnc1	ENSMUSG00000040430#chr11#-#107077991l107078110l107069205l107073972l107087544l107087608#E#SE	0.589	0.264	0.325	5.45456E-05	Exclusion	24
SE	Pitpnc1	ENSMUSG00000040430#chr11#-#107077991l107078110l107069205l107073972l107087544l107087608#E#SE	0.483	0.188	0.295	6.35516E-10	Exclusion	26
SE	Bptf	ENSMUSG00000040481#chr11#-#106948025l106948211l106943826l106944014l106957029l106957239#I#SE	0.284	0.722	-0.438	4.57611E-05	Inclusion	26
SE	Bptf	ENSMUSG00000040481#chr11#-#106948025l106948211l106943826l106944014l106957029l106957239#I#SE	0.307	0.708	-0.401	0.001174001	Inclusion	28
SE	Bptf	ENSMUSG00000040481#chr11#-#106956315l106956504l106943826l106944014l106957029l106957239#I#SE	0.495	0.848	-0.353	0.000105544	Inclusion	26
SE	Bptf	ENSMUSG00000040481#chr11#-#106956315l106956504l106943826l106944014l106957029l106957239#I#SE	0.53	0.802	-0.272	0.018410714	Inclusion	28
SE	Otud6b	ENSMUSG00000040550#chr4#-#14749838l14749919l14745322l14745635l14752645l14752800#E#SE	1	0.362	0.638	0.003886242	Exclusion	24
SE	Otud6b	ENSMUSG00000040550#chr4#-#14749838l14749919l14745322l14745635l14752645l14752800#E#SE	0.81	0.393	0.417	1.6051E-07	Exclusion	26
SE	Ranbp17	ENSMUSG00000040594#chr11#-#33400679l33400770l33393250l33393417l33404681l33404828#E#SE	1	0.096	0.904	0.004285077	Exclusion	24
SE	Ranbp17	ENSMUSG00000040594#chr11#-#33400679l33400770l33393250l33393417l33404681l33404828#E#SE	1	0.291	0.709	0.004775728	Exclusion	28
SE	Crocc	ENSMUSG00000040860#chr4#-#140577568l140577732l140576188l140576404l140577958l140578079#E#SE	1	0.32	0.68	0.001093178	Exclusion	26
SE	Crocc	ENSMUSG00000040860#chr4#-#140577568l140577732l140576188l140576404l140577958l140578079#E#SE	1	0.127	0.873	0.000418654	Exclusion	28
SE	Rfx3	ENSMUSG00000040929#chr19#-#27997697l27997756l27975268l27975393l28085461l28085656#E#SE	0.609	0.118	0.491	0.031800802	Exclusion	24
SE	Rfx3	ENSMUSG00000040929#chr19#-#27997697l27997756l27975268l27975393l28085461l28085656#E#SE	0.696	0	0.696	9.49443E-07	Exclusion	26
SE	Uspl1	ENSMUSG00000041264#chr5#+#149999283l149999410l149996242l149996382l149999920l150000049#E#SE	0.42	0.114	0.306	0.003129956	Exclusion	24
SE	Uspl1	ENSMUSG00000041264#chr5#+#149999283l149999410l149996242l149996382l149999920l150000049#E#SE	0.41	0.197	0.213	0.004367682	Exclusion	26
SE	Uspl1	ENSMUSG00000041264#chr5#+#149999283l149999410l149996242l149996382l149999920l150000049#E#SE	0.442	0.105	0.337	2.92245E-05	Exclusion	28
SE	Uspl1	ENSMUSG00000041264#chr5#+#149999283l149999452l149996135l149996382l149999920l150000049#E#SE	0.516	0.15	0.366	0.000280065	Exclusion	24
SE	Uspl1	ENSMUSG00000041264#chr5#+#149999283l149999452l149996135l149996382l149999920l150000049#E#SE	0.495	0.237	0.258	0.000272238	Exclusion	26
SE	Uspl1	ENSMUSG00000041264#chr5#+#149999283l149999452l149996135l149996382l149999920l150000049#E#SE	0.493	0.19	0.303	0.000485675	Exclusion	28
SE	Zfp740	ENSMUSG00000046897#chr15#+#102035659l102035736l102035001l102035314l102038201l102038351#E#SE	0.478	0.242	0.236	0.005051145	Exclusion	26

SE	Zfp740	ENSMUSG00000046897#chr15#+#102035659l102035736l102035001l102035314l102038201l102038351#E#SE	0.554	0.216	0.338	0.000269245	Exclusion	28
SE	Gphn	ENSMUSG00000047454#chr12#+#79594936l79595044l79593024l79593297l79605603l79605738#E#SE	0.664	0.265	0.399	6.28871E-08	Exclusion	24
SE	Gphn	ENSMUSG00000047454#chr12#+#79594936l79595044l79593024l79593297l79605603l79605738#E#SE	0.53	0.306	0.224	3.78517E-05	Exclusion	26
SE	Gphn	ENSMUSG00000047454#chr12#+#79594936l79595044l79593024l79593297l79605603l79605738#E#SE	0.524	0.308	0.216	0.000787604	Exclusion	28
SE	Tnrc6b	ENSMUSG00000047888#chr15#+#80713373l80713532l80709296l80711636l80714636l80714812#I#SE	0.777	1	-0.223	0.018517812	Inclusion	26
SE	Tnrc6b	ENSMUSG00000047888#chr15#+#80713373l80713532l80709296l80711636l80714636l80714812#I#SE	0.772	1	-0.228	0.038275855	Inclusion	28
SE	1110034B05Rik	ENSMUSG00000048495#chr1#-#57450428l57450538l57450193l57450331l57450890l57450935#I#SE	0.12	0.333	-0.213	0.016149843	Inclusion	24
SE	1110034B05Rik	ENSMUSG00000048495#chr1#-#57450428l57450538l57450193l57450331l57450890l57450935#I#SE	0.102	0.432	-0.33	3.53878E-07	Inclusion	26
SE	1110034B05Rik	ENSMUSG00000048495#chr1#-#57450428l57450538l57450193l57450331l57450890l57450935#I#SE	0.039	0.518	-0.479	5.8049E-08	Inclusion	28
SE	1110034B05Rik	ENSMUSG00000048495#chr1#-#57450513l57450538l57450193l57450331l57450890l57450935#I#SE	0.103	0.467	-0.364	0.003603634	Inclusion	24
SE	1110034B05Rik	ENSMUSG00000048495#chr1#-#57450513l57450538l57450193l57450331l57450890l57450935#I#SE	0.146	0.58	-0.434	4.61751E-06	Inclusion	26
SE	1110034B05Rik	ENSMUSG00000048495#chr1#-#57450513l57450538l57450193l57450331l57450890l57450935#I#SE	0.091	0.6	-0.509	0.000204069	Inclusion	28
SE	Setd8	ENSMUSG00000049327#chr5#+#124895977l124896093l124889938l124890024l124897222l124897379#I#SE	0.207	1	-0.793	0.021326891	Inclusion	24
SE	Setd8	ENSMUSG00000049327#chr5#+#124895977l124896093l124889938l124890024l124897222l124897379#I#SE	0.299	1	-0.701	0.035095446	Inclusion	26
SE	Setd8	ENSMUSG00000049327#chr5#+#124895977l124896093l124889938l124890024l124897222l124897379#I#SE	0.343	1	-0.657	0.044198707	Inclusion	28
SE	Mdm4	ENSMUSG00000054387#chr1#-#134901230l134901298l134900367l134900467l134905713l134905769#E#SE	0.673	0.431	0.242	0.03411172	Exclusion	24
SE	Mdm4	ENSMUSG00000054387#chr1#-#134901230l134901298l134900367l134900467l134905713l134905769#E#SE	0.74	0.512	0.228	0.005589267	Exclusion	26
SE	Mdm4	ENSMUSG00000054387#chr1#-#134901230l134901298l134900367l134900467l134905713l134905769#E#SE	0.717	0.476	0.241	0.007297668	Exclusion	28
SE	Spna2	ENSMUSG00000057738#chr2#+#29869677l29869692l29869195l29869358l29871108l29871240#I#SE	0.445	0.796	-0.351	4.40026E-05	Inclusion	24
SE	Spna2	ENSMUSG00000057738#chr2#+#29869677l29869692l29869195l29869358l29871108l29871240#I#SE	0	0.759	-0.759	0	Inclusion	26
SE	Palld	ENSMUSG00000058056#chr8#-#64013654l64013705l64012150l64012372l64014482l64014581#I#SE	0.193	0.417	-0.224	0.046130036	Inclusion	24
SE	Palld	ENSMUSG00000058056#chr8#-#64013654l64013705l64012150l64012372l64014482l64014581#I#SE	0.198	0.516	-0.318	5.63603E-05	Inclusion	26
SE	Palld	ENSMUSG00000058056#chr8#-#64013654l64013705l64012150l64012372l64014482l64014581#I#SE	0.296	0.544	-0.248	0.025509367	Inclusion	28
SE	Wdr91	ENSMUSG00000058486#chr6#-#34859676l34859827l34859360l34859540l34860696l34860836#I#SE	0.049	0.316	-0.267	0.006323183	Inclusion	24
SE	Wdr91	ENSMUSG00000058486#chr6#-#34859676l34859827l34859360l34859540l34860696l34860836#I#SE	0.036	0.333	-0.297	8.12814E-05	Inclusion	28
SE	Wdr91	ENSMUSG00000058486#chr6#-#34859713l34859827l34859460l34859540l34860696l34860842#I#SE	0.047	0.306	-0.259	0.013206463	Inclusion	24
SE	Wdr91	ENSMUSG00000058486#chr6#-#34859713l34859827l34859460l34859540l34860696l34860842#I#SE	0.012	0.22	-0.208	0.002818552	Inclusion	28
SE	Gtf2i	ENSMUSG00000060261#chr5#-#134748393l134748456l134742412l134742526l134750408l134750465#I#SE	0.586	0.824	-0.238	0.000143312	Inclusion	24

SE	Gtf2i	ENSMUSG00000060261#chr5#-#134748393l134748456l134742412l134742526l134750408l134750465#I#SE	0.68	0.886	-0.206	9.73664E-07	Inclusion	26
SE	Lmtk3	ENSMUSG00000062044#chr7#+#53043015l53043124l53042763l53042840l53043273l53043392#E#SE	1	0.407	0.593	0.013705772	Exclusion	24
SE	Lmtk3	ENSMUSG00000062044#chr7#+#53043015l53043124l53042763l53042840l53043273l53043392#E#SE	0.668	0.365	0.303	0.033228185	Exclusion	26
SE	Lmtk3	ENSMUSG00000062044#chr7#+#53043015l53043124l53042763l53042840l53043273l53043392#E#SE	1	0.407	0.593	0.00431559	Exclusion	28
SE	Dzip3	ENSMUSG00000064061#chr16#-#48951655l48952273l48950113l48950146l48953839l48953916#I#SE	0.324	0.705	-0.381	0.00637449	Inclusion	24
SE	Dzip3	ENSMUSG00000064061#chr16#-#48951655l48952273l48950113l48950146l48953839l48953916#I#SE	0.317	0.549	-0.232	0.016667737	Inclusion	26
SE	Med14	ENSMUSG00000064127#chrX#-#12266454l12266586l12264144l12264327l12270710l12270822#E#SE	0.718	0.513	0.205	0.046360062	Exclusion	24
SE	Med14	ENSMUSG00000064127#chrX#-#12266454l12266586l12264144l12264327l12270710l12270822#E#SE	0.659	0.447	0.212	0.0143954	Exclusion	28
SE	Nnat	ENSMUSG00000067786#chr2#+#157386948l157386975l157385851l157385996l157387277l157388240#E#SE	0.886	0.658	0.228	7.26921E-11	Exclusion	24
SE	Nnat	ENSMUSG00000067786#chr2#+#157386948l157386975l157385851l157385996l157387277l157388240#E#SE	0.899	0.644	0.255	0	Exclusion	28
SE	Nnat	ENSMUSG00000067786#chr2#+#157386948l157387024l157385842l157385996l157387277l157387974#E#SE	0.799	0.517	0.282	1.74757E-11	Exclusion	24
SE	Nnat	ENSMUSG00000067786#chr2#+#157386948l157387024l157385842l157385996l157387277l157387974#E#SE	0.756	0.529	0.227	1.67755E-13	Exclusion	26
SE	Nnat	ENSMUSG00000067786#chr2#+#157386948l157387024l157385842l157385996l157387277l157387974#E#SE	0.815	0.491	0.324	0	Exclusion	28
SE	Nnat	ENSMUSG00000067786#chr2#+#157386948l157387029l157385845l157385996l157387277l157388258#E#SE	0.853	0.607	0.246	1.90846E-11	Exclusion	24
SE	Nnat	ENSMUSG00000067786#chr2#+#157386948l157387029l157385845l157385996l157387277l157388258#E#SE	0.816	0.615	0.201	3.00204E-13	Exclusion	26
SE	Nnat	ENSMUSG00000067786#chr2#+#157386948l157387029l157385845l157385996l157387277l157388258#E#SE	0.864	0.568	0.296	0	Exclusion	28
SE	Csde1	ENSMUSG00000068823#chr3#+#102844363l102844456l102843855l102843965l102845067l102845165#E#SE	1	0.413	0.587	1.85074E-13	Exclusion	24
SE	Csde1	ENSMUSG00000068823#chr3#+#102844363l102844456l102843855l102843965l102845067l102845165#E#SE	1	0.5	0.5	0	Exclusion	26
SE	Eif2s3y	ENSMUSG00000069049#chrY#+#349821l349916l348490l348612l351076l351235#E#SE	0.793	0.516	0.277	0.002716723	Exclusion	24
SE	Eif2s3y	ENSMUSG00000069049#chrY#+#349821l349916l348490l348612l351076l351235#E#SE	0.826	0.478	0.348	1.4982E-06	Exclusion	28
SE	Strada	ENSMUSG00000069631#chr11#-#106045875l106045933l106034992l106035095l106048414l106048494#I#SE	0.372	1	-0.628	1.88428E-05	Inclusion	26
SE	Strada	ENSMUSG00000069631#chr11#-#106045875l106045933l106034992l106035095l106048414l106048494#I#SE	0.24	1	-0.76	0.000149312	Inclusion	28
SE	Prss36	ENSMUSG00000070371#chr7#-#135077652l135077794l135077080l135077346l135077903l135078141#I#SE	0.128	0.637	-0.509	0.020482179	Inclusion	24
SE	Prss36	ENSMUSG00000070371#chr7#-#135077652l135077794l135077080l135077346l135077903l135078141#I#SE	0.294	1	-0.706	0.00171793	Inclusion	28
SE	Chchd 2	ENSMUSG00000070493#chr5#-#130359804l130360054l130358299l130358450l130363067l130363340#E#SE	1	0	1	0.044319689	Exclusion	26
SE	Chchd 2	ENSMUSG00000070493#chr5#-#130359804l130360054l130358299l130358450l130363067l130363340#E#SE	1	0	1	0.043527717	Exclusion	28
SE	Srsf3	ENSMUSG00000071172#chr17#+#29176398l29176854l29175434l29175569l29177719l29177758#I#SE	0.621	0.828	-0.207	9.96483E-05	Inclusion	26
SE	Srsf3	ENSMUSG00000071172#chr17#+#29176398l29176854l29175434l29175569l29177719l29177758#I#SE	0.704	1	-0.296	8.94105E-10	Inclusion	28
SE	Tia1	ENSMUSG00000071337#chr6#+#86373599l86373665l86369922l86370405l86374338l86374417#I#SE	0.121	0.337	-0.216	0.001306632	Inclusion	24
SE	Tia1	ENSMUSG00000071337#chr6#+#86373599l86373665l86369922l86370405l86374338l86374417#I#SE	0.145	0.407	-0.262	1.15551E-06	Inclusion	28

SE	Dtnb	ENSMUSG00000071454#chr12#+#3774569l3774610l3773550l3773640l3779618l3779654#I#SE	0.687	0.955	-0.268	0.039148513	Inclusion	26
SE	Dtnb	ENSMUSG00000071454#chr12#+#3774569l3774610l3773550l3773640l3779618l3779654#I#SE	0.655	1	-0.345	0.029581831	Inclusion	28
SE	Tomm5	ENSMUSG00000078713#chr4#-#45119710l45119760l45118083l45118516l45120784l45120980#I#SE	0	0.237	-0.237	0.000556512	Inclusion	24
SE	Tomm5	ENSMUSG00000078713#chr4#-#45119710l45119760l45118083l45118516l45120784l45120980#I#SE	0	0.359	-0.359	3.10973E-12	Inclusion	26
SE	Sec61 g	ENSMUSG00000078974#chr11#-#16404738l16404841l16401640l16401810l16406375l16406475#E#SE	1	0.612	0.388	4.95593E-08	Exclusion	26
SE	Sec61 g	ENSMUSG00000078974#chr11#-#16404738l16404841l16401640l16401810l16406375l16406475#E#SE	1	0.046	0.954	1.55431E-15	Exclusion	28
SE	Rab7	ENSMUSG00000079477#chr6#-#87965625l87965712l87963631l87963692l87995066l87995239#I#SE	0.029	1	-0.971	4.95438E-07	Inclusion	24
SE	Rab7	ENSMUSG00000079477#chr6#-#87965625l87965712l87963631l87963692l87995066l87995239#I#SE	0.029	1	-0.971	1.66533E-14	Inclusion	26
SE	Hbxip	ENSMUSG00000087260#chr3#+#107082787l107082849l107081775l107082031l107084826l107084944#I#SE	0.3	1	-0.7	0.001180992	Inclusion	24
SE	Hbxip	ENSMUSG00000087260#chr3#+#107082787l107082849l107081775l107082031l107084826l107084944#I#SE	0.404	1	-0.596	6.09594E-05	Inclusion	28
SE	24100 04N09 Rik	ENSMUSG00000087590#chr18#+#33955036l33955099l33954574l33954778l33955506l33955640#E#SE	1	0.691	0.309	0.000500305	Exclusion	24
SE	24100 04N09 Rik	ENSMUSG00000087590#chr18#+#33955036l33955099l33954574l33954778l33955506l33955640#E#SE	0.96	0.751	0.209	0.001251603	Exclusion	26
SE	24100 04N09 Rik	ENSMUSG00000087590#chr18#+#33955036l33955099l33954574l33954778l33955506l33955640#E#SE	0.959	0.727	0.232	0.007094722	Exclusion	28
SE	Ttbk2	ENSMUSG00000090100#chr2#-#120650977l120651051l120648208l120648344l120675791l120676154#E#SE	0.455	0.148	0.307	0.036596761	Exclusion	26
SE	Ttbk2	ENSMUSG00000090100#chr2#-#120650977l120651051l120648208l120648344l120675791l120676154#E#SE	0.68	0	0.68	4.37483E-05	Exclusion	28

APPENDIX B - Illumina microarray analysis in NPCs

Gene me	ENSEMBL	Genomic Location [mm9]	logFC	AveExpr	adj.P.Val
Ass1	ENSMUSG00000076441	chr2:31376010:31376059:	3.564970315	8.207397658	9.11244E-10
Pde1a	ENSMUSG00000059173	chr2:79705263:79705312:-	3.435639359	8.704254116	1.08037E-07
Spp1	ENSMUSG00000029304	chr5:104869796:104869845:	3.313298809	9.956529887	6.82138E-07
Ckmt1	ENSMUSG00000000308	chr2:121189400:121189449:	3.265851	8.83116845	3.39061E-09
Pde1a	ENSMUSG00000059173	chr2:79705198:79705247:-	3.249381506	8.36479476	1.72272E-08
Diras2	ENSMUSG00000047842	chr13:52599864:52599913:-	3.156059725	9.797755365	1.46631E-08
Reln	ENSMUSG00000042453	chr5:21390390:21390439:-	3.133400919	10.73717168	1.00059E-05
Rgs4	ENSMUSG00000038530	chr1:171672462:171672511:-	3.091259594	8.929218969	2.41203E-08
Pde1a	ENSMUSG00000059173	chr2:79705238:79705287:-	3.086248947	8.26020787	8.78553E-08
Chchd10	ENSMUSG00000049422	chr10:75400420:75400469:	3.014880548	10.29765602	4.3113E-09
Sst	ENSMUSG00000004366	chr16:23889780:23889829:-	3.008862399	10.1509938	8.05448E-06
Tceal5	ENSMUSG00000054034	chrX:132735583:132735632:-	2.924855323	9.921456207	1.19653E-08
Vgf	ENSMUSG00000037428	chr5:137508882:137508931:	2.898145305	7.998305687	9.36679E-08
Wfdc2	ENSMUSG00000017723	chr2:164393913:164393962:	2.866010397	8.161025417	3.68859E-06
Cpne4	ENSMUSG00000032564	chr9:104936340:104936389:	2.864780419	8.246749092	6.58829E-07
Chgb	ENSMUSG00000027350	chr2:132619745:132619794:	2.849264599	8.230226958	8.35499E-08
Glra2	ENSMUSG00000018589	chrX:161567314:161567363:-	2.826266394	9.462544539	6.51692E-09
Clu	ENSMUSG00000022037	chr14:66600225:66600274:	2.816170447	9.216392843	6.38319E-07
Thbs2	ENSMUSG00000023885	chr17:14804242:14804291:-	2.763961706	8.135087879	6.74303E-06
AW555464	ENSMUSG00000072825	chr12:113984610:113984659:	2.719016041	9.080603603	4.3113E-09
Ctgf	ENSMUSG00000019997	chr10:24318317:24318366:	2.705294478	8.507877829	9.8647E-07
Islr2	ENSMUSG00000051243	chr9:58044390:58044439:-	2.69224379	10.31961359	1.808E-08
Cntp2	ENSMUSG00000039419	chr6:47249039:47249088:	2.660152103	8.239015728	2.97846E-07
Calb2	ENSMUSG00000003657	chr8:112666522:112666571:-	2.660013342	8.985639029	4.92479E-08
Gpnmb	ENSMUSG00000029816	chr6:49006694:49006743:	2.602732928	8.041806321	1.39543E-06
Stmn2	ENSMUSG00000027500	chr3:8561306:8561355:	2.575619451	11.24311788	4.35467E-09
Slc17a6	ENSMUSG00000030500	chr7:58926243:58926291:	2.556824473	8.951167373	2.41203E-08
Atp1b1	ENSMUSG00000026576	chr1:166367693:166367742:-	2.524809565	10.87454203	2.16234E-08
Scg2	ENSMUSG00000050711	chr1:79431994:79432043:-	2.515681693	7.783009742	3.77762E-08
Dcxr	ENSMUSG00000039450	chr11:120587073:120587122:-	2.495223756	8.706675964	1.19653E-08
Mmp3	ENSMUSG00000043613	chr9:7455747:7455796:	2.482254928	7.943822559	7.2815E-06
Djc6	ENSMUSG00000028528	chr4:101315165:101315214:	2.474622792	9.914499928	1.47995E-07
Svop	ENSMUSG00000042078	chr5:114477006:114477055:-	2.460106771	10.42718912	2.2996E-08
Mmp3	ENSMUSG00000043613	chr9:7451773:7451822:	2.447018327	7.68048952	8.82638E-07
Lgals3	ENSMUSG00000050335	chr14:48005397:48005446:	2.441480013	7.607698099	9.88866E-06

Tmem130	ENSMUSG00000043388	chr5:145496876:145496925:-	2.43076195	9.338854613	2.16234E-08
Gad1	ENSMUSG00000070880	chr2:70439916:70439965:	2.429121842	8.167205651	1.82629E-06
Grp	ENSMUSG00000024517	chr18:66046055:66046104:	2.418855948	7.811330581	2.66787E-08
Cntp4	ENSMUSG00000031772	chr8:115406212:115406261:	2.387562498	8.745875467	4.35467E-09
Pacsin1	ENSMUSG00000040276	chr17:27847915:27847964:	2.342066261	8.735841391	1.35588E-08
Gad1	ENSMUSG00000070880	chr2:70439915:70439964:	2.340566895	7.974658351	1.65063E-06
Djc6	ENSMUSG00000028528	chr4:101315184:101315233:	2.325789271	9.521114953	1.43155E-07
Sv2b	ENSMUSG00000053025	chr7:82259830:82259879:-	2.288689286	8.189187745	2.2996E-08
Cav1	ENSMUSG00000007655	chr6:17291157:17291206:	2.288468925	10.0586779	3.87007E-07
Nrip3	ENSMUSG00000034825	chr7:116901635:116901684:-	2.2818558	8.673110708	1.01346E-06
2900011O08Rik	ENSMUSG00000044117	chr16:14100833:14100882:	2.270229597	9.314980426	2.79454E-07
Fabp3	ENSMUSG00000028773	chr4:129992430:129992479:	2.262100041	8.834149907	3.39061E-09
Lmo2	ENSMUSG00000032698	chr2:103821843:103821892:	2.254401831	8.190512678	2.16957E-07
Tbr1	ENSMUSG00000035033	chr2:61651395:61651444:	2.238999699	8.070376061	1.77532E-08
Fam131a	ENSMUSG00000050821	chr16:20702982:20703031:	2.236614017	9.22712188	1.95452E-07
Ly6h	ENSMUSG00000022577	chr15:75395640:75395689:-	2.231833574	10.87706077	4.55059E-08
Rcan2	ENSMUSG00000039601	chr17:44176265:44176314:	2.22182535	8.877080698	1.20269E-08
Kif5c	ENSMUSG00000026764	chr2:49630170:49630219:	2.215661607	11.15341511	2.28364E-08
Ly6h	ENSMUSG00000022577	chr15:75395616:75395665:-	2.214174919	10.45930638	5.66588E-08
Stmn4	ENSMUSG00000022044	chr14:66976798:66976847:	2.206613039	10.11676564	3.63044E-09
Rtn1	ENSMUSG00000021087	chr12:73337524:73337573:-	2.203553717	11.31133748	4.3113E-09
Gdf10	ENSMUSG00000021943	chr14:34748248:34748297:	2.199188375	7.517560479	4.55059E-08
AI593442	ENSMUSG00000078307	chr9:52484418:52484467:-	2.193317042	9.201835573	2.99635E-06
Rcan2	ENSMUSG00000039601	chr17:44175826:44175875:	2.181336141	8.046769738	1.20269E-08
Nsg2	ENSMUSG00000020297	chr11:31958836:31958885:	2.180971963	10.97788962	1.50773E-07
Caln1	ENSMUSG00000060371	chr5:131315937:131315986:	2.176833972	9.094014491	2.82618E-07
S100a11		chr3:93329926:93329975:	2.169173223	10.41362738	5.49827E-08
Areg	ENSMUSG00000029378	chr5:91577301:91577350:	2.167778653	8.026643158	2.92153E-07
Dcxr	ENSMUSG00000039450	chr11:120587755:120587804:-	2.166259784	8.505098604	3.35938E-07
Fibcd1	ENSMUSG00000026841	chr2:31668838:31668887:-	2.160798532	7.978420443	1.01294E-06
Mapt	ENSMUSG00000018411	chr11:104189419:104189468:	2.146886255	10.75848268	2.81094E-07
Rnf182	ENSMUSG00000044164	chr13:43763797:43763846:	2.141573487	8.367557989	3.45414E-07
2900011O08Rik	ENSMUSG00000044117	chr16:14094034:14094083:	2.140480839	8.58436942	1.92911E-07
Stmn4	ENSMUSG00000022044	chr14:66976793:66976842:	2.119520899	9.863605618	8.17687E-08
Sh3gl2	ENSMUSG00000028488	chr4:85035162:85035211:	2.102637762	11.33416393	5.47388E-08
Cend1	ENSMUSG00000060240	chr7:148612756:148612805:-	2.101009031	7.524457548	2.41203E-08
Sult4a1	ENSMUSG00000018865	chr15:83906555:83906604:-	2.099431402	10.11868332	2.61501E-08
Rasgrp1	ENSMUSG00000027347	chr2:117105869:117105918:-	2.098895785	7.242684921	6.97101E-07

Tspyl3	ENSMUSG00000074671	chr2:153048225:153048274:-	2.09486525	8.40713865	2.2996E-08
Ptpre	ENSMUSG00000041836	chr7:142877677:142877726:	2.092092511	8.260696395	3.31362E-08
Mcf2l	ENSMUSG00000031442	chr8:13020304:13020353:	2.090551433	9.280508461	2.45465E-07
Slit2	ENSMUSG00000031558	chr5:48696452:48696501:	2.090038756	7.87497841	1.20269E-08
Gap43	ENSMUSG00000047261	chr16:42248877:42248926:-	2.087275437	11.53065336	3.63044E-09
Nuak1	ENSMUSG00000020032	chr10:83834184:83834233:-	2.082625476	10.07655171	3.31476E-07
Thy1	ENSMUSG00000032011	chr9:43856488:43856537:	2.072401495	8.853765382	1.19653E-08
Gpr123	ENSMUSG00000025475	chr7:147063636:147063685:	2.069556471	7.905065947	6.97101E-07
Fas	ENSMUSG00000024778	chr19:34401880:34401929:	2.069230899	7.489627834	2.45465E-07
Btbd11	ENSMUSG00000020042	chr10:85122861:85122910:	2.069211427	8.985323271	2.41203E-08
Tmod1	ENSMUSG00000028328	chr4:46127321:46127370:	2.063744541	7.637228926	1.91711E-07
Anxa3	ENSMUSG00000029484	chr5:97274605:97274654:	2.038554257	11.06691478	7.20662E-08
6030405A18Rik	ENSMUSG00000056306	chr3:54701160:54701209:-	2.036936031	9.278467266	8.09756E-08
Plch2	ENSMUSG00000029055	chr4:154357524:154357573:-	2.036805881	7.876190957	9.64608E-07
Gabrg2	ENSMUSG00000020436	chr11:41725837:41725886:-	2.030760754	7.928915685	2.06092E-08
Rell2	ENSMUSG00000044024	chr18:38118769:38118817:	2.028252727	9.027106287	3.62344E-08
Mtap1b	ENSMUSG00000052727	chr13:100204461:100204510:-	2.025932458	10.42298499	1.96301E-07
Mmp3	ENSMUSG00000043613	chr9:7449846:7449895:	2.02144355	7.474403836	5.58056E-06
Anxa3	ENSMUSG00000029484	chr5:97274679:97274728:	2.020075017	11.54594614	3.63803E-07
Mllt11	ENSMUSG00000053192	chr3:95023109:95023158:-	2.019597566	12.3816904	4.92479E-08
Go1	ENSMUSG00000031748	chr8:96492013:96492062:	2.019141051	9.735326743	1.38868E-07
Eno2	ENSMUSG00000004267	chr6:124710401:124710450:-	2.014026421	9.330140048	4.92479E-08
Hspb8	ENSMUSG00000041548	chr5:116858761:116858810:-	2.010706053	7.789348153	3.31362E-08
Go1	ENSMUSG00000031748	chr8:96492548:96492597:	1.996494418	8.442032524	4.40713E-08
Ccng1	ENSMUSG00000020326	chr11:40564942:40564942:-,chr11:40564813:40564861:-	1.992059501	10.60455415	5.66588E-08
Syngr3	ENSMUSG00000007021	chr17:24822304:24822353:-	1.986896786	9.462028074	4.17833E-08
Tes	ENSMUSG00000029552	chr6:17055631:17055680:	1.980681543	8.745767617	4.92479E-08
Pqlc3	ENSMUSG00000045679	chr12:16995838:16995887:-	1.979675954	7.809520414	4.70894E-08
Prickle1	ENSMUSG00000036158	chr15:93329646:93329695:-	1.974491939	9.083180817	6.21833E-08
Eef1a2	ENSMUSG00000016349	chr2:180882407:180882456:-	1.974053655	9.032387031	1.75247E-07
Tuft1	ENSMUSG00000005968	chr3:94416746:94416795:-	1.971944848	8.334717091	4.17833E-08
Dcn	ENSMUSG00000019929	chr10:96980254:96980303:	1.971125126	8.067043625	3.13936E-07
Vsnl1	ENSMUSG00000054459	chr12:11332158:11332207:-	1.97088128	8.260572397	4.65576E-08
Ccl27a	ENSMUSG00000073888	chr4:41716429:41716478:-	1.968303059	9.347999498	1.42556E-07
A730017C20Rik	ENSMUSG00000050875	chr18:59236484:59236533:	1.959522056	8.312304399	2.15232E-07
Ccng1	ENSMUSG00000020326	chr11:40562289:40562338:-	1.958090673	11.37540147	1.21743E-07
Klc1	ENSMUSG00000021288	chr12:113032813:113032862:	1.953449832	10.81504311	1.10868E-06

Ly6h	ENSMUSG00000022577	chr15:75396044:75396093:-	1.952885	9.17657423	5.39063E-07
Gabrg2	ENSMUSG00000020436	chr11:41729812:41729861:-	1.950244774	7.55054332	1.06835E-07
Chst8	ENSMUSG00000060402	chr7:35459805:35459854:-	1.942490644	8.659563204	7.53135E-08
Trnp1	ENSMUSG00000056596	chr4:133047103:133047152:-	1.931656051	9.208277601	6.27541E-07
Adra2a	ENSMUSG00000033717	chr19:54123316:54123365:	1.929918993	8.361352755	7.85599E-08
Fezf2	ENSMUSG00000021743	chr14:13174738:13174787:-	1.927942807	8.046576599	7.53135E-08
Rspo3	ENSMUSG00000019880	chr10:29173225:29173274:-	1.923757881	7.945831128	6.86547E-06
Esm1	ENSMUSG00000042379	chr13:114008196:114008245:	1.920289958	7.102896459	2.11362E-05
Cadps	ENSMUSG00000054423	chr14:13205204:13205253:-	1.919061869	8.725552828	1.92911E-07
Syp	ENSMUSG00000031144	chrX:7230191:7230240:	1.898034595	10.29632774	4.12952E-08
Gabrg2	ENSMUSG00000020436	chr11:41725711:41725760:-	1.892929885	7.43053605	2.2996E-08
Syt1	ENSMUSG00000035864	chr10:107935530:107935579:-	1.89144225	8.438377927	2.15232E-07
Rnf182	ENSMUSG00000044164	chr13:43763554:43763603:	1.8808018	8.13866838	2.79454E-07
Olfm1	ENSMUSG00000026833	chr2:28085714:28085763:	1.875797215	9.995000514	1.92911E-07
Rprm	ENSMUSG00000075334	chr2:53936662:53936711:-	1.875294494	10.91626947	8.78918E-08
Arpp21	ENSMUSG00000032503	chr9:111968061:111968110:-	1.870623468	8.296374338	5.39063E-07
Rec8	ENSMUSG00000002324	chr14:56244151:56244200:	1.856569889	7.799583302	0.001091467
Clstn3	ENSMUSG00000008153	chr6:124380896:124380945:-	1.856226438	8.683786153	2.81094E-07
Nt	ENSMUSG00000067786	chr2:157387933:157387982:	1.852117025	9.238077986	0.000117476
Cplx1	ENSMUSG00000033615	chr5:108947597:108947646:-	1.851637969	10.97560419	3.36216E-08
Cdkn1a	ENSMUSG00000023067	chr17:29237186:29237235:	1.847923667	9.586610038	2.54291E-06
Acaa1b	ENSMUSG00000010651	chr9:119057258:119057307:-	1.84155876	7.479317049	3.82088E-08
Sv2a	ENSMUSG00000038486	chr3:95998908:95998957:	1.835107906	9.507716889	7.06899E-07
Epb4.9	ENSMUSG00000022099	chr14:71003542:71003591:-	1.834724434	7.798608148	2.62296E-08
Sytl2	ENSMUSG00000030616	chr7:97558600:97558649:	1.831148247	7.861867047	1.41537E-07
Trp53inp1	ENSMUSG00000028211	chr4:11100946:11100995:	1.830298498	10.2655528	1.43155E-07
Klc1	ENSMUSG00000021288	chr12:113032834:113032883:	1.82614945	10.15801374	1.92911E-07
Eef1a2	ENSMUSG00000016349	chr2:180882514:180882563:-	1.823473403	8.75781201	4.36499E-07
Vstm2l	ENSMUSG00000037843	chr2:157770386:157770435:	1.81994371	9.294811288	1.3439E-06
Ak1	ENSMUSG00000026817	chr2:32490205:32490254:	1.812141516	8.844321123	1.92801E-08

Timp2	ENSMUSG00000017466	chr11:118162613:118162662:-	1.810895398	10.19662	2.16234E-08
Olfm1	ENSMUSG00000026833	chr2:28068159:28068207:,chr 2:28069621:28069621:	1.799691634	9.920379689	9.21744E-08
Rbfox1	ENSMUSG00000008658	chr16:7409979:7410028:	1.799047784	9.817983368	4.02393E-07
Slc32a1	ENSMUSG00000037771	chr2:158441306:158441355:	1.797771387	8.391259383	8.75626E-05
Kif5a	ENSMUSG00000074657	chr10:126662984:126663033: -	1.796077292	8.306379628	1.78496E-07
Blcap	ENSMUSG00000067787	chr2:157382437:157382486:-	1.794392733	10.06205957	2.89363E-07
Cckbr	ENSMUSG00000030898	chr7:112584663:112584712:	1.785380679	7.146504096	5.07583E-06
Hs3st1	ENSMUSG00000051022	chr5:40005562:40005611:-	1.784891344	8.305792753	2.89363E-07
Mmp10	ENSMUSG00000047562	chr9:7509909:7509958:	1.77959258	7.408360027	1.10242E-05
Sema5a	ENSMUSG00000022231	chr15:32625932:32625981:	1.774912009	8.580051923	1.83568E-07
Ociad2	ENSMUSG00000029153	chr5:73714223:73714272:-	1.772175619	8.004075676	4.57133E-07
Ddit4l	ENSMUSG00000046818	chr3:137291137:137291186:	1.770586718	10.7134216	1.808E-08
Ralyl	ENSMUSG00000039717	chr3:14181876:14181925:	1.768528233	8.628420739	5.18295E-07
Gas6	ENSMUSG00000031451	chr8:13465655:13465704:-	1.76192312	9.880323627	1.41537E-07
Trim2	ENSMUSG00000027993	chr3:83967838:83967887:-	1.755468663	10.08747792	1.42864E-07
Dcx	ENSMUSG00000031285	chrX:140290608:140290657:-	1.74119828	10.19251291	8.23796E-07
AI836003	ENSMUSG00000029875	chr15:98000214:98000263:	1.737144718	7.417738872	1.32273E-07
Rab3a	ENSMUSG00000031840	chr8:73282334:73282383:	1.727763507	10.3493317	1.18815E-07
Bgn	ENSMUSG00000031375	chrX:70741170:70741219:	1.727321379	8.041803099	9.71782E-06
Odz4	ENSMUSG00000048078	chr7:104055104:104055153:	1.724782483	9.161422521	0.000523589
Dync1i1	ENSMUSG00000029757	chr6:5960517:5960566:	1.721550294	7.995802216	8.93206E-07
Rit2	ENSMUSG00000057455	chr18:31134123:31134172:-	1.716299129	7.506507438	9.39361E-07
Calb2	ENSMUSG00000003657	chr8:112676542:112676591:-	1.714541779	7.55915669	1.65208E-06
Ndrg4	ENSMUSG00000036564	chr8:98238732:98238781:	1.708167041	8.18665043	5.48069E-07
Pde4dip	ENSMUSG00000038170	chr3:97493882:97493931:-	1.706872128	8.644312708	6.38956E-07
Cartpt	ENSMUSG00000021647	chr13:100668836:100668885: -	1.705858647	7.017372228	2.22001E-06
Tmem108	ENSMUSG00000042757	chr9:103387036:103387085:-	1.705048218	8.148300203	1.92911E-07
Angpt2	ENSMUSG00000031465	chr8:18691380:18691429:-	1.702688529	11.81446131	3.07055E-06
Galnt9	ENSMUSG00000033316	chr5:111050240:111050289:	1.700348276	7.662434461	1.01294E-06
Nrn1	ENSMUSG00000039114	chr13:36817911:36817960:-	1.696379964	9.926411511	3.80341E-06
Syt5	ENSMUSG00000004961	chr7:4491693:4491742:-	1.695897671	8.059856393	7.8339E-07
Sv2a	ENSMUSG00000038486	chr3:95998899:95998948:	1.692011854	9.347718439	9.45522E-08
Darc	ENSMUSG00000037872	chr1:175262178:175262227:-	1.68896904	8.093282292	8.53537E-07
Dync1i1	ENSMUSG00000029757	chr6:5977664:5977713:	1.686579586	8.113504401	1.01346E-06
Dcx	ENSMUSG00000031285	chrX:140290666:140290715:-	1.684231646	9.491145661	2.03699E-06
H2afj	ENSMUSG00000060032	chr6:136758013:136758062:	1.682298386	8.638101067	2.41203E-08

cad	ENSMUSG00000041073	chr11:6498008:6498013:-,chr11:6497869:6497912:-	1.681478401	8.244357866	8.17687E-08
Chst1	ENSMUSG00000027221	chr2:92455211:92455260:	1.680292425	9.101702277	1.18815E-07
Cyb561	ENSMUSG00000019590	chr11:105795289:105795338:-	1.679939117	7.37190712	8.29358E-08
Nol4	ENSMUSG00000041923	chr18:22852231:22852280:-	1.676609433	8.413360579	3.41658E-07
Robo1	ENSMUSG00000022883	chr16:73045994:73046043:	1.675201732	9.610967844	2.1692E-06
Mcf2l	ENSMUSG00000031442	chr8:13020401:13020450:	1.669769501	8.399934295	4.92479E-08
cc2	ENSMUSG00000026932	chr2:25911166:25911215:-	1.669124834	9.189241302	1.55536E-07
Cdkn1a	ENSMUSG00000023067	chr17:29237369:29237418:	1.667947205	9.877105921	1.46882E-05
Igf2	ENSMUSG00000048583	chr7:149836752:149836801:-	1.664653071	7.828411996	0.000160784
Diras1	ENSMUSG00000043670	chr10:80482348:80482397:-	1.661271066	9.283155282	4.07309E-07
Hba-a1		chr11:32183968:32184017:	1.65715046	7.302464914	2.06092E-08
Tesc	ENSMUSG00000029359	chr5:118511628:118511677:	1.656347893	7.611160362	3.41658E-07
St6galc5		chr3:152483122:152483171:-	1.654307502	8.54231315	1.48508E-06
Mmp13	ENSMUSG00000050578	chr9:7283143:7283192:	1.654097488	7.226792443	1.32336E-05
Anxa5	ENSMUSG00000027712	chr3:36348108:36348157:-	1.652881873	9.938127549	1.58257E-06
Lhfpl2	ENSMUSG00000045312	chr13:94965110:94965159:	1.647603006	9.030595991	4.92479E-08
Snca	ENSMUSG00000025889	chr6:60681879:60681928:-	1.646299415	11.15278707	1.29019E-07
Slc5a3	ENSMUSG00000039680	chr16:92112240:92112289:	1.636044713	11.99037253	3.44844E-06
Cox6b2	ENSMUSG00000051811	chr7:4703418:4703467:-	1.633173019	8.019840646	9.84059E-08
Ppp2r2c	ENSMUSG00000029120	chr5:37345892:37345941:	1.629866551	7.563213571	1.10445E-06
Snca	ENSMUSG00000025889	chr6:60681957:60682006:-	1.628258265	9.528202769	5.72287E-07
l		chr19:47099097:47099146:	1.625918468	8.521409182	4.00582E-07
Psd2	ENSMUSG00000024347	chr18:36173787:36173836:	1.624943198	8.334698424	4.75685E-07
Apod	ENSMUSG00000022548	chr16:31311122:31311171:-	1.62473747	7.086391119	0.000109557
Pnma2	ENSMUSG00000046204	chr14:67538778:67538827:	1.612984572	8.991650905	3.44222E-08
Sgk1	ENSMUSG00000019970	chr10:21719378:21719427:	1.611904857	9.531845493	1.88475E-05
Mmp24	ENSMUSG00000027612	chr2:155643913:155643962:	1.60529566	8.174934961	7.20153E-07
Serpi3n	ENSMUSG00000021091	chr12:105652409:105652458:	1.603483213	7.090318409	9.77828E-07
Gabrb3	ENSMUSG00000033676	chr7:65083842:65083891:	1.597145817	9.114008125	3.95405E-07
Ccng1	ENSMUSG00000020326	chr11:40564431:40564480:-	1.594844326	9.478460554	2.36108E-07
Phlda3	ENSMUSG00000041801	chr1:137665353:137665402:	1.592953636	10.20114787	3.13689E-07
Epb4.1l1	ENSMUSG00000027624	chr2:156368591:156368640:	1.591169315	8.462519592	8.05352E-07
Stx1a	ENSMUSG00000007207	chr5:135526879:135526928:	1.586208129	9.606395721	2.48585E-07
Celsr3	ENSMUSG00000023473	chr9:108755165:108755214:	1.584060933	8.959934777	0.000465667
Scn3b	ENSMUSG00000049281	chr9:40098150:40098199:	1.583803018	7.576340611	1.18815E-07
Asphd1	ENSMUSG00000046378	chr7:134089612:134089661:-	1.580200878	7.429546901	1.33781E-07
Bcl11b	ENSMUSG00000048251	chr12:109153448:109153497:-	1.57898357	10.41051396	6.27541E-07

Sparc	ENSMUSG00000018593	chr11:55208464:55208512:-	1.577288069	10.2755909	2.82954E-06
Ifitm2	ENSMUSG00000060591	chr7:148141590:148141639:-	1.576071613	9.792638391	8.34197E-06
Slc6a17	ENSMUSG00000027894	chr3:107270475:107270524:-	1.565425808	7.860586166	1.06739E-07
Coro1a	ENSMUSG00000030707	chr7:133843446:133843495:-	1.56101597	9.036346817	8.7785E-07
Rab9b	ENSMUSG00000043463	chrX:133392799:133392848:-	1.555485033	7.924708364	4.4898E-07
Gabrb1	ENSMUSG00000029212	chr5:72500049:72500075:,chr 5:72513188:72513210:	1.554142511	7.179337715	4.71094E-06
Dusp4	ENSMUSG00000031530	chr8:35882724:35882773:	1.552207345	8.645648523	2.13608E-07
Slco1c1	ENSMUSG00000030235	chr6:141517967:141518016:	1.551608474	7.1895859	1.70358E-06
Fam177a	ENSMUSG00000095595; ENSMUSG00000094103	chr12:56240502:56240551:	1.551536507	9.148790812	2.85189E-08
Nmbr	ENSMUSG00000019865	chr10:14490179:14490228:	1.548290034	6.982584374	7.83822E-06
Actl6b	ENSMUSG00000029712	chr5:138008558:138008571:,c hr5:138010534:138010569:	1.54816387	7.478642945	4.55059E-08
Sparc	ENSMUSG00000018593	chr11:55223447:55223496:-	1.547015555	10.04784233	4.38271E-06
Sphkap		chr1:83252297:83252346:-	1.546101086	8.066206811	4.43263E-08
Pfkp	ENSMUSG00000021196	chr13:6597149:6597198:-	1.544214761	9.294381995	1.51009E-06
Cd200	ENSMUSG00000022661	chr16:45383222:45383271:-	1.544134724	7.683900329	1.82637E-07
Coro1a	ENSMUSG00000030707	chr7:133844098:133844104:-, chr7:133843944:133843986:-	1.540688854	8.616953543	5.05653E-06
C1qtnf4	ENSMUSG00000040794	chr2:90730244:90730293:	1.540108346	8.128104368	3.07055E-06
Erc2	ENSMUSG00000040640	chr14:29291366:29291415:	1.540099182	8.477300469	1.00777E-06
Nol4	ENSMUSG00000041923	chr18:22852007:22852056:-	1.533240258	8.282062745	2.16234E-08
Zcchc18	ENSMUSG00000031428	chrX:133530699:133530748:	1.528742344	11.96649502	1.5662E-07
Rtn1	ENSMUSG00000021087	chr12:73313115:73313164:-	1.528656163	12.76777479	6.78752E-08
Car2	ENSMUSG00000027562	chr3:14895036:14895085:	1.528403416	8.513604886	1.21003E-05
Cyba	ENSMUSG00000006519	chr8:124948937:124948986:-	1.527024552	8.36208744	3.40756E-06
Jakmip1	ENSMUSG00000063646	chr5:37516410:37516459:	1.525911926	8.452932689	2.69923E-07
Sema5a	ENSMUSG00000022231	chr15:32625930:32625979:	1.524443947	8.165986458	3.91387E-08
Syn1	ENSMUSG00000037217	chrX:20437762:20437811:-	1.521078006	9.319293951	6.48807E-07
Bzrap1	ENSMUSG00000034156	chr11:87599271:87599320:	1.520132559	8.242860785	0.000225839
Crtac1	ENSMUSG00000042401	chr19:42357579:42357628:-	1.518471175	8.259897097	1.75247E-07
Nefm	ENSMUSG00000022054	chr14:68738058:68738107:-	1.515836117	8.019515492	2.29911E-07
Fam49a	ENSMUSG00000020589	chr12:12382992:12383041:	1.509216845	11.22241568	1.8486E-07
Spnb3	ENSMUSG00000067889	chr19:4752085:4752134:	1.50887686	8.642651972	6.37974E-07
Rbfox3	ENSMUSG00000025576	chr11:118351137:118351186:-	1.503396685	9.591646781	4.44372E-06
Chl1	ENSMUSG00000030077	chr6:103664507:103664556:	1.502304322	8.154101782	3.19656E-06
Cds1	ENSMUSG00000029330	chr5:102252635:102252684:	1.501685973	7.573775576	1.8486E-07
Ank3	ENSMUSG00000069601	chr10:69486582:69486631:	1.498792043	7.727759177	5.0555E-06
Arhgap20	ENSMUSG00000053199	chr9:51661111:51661160:	1.497415601	7.853172965	3.31476E-07

Thrsp	ENSMUSG00000035686	chr7:104561925:104561974:-	1.495563566	7.642386893	5.98717E-06
Cxcl12	ENSMUSG00000061353	chr6:117123722:117123771:	1.495442364	7.621409194	1.81894E-05
Srxn1	ENSMUSG00000032802	chr2:151936737:151936786:	1.494015941	8.211751886	3.60929E-07
Actl6b	ENSMUSG00000029712	chr5:138010633:138010682:	1.493788159	8.043726136	5.79333E-08
Pdgfa		chr5:139452401:139452450:-	1.489629697	10.3562567	3.77845E-06
Ap3b2	ENSMUSG00000062444	chr7:88605505:88605554:-	1.485669753	8.154247865	3.87172E-07
Epb4.1l1	ENSMUSG00000027624	chr2:156368648:156368697:	1.484302248	7.951435058	2.85954E-07
Rab3d	ENSMUSG00000019066	chr9:21712036:21712085:-	1.483549804	8.636004454	1.63209E-06
Plcd4	ENSMUSG00000026173	chr1:74611086:74611086:,chr 1:74611606:74611654:	1.480037707	7.848661358	9.8647E-07
Pdlim1	ENSMUSG00000055044	chr19:40296825:40296874:-	1.475348383	9.642314335	6.36794E-06
Gria1	ENSMUSG00000020524	chr11:57131239:57131288:	1.474184178	7.53163032	7.11223E-07
Ccdc3	ENSMUSG00000026676	chr2:5151806:5151855:	1.471417515	7.718175262	3.94454E-06
Prokr2	ENSMUSG00000050558	chr2:132197621:132197670:-	1.467953611	7.09159689	7.59591E-07
Fam167a	ENSMUSG00000035095	chr14:64084105:64084154:	1.467395127	7.46668127	5.96321E-07
Cryab	ENSMUSG00000032060	chr9:50562673:50562722:	1.466903799	7.385390978	1.69477E-07
Bbc3	ENSMUSG00000002083	chr7:16903413:16903462:	1.46653538	10.56195948	8.22587E-06
Scg5	ENSMUSG00000023236	chr2:113616801:113616850:-	1.457333405	9.697319008	8.78553E-08
Spock3	ENSMUSG00000054162	chr8:65835353:65835402:	1.456479203	6.904682613	8.77299E-08
Galt	ENSMUSG00000036073	chr4:41705454:41705503:	1.454827289	9.054025247	9.87024E-07
Rps6kl1	ENSMUSG00000019235	chr12:86476728:86476777:-	1.442163396	8.383407709	9.82461E-07
Phlda3	ENSMUSG00000041801	chr1:137665204:137665253:	1.439996307	9.982855904	5.91254E-07
Celf4	ENSMUSG00000024268	chr18:25637894:25637943:-	1.439462875	7.844067149	2.28391E-07
Kctd12		chr14:103377115:103377164:-	1.435034956	8.075549303	3.50466E-08
Tmod2	ENSMUSG00000032186	chr9:75413566:75413615:-	1.43138446	9.93082255	4.19433E-07
Jazf1	ENSMUSG00000063568	chr6:52718931:52718980:-	1.431022232	8.175688136	1.71778E-06
Usp29	ENSMUSG00000051527	chr7:6919760:6919809:	1.430385766	7.596346532	1.77521E-06
Cck	ENSMUSG00000032532	chr9:121399159:121399208:-	1.427542075	7.113086974	0.000289589
Trp53inp1	ENSMUSG00000028211	chr4:11101237:11101286:	1.426349506	9.12772851	1.49726E-06
Tcfap2c	ENSMUSG00000028640	chr2:172384008:172384057:	1.425742604	7.452751666	1.25778E-06
Gz	ENSMUSG00000040009	chr10:74478486:74478535:	1.423760248	9.704529637	8.45842E-05
Rasgef1c	ENSMUSG00000020374	chr11:49793566:49793615:	1.417431688	7.136277537	5.58224E-07
Hbegf	ENSMUSG00000024486	chr18:36664987:36665036:-	1.417164234	8.571134635	1.18334E-06
Lrp11	ENSMUSG00000019796	chr10:7345037:7345086:	1.41287622	10.14675131	1.99205E-07
Sh3gl2	ENSMUSG00000028488	chr4:85031735:85031784:	1.412166468	8.132421041	5.25526E-06
1700047I17Rik2		chr12:56306718:56306767:	1.409038363	8.263563512	1.95389E-07
Chst2	ENSMUSG00000033350	chr9:95304928:95304977:-	1.406301071	8.640935002	1.25778E-06
Ppp1r13b	ENSMUSG00000021285	chr12:113067059:113067108:-	1.403195846	7.698985952	6.27541E-07

Tiam2	ENSMUSG00000023800	chr17:3519205:3519254:	1.398685319	7.925093508	2.79228E-08
D3Bwg0562e	ENSMUSG00000044667	chr3:117022692:117022741:-	1.395678491	7.303336329	1.18815E-07
Rell2	ENSMUSG00000044024	chr18:38116138:38116187:	1.395650978	7.327177225	5.58129E-06
Rab15	ENSMUSG00000021062	chr12:77899014:77899063:-	1.38931792	9.36535627	5.85376E-07
Dos	ENSMUSG00000035640	chr10:79593419:79593468:-	1.387282526	9.779515792	1.76054E-07
Aak1	ENSMUSG00000057230	chr6:86941544:86941593:	1.383512553	7.931953011	6.05376E-08
Gpr176	ENSMUSG00000040133	chr2:118103002:118103051:-	1.381988986	7.452157119	9.8759E-08
Rab6b	ENSMUSG00000032549	chr9:103087402:103087451:	1.381689626	10.79156815	2.86241E-07
Mapk8	ENSMUSG00000021936	chr14:34191151:34191200:-	1.375550118	9.178409896	1.99205E-07
Mmp2	ENSMUSG00000031740	chr8:95377093:95377142:	1.373938797	8.191793923	4.52213E-06
Celf4	ENSMUSG00000024268	chr18:25649671:25649720:-	1.37366297	7.457681447	4.56165E-06
Inpp5f	ENSMUSG00000042105	chr7:135839572:135839621:	1.373555807	11.80476951	1.32273E-07
Pqlc3	ENSMUSG00000045679	chr12:17000259:17000303:-,chr12:16999121:16999125:-	1.372368666	7.418043451	1.92911E-07
Adcy2	ENSMUSG00000021536	chr13:68759059:68759108:-	1.371202853	8.537707575	1.67168E-07
Emp3	ENSMUSG00000040212	chr7:53175687:53175736:-	1.371058046	7.105142823	1.24635E-06
Gdap1	ENSMUSG00000025777	chr1:17154189:17154238:	1.367903097	10.07210335	4.13035E-07
Ef5	ENSMUSG00000048915	chr17:62954145:62954194:-	1.367418109	8.724209202	3.93683E-07
Slc17a7	ENSMUSG00000070570	chr7:52431216:52431265:	1.364526413	7.094169546	1.63209E-06
Mapre2	ENSMUSG00000024277	chr18:24052231:24052280:	1.35981669	11.07705071	2.73941E-07
Chd5	ENSMUSG00000005045	chr4:151764083:151764132:	1.357769194	7.739524501	4.70794E-05
Prkcz	ENSMUSG00000029053	chr4:154634242:154634291:-	1.35669466	9.496388258	2.85954E-07
Tubb4	ENSMUSG00000062591	chr17:57219644:57219693:-	1.356426947	8.049779824	7.39652E-07
Tagln3	ENSMUSG00000022658	chr16:45711612:45711661:-	1.356336053	10.13445107	7.57474E-05
Rhod	ENSMUSG00000041845	chr19:4425825:4425874:-	1.354487382	8.405001253	5.66588E-08
S100a6	ENSMUSG00000001025	chr3:90418228:90418277:	1.351071931	7.563896229	1.80269E-05
Angpt2	ENSMUSG00000031465	chr8:18714160:18714209:-	1.350151067	8.058752108	1.58618E-06
Coro1a	ENSMUSG00000030707	chr7:133845556:133845605:-	1.349628477	7.70156967	1.30002E-06
Slco3a1	ENSMUSG00000025790	chr7:81429226:81429275:-	1.349400217	8.2408985	7.13949E-06
Rusc2	ENSMUSG00000035969	chr4:43439820:43439869:	1.346828164	10.36276672	2.30037E-06
Tbc1d9	ENSMUSG00000031709	chr8:85795693:85795742:	1.346614308	8.343568063	1.96301E-07
Hsd11b1	ENSMUSG00000016194	chr1:195048145:195048194:-	1.335865106	6.881133541	3.72559E-07
Col4a1	ENSMUSG00000031502	chr8:11198791:11198840:-	1.335469112	7.793427814	0.000400716
Rtn1	ENSMUSG00000021087	chr12:73313088:73313137:-	1.334567296	12.52604461	7.20153E-07
Serpini1	ENSMUSG00000027834	chr3:75445770:75445819:	1.334123748	7.91217935	1.74444E-06
Fas	ENSMUSG00000024778	chr19:34391081:34391130:	1.332737983	7.22823441	1.36462E-06
Rapgef4	ENSMUSG00000049044	chr2:72091024:72091051:,chr2:72094306:72094327:	1.325422057	7.443745187	3.15182E-07
Gdap1	ENSMUSG00000025777	chr1:17153992:17154041:	1.325020748	8.804275455	5.18726E-07

Mbp	ENSMUSG00000041607	chr18:82727885:82727934:	1.323972877	7.370259274	2.24903E-05
Romo1	ENSMUSG00000067847	chr2:155970134:155970183:	1.320183577	7.569573201	2.2475E-06
Pcdh20	ENSMUSG00000050505	chr14:88865883:88865932:-	1.31992097	7.514919356	5.63484E-06
Atp6v1g2	ENSMUSG00000024403	chr17:35375614:35375663:	1.318069978	8.899954944	8.57452E-08
March4	ENSMUSG00000039372	chr1:72473836:72473885:-	1.316982598	7.760250943	1.64925E-06
Stxbp1	ENSMUSG00000026797	chr2:32643520:32643569:-	1.315614341	11.63447956	6.14457E-07
Kcnk1	ENSMUSG00000033998	chr8:128554409:128554458:	1.313573053	7.984367798	1.43155E-07
Cxadr	ENSMUSG00000022865	chr16:78340631:78340680:	1.30957845	10.41812336	8.28783E-06
Slc24a3	ENSMUSG00000063873	chr2:145467619:145467668:	1.309455893	9.30403583	1.06978E-06
Col6a1	ENSMUSG00000001119	chr10:76171561:76171610:-	1.308545252	6.909411287	4.06391E-05
Elmod1	ENSMUSG00000041986	chr9:53767420:53767469:-	1.307960202	8.031414068	2.96492E-07
Cplx2	ENSMUSG00000025867	chr13:54479987:54480036:	1.302861246	8.335773122	1.50338E-05
Rnf208	ENSMUSG00000044628	chr2:25099692:25099741:	1.301707586	10.35032643	5.35937E-06
Syt4	ENSMUSG00000024261	chr18:31599054:31599103:-	1.298047948	11.22266993	4.98603E-05
Dpysl5	ENSMUSG00000029168	chr5:31101562:31101611:	1.295673273	9.306479972	3.60042E-06
Cav2	ENSMUSG00000000058	chr6:17231898:17231947:	1.294606471	7.687307065	1.35319E-05
Uchl1	ENSMUSG00000029223	chr5:67078100:67078149:	1.294441457	10.67791886	2.30367E-07
Fbll1	ENSMUSG00000051062	chr11:35611270:35611319:-	1.293855876	7.604465482	3.36514E-05
Elavl3	ENSMUSG00000003410	chr9:21822543:21822592:-	1.293782681	8.302549067	4.38271E-06
Vamp2	ENSMUSG00000020894	chr11:68905817:68905866:	1.293750517	10.12071718	1.06739E-07
Sorl1	ENSMUSG00000049313	chr9:41782068:41782117:-	1.291731228	7.668288415	8.46226E-06
Snph	ENSMUSG00000027457	chr2:151416409:151416458:-	1.287711392	7.701278948	4.17833E-08
Prkcz	ENSMUSG00000029053	chr4:154636543:154636592:-	1.28391557	8.209945629	6.14359E-06
Tmem35	ENSMUSG00000033578	chrX:130839990:130840039:	1.283276939	9.575966528	1.34795E-05
Adora1	ENSMUSG00000042429	chr1:136098200:136098249:-	1.282920327	8.62133925	3.06116E-07
Abat	ENSMUSG00000057880	chr16:8621538:8621587:	1.281425983	9.350388983	0.000139825
Epb4.9	ENSMUSG00000022099	chr14:71003803:71003852:-	1.280267586	7.060330299	2.15232E-07
Mpped1	ENSMUSG00000041708	chr15:83688601:83688650:	1.277337091	9.582032616	2.43317E-06
Elmo1	ENSMUSG00000041112	chr13:20698099:20698148:	1.275431738	10.98764753	1.09268E-07
Rasl11b	ENSMUSG00000049907	chr5:74595297:74595346:	1.274306407	9.297467333	7.28793E-06
Lm	ENSMUSG00000028063	chr3:88287992:88288041:-	1.273096152	9.126791671	4.17603E-06
Stmn3	ENSMUSG00000027581	chr2:181041947:181041996:-	1.272809242	10.27669129	2.19763E-06
Mast1	ENSMUSG00000053693	chr8:87435893:87435942:-	1.272014436	7.868236767	4.94047E-06
Scg3	ENSMUSG00000032181	chr9:75491634:75491683:-	1.271694144	9.714292127	1.0313E-06
Vamp8	ENSMUSG00000050732	chr6:72335493:72335542:-	1.270303121	7.089104023	1.75247E-07
Prmt2	ENSMUSG00000020230	chr10:75670186:75670235:-	1.270205989	11.42276125	3.60929E-07
1300014I06Rik	ENSMUSG00000021411	chr13:34720338:34720387:-	1.267420337	7.703133413	2.76475E-06
Prmt2	ENSMUSG00000020230	chr10:75670130:75670179:-	1.265601024	11.81964109	1.78211E-07

Nell2	ENSMUSG00000022454	chr15:95050515:95050564:-	1.265417024	8.969848739	4.17582E-05
Stxbp2	ENSMUSG00000004626	chr8:3642663:3642712:	1.263570768	7.701598744	0.000122338
Dlg2	ENSMUSG00000052572	chr7:99597248:99597297:	1.262277712	7.358898574	5.19344E-08
Klk8	ENSMUSG00000064023	chr7:51059063:51059112:	1.261505047	7.600696854	6.46152E-07
Olfml2b	ENSMUSG00000038463	chr1:172612689:172612738:	1.260819968	8.088075454	1.3439E-06
Rab11fip5	ENSMUSG00000051343	chr6:85285117:85285166:-	1.258884826	8.779356843	2.97106E-07
Dusp8	ENSMUSG00000037887	chr7:149267582:149267631:-	1.258654284	8.940153621	5.36415E-07
Serpinf1	ENSMUSG00000000753	chr11:75223539:75223588:-	1.25393558	7.885276043	0.002544778
Dpysl3	ENSMUSG00000024501	chr18:43487995:43488044:-	1.252911247	11.88338934	2.28101E-06
Gprasp1	ENSMUSG00000043384	chrX:132337741:132337790:	1.252576236	11.0612465	1.8922E-06
Arhgdib	ENSMUSG00000030220	chr6:136872439:136872488:-	1.250141948	6.995491172	3.02802E-06
Prl2c3	ENSMUSG00000056457	chr13:12892287:12892336:-	1.247544524	7.007402757	8.82584E-05
Wnt8b	ENSMUSG00000036961	chr19:44586929:44586978:	1.246763115	6.958548289	0.000126085
Pik3r3	ENSMUSG00000028698	chr4:115975245:115975294:	1.245068267	10.66864486	1.43155E-07
Ctsk	ENSMUSG00000028111	chr3:95313042:95313091:	1.244188763	7.340596606	0.000100508
Ifi27l1	ENSMUSG00000064215	chr12:104678303:104678352:	1.242461905	7.175148119	5.2773E-06
Gprin1	ENSMUSG00000069227	chr13:54838057:54838106:-	1.237231092	10.98180776	2.19747E-06
Ctxn1	ENSMUSG00000048644	chr8:4257928:4257977:-	1.236871713	9.2591253	4.18521E-06
Myt1l	ENSMUSG00000061911	chr12:30604856:30604903:,chr12:30605206:30605207:	1.236591188	8.265914648	2.90382E-05
Spsb1	ENSMUSG00000039911	chr4:149270463:149270512:-	1.236521099	8.380636787	1.6236E-06
Cd200	ENSMUSG00000022661	chr16:45382738:45382786:-	1.2363346	7.042267836	1.13944E-06
Trnp1	ENSMUSG00000056596	chr4:133047240:133047289:-	1.232447852	6.972821237	4.07739E-05
6330403K07Rik		chr11:70845729:70845778:-	1.230742455	11.09344496	5.30344E-06
Mapre2	ENSMUSG00000024277	chr18:24051899:24051948:	1.228591411	8.578536096	9.39161E-08
Srxn1	ENSMUSG00000032802	chr2:151935522:151935571:	1.227383729	7.722699703	5.6218E-06
Crmp1	ENSMUSG00000029121	chr5:37682791:37682840:	1.22439088	9.984347251	2.39855E-06
Gucy1a3	ENSMUSG00000033910	chr3:81896463:81896512:-	1.220010881	8.984168401	4.30393E-05
Fam164a	ENSMUSG00000043542	chr3:7553480:7553529:	1.219125027	10.47978003	3.57661E-07
Nxph2	ENSMUSG00000069132	chr2:23257259:23257308:	1.219081543	7.615116785	8.96466E-05
Otx2	ENSMUSG00000021848	chr14:49278180:49278229:-	1.217321625	7.0359337	1.22393E-05
Ifi27l1	ENSMUSG00000064215	chr12:104678265:104678314:	1.216913799	7.214111122	3.57536E-06
Sh3gl2	ENSMUSG00000028488	chr4:85031737:85031786:	1.215425653	7.695029734	1.09035E-05
Klhl8	ENSMUSG00000029312	chr5:104291504:104291553:-	1.214253516	7.740338518	1.67693E-07
Arpp21	ENSMUSG00000032503	chr9:112083679:112083728:-	1.213058344	8.429542804	2.24243E-07
Cdh13	ENSMUSG00000031841	chr8:121836613:121836635:,chr8:121837873:121837899:	1.212331985	9.633227147	1.07729E-05
cad	ENSMUSG00000041073	chr11:6498272:6498318:-,chr11:6498128:6498130:-	1.211379897	8.044227192	8.09128E-07
Phactr1	ENSMUSG00000054728	chr13:43233690:43233739:	1.210085368	8.078660952	5.6305E-07

Id4	ENSMUSG00000021379	chr13:48358659:48358708:	1.210044041	8.245098317	4.2001E-06
Rbbp6	ENSMUSG00000030779	chr7:130123025:130123074:	1.209714598	7.445424293	1.75009E-06
Plcd4	ENSMUSG00000026173	chr1:74589552:74589601:	1.206752698	7.097562626	1.21213E-07
Syn1	ENSMUSG00000037217	chrX:20437659:20437708:-	1.203838733	9.537161951	2.03699E-06
Id2	ENSMUSG00000020644	chr12:25779265:25779314:-	1.203785981	9.670603036	2.90449E-07
Adcy8	ENSMUSG00000022376	chr15:64530760:64530809:-	1.202148231	7.703459064	2.44118E-06
Cxadr	ENSMUSG00000022865	chr16:78340725:78340774:	1.201837502	11.03273792	8.03394E-06
Lum	ENSMUSG00000036446	chr10:97034583:97034632:	1.200760011	7.004516209	2.60538E-05
Tceal1	ENSMUSG00000049536	chrX:133243792:133243841:	1.20033471	7.731393934	9.85798E-06
Camkv	ENSMUSG00000032936	chr9:107851695:107851744:	1.196565894	7.654221297	5.79895E-06
St8sia5	ENSMUSG00000025425	chr18:77493863:77493912:	1.196541567	6.92856957	5.85376E-07
Ldb2	ENSMUSG00000039706	chr5:44864103:44864152:-	1.195744856	8.912185152	2.21865E-06
Atp2b2	ENSMUSG00000030302	chr6:113695955:113696004:-	1.193905287	7.056737059	1.61284E-06
Col4a2	ENSMUSG00000031503	chr8:11448896:11448945:	1.191543517	7.194201709	9.78857E-05
Palm	ENSMUSG00000035863	chr10:79283446:79283495:	1.190643215	8.960902778	1.82394E-07
Serpinb6a	ENSMUSG00000060147	chr13:34009975:34010024:-	1.189409927	9.070390334	1.14104E-05
Rab3b	ENSMUSG00000003411	chr4:108615728:108615777:	1.188529433	7.389992947	1.58504E-06
Pqlc3	ENSMUSG00000045679	chr12:16995783:16995832:-	1.187662818	6.846165999	7.71069E-06
6430598A04Rik	ENSMUSG00000045348	chr5:138172497:138172546:-	1.186636715	7.609538558	1.92911E-07
Kalrn	ENSMUSG00000061751	chr16:33975469:33975518:-	1.18626242	7.515412479	0.00052405
Reep5	ENSMUSG00000005873	chr18:34504768:34504817:-	1.184406492	9.967773343	5.19708E-07
Sphk1	ENSMUSG00000061878	chr11:116397901:116397950:	1.183056931	8.618935771	2.49425E-05
Rprml	ENSMUSG00000046215	chr11:103511773:103511822:	1.181451273	7.079403068	7.66899E-05
Wdr6	ENSMUSG00000066357	chr9:108475117:108475166:-	1.180246342	10.03662804	8.72337E-06
Cxcl12	ENSMUSG00000061353	chr6:117121533:117121582:	1.179035478	7.42130637	0.000154668
Sgip1	ENSMUSG00000028524	chr4:102643467:102643516:	1.178858742	7.58809274	7.2815E-06
Hist2h2aa1	ENSMUSG00000064220; ENSMUSG00000063954	chr3:96043643:96043692:-	1.178507308	7.226670962	8.78918E-08
Synm	ENSMUSG00000030554	chr7:74877798:74877847:-	1.178397335	7.312797775	1.21743E-07
Enpp5	ENSMUSG00000023960	chr17:44223309:44223358:	1.17830953	9.18641706	4.13157E-07
Ercc5	ENSMUSG00000026048	chr1:44237738:44237787:	1.175718861	10.17316826	1.79293E-06
4833424O15Rik	ENSMUSG00000033342	chr3:117392050:117392099:	1.175180651	7.946386105	2.56275E-06
Hsbp1	ENSMUSG00000031839	chr8:121872380:121872429:	1.174229731	11.20518592	3.67453E-06
Lix1	ENSMUSG00000047786	chr17:17539897:17539946:	1.173748386	8.519456963	8.82102E-06
Cort	ENSMUSG00000028971	chr4:148499316:148499365:-	1.170936202	6.976043168	5.56538E-05
Dcn	ENSMUSG00000019929	chr10:96969288:96969337:	1.170439863	7.080771308	1.73367E-05
Fam155a	ENSMUSG00000079157	chr8:9206089:9206138:-	1.165354038	8.981435061	4.07309E-07
AI593442	ENSMUSG00000078307	chr9:52482564:52482613:-	1.164136503	7.001704068	5.65904E-06

Sema4f	ENSMUSG00000000627	chr6:82862085:82862134:-	1.163708915	6.994479849	7.52977E-06
Zbtb8b	ENSMUSG00000048485	chr4:129103778:129103827:-	1.162733033	7.090001746	3.2831E-07
Fam49b	ENSMUSG00000022378	chr15:63760888:63760937:-	1.161429943	9.223330008	1.63209E-06
Gxylt2	ENSMUSG00000030074	chr6:100754964:100755013:	1.160697045	7.193890867	2.37713E-05
Pmaip1	ENSMUSG00000024521	chr18:66624125:66624174:	1.160419603	7.098515009	2.91874E-07
Fbxo32	ENSMUSG00000022358	chr15:58011999:58012048:-	1.158871143	7.519761486	2.76761E-06
Sln	ENSMUSG00000042045	chr9:53701457:53701506:	1.157411443	6.681577648	0.000255785
Pak3	ENSMUSG00000031284	chrX:140225796:140225845:	1.154347945	10.27632821	9.8647E-07
Ptpro	ENSMUSG00000030223	chr6:137411117:137411166:	1.15414939	9.48725861	5.87305E-06
Mgst3	ENSMUSG00000026688	chr1:169302611:169302660:-	1.153721953	9.467994701	4.02025E-05
Smarca2	ENSMUSG00000024921	chr19:26852604:26852653:	1.150417294	11.14579806	5.5677E-07
Col6a1	ENSMUSG00000001119	chr10:76171758:76171807:-	1.148078218	6.823241547	4.38345E-05
Fry	ENSMUSG00000056602	chr5:151299954:151300003:	1.14618966	7.596902742	2.79454E-07
Sparcl1	ENSMUSG00000029309	chr5:104508469:104508518:-	1.145820148	7.77112248	2.23255E-05
Gpr83	ENSMUSG00000031932	chr9:14673626:14673675:	1.145135438	7.284610618	5.14922E-06
Ube2n	ENSMUSG00000074781	chr10:95007923:95007972:	1.14436195	10.20606701	9.39361E-07
D10Bwg1379e	ENSMUSG00000019852	chr10:18308109:18308158:-	1.141355001	7.322052304	7.6288E-06
Apoe	ENSMUSG00000002985	chr7:20281959:20282008:-	1.139814357	8.740644181	4.6615E-05
Gprasp1	ENSMUSG00000043384	chrX:132337156:132337205:	1.138972528	9.034103337	4.51532E-06
Rusc2	ENSMUSG00000035969	chr4:43439817:43439866:	1.136552022	10.11118859	1.96301E-07
Cdh13	ENSMUSG00000031841	chr8:121029560:121029609:	1.136438408	8.992381257	2.20225E-05
Cxxc4	ENSMUSG00000044365	chr3:133924778:133924827:	1.134660786	8.039421107	2.9149E-05
Znrf2	ENSMUSG00000058446	chr6:54839346:54839395:	1.132034522	10.10767121	3.52166E-05
Sulf1	ENSMUSG00000016918	chr1:12850255:12850304:	1.131128778	7.098593743	0.001623072
Lm	ENSMUSG00000028063	chr3:88287147:88287196:-	1.130215095	10.01034502	6.46952E-06
Fam129b	ENSMUSG00000026796	chr2:32780677:32780726:	1.127959717	9.274671248	1.154E-06
Rasl11b	ENSMUSG00000049907	chr5:74595389:74595438:	1.126473351	9.102526341	9.92881E-06
1110008P14Rik	ENSMUSG00000039195	chr2:32234748:32234797:-	1.125247243	9.703635023	2.81678E-06
Arg2	ENSMUSG00000021125	chr12:80257029:80257078:	1.124801131	6.786326544	3.32465E-05
Nell2	ENSMUSG00000022454	chr15:95126620:95126669:-	1.124423921	7.683971936	1.62642E-05
Cdk5r1	ENSMUSG00000048895	chr11:80294579:80294628:	1.121093637	12.2981684	6.97101E-07
Ptprd	ENSMUSG00000028399	chr4:75587440:75587489:-	1.120868899	9.627907625	9.58355E-05
Sez6l2	ENSMUSG00000030683	chr7:134111756:134111770:,chr7:134113567:134113601:	1.120868514	7.365234441	2.81277E-05
Slc8a1	ENSMUSG00000054640	chr17:81785132:81785181:-	1.11945554	8.586064591	1.41562E-06
Rab11fip5	ENSMUSG00000051343	chr6:85285122:85285171:-	1.119145441	8.361165204	1.72526E-07
Prokr1	ENSMUSG00000049409	chr6:87528629:87528678:-	1.118350685	7.84538473	6.56165E-05
Palm	ENSMUSG00000035863	chr10:79283071:79283120:	1.117068433	7.696684805	9.37161E-06

Ephx4	ENSMUSG00000033805	chr5:107848803:107848852:	1.115932796	7.801309688	2.39935E-05
Runx1t1	ENSMUSG00000006586	chr4:13818157:13818206:	1.11440567	8.411079559	4.38271E-06
S100a10	ENSMUSG00000041959	chr3:93368411:93368460:	1.113590756	9.359746261	0.000115617
Cartpt	ENSMUSG00000021647	chr13:100668905:100668954:-	1.113379666	6.948556243	3.11239E-05
Dapk1	ENSMUSG00000021559	chr13:60864054:60864103:	1.109155155	7.54707686	5.99411E-06
Slc40a1	ENSMUSG00000025993	chr1:45965105:45965154:-	1.108896015	7.005308082	0.000385845
Stac	ENSMUSG00000032502	chr9:111463994:111464043:-	1.108149493	7.824796282	1.55474E-06
Akr1c13		chr13:4193303:4193352:	1.107900576	6.887981086	7.52511E-05
Apbb1	ENSMUSG00000037032	chr7:112707107:112707156:-	1.106281268	9.728152909	1.22799E-06
Rufy3	ENSMUSG00000029291	chr5:89071420:89071469:	1.105323489	10.2103124	7.00624E-07
Enc1	ENSMUSG00000041773	chr13:98022565:98022614:	1.104067136	11.39710176	4.35628E-06
Aplp1	ENSMUSG00000006651	chr7:31220310:31220359:-	1.102967891	8.021406656	2.01231E-06
Cacng5	ENSMUSG00000040373	chr11:107736236:107736285:-	1.100982584	8.829165747	0.00294654
Sel1l3	ENSMUSG00000029189	chr5:53498590:53498639:-	1.100142722	8.094248516	5.14922E-06
Emid2	ENSMUSG00000004415	chr5:137217674:137217723:-	1.100047935	7.558294677	9.63396E-05
Lix1	ENSMUSG00000047786	chr17:17580656:17580705:	1.098708703	8.192972569	0.00026867
Larp6	ENSMUSG00000034839	chr9:60586214:60586263:	1.098290039	7.96587205	5.25347E-06
Nuak1	ENSMUSG00000020032	chr10:83834497:83834546:-	1.097022448	7.296151585	2.21532E-05
Prkar1b	ENSMUSG00000025855	chr5:139493573:139493622:-	1.096412313	7.458235581	8.336E-07
Ccnd2	ENSMUSG00000000184	chr6:127079637:127079686:-	1.096115927	12.70141098	1.50742E-06
Parp6	ENSMUSG00000025237	chr9:59497979:59498028:	1.095095201	9.694326566	1.13944E-06
Igfbp7	ENSMUSG00000036256	chr5:77778386:77778435:-	1.094953039	7.657986969	0.001616895
Stx7	ENSMUSG00000019998	chr10:23908324:23908373:	1.094155907	11.09567248	4.55649E-06
Mapkapk3	ENSMUSG00000032577	chr9:107157498:107157547:-	1.092445947	7.77487617	8.43085E-07
Crhbp	ENSMUSG00000021680	chr13:96201660:96201709:-	1.092408343	7.290267069	0.002868347
Gstt3	ENSMUSG00000001665	chr10:75236901:75236950:-	1.092385507	6.964957921	3.9429E-05
Hecw2	ENSMUSG00000042807	chr1:53987687:53987736:-	1.092055365	7.192433843	1.45705E-06
Gria1	ENSMUSG00000020524	chr11:57140964:57141013:	1.087885038	7.110642657	5.66565E-05
Atp2a2	ENSMUSG00000029467	chr5:122903757:122903806:-	1.087702029	10.67066389	1.53688E-05
Tmem120a	ENSMUSG00000039886	chr5:136211545:136211594:-	1.087234515	9.950136743	3.60257E-07
Fbxo25	ENSMUSG00000038365	chr8:13940328:13940377:	1.087198249	9.534788223	4.74937E-06
Ngfr	ENSMUSG00000000120	chr11:95430274:95430323:-	1.087172322	7.117541049	7.70466E-06
Pja2	ENSMUSG00000024083	chr17:64632511:64632560:-	1.087139933	11.2141633	1.87919E-06
gk	ENSMUSG00000034744	chr6:83746931:83746980:	1.085525666	9.901334309	0.001035789
Eif4a2	ENSMUSG00000022884	chr16:23111608:23111657:	1.085381392	11.557299	1.93493E-05
Ppp2r2b	ENSMUSG00000024500	chr18:43058456:43058505:-	1.085320239	8.651709637	6.21925E-06
Bhlhe22	ENSMUSG00000025128	chr3:17957205:17957254:	1.085215013	7.359952608	0.000178421

Iqsec3	ENSMUSG00000040797	chr6:121323200:121323249:-	1.084965664	7.018813918	1.87993E-05
G14	ENSMUSG00000024697	chr19:16685191:16685240:	1.082088409	7.716171721	9.08256E-05
Trafd1	ENSMUSG00000042726	chr5:121821820:121821869:-	1.081813239	10.45758887	9.93102E-06
Mpp3	ENSMUSG00000052373	chr11:101861578:101861627:-	1.080429838	7.92407837	6.3613E-06
Pfkp	ENSMUSG00000021196	chr13:6620232:6620281:-	1.077939556	8.059127223	1.66477E-06
Rac3	ENSMUSG00000018012	chr11:120584580:120584629:	1.077133122	8.379488042	5.36767E-07
Ccnd1	ENSMUSG00000070348	chr7:152115983:152116032:-	1.07519144	13.5660612	0.000180837
Csdc2	ENSMUSG00000042109	chr15:81781303:81781352:	1.074477496	8.49910616	3.38843E-06
Sat1	ENSMUSG00000025283	chrX:151647992:151648041:-	1.070942068	9.85732332	6.43262E-05
Gria1	ENSMUSG00000020524	chr11:57140966:57141015:	1.067557804	7.058504797	7.31322E-05
Sqstm1	ENSMUSG00000015837	chr11:50014169:50014218:-	1.067440308	10.85734629	5.21435E-06
Slc1a1	ENSMUSG00000024935	chr19:28988294:28988343:	1.06705227	8.380297679	5.25347E-06
Ptprd	ENSMUSG00000028399	chr4:75587454:75587503:-	1.064120575	9.554428797	3.25708E-05
Pltp	ENSMUSG00000017754	chr2:164665235:164665284:-	1.062746883	7.136324081	9.16173E-07
Dclk1	ENSMUSG00000027797	chr3:55340502:55340551:	1.057431805	10.06283318	6.11286E-07
Prr13	ENSMUSG00000023048	chr15:102293096:102293145:	1.057205197	11.29868501	8.34197E-06
Dkk3	ENSMUSG00000030772	chr7:119259613:119259662:-	1.057088807	8.496529464	0.001301342
Ica1l	ENSMUSG00000026018	chr1:60045940:60045989:-	1.056035679	7.040963418	4.72036E-06
Gatsl3	ENSMUSG00000020424	chr11:4122291:4122340:	1.0550861	7.175078265	8.16337E-07
Ccl27a	ENSMUSG00000073888	chr4:41716717:41716766:-	1.054164876	7.512302365	6.65037E-07
Eps8	ENSMUSG00000015766	chr6:137430688:137430737:-	1.050554472	7.895311834	7.11223E-07
Npas4	ENSMUSG00000045903	chr19:4984596:4984645:-	1.049277863	6.803222313	0.000276507
Cstb	ENSMUSG00000005054	chr10:77890170:77890219:	1.048619923	12.09120066	1.02855E-06
Plcd4	ENSMUSG00000026173	chr1:74611689:74611738:	1.04722381	6.9386931	1.83188E-05
Ifitm3	ENSMUSG00000025492	chr7:148195586:148195635:-	1.042435134	9.114646336	0.000483992
Dlk2	ENSMUSG00000047428	chr17:46440050:46440099:	1.041723002	8.181758378	4.56165E-06
Timp1	ENSMUSG00000001131	chrX:20451675:20451724:	1.041297459	8.7373742	6.83928E-06
Ptpro	ENSMUSG00000030223	chr6:137368850:137368899:	1.041244916	7.35270241	8.34197E-06
Socs2	ENSMUSG00000020027	chr10:94875043:94875092:-	1.040983584	9.659035929	1.80427E-05
Thsd7b	ENSMUSG00000042581	chr1:132115331:132115380:	1.038537762	6.988896771	0.00012788
Igdcc4	ENSMUSG00000032816	chr9:64985471:64985520:	1.036649703	10.29119683	0.000315707
Pacs2	ENSMUSG00000021143	chr12:114312520:114312569:	1.035613472	10.96122974	1.7982E-05
Zmat3	ENSMUSG00000027663	chr3:32234129:32234178:-	1.035397164	9.612406487	4.57133E-07
Adam23	ENSMUSG00000025964	chr1:63642598:63642647:	1.035055482	8.357449063	6.15243E-05
Gjd2	ENSMUSG00000068615	chr2:113835489:113835538:-	1.034890708	7.836450647	1.7499E-05
Icam1	ENSMUSG00000037405	chr9:20832883:20832932:	1.034839477	7.200974952	4.11575E-05
Pkia	ENSMUSG00000027499	chr3:7445021:7445070:	1.033923828	11.35959782	1.50742E-05
Slc19a2	ENSMUSG00000040918	chr1:166195371:166195420:	1.03384507	9.826623397	3.69223E-05

B930041F14Rik	ENSMUSG00000074738	chr4:155070519:155070568:	1.033707554	10.60424715	2.5741E-06
Dgkg	ENSMUSG00000022861	chr16:22468713:22468762:-	1.032296702	7.426642123	5.96541E-05
6430548M08Rik	ENSMUSG00000031824	chr8:122687226:122687275:	1.031936959	7.9324255	1.16253E-05
Eef1a2	ENSMUSG00000016349	chr2:180888469:180888518:-	1.030176096	7.113901872	2.55842E-05
Crabp1	ENSMUSG00000032291	chr9:54620793:54620842:	1.029543237	6.937298937	0.000111538
Map1lc3a	ENSMUSG00000027602	chr2:155103551:155103600:	1.028580479	8.527965607	7.23075E-06
Pcyt1b	ENSMUSG00000035246	chrX:90995029:90995078:	1.027892115	7.860160376	5.00916E-07
Ccnd1	ENSMUSG00000070348	chr7:152115984:152116033:-	1.027430893	13.90117783	5.97026E-05
Stk32b	ENSMUSG00000029123	chr5:37838136:37838185:-	1.027097819	7.688086238	8.03394E-06
Crym	ENSMUSG00000030905	chr7:127330118:127330167:-	1.027035505	7.329239933	1.80269E-05
Fam164a	ENSMUSG00000043542	chr3:7553489:7553538:	1.026690743	9.197989202	1.67875E-06
Lrdd	ENSMUSG00000025507	chr7:148624604:148624653:-	1.024909806	7.962387124	9.85903E-05
Garnl3	ENSMUSG00000038860	chr2:32841966:32842015:-	1.023981073	9.019203059	6.16492E-05
Dennd2c	ENSMUSG00000007379	chr3:102973452:102973501:	1.023394523	6.990510663	1.63209E-06
Aard	ENSMUSG00000068522	chr15:51876950:51876999:	1.022770801	9.591164012	7.01036E-06
Ccdc120	ENSMUSG00000031150	chrX:7309030:7309079:-	1.02199943	8.725002034	7.32449E-06
Mgst3	ENSMUSG00000026688	chr1:169303925:169303974:-	1.021528166	8.645402067	0.000544659
Ldoc1l	ENSMUSG00000055745	chr15:84383915:84383964:-	1.021015128	9.737816102	1.46805E-06
Abhd4	ENSMUSG00000040997	chr14:54888630:54888679:	1.020656086	9.663407838	4.49151E-05
Mdm2	ENSMUSG00000020184	chr10:117126367:117126416:-	1.018563015	10.77290141	8.38192E-05
Scrn1		chr6:54456378:54456427:-	1.016017202	8.559903734	1.55474E-06
Gucy1a3	ENSMUSG00000033910	chr3:81898142:81898191:-	1.014962762	7.433012358	4.5124E-05
Nr4a2	ENSMUSG00000026826	chr2:56960685:56960734:-	1.014867399	7.533006185	2.25111E-06
Tnfaip8	ENSMUSG00000062210	chr18:50251038:50251087:	1.014361514	9.388022887	8.21975E-06
Epha3	ENSMUSG00000052504	chr16:63545096:63545145:-	1.013868792	7.669479845	1.14775E-05
Arhgap44	ENSMUSG00000033389	chr11:64815676:64815725:-	1.013154067	9.013647005	1.57679E-06
Alcam	ENSMUSG00000022636	chr16:52251265:52251314:-	1.012628857	8.81559121	1.22525E-05
Thsd7b	ENSMUSG00000042581	chr1:132115759:132115808:	1.012294263	6.683921153	0.000112084
Pdp1	ENSMUSG00000049225	chr4:11887874:11887923:-	1.011464755	7.364492239	3.11239E-05
Stmn1	ENSMUSG00000028832	chr4:134029501:134029550:	1.011239026	10.39796925	0.000144941
Mcc	ENSMUSG00000071856	chr18:44585165:44585214:-	1.010951264	8.164994583	2.55796E-06
Ecm1	ENSMUSG00000028108	chr3:95538235:95538284:-	1.010083887	7.037412751	0.001700642
Ankrd12	ENSMUSG00000034647	chr17:66317159:66317208:-	1.00986178	8.637215608	3.94215E-05
6430527G18Rik	ENSMUSG00000034168	chr12:88222183:88222232:-	1.009407294	11.62769253	1.79091E-06
Dpp10	ENSMUSG00000036815	chr1:125229254:125229303:-	1.008826453	7.047104511	5.00698E-06
Pdrg1	ENSMUSG00000027472	chr2:152834936:152834985:-	1.008603747	9.437571982	1.37773E-05
Gng3	ENSMUSG00000071658	chr19:8911455:8911504:-	1.007187638	8.089659068	5.35393E-06
Syt16	ENSMUSG00000044912	chr12:75368796:75368845:	1.00654766	9.269396181	1.05952E-05

Adcy1	ENSMUSG00000020431	chr11:7078133:7078182:	1.005842213	7.417828672	5.01536E-06
Msx1	ENSMUSG00000048450	chr5:38212320:38212369:-	1.005568583	6.966939988	3.90199E-06
Cdkl2	ENSMUSG00000029403	chr5:92435511:92435560:-	1.005271428	6.928563249	1.13944E-06
Nol4	ENSMUSG00000041923	chr18:22928294:22928343:-	1.004117209	6.832311232	1.5405E-05
Larp6	ENSMUSG00000034839	chr9:60586262:60586311:	1.003044126	7.702907546	2.20535E-05
Mmd	ENSMUSG00000003948	chr11:90139693:90139742:	1.002174603	10.48487024	2.56275E-06
Bcl2l1	ENSMUSG00000007659	chr2:152607465:152607514:-	1.002037914	7.829413577	2.86385E-06
Klf6	ENSMUSG00000000078	chr13:5864529:5864578:	1.00160062	8.180322059	7.98638E-06
Tulp4		chr17:6240371:6240420:	1.000878007	10.84762611	5.25347E-06
Tmem179	ENSMUSG00000054013	chr12:113738703:113738752:-	1.000231275	7.071015846	4.42007E-07
Rapgef5	ENSMUSG00000041992	chr12:118994896:118994945:	0.999952219	7.13574528	1.18334E-06
Gjd2	ENSMUSG00000068615	chr2:113835526:113835575:-	0.996463644	7.273988962	4.35753E-05
Adcyap1	ENSMUSG00000024256	chr17:93604568:93604617:	0.996381396	6.728338246	2.11362E-05
Dcaf4	ENSMUSG00000021222	chr12:84882576:84882625:	0.996046404	9.191224006	2.16109E-06
ENSMUSG00000068790	ENSMUSG00000096775	chr14:4144118:4144167:	0.995492532	10.5675665	6.14359E-06
Tnfsf18	ENSMUSG00000066755	chr1:163435049:163435098:	0.994568374	6.686800425	0.000658834
Pnck	ENSMUSG00000002012	chrX:70901475:70901524:-	0.994332474	7.59123021	1.95873E-05
Hecw2	ENSMUSG00000042807	chr1:53989973:53990022:-	0.993621297	7.341638614	2.70334E-05
Sybu	ENSMUSG00000022340	chr15:44503819:44503868:-	0.992289792	10.28439975	4.70245E-05
Plcl2	ENSMUSG00000038910	chr17:50827594:50827643:	0.990851562	8.355435201	4.51532E-06
Fam158a	ENSMUSG00000022217	chr14:56200387:56200436:-	0.990670452	7.487879208	7.93511E-06
Atp6v0d1	ENSMUSG00000013160	chr8:108048801:108048850:-	0.989646267	11.37180649	4.25348E-05
Pmm1	ENSMUSG00000022474	chr15:81781844:81781893:-	0.986239427	10.15552829	0.000300113
Rufy3	ENSMUSG00000029291	chr5:89071591:89071640:	0.984960224	11.00534267	1.38331E-06
Gng4	ENSMUSG00000021303	chr13:13919897:13919946:	0.98370821	7.232216778	4.90167E-05
Lm	ENSMUSG00000028063	chr3:88288537:88288543:-,chr3:88288034:88288076:-	0.983441486	8.502422883	6.97101E-07
Cort	ENSMUSG00000028971	chr4:148499369:148499418:-	0.981128967	7.088652281	0.003370594
Ramp3	ENSMUSG00000041046	chr11:6576648:6576697:	0.980164861	6.740087622	2.80683E-06
March4	ENSMUSG00000039372	chr1:72474375:72474424:-	0.978727818	7.169694914	9.87678E-05
Enox1	ENSMUSG00000022012	chr14:78121036:78121085:	0.97688083	8.637822114	7.33617E-07
Renbp	ENSMUSG00000031387	chrX:71167468:71167517:-	0.976797312	8.903936897	3.28229E-05
Sh3kbp1	ENSMUSG00000040990	chrX:156411741:156411790:	0.976085572	8.425645859	4.35628E-06
Djb9	ENSMUSG00000014905	chr12:45307126:45307175:-	0.974918366	9.027008895	4.0223E-05
Atp9a	ENSMUSG00000027546	chr2:168460278:168460327:-	0.973794481	8.351198473	7.67341E-06
Mtap1b	ENSMUSG00000052727	chr13:100194560:100194609:-	0.971840533	7.31561818	2.47165E-06
Vat1l	ENSMUSG00000046844	chr8:116897837:116897886:	0.971514633	8.493506396	2.12155E-06
Lhx5	ENSMUSG00000029595	chr5:120891110:120891159:	0.970756804	6.577408693	2.95929E-05

Ubtd1	ENSMUSG00000025171	chr19:42109022:42109071:	0.969846158	8.086881931	1.24549E-05
Rundc3b	ENSMUSG00000040570	chr5:8490647:8490696:-	0.969785381	7.565198602	0.000158505
Bclp2		chr3:105820901:105820950:-	0.969329405	6.495268832	1.00961E-06
Gsta4	ENSMUSG00000032348	chr9:78056899:78056948:	0.968068573	8.046238974	6.20973E-05
Spnb2	ENSMUSG00000020315	chr11:30000576:30000625:-	0.967727277	8.950023542	9.33058E-05
Pmm1	ENSMUSG00000022474	chr15:81782387:81782436:-	0.96718094	10.52771609	0.000794498
Rhof	ENSMUSG00000029449	chr5:123568488:123568537:-	0.966786694	7.150177499	3.26225E-06
Higd2a	ENSMUSG00000025868	chr13:54692328:54692377:	0.966253894	12.94434885	1.16241E-06
Ankrd12	ENSMUSG00000034647	chr17:66373464:66373513:-	0.966218437	8.134381304	1.39069E-05
Gng7	ENSMUSG00000048240	chr10:80411412:80411461:-	0.965758155	8.634830803	7.9599E-06
Stard10	ENSMUSG00000030688	chr7:108494530:108494579:	0.964723353	7.796664514	9.80047E-05
Slc27a3	ENSMUSG00000027932	chr3:90189181:90189230:-	0.96367723	9.44561106	5.97999E-07
Jph4	ENSMUSG00000022208	chr14:55726278:55726327:-	0.961449181	7.51826511	4.88002E-06
Cxxc4	ENSMUSG00000044365	chr3:133903528:133903577:	0.960964801	7.93207269	0.000206858
Magee1	ENSMUSG00000031227	chrX:102319145:102319194:	0.960368035	10.67664664	4.52213E-06
Cbs	ENSMUSG00000024039	chr17:31749945:31749994:-	0.958954813	8.482256981	1.03934E-05
Nrxn1	ENSMUSG00000024109	chr17:90458838:90458887:-	0.958727374	8.937867794	0.00101094
Sema3f	ENSMUSG00000034684	chr9:107583840:107583889:-	0.957858903	8.403542174	4.21889E-06
Ercc5	ENSMUSG00000026048	chr1:44237820:44237869:	0.956987855	10.79657823	3.91025E-06
Tubg2	ENSMUSG00000045007	chr11:101023031:101023080:	0.956474761	9.117788067	1.12997E-05
Pqlc3	ENSMUSG00000045679	chr12:17000267:17000316:-	0.955994935	6.870937019	1.51563E-05
Sh3bgrl3	ENSMUSG00000028843	chr4:133683597:133683646:-	0.955638199	10.78768523	2.02003E-05
Atp6v1h	ENSMUSG00000033793	chr1:5152255:5152304:	0.95454429	11.77276463	2.19344E-05
Whrn	ENSMUSG00000039137	chr4:63075996:63076045:-	0.954158616	9.01818669	0.000374584
Rapgefl1	ENSMUSG00000038020	chr11:98714234:98714283:	0.953388846	7.842876932	3.69994E-05
Bag3	ENSMUSG00000030847	chr7:135690226:135690275:	0.952471219	10.90216247	9.16173E-07
Gpr21	ENSMUSG00000053164	chr2:37374669:37374718:	0.95191246	7.127473256	5.8406E-06
Akap12	ENSMUSG00000038587	chr10:5987476:5987525:-	0.951707735	11.07424877	4.47591E-06
Camk1d	ENSMUSG00000039145	chr2:5218078:5218127:-	0.950087419	6.946439262	1.57218E-06
Scn3b	ENSMUSG00000049281	chr9:40096479:40096528:	0.949041076	6.810942662	9.61659E-07
Gpr12	ENSMUSG00000041468	chr5:147394028:147394077:-	0.948645288	6.964560962	7.53441E-05
Mdm2	ENSMUSG00000020184	chr10:117126034:117126083:-	0.948467177	11.27631973	0.00014475
Sema3f	ENSMUSG00000034684	chr9:107583842:107583891:-	0.947485366	7.890275622	3.66765E-06
Cpped1	ENSMUSG00000065979	chr16:11803871:11803920:-	0.947243756	9.885276689	0.00023336
Dynll2	ENSMUSG00000020483	chr11:87794143:87794192:-	0.94497895	8.937824979	8.71449E-06
Pcsk2	ENSMUSG00000027419	chr2:143641826:143641875:	0.944976934	7.098396349	4.80499E-06
Nin	ENSMUSG00000021068	chr12:71120083:71120132:-	0.944207452	8.795957396	0.000100068
Slc25a45	ENSMUSG00000024818	chr19:5885609:5885658:	0.943930088	7.431038551	1.38357E-05

4833424O15Rik	ENSMUSG00000033342	chr3:117392212:117392261:	0.940814893	7.326425517	1.1715E-05
St8sia3	ENSMUSG00000056812	chr18:64431431:64431480:	0.940237613	6.826623781	6.72228E-06
Lrrc24	ENSMUSG00000033707	chr15:76545808:76545857:-	0.939375516	7.610403828	7.01036E-06
Itm2a	ENSMUSG00000031239	chrX:104594929:104594978:-	0.937271095	9.342972497	1.36009E-05
Ngef	ENSMUSG00000026259	chr1:89373684:89373733:-	0.936832466	6.809044447	3.80086E-05
Grip1	ENSMUSG00000034813	chr10:119512355:119512404:	0.935850507	8.78493297	0.000178279
Scoc	ENSMUSG00000063253	chr8:85958954:85959003:-	0.935833029	10.4634643	3.50004E-05
Dapk1	ENSMUSG00000021559	chr13:60864045:60864094:	0.933988277	7.885393687	3.07055E-06
Mansc1	ENSMUSG00000032718	chr6:134559329:134559378:-	0.933940164	7.40395863	2.33636E-05
Ldb2	ENSMUSG00000039706	chr5:44863928:44863977:-	0.933693722	7.69821311	1.87583E-06
Sp47	ENSMUSG00000009894	chr11:59235030:59235079:-	0.932398065	8.796546993	0.000204761
Pld3	ENSMUSG00000003363	chr7:28318674:28318723:-	0.93183493	9.362710614	6.87988E-06
Timp1	ENSMUSG00000001131	chrX:20451683:20451732:	0.931393958	8.597507316	3.59119E-05
Acot7	ENSMUSG00000028937	chr4:151645779:151645828:	0.930350313	11.43365262	2.25016E-06
Upp1	ENSMUSG00000020407	chr11:9035989:9036038:	0.92985506	10.39287525	9.43604E-05
Kifap3	ENSMUSG00000026585	chr1:165846972:165847021:	0.929438822	9.908245351	2.81356E-06
Spock1	ENSMUSG00000056222	chr13:57528162:57528211:-	0.929277991	6.885399104	7.47995E-05
Coro2b	ENSMUSG00000041729	chr9:62267571:62267620:-	0.928157113	9.023336971	3.19253E-05
Atp6v0d1	ENSMUSG00000013160	chr8:108054743:108054792:-	0.927752498	10.694813	7.45757E-06
Snrpn		chr7:67128022:67128071:-	0.927629151	12.5782002	1.00423E-06
Clip1		chr5:124027902:124027951:-	0.927255438	9.253566308	1.87778E-05
Nfe2l2	ENSMUSG00000015839	chr2:75516564:75516613:-	0.924974446	8.397299908	5.05362E-05
Cish	ENSMUSG00000032578	chr9:107204093:107204142:	0.924723538	8.092292894	2.12699E-05
Fahd1	ENSMUSG00000045316	chr17:24985961:24986010:-	0.921574509	9.287755903	0.000122151
Upp1	ENSMUSG00000020407	chr11:9035167:9035216:	0.921195738	8.392761661	5.14156E-05
3110035E14Rik	ENSMUSG00000067879	chr1:9616688:9616737:	0.919890388	8.428174283	0.000107397
Cotl1	ENSMUSG00000031827	chr8:122333250:122333299:-	0.919719959	10.8879986	6.31544E-06
Ss18l1	ENSMUSG00000039086	chr2:179804711:179804760:	0.918928935	7.941364682	8.53537E-07
Adap1	ENSMUSG00000056413	chr5:139748063:139748112:-	0.918717238	6.799616656	2.80683E-06
Lingo2	ENSMUSG00000045083	chr4:35654808:35654857:-	0.918149828	6.895545044	4.68774E-07
Ss18l1	ENSMUSG00000039086	chr2:179802804:179802853:	0.918001553	7.288435313	4.51532E-06
Plk2	ENSMUSG00000021701	chr13:111190807:111190856:	0.916805327	9.740779689	7.19196E-05
Nsg1	ENSMUSG00000029126	chr5:38528564:38528613:-	0.916307678	7.858460152	0.00080241
Dic1	ENSMUSG00000061322	chr4:41585070:41585119:	0.916140459	7.071885692	2.8601E-05
Tcea3	ENSMUSG00000001604	chr4:135827154:135827203:	0.916132679	6.871341287	6.36787E-06
Dt	ENSMUSG00000024302	chr18:23762656:23762705:	0.916006011	8.461911983	0.000300924
Mt3	ENSMUSG00000031760	chr8:96676667:96676716:	0.915897887	10.24638475	0.001156848
Loxl1	ENSMUSG00000032334	chr9:58136500:58136549:-	0.915652647	8.416315901	0.002011966

Bace2	ENSMUSG00000040605	chr16:97646156:97646205:	0.914796737	7.323675151	2.06339E-05
Atp6v1e1	ENSMUSG00000019210	chr6:120745343:120745392:-	0.913569937	12.90390951	3.50156E-06
Casp1	ENSMUSG00000025888	chr9:5306714:5306763:	0.913174383	6.638348655	7.31725E-07
Ooep	ENSMUSG00000032346	chr9:78225317:78225366:-	0.913011846	6.836691014	1.22152E-05
Slitrk4	ENSMUSG00000046699	chrX:61522862:61522911:-	0.912812833	7.194046282	0.000946497
Klf6	ENSMUSG00000000078	chr13:5866959:5867008:	0.912335455	11.53937165	2.34127E-05
Elavl2	ENSMUSG00000008489	chr4:90917663:90917712:-	0.911991749	8.993615265	6.21643E-06
Rgs17	ENSMUSG00000019775	chr10:4505259:4505269:,chr1 0:4513400:4513438:	0.911658044	8.017651718	1.17201E-05
Rhoj	ENSMUSG00000046768	chr12:76502356:76502405:	0.911265978	8.560935732	1.6524E-05
Laptm5	ENSMUSG00000028581	chr4:130491984:130492033:	0.909393381	7.179262879	0.005760164
Hsd11b1	ENSMUSG00000016194	chr1:195048163:195048212:-	0.908911035	6.750824262	3.94218E-06
Gabrg2	ENSMUSG00000020436	chr11:41724340:41724389:-	0.903516361	6.754996656	2.20535E-05
Nub1	ENSMUSG00000028954	chr5:24215900:24215949:	0.902919969	8.996579307	3.59119E-05
Syne1	ENSMUSG00000019769; ENSMUSG00000096054	chr10:5009299:5009348:	0.902568789	6.711042608	2.24217E-05
Usp16	ENSMUSG00000025616	chr16:87481148:87481197:	0.902486959	9.292158206	5.64834E-06
Cadps2	ENSMUSG00000017978	chr6:23212864:23212913:-	0.902294332	7.988321182	6.63059E-06
Apba2	ENSMUSG00000030519	chr7:71889330:71889379:	0.902094635	8.073317192	3.03086E-06
Kifap3	ENSMUSG00000026585	chr1:165846921:165846970:	0.899575743	8.664664753	1.22525E-05
Csrnp3	ENSMUSG00000044647	chr2:65861141:65861190:	0.899380701	7.297920558	8.01428E-05
Apba2	ENSMUSG00000030519	chr7:71898512:71898561:	0.899217112	8.177504683	2.80683E-06
Lm	ENSMUSG00000028063	chr3:88288560:88288609:-	0.899014613	8.485420112	5.48338E-06
Fbxw7	ENSMUSG00000028086	chr3:84756223:84756272:	0.898883161	6.894798147	4.29506E-06
BC031353	ENSMUSG00000034858	chr9:74879634:74879683:	0.898282801	9.320928604	0.000144297
Cntp4	ENSMUSG00000031772	chr8:115405817:115405866:	0.8981716	6.95038722	9.62497E-07
Chst15	ENSMUSG00000030930	chr7:139427967:139428016:-	0.897447898	7.483541963	1.86626E-05
Fam78b	ENSMUSG00000060568	chr1:169020823:169020872:	0.897109175	6.84328752	7.08722E-06
Sema6b	ENSMUSG00000001227	chr17:56262526:56262575:-	0.896886515	7.876169519	6.44893E-06
Slc35f3	ENSMUSG00000057060	chr8:128919284:128919333:	0.896450099	7.154187708	1.22525E-05
Upp1	ENSMUSG00000020407	chr11:9034860:9034909:	0.895385967	9.004827789	9.33058E-05
Fsd1	ENSMUSG00000011589	chr17:56136175:56136224:	0.894394162	9.27530651	3.35131E-05
Ntsr1	ENSMUSG00000027568	chr2:180279550:180279599:	0.894351697	7.336695482	2.97253E-06
Adamts18		chr8:116221698:116221747:-	0.893399481	6.856782515	3.97559E-06
Kcnip1	ENSMUSG00000053519	chr11:33530536:33530585:-	0.892917107	7.225856387	6.13636E-05
Crct1	ENSMUSG00000027913	chr3:92818270:92818319:-	0.891051103	6.712340541	0.000255785
Gabarap	ENSMUSG00000018567	chr11:69807994:69808043:	0.889721443	11.80910408	0.000119521
Sorcs2	ENSMUSG00000029093	chr5:36360281:36360330:-	0.889647096	7.064146278	6.41859E-06
Coro1a	ENSMUSG00000030707	chr7:133843835:133843884:-	0.889219848	7.006545716	6.76762E-06

Tes	ENSMUSG00000029552	chr6:17015262:17015311:	0.888901915	6.816459851	0.000270039
Zic3	ENSMUSG00000067860	chrX:55289010:55289059:	0.888787525	7.648490668	0.004413007
Ei24	ENSMUSG00000062762	chr9:36587116:36587165:-	0.88819438	10.9739756	1.43366E-05
Mtpn	ENSMUSG00000029840	chr6:35459533:35459582:-	0.884870966	10.16675257	1.33675E-05
Gpr85	ENSMUSG00000048216	chr6:13785205:13785254:-	0.88472905	9.570643547	3.49244E-05
Lix1	ENSMUSG00000047786	chr17:17580655:17580704:	0.884404773	7.756729933	0.00085315
Gm5468		chr15:25344482:25344531:	0.883792195	7.068654422	1.97925E-06
Npy	ENSMUSG00000029819	chr6:49779390:49779439:	0.882982919	7.330375987	0.000998783
Galt	ENSMUSG00000036073	chr4:41704400:41704449:	0.882730515	6.952078692	1.30802E-06
Trim3	ENSMUSG00000036989	chr7:112759204:112759253:-	0.881792726	8.658074063	4.47591E-06
Bdh2	ENSMUSG00000028167	chr3:134967304:134967353:	0.880582789	7.793825124	0.000160784
Syn2	ENSMUSG00000009394	chr6:115224937:115224986:	0.880484065	8.982362709	7.67341E-06
Snx16	ENSMUSG00000027534	chr3:10418817:10418866:-	0.879248016	8.167155429	5.70907E-05
Itga11	ENSMUSG00000032243	chr9:62631670:62631719:	0.878449223	6.817752667	7.37877E-05
Ryr3	ENSMUSG00000057378	chr2:112472282:112472331:-	0.878372958	6.678314395	0.000922727
Zfp238	ENSMUSG00000063659	chr1:179380235:179380284:	0.877378015	10.7478225	9.89424E-06
Cbln1	ENSMUSG00000031654	chr8:89992824:89992873:-	0.877301335	9.026178041	0.000153481
Arl4c	ENSMUSG00000049866	chr1:90597624:90597673:-	0.876408795	8.860695704	1.12716E-05
Xpo7		chr14:71060330:71060379:	0.876407984	7.187398884	5.57448E-06
Dner	ENSMUSG00000036766	chr1:84366549:84366598:-	0.875879085	12.06008897	5.20695E-06
Hpca	ENSMUSG00000028785	chr4:128789088:128789137:-	0.874805192	7.552393903	0.000652129
Dusp6	ENSMUSG00000019960	chr10:98729743:98729792:	0.874638777	9.572200566	0.000400377
Smpd1	ENSMUSG00000037049	chr7:112706757:112706806:	0.87343138	10.56519382	1.75682E-06
Abcb9	ENSMUSG00000029408	chr5:124511928:124511977:-	0.872851496	8.031276949	0.000138459
Atp6v1f	ENSMUSG00000004285	chr6:29420447:29420496:	0.872666355	11.79722424	7.26742E-05
Ezr	ENSMUSG00000052397	chr17:6942897:6942946:-	0.870161857	9.2292443	5.32968E-05
Pdlim7	ENSMUSG00000021493	chr13:55599781:55599830:-	0.869734368	7.836925901	0.002965086
Rnf11	ENSMUSG00000028557	chr4:109125503:109125552:-	0.868437856	11.09012335	2.14908E-05
Macrod2		chr2:142218051:142218100:	0.868376392	7.143434369	8.89542E-05
Camta2	ENSMUSG00000040712	chr11:70482998:70483047:-	0.868271932	10.7818744	0.00211072
Ncdn	ENSMUSG00000028833	chr4:126421238:126421287:-	0.868222228	7.996491203	0.000129506
Wnt7b	ENSMUSG00000022382	chr15:85365991:85366040:-	0.868126931	10.39626296	0.000115324
Fgf13	ENSMUSG00000031137	chrX:56315651:56315700:-	0.868092647	9.107324429	4.38345E-05
Ywhag	ENSMUSG00000051391	chr5:136384367:136384416:-	0.868042031	11.5746942	7.42983E-06
Spock2	ENSMUSG00000058297	chr10:59596584:59596633:	0.867931538	7.494076265	4.43669E-06
Bach2	ENSMUSG00000040270	chr4:32668044:32668093:	0.867645467	10.79158413	0.001377143
Lypd6b	ENSMUSG00000026765	chr2:49804193:49804242:	0.866350414	7.066362915	0.000157114
Atp6v0d1	ENSMUSG00000013160	chr8:108048457:108048506:-	0.866320251	11.92102934	8.8601E-06

Nrp1	ENSMUSG00000025810	chr8:131027112:131027161:	0.866230822	8.716062922	0.000920976
Ehd4	ENSMUSG00000027293	chr2:119915286:119915335:-	0.865860765	8.706882823	2.27809E-06
Eif4a2	ENSMUSG00000022884	chr16:23113891:23113940:	0.864548285	12.48096173	0.000221186
Grip1	ENSMUSG00000034813	chr10:119512517:119512566:	0.864286551	9.49293407	0.000129185
Sp91	ENSMUSG00000033419	chr9:86660092:86660141:-	0.863659604	7.102956925	0.000605855
AI413582	ENSMUSG00000062753	chr17:27701094:27701114:-,c hr17:27700933:27700961:-	0.863189555	8.470543342	1.35319E-05
Abr	ENSMUSG00000017631	chr11:76230498:76230547:-	0.861789906	8.671619263	7.64192E-05
Trp53inp2	ENSMUSG00000038375	chr2:155215184:155215233:	0.861481412	9.123096476	7.31728E-06
Prkce	ENSMUSG00000045038	chr17:87029433:87029482:	0.861469596	7.046171126	4.43859E-05
Tceb1		chr1:16632247:16632296:-	0.861331015	9.702572784	2.94192E-05
Smpd3	ENSMUSG00000031906	chr8:108776826:108776875:-	0.860185871	8.335067457	7.26183E-05
Dok5	ENSMUSG00000027560	chr2:170704710:170704759:	0.8585895	7.585348801	3.80086E-05
Rac3	ENSMUSG00000018012	chr11:120584578:120584627:	0.856954056	8.130868629	5.55766E-05
Cacng5	ENSMUSG00000040373	chr11:107736307:107736356:-	0.856848977	7.709809207	0.002302231
Pja2	ENSMUSG00000024083	chr17:64630413:64630462:-	0.855914463	11.15592972	3.47657E-06
Rasgrf1	ENSMUSG00000032356	chr9:89921695:89921744:	0.855679755	6.745630838	1.7172E-05
D0H4S114	ENSMUSG00000042834	chr18:33596731:33596780:-	0.854874704	12.97763518	6.79894E-05
Pcdhb3	ENSMUSG00000045498	chr18:37463497:37463546:	0.854447196	6.94771767	2.42539E-06
Dusp15	ENSMUSG00000042662	chr2:152771166:152771215:-	0.853674343	7.315503772	7.61785E-05
Cbs	ENSMUSG00000024039	chr17:31749952:31750001:-	0.853516614	8.481764718	4.24328E-05
Rufy3	ENSMUSG00000029291	chr5:89071595:89071644:	0.85329674	10.40563271	1.98432E-05
Id1	ENSMUSG00000042745	chr2:152562859:152562908:	0.852259241	9.719755539	0.000206198
Ccnd1	ENSMUSG00000070348	chr7:152117120:152117169:-	0.852102248	11.81833178	1.87091E-05
Lynx1	ENSMUSG00000022594	chr15:74578304:74578353:-	0.851733739	8.770405914	9.32947E-06
Lrrc28	ENSMUSG00000030556	chr7:74658397:74658446:-	0.85120276	9.793014951	8.10582E-05
Sema7a	ENSMUSG00000038264	chr9:57810525:57810574:	0.85057094	7.93591552	2.68793E-05
Cdc42ep3	ENSMUSG00000036533	chr17:79733511:79733560:-	0.850200842	8.15329686	5.64834E-06
Akap7	ENSMUSG00000039166	chr10:24889980:24890029:-	0.849487895	9.183162349	1.85643E-05
Rln1	ENSMUSG00000039097	chr19:29406395:29406444:-	0.849313821	7.361235195	1.34303E-05
Ntm	ENSMUSG00000059974	chr9:28816831:28816880:-	0.848188493	9.258445557	1.34306E-05
Gpr27	ENSMUSG00000072875	chr6:99643684:99643733:	0.847233847	7.095344658	5.21557E-05
Itga3	ENSMUSG00000001507	chr11:94905825:94905874:-	0.846865572	6.672354701	5.20078E-05
Uba5	ENSMUSG00000032557	chr9:103951571:103951620:-	0.846462555	10.62657631	1.59834E-05
Pramef8	ENSMUSG00000046862	chr4:143010804:143010853:	0.845789052	8.400763057	0.000217721
Kif1b	ENSMUSG00000063077	chr4:148550737:148550786:-	0.845553983	11.15924347	0.000120638
Snrk	ENSMUSG00000038145	chr9:122078708:122078757:	0.845549474	9.927011938	4.80499E-06
Arhgap23	ENSMUSG00000049807	chr11:97363401:97363450:	0.845520295	8.132365788	4.38921E-06

Map3k12	ENSMUSG00000023050	chr15:102329960:102330009:-	0.844869407	9.179239469	6.56156E-05
Rgmb	ENSMUSG00000048027	chr17:15943286:15943335:-	0.844733814	7.174154506	6.44947E-06
Nrp1	ENSMUSG00000025810	chr8:131027106:131027155:	0.84466288	8.928614425	0.002842096
Igtp	ENSMUSG00000078853	chr11:58020810:58020859:	0.844279461	6.769651815	7.11642E-06
Atp6v0d1	ENSMUSG00000013160	chr8:108063311:108063360:-	0.844031425	10.64323604	1.49155E-05
Dynlrb1	ENSMUSG00000047459	chr2:155075682:155075731:	0.843708689	11.96531507	8.30675E-06
Gabarapl1	ENSMUSG00000030161	chr6:129492032:129492081:	0.843387766	9.99767267	5.25448E-06
Slc39a12	ENSMUSG00000036949	chr2:14416079:14416128:	0.84315337	6.829604232	0.000124834
1110012L19Rik	ENSMUSG00000045237	chrX:67642222:67642271:	0.843085068	8.117694913	0.000119729
Nelf	ENSMUSG00000006476	chr2:24918187:24918236:	0.842052964	9.956961936	3.55678E-05
Sh3kbp1	ENSMUSG00000040990	chrX:156411830:156411879:	0.841889127	8.600582632	1.22901E-05
Pitpnm2	ENSMUSG00000029406	chr5:124568794:124568843:-	0.841077304	8.155644133	0.001916181
Psme1	ENSMUSG00000022216	chr14:56200177:56200226:	0.840867779	10.1871996	1.32441E-05
Arhgdig	ENSMUSG00000073433	chr17:26336559:26336608:-	0.839565517	8.914446745	0.000356674
Trafd1	ENSMUSG00000042726	chr5:121823199:121823248:-	0.839447513	7.874280315	5.57448E-06
Fam19a1	ENSMUSG00000059187	chr6:96604865:96604914:	0.839439528	6.511963006	1.63053E-05
Cntn6	ENSMUSG00000030092	chr6:104813152:104813201:	0.839150729	7.094426269	8.61998E-05
Armcx1	ENSMUSG00000033460	chrX:131256132:131256181:	0.838427509	8.765193339	0.001288078
Mff	ENSMUSG00000026150	chr1:82738415:82738464:	0.837179222	8.71757931	6.65954E-06
Iqgap1	ENSMUSG00000030536	chr7:87857713:87857762:-	0.836718606	10.22691013	0.000245812
Tbc1d25	ENSMUSG00000039201	chrX:7731880:7731929:-	0.836146991	7.787441551	3.23895E-05
Tmem38a	ENSMUSG00000031791	chr8:75110907:75110956:	0.836068062	8.010551165	0.000213252
Spag6	ENSMUSG00000022783	chr16:16753228:16753277:-	0.834794213	7.021196324	0.000158556
Gas7	ENSMUSG00000033066	chr11:67498226:67498275:	0.833988615	7.25071822	2.19199E-06
Fnbp1l	ENSMUSG00000039735	chr3:122241852:122241901:-	0.833561614	11.53407201	1.16254E-05
Has3	ENSMUSG00000031910	chr8:109406619:109406668:	0.832833724	6.885868936	8.05125E-06
Slc7a4	ENSMUSG00000022756	chr16:17573197:17573246:-	0.832804469	7.51076319	0.000137415
Dt	ENSMUSG00000024302	chr18:23755978:23756027:	0.832394756	7.99075435	0.000484968
March1	ENSMUSG00000036469	chr8:68994108:68994157:	0.831131554	6.972674159	1.21003E-05
Sh3bp2	ENSMUSG00000054520	chr5:34906187:34906236:	0.831029215	8.94857442	6.14359E-06
Slc2a13	ENSMUSG00000036298	chr15:91098458:91098507:-	0.830054881	7.804687981	6.63399E-05
1110012L19Rik	ENSMUSG00000045237	chrX:67639259:67639308:	0.829919539	8.629108888	0.000730919
PGC-1v	ENSMUSG00000029167	chr5:51849328:51849377:-	0.829511424	8.813005156	3.31226E-05
Neurod1	ENSMUSG00000034701	chr2:79292820:79292869:-	0.828777325	6.818767383	5.2773E-06
Rusc1	ENSMUSG00000041263	chr3:88888056:88888105:-	0.828423817	7.54371918	1.22638E-05
Wsb2	ENSMUSG00000029364	chr5:117828263:117828312:	0.827718543	11.94627437	4.44372E-06
Scrn1	ENSMUSG00000019124	chr6:54458993:54459042:-	0.827506341	7.256386625	9.39815E-05

Pnpo	ENSMUSG00000018659	chr11:96803737:96803786:-	0.827378691	7.138108436	2.21585E-05
Slc7a8	ENSMUSG00000022180	chr14:55341288:55341337:-	0.824651046	6.727414509	0.000102792
Kcnma1	ENSMUSG00000063142	chr14:24119139:24119188:-	0.822327359	6.941908411	0.00046422
Abcb9	ENSMUSG00000029408	chr5:124511927:124511976:-	0.820780372	7.731207001	0.000353577
Dos	ENSMUSG00000035640	chr10:79593574:79593623:-	0.82044181	7.612210536	2.55348E-05
Tmtc4	ENSMUSG00000041594	chr14:123319259:123319308: -	0.819821003	6.827806992	3.64217E-05
Elmo1	ENSMUSG00000041112	chr13:20565046:20565095:	0.819811569	7.195101066	3.17733E-05
Spink2	ENSMUSG00000053030	chr5:77634151:77634200:-	0.81962952	6.980755271	4.60868E-05
Jph3	ENSMUSG00000025318	chr8:124314410:124314459:	0.818345689	7.053094996	5.49288E-06
Parm1	ENSMUSG00000034981	chr5:92052926:92052975:	0.817952384	7.863036388	6.48925E-05
Itsn1	ENSMUSG00000022957	chr16:91909480:91909529:	0.817944636	7.162209742	8.51917E-06
2310035C23Rik	ENSMUSG00000026319	chr1:107637041:107637090:	0.817719553	7.857272594	2.33912E-05
P2ry1	ENSMUSG00000027765	chr3:60812677:60812726:	0.816774494	7.367571802	1.18054E-05
Tnfrsf10b	ENSMUSG00000022074	chr14:70182289:70182338:	0.816665723	6.841151356	3.43981E-06
Ppp3cb	ENSMUSG00000021816	chr14:21319408:21319457:-	0.816464103	11.8399039	7.01026E-06
Crip2	ENSMUSG00000006356	chr12:114383649:114383698:	0.816422477	12.66082841	5.41661E-06
Zfp597	ENSMUSG00000039789	chr16:3861578:3861627:-	0.814525558	8.800192608	5.3745E-06
Mapk9	ENSMUSG00000020366	chr11:49699461:49699510:	0.814484511	10.78086421	7.66954E-06
Tceal6	ENSMUSG00000031409	chrX:131743421:131743470:-	0.814467377	8.051972254	1.21674E-05
Mapk8ip2	ENSMUSG00000022619	chr15:89292754:89292803:	0.814201241	8.985469117	4.15873E-05
Ccdc92	ENSMUSG00000037979	chr5:125315426:125315475:-	0.813036212	9.842324681	5.25347E-06
Nell2	ENSMUSG00000022454	chr15:95061728:95061734:-,c hr15:95059697:95059739:-	0.812691761	7.243888174	0.000655046
Dusp1	ENSMUSG00000024190	chr17:26642678:26642727:-	0.810999283	10.91670997	0.000105995
Bid	ENSMUSG00000004446	chr6:120843364:120843413:-	0.810276739	7.571444482	2.28101E-06
Mdk	ENSMUSG00000027239	chr2:91770094:91770143:-	0.810199945	10.6534514	0.000424324
Rab40c	ENSMUSG00000025730	chr17:26019146:26019195:-	0.810021362	10.57677936	8.17398E-07
Cd151	ENSMUSG00000025510	chr7:148657124:148657173:	0.809430817	10.78324772	1.60453E-05
Gnb5	ENSMUSG00000032192	chr9:75193427:75193476:	0.80837872	9.331174077	1.81894E-05
Wdr37	ENSMUSG00000021147	chr13:8856116:8856165:-	0.803970607	7.865626583	1.37369E-05
Tnfrsf12a	ENSMUSG00000023905	chr17:23812760:23812809:-	0.80357269	10.111318	5.87019E-05
Rab6	ENSMUSG00000030704	chr7:107778384:107778433:	0.803154933	11.08399031	1.21003E-05
Fhdc1	ENSMUSG00000041842	chr3:84248086:84248135:-	0.802700302	7.29097131	0.000319551
Pak7	ENSMUSG00000039913	chr2:135907997:135908046:-	0.800849174	6.905539053	2.52513E-05
Pygb	ENSMUSG00000033059	chr2:150657139:150657188:	0.799781648	9.72304404	0.000188609
Prr7	ENSMUSG00000034686	chr13:55574366:55574415:	0.799703998	8.970712044	0.000897961
Acot7	ENSMUSG00000028937	chr4:151635078:151635127:	0.799350403	9.491435984	1.7465E-05
Pth2r	ENSMUSG00000025946	chr1:65435261:65435310:	0.799127731	6.577650845	0.000191227

Sept3	ENSMUSG00000022456	chr15:82122180:82122229:	0.796133318	9.273672388	2.79591E-05
Col5a1	ENSMUSG00000026837	chr2:27892889:27892938:	0.795125343	9.780078314	0.00364271
Ednra	ENSMUSG00000031616	chr8:80186996:80187045:-	0.794593661	7.69326501	2.28482E-05
Thra	ENSMUSG00000058756	chr11:98625661:98625710:	0.79455317	9.417687916	1.64094E-05
Shh	ENSMUSG00000002633	chr5:28783901:28783950:-	0.793959266	6.590459445	0.000103156
Klhl26	ENSMUSG00000055707	chr8:72974246:72974295:-	0.793908941	10.15390425	4.41412E-06
Acta2	ENSMUSG00000035783	chr19:34316067:34316116:-	0.793864577	8.554580165	0.004667752
Hsd11b1	ENSMUSG00000016194	chr1:195048157:195048206:-	0.793810423	6.653753889	6.82259E-05
Cac2d1	ENSMUSG00000040118	chr5:15876791:15876840:	0.7917091	8.723669364	0.002239501
Psme2	ENSMUSG00000079197; ENSMUSG00000078153	chr14:56209737:56209786:-	0.79170225	8.695732328	0.000160784
Cxx1c	ENSMUSG00000051851	chrX:50911209:50911258:	0.790803324	8.328913983	1.9213E-05
Phactr1	ENSMUSG00000054728	chr13:42778114:42778163:	0.790681697	6.586957598	6.0154E-06
nos1	ENSMUSG00000072437	chr19:60833889:60833938:	0.790434463	8.318124937	0.000163327
Trp53bp1	ENSMUSG00000043909	chr2:121024187:121024236:-	0.79041131	10.77520644	5.86024E-05
Sbk1	ENSMUSG00000042978	chr7:133438414:133438463:	0.790165922	12.61840764	9.82791E-06
Cltb	ENSMUSG00000047547	chr13:54694868:54694917:-	0.789931538	8.28152114	8.78646E-06
Fgd4	ENSMUSG00000022788	chr16:16422840:16422889:-	0.789590431	6.686046719	8.34197E-06
gk	ENSMUSG00000034744	chr6:83751510:83751559:	0.789216644	8.363567073	1.60246E-05
Sgsm2	ENSMUSG00000038351	chr11:74663048:74663097:-	0.788967554	7.273948516	0.0004075
Slc1a2	ENSMUSG00000005089	chr2:102621822:102621871:	0.788747395	7.777681923	1.2421E-05
Sept5	ENSMUSG00000072214	chr16:18622572:18622621:-	0.788501631	8.376418262	6.18708E-05
Exoc4	ENSMUSG00000029763	chr6:33922238:33922287:	0.788091356	9.544752234	6.14359E-06
Atp9a	ENSMUSG00000027546	chr2:168475059:168475108:-	0.7876573	7.597515583	7.66899E-05
Wnk2	ENSMUSG00000037989	chr13:49131734:49131783:-	0.786209242	8.320950547	0.000219837
E130309F12Rik	ENSMUSG00000063446	chr4:49336299:49336348:	0.785332267	8.440793447	2.40044E-05
Rabgef1	ENSMUSG00000025340	chr5:130690108:130690157:	0.785213707	10.01432861	1.48065E-05
Fbxo32	ENSMUSG00000022358	chr15:58039548:58039597:-	0.785197228	6.637281375	5.50447E-05
Pgrmc1	ENSMUSG00000006373	chrX:34145704:34145753:	0.785166258	9.518613373	0.000924667
Kndc1	ENSMUSG00000066129	chr7:147127344:147127393:	0.785098405	7.411489892	0.001160715
Ccdc80	ENSMUSG00000022665	chr16:45127495:45127544:	0.784562404	7.242794764	0.000133117
Elk3	ENSMUSG00000008398	chr10:92712317:92712366:-	0.784308304	10.53006683	5.21435E-06
Gmpr	ENSMUSG00000000253	chr13:45641365:45641414:	0.78310861	7.702614612	3.55808E-05
Scamp1	ENSMUSG00000021687	chr13:94971463:94971512:-	0.782417602	11.57625713	6.32647E-06
Slco3a1	ENSMUSG00000025790	chr7:81463394:81463443:-	0.78192301	6.782618464	0.000218952
AK197526		chr6:87949393:87949442:-	0.781243154	11.02679052	1.03663E-06
Gpr85	ENSMUSG00000048216	chr6:13785556:13785605:-	0.781131337	7.556745284	0.000411771
Lm	ENSMUSG00000028063	chr3:88287969:88288014:-,chr3:88287865:88287868:-	0.780843864	7.450567584	0.000199441

Ssu72	ENSMUSG00000029038	chr4:155107711:155107760:	0.78004445	11.92221371	1.39645E-05
Triobp	ENSMUSG00000033088	chr15:78836241:78836290:	0.779511351	12.01979227	4.29222E-05
gk	ENSMUSG00000034744	chr6:83751119:83751168:	0.779389427	8.211218029	2.95571E-05
Ifngr2	ENSMUSG00000022965	chr16:91563208:91563257:	0.778840696	8.191212971	0.000100655
Nfix	ENSMUSG00000001911	chr8:87245559:87245608:-	0.778476166	11.65139776	0.000457177
Sgip1	ENSMUSG00000028524	chr4:102643594:102643643:	0.778122872	7.378563098	0.000230305
Atg16l1	ENSMUSG00000026289	chr1:89688708:89688757:	0.778093451	9.659199573	0.00076889
Pak1	ENSMUSG00000030774	chr7:105059723:105059772:	0.777988918	8.07015843	0.00065469
Triobp	ENSMUSG00000033088	chr15:78836224:78836273:	0.777413466	12.10131732	4.53668E-05
Hpcal1	ENSMUSG00000071379	chr12:17798250:17798299:	0.776788709	8.228963295	0.00011215
Trafd1	ENSMUSG00000042726	chr5:121822263:121822312:-	0.776704728	7.6497469	9.13411E-05
Atp2a2	ENSMUSG00000029467	chr5:122903580:122903629:-	0.775412983	10.63278584	0.000254836
Gq	ENSMUSG00000024639	chr19:16459714:16459763:	0.774716443	10.1044874	0.000158791
Nln		chr13:104813400:104813449:-	0.774638015	9.203643089	3.22732E-05
Chrnb2	ENSMUSG00000027950	chr3:89557752:89557801:-	0.774247909	6.759546737	3.11239E-05
Cdh7	ENSMUSG00000026312	chr1:112035299:112035348:	0.773847686	6.458387819	1.0738E-05
Hcn2	ENSMUSG00000020331	chr10:79198800:79198849:	0.772628254	7.6765109	6.02315E-05
Hist1h4h	ENSMUSG00000096010; ENSMUSG00000067455; ENSMUSG00000064288; ENSMUSG00000069306; ENSMUSG00000069305; ENSMUSG00000060639; ENSMUSG00000060981; ENSMUSG00000069274; ENSMUSG00000061482; ENSMUSG00000060678; ENSMUSG00000069266; ENSMUSG00000060093; ENSMUSG00000091405	chr13:23622965:23623014:	0.771932892	8.054387743	4.5124E-05
St18	ENSMUSG00000033740	chr1:6850950:6850999:	0.771793293	6.675256032	6.14359E-06
Zic4	ENSMUSG00000036972	chr9:91283696:91283745:	0.771703404	6.345426826	0.000209544
Rnf14	ENSMUSG00000060450	chr18:38477304:38477353:	0.771247022	11.47732069	4.73555E-06
Arf2	ENSMUSG00000062421	chr11:103846532:103846581:	0.771121091	10.25752374	3.48932E-05
Rasl10b	ENSMUSG00000020684	chr11:83234351:83234400:	0.770143054	7.06254933	8.5082E-06
Gdap1l1	ENSMUSG00000017943	chr2:163279593:163279642:	0.769326593	8.349796491	0.000231197
Mast1	ENSMUSG00000053693	chr8:87436113:87436162:-	0.768649935	7.053224282	2.7116E-05
Tex264	ENSMUSG00000040813	chr9:106561142:106561191:-	0.767872219	9.790956121	1.87113E-05
Dennd3	ENSMUSG00000036661	chr15:73402524:73402573:	0.767378444	7.532230665	0.000705295
Ssbp2	ENSMUSG00000003992	chr13:91820237:91820243:,chr13:91823287:91823322:,chr13:91824816:91824822:	0.766995492	9.526627494	1.70476E-05
Fam110b	ENSMUSG00000049119	chr4:5726858:5726907:	0.766930852	8.939837505	3.11239E-05
Kcnu1	ENSMUSG00000031576	chr8:27048294:27048343:	0.765833963	6.938779693	0.000122701
Slc6a6	ENSMUSG00000030096	chr6:91708824:91708873:	0.765682053	11.38994488	0.000681403

Myl6	ENSMUSG00000090841	chr10:127929285:127929307:-,chr10:127929166:127929192:-	0.765513911	12.58612093	7.80302E-05
Prkcd	ENSMUSG00000021948	chr14:31408860:31408909:-	0.76480391	7.653096354	8.09835E-05
Nln	ENSMUSG00000021710	chr13:104813559:104813608:-	0.764170614	9.779210722	6.96286E-05
Prkag2	ENSMUSG00000028944	chr5:24368859:24368908:-	0.764086	8.867218433	2.26855E-05
Caskin1	ENSMUSG00000033597	chr17:24645466:24645515:	0.763928165	8.196464603	0.000372172
Ntrk2	ENSMUSG00000055254	chr13:59230780:59230829:	0.763504901	7.262585357	0.008702071
Zfp238	ENSMUSG00000063659	chr1:179374882:179374931:	0.762885426	7.574101622	0.002142684
Isca1	ENSMUSG00000044792	chr13:59857302:59857351:-	0.762487929	10.39626838	8.08528E-06
Ppp1r14c	ENSMUSG00000040653	chr10:6922971:6923020:-	0.762218524	8.210336213	0.000454807
8430410K20Rik	ENSMUSG00000041124	chr9:4386549:4386598:	0.761876908	10.95013897	1.64094E-05
Glipr2	ENSMUSG00000028480	chr4:43991772:43991821:	0.76106945	9.233889938	0.007807577
Gnpda1	ENSMUSG00000052102	chr18:38497793:38497842:-	0.760480662	8.615600687	0.000411505
Aifm2	ENSMUSG00000020085	chr10:61201321:61201370:	0.75957148	7.903198205	1.884E-05
4931408A02Rik	ENSMUSG00000039903	chr16:90894825:90894874:	0.759021717	7.836746563	0.000579782
6030419C18Rik	ENSMUSG00000066607	chr9:58347387:58347436:	0.758851048	7.805057974	1.55132E-05
Ctnnbip1	ENSMUSG00000028988	chr4:148940343:148940392:	0.75798405	10.44741247	0.000321738
Fam101a	ENSMUSG00000037962	chr5:125492697:125492746:	0.757949018	8.76589969	0.000894032
Lancl1	ENSMUSG00000026000	chr1:67053511:67053560:-	0.757807726	9.887055618	2.04407E-05
Atp5g1	ENSMUSG00000006057	chr11:95934857:95934906:-	0.757748904	12.60431168	3.40832E-05
Cadm1	ENSMUSG00000032076	chr9:47660926:47660975:	0.757379989	9.971627871	0.002350675
Gri	ENSMUSG00000022564	chr15:76080253:76080302:	0.757270973	12.81020963	6.31387E-05
Rnf11	ENSMUSG00000028557	chr4:109125525:109125574:-	0.756829449	10.04498301	0.000145004
Ank1	ENSMUSG00000031543	chr8:24260696:24260745:	0.756471087	7.005073071	4.54136E-05
Pld3	ENSMUSG00000003363	chr7:28317272:28317321:-	0.75625539	7.915101215	2.15688E-05
Bend6	ENSMUSG00000042182	chr1:33909014:33909063:-	0.75608451	7.770499913	5.96139E-05
Wdr37	ENSMUSG00000021147	chr13:8804495:8804544:-	0.755724988	7.539506386	6.08761E-05
Ppp2r5b	ENSMUSG00000024777	chr19:6228265:6228314:-	0.75546318	7.62734195	5.31279E-05
Ube2e2	ENSMUSG00000058317	chr14:19406237:19406286:-	0.754654483	11.03512959	2.01022E-06
Chrm3	ENSMUSG00000046159	chr13:9875922:9875971:-	0.753430141	6.934504158	5.72906E-06
Syngr1	ENSMUSG00000022415	chr15:79949508:79949557:	0.75318719	6.894945508	1.37327E-05
Ankrd56	ENSMUSG00000045314	chr5:93470452:93470501:-	0.752640706	6.511211823	0.000115484
Dok5	ENSMUSG00000027560	chr2:170704709:170704758:	0.752465596	7.347949093	2.54678E-05
Tcfap2c	ENSMUSG00000028640	chr2:172383694:172383743:	0.752356943	6.781272131	2.49812E-05
Camk2b	ENSMUSG00000057897	chr11:5869822:5869871:-	0.750924974	11.40718642	0.000757592
Gpr158	ENSMUSG00000045967	chr2:21751924:21751973:	0.749935367	7.226679852	6.53719E-06
Atp5sl	ENSMUSG00000057229	chr7:26410337:26410386:	0.749896332	7.730584553	9.53938E-06
Hagh	ENSMUSG00000024158	chr17:25000641:25000690:	0.749718291	8.710431507	1.70004E-05

Lix1	ENSMUSG00000047786	chr17:17594522:17594571:	0.748904265	7.571886644	0.001295217
Sgsm1	ENSMUSG00000042216	chr5:113672531:113672580:-	0.748549942	7.270335457	0.001010835
Insr	ENSMUSG00000005534	chr8:3153647:3153696:-	0.748519373	9.129473053	6.59974E-05
Atat1	ENSMUSG00000024426	chr17:36036989:36037038:-	0.748405932	8.653124831	5.57783E-06
Vat1	ENSMUSG00000034993	chr11:101320320:101320369:-	0.748163081	8.077564265	0.000144941
Caskin1	ENSMUSG00000033597	chr17:24645242:24645291:	0.748134671	7.400035481	0.00017487
Atp6v1b2	ENSMUSG00000006273	chr8:71637332:71637381:	0.748014697	11.42066716	4.53231E-06
Arntl	ENSMUSG00000055116	chr7:120457242:120457291:	0.748002689	8.907677681	2.19625E-06
Pfn2	ENSMUSG00000027805	chr3:57646214:57646263:-	0.747893571	11.72070985	8.34197E-06

APPENDIX C - RNA-sequencing differential gene expression analysis in NPCs

Gene Name	RPKM EtOH	RPKM OHT	log2 Fold Change	p-value
Tgm6	0	0.0169779	1,7977E+308	0.0177378
Slc5a11	0	0.0203926	1,7977E+308	0.0276792
Best3	0	0.016824	1,7977E+308	0.0296258
2310033E01Rik	0	0.0758708	1,7977E+308	0.0309638
9330175E14Rik	0	0.0287291	1,7977E+308	0.0355302
Cntnap3	0	0.00787291	1,7977E+308	0.0398235
Myl2	0	0.0784582	1,7977E+308	0.042654
Lrrc69	0	0.0340313	1,7977E+308	0.0436869
Rxfp4	0	0.0328147	1,7977E+308	0.0437014
Ly6d	0	0.0674338	1,7977E+308	0.0447141
Ptprv	0.137966	2.8184	4.3525	0
Rec8	0.3924	6.01404	3.93794	0
Them5	0.0112913	0.169986	3.91213	0.0119719
Scn4b	0.00330738	0.0453996	3.77892	0.0107074
Perp	0.40015	4.63691	3.53455	0
Cd80	0.0394448	0.438148	3.47351	1.67616E-06
Lao1	0.00652136	0.0708602	3.44173	0.0320764
D730039F16Rik	0.019861	0.215123	3.43715	5.91003E-05
Serpinb11	0.00692503	0.073397	3.40583	0.043482
Ltb4r1	0.0125669	0.132662	3.40005	0.0152619
Grhl3	0.0645272	0.671497	3.3794	1.17684E-13
Icam1	0.143347	1.48232	3.37027	0
Shh	0.05045	0.500066	3.30919	8.77881E-10
Ptk2b	0.0448615	0.440644	3.29606	1.88982E-12
Adm2	0.0354349	0.340663	3.2651	0.00113635
BC037703	0.100894	0.933804	3.21027	0
Gria1	0.18761	1.72966	3.20467	0
St14	0.0498824	0.456991	3.19556	1.51879E-13
Gbp11	0.00524351	0.0471304	3.16805	0.036406
Car10	0.161162	1.37538	3.09324	0
Cidea	0.0389013	0.325058	3.06281	0.00402924
Sec14l5	0.210763	1.7556	3.05827	0
H2-Eb1	0.051101	0.421556	3.0443	3.59235E-06
Cryab	2.78743	22.6075	3.0198	0
Ckmt1	1.67982	13.5343	3.01024	0

Wnt2	0.0149405	0.118546	2.98815	0.00387934
Rhbdf2	0.0853297	0.670265	2.97361	4.44089E-16
Rcsd1	0.0209156	0.160915	2.94365	0.000912852
1700007K13Rik	1.72415	13.1889	2.93536	0
Prrg4	0.50922	3.87266	2.92697	0
Fas	1.19862	9.06643	2.91916	0
Cd177	0.00591874	0.0446608	2.91565	0.0423124
Adrb3	0.0132804	0.0984189	2.88964	0.00235066
Casp14	0.012095	0.0869958	2.84654	0.00920128
Podn	0.102711	0.724041	2.81748	1.15463E-14
Ptpn7	0.0539875	0.3784	2.80922	1.74139E-09
Cox6a2	0.443871	3.07179	2.79087	1.01971E-10
Crybb1	0.0313041	0.215477	2.78311	0.0201249
Crispld2	0.72721	4.96886	2.77247	0
Gm5424	0.691794	4.70006	2.76426	0
Pm20d1	0.025439	0.172553	2.76193	1.10183E-05
Cyp4f14	0.0301555	0.203694	2.75591	0.000169947
P2ry6	0.0140695	0.0949933	2.75526	0.0148858
Itgb2	0.0148974	0.0968157	2.70018	0.00250393
Hsd17b1	0.0584125	0.378965	2.69771	0.00013373
Sp9	0.0293469	0.190147	2.69584	4.23879E-05
9530053A07Rik	0.168059	1.07405	2.67602	0
Tnfsf18	0.486002	3.09191	2.66946	0
Cpz	0.011597	0.0737669	2.66923	0.0222818
4833427G06Rik	0.0443226	0.281346	2.66623	0.0146571
Eef1a2	0.131877	0.829852	2.65366	8.90688E-11
Tslp	0.0880286	0.548021	2.63819	6.20056E-05
Svop	1.8844	11.6321	2.62593	0
Cend1	2.12866	13.0512	2.61616	0
Ankrd34c	0.0494855	0.300419	2.6019	2.92529E-06
Serpinb8	0.0229934	0.139038	2.59619	0.00205111
Tshr	0.0696974	0.42122	2.5954	2.45801E-11
Mal	0.0440199	0.264556	2.58735	6.18367E-05
Cyyr1	0.0450659	0.269564	2.58052	0.000051296
Trp73	0.00994603	0.0580874	2.54603	0.0451651
Gjc2	0.0168785	0.0985687	2.54594	0.0330894
Tmc3	0.0343167	0.198978	2.53562	4.98959E-07
Rgs8	0.0958673	0.548183	2.51555	1.9984E-15

Fam26e	0.0606927	0.34574	2.51009	6.38751E-05
Plscr2	0.0609364	0.342613	2.4912	4.45152E-05
Dusp15	0.667175	3.73607	2.48539	1.51367E-05
Ysk4	0.00657678	0.0365295	2.47361	0.0300825
Shpk	0.423183	2.3102	2.44866	0
March4	0.0973181	0.529632	2.44421	1.92801E-12
Klhdc7a	0.716789	3.81012	2.41022	0
Abca13	0.00245959	0.0128308	2.38313	0.0091811
Ppp2r2c	1.12662	5.87155	2.38174	0
Dsp	0.0050619	0.026319	2.37835	0.00422101
Thbs2	0.194815	1.00995	2.37411	0
Ddo	0.0208975	0.107839	2.36748	0.00167301
Hsf4	0.0219991	0.11304	2.36131	0.0215703
Epx	0.0171572	0.0879173	2.35733	0.00756985
Alox5	0.189946	0.971985	2.35535	6.7768E-13
Calhm2	0.062581	0.320017	2.35435	2.04738E-05
Fbln5	0.173963	0.888137	2.352	0
Nupr1	2.10435	10.7319	2.35046	0
Mag	0.18034	0.919461	2.35007	1.4396E-11
Gstt3	0.499852	2.54583	2.34856	0
ORF63	0.0389362	0.195013	2.32439	0.00244193
Trib3	0.666839	3.33319	2.32149	0
Sucnr1	0.0183281	0.0912121	2.31517	0.0406026
Gfap	0.221188	1.0971	2.31035	9.61958E-09
Espn	0.115627	0.564825	2.28832	0.00745824
Rhbdl2	0.109578	0.533114	2.28249	4.96797E-05
Gjb6	0.0169592	0.0820863	2.27507	0.0411475
Abca1	0.932046	4.48229	2.26576	0
Enpep	0.0143139	0.0683886	2.25634	0.00310717
5033411D12Rik	0.0241546	0.115372	2.25592	0.0162918
Gad1	0.110088	0.525241	2.25433	6.86821E-10
Slc39a12	0.864032	4.08113	2.23981	0
Parp10	0.0371282	0.175134	2.23788	0.000511985
Cdh18	0.0249284	0.117447	2.23614	0.00222123
Tmem130	0.012984	0.0611225	2.23497	0.024887
Nipal4	0.0628831	0.295936	2.23454	5.13257E-07
Scg2	0.0438093	0.206033	2.23356	0.000165042
Def6	0.101807	0.473505	2.21755	2.89644E-07

Col22a1	0.0934463	0.433349	2.21332	5.79181E-12
Pdk4	0.246775	1.13725	2.20427	2.17604E-14
Tgfbi	0.0275718	0.126692	2.20006	0.00187223
Creb3l1	0.893183	4.09057	2.19527	0
9930013L23Rik	0.258393	1.18068	2.19198	0
Tcea3	0.607967	2.76091	2.18308	1.32783E-12
Npas2	0.111934	0.506568	2.17811	1.91315E-10
Cd38	0.0598413	0.268443	2.1654	5.90018E-06
Pla2g5	0.0302863	0.135089	2.15718	0.0119152
Ass1	0.0769896	0.343012	2.15552	0.00015255
Prdm1	0.324025	1.44323	2.15512	0
Mbp	2.34746	10.4377	2.15263	0
A330076H08Rik	0.413407	1.82576	2.14287	1.43552E-12
AW555464	0.914223	4.02672	2.13899	0
Chchd10	0.906825	3.99076	2.13777	1.43441E-12
Il7	0.0299053	0.131504	2.13663	0.00253934
A730017C20Rik	0.152866	0.663943	2.11879	0.000530391
Pla2r1	0.0111337	0.0483091	2.11736	0.00521004
Fut1	0.0216066	0.0937236	2.11694	0.00917906
P2rx6	0.150025	0.647404	2.10946	2.61181E-05
Klk13	0.0427106	0.184114	2.10793	0.0274638
Xkrx	0.0343797	0.148118	2.10711	0.000670888
Mmp28	0.0401109	0.172214	2.10214	0.00563205
Kcnj15	0.0168242	0.0720939	2.09934	0.00471817
Lpin3	0.100106	0.428913	2.09916	4.68067E-08
Slc7a3	2.45215	10.4372	2.08962	0
Pltp	0.921519	3.9171	2.0877	0.000476086
Casp1	0.164328	0.69787	2.08638	1.16851E-06
Ggta1	0.547011	2.31164	2.07927	7.50733E-13
Gypa	0.0566676	0.239164	2.07741	0.000770931
Glp2r	0.0152479	0.0643482	2.07729	0.00286527
St18	0.00829512	0.0349474	2.07485	0.0139976
Diras2	0.563105	2.36304	2.06917	0
Tap1	1.5329	6.39227	2.06006	0
Zbtb8b	0.0224495	0.0935185	2.05857	0.00348164
Hs3st2	0.179778	0.739527	2.04039	1.22052E-08
Atp13a4	0.0319663	0.13139	2.03923	0.000514152
Olfr287	4.11909	16.9186	2.03821	0

Extl1	0.130193	0.534327	2.03707	8.65567E-10
Fbxo32	1.2488	5.11695	2.03474	0
Ccdc114	0.0197693	0.0809414	2.03362	0.0188698
S1pr3	0.0908122	0.370577	2.02881	1.32842E-08
Gdf15	1.26572	5.1601	2.02745	6.32827E-14
Aldh1a1	0.214718	0.8659	2.01176	1.27233E-08
Kndc1	0.0471396	0.189682	2.00857	6.03013E-08
Agt	0.524515	2.10568	2.00523	3.73301E-12
Fgf18	0.128593	0.51495	2.00162	0.000362416
Apobec1	4.24891	16.8879	1.99083	0
Hmgcll1	0.226392	0.89686	1.98606	1.68752E-11
Adrb2	0.125149	0.492664	1.97695	1.58604E-06
Olfml1	0.0439026	0.17272	1.97606	0.0031771
Pygm	1.45261	5.66831	1.96427	0
Sp6	0.0698306	0.270688	1.9547	4.65516E-06
Slc26a3	0.0203851	0.0790091	1.9545	0.0186874
Slco1c1	0.0230897	0.0888917	1.9448	0.0373116
Efna3	0.839623	3.22534	1.94164	1.55393E-11
Tnfrsf10b	2.52663	9.68553	1.93862	0
E030003E18Rik	0.111596	0.426019	1.93263	0.00126829
Cd55	0.0947709	0.361737	1.93243	7.75607E-06
Scnn1a	0.0319623	0.121521	1.92676	0.0010336
Agbl2	0.0792505	0.300897	1.92478	1.85708E-06
Pqlc3	1.27083	4.81102	1.92057	3.9968E-15
Pla2g7	31.8714	120.521	1.91895	0
Gimap8	0.084552	0.315286	1.89875	2.12558E-06
Ermn	0.0161434	0.0599757	1.89343	0.0184281
5430435G22Rik	0.0562105	0.208715	1.89262	0.000406674
Apod	0.0454461	0.168455	1.89013	0.00545978
Gpr75	0.380525	1.40911	1.88872	9.64503E-09
Clu	2.6888	9.9567	1.8887	0
Pvrl4	0.0466378	0.172677	1.88851	0.00033784
Rab42-ps	0.10213	0.377562	1.88631	0.0152549
Kcnk13	0.09289	0.343146	1.88523	3.10473E-05
Fndc5	1.42255	5.21401	1.87391	0
Celf5	1.03616	3.78302	1.8683	0
Pamr1	0.0237197	0.0863713	1.86447	0.0125298
Sod3	0.427017	1.53945	1.85005	5.67024E-10

Cftr	0.0278861	0.100497	1.84953	0.000115734
Olfr288	0.278406	1.00133	1.84666	2.15636E-08
Scube3	0.0151193	0.0542552	1.84337	0.0429941
Rasgef1a	0.135447	0.485221	1.84091	1.83041E-07
Mmp2	0.665702	2.379	1.83741	9.10383E-15
Adra2a	0.0305217	0.107995	1.82306	0.00165254
Wdr72	0.0239773	0.0848053	1.82249	0.00123443
Ank3	1.16886	4.12957	1.82089	0
Ky	0.0984402	0.345871	1.81291	5.2633E-08
P2rx3	0.143777	0.504877	1.8121	2.33219E-08
Apob48r	0.0268667	0.0942441	1.81059	0.00426181
Syne1	0.0876188	0.307232	1.81002	1.51631E-08
Rspo3	0.0242028	0.0848403	1.80958	0.0251262
Mapk13	0.0408943	0.143239	1.80846	0.0310055
Thrsp	3.94065	13.7937	1.8075	0
Synpo	0.121582	0.422191	1.79597	5.54415E-05
Pacsin1	0.418458	1.4403	1.78321	1.29528E-05
Rln1	0.366795	1.25992	1.78029	0.000111694
Irgm2	0.0421171	0.144289	1.77648	0.000755001
Rarb	1.99584	6.81511	1.77174	0
Nr5a2	0.0888029	0.303205	1.77161	8.45461E-06
Trim34	0.0254202	0.0867777	1.77135	0.0198198
Sgca	0.0894378	0.304317	1.76662	0.00239395
Arhgef19	0.283257	0.961767	1.76358	9.28003E-10
Stmn2	0.032	0.108269	1.75848	0.027862
Zfr2	0.0851474	0.287476	1.75541	1.50778E-05
Glp1r	0.0622077	0.209878	1.75439	0.00857912
Gm4659	0.11639	0.390533	1.74648	9.02261E-06
Plxdc2	1.81903	6.10118	1.74591	0
Mr1	0.151594	0.505923	1.73871	2.8126E-06
Gda	0.00923917	0.0308332	1.73865	0.0442314
Fibin	0.0278153	0.0925856	1.73491	0.0337675
Olfm3	0.109101	0.363057	1.73453	1.28754E-06
Ndrg4	9.04006	30.0806	1.73443	0
Ephx2	0.251745	0.837064	1.73338	4.27635E-07
Cdkn1a	65.0609	215.997	1.73115	0
Kcna4	0.110143	0.364261	1.7256	2.6356E-07
Plek2	0.150705	0.498137	1.72481	0.000110099

Dcxr	7.47083	24.6371	1.72149	0
Cgref1	3.55609	11.6961	1.71766	4.44089E-15
Abcc8	0.0117485	0.0385843	1.71553	0.0304978
Notum	0.0268959	0.088231	1.7139	0.0422035
Robo3	0.0677218	0.222046	1.71317	9.30031E-06
Cnga3	0.0311429	0.101851	1.70949	0.00438578
Areg	0.471107	1.54065	1.70942	5.67493E-07
9230105E10Rik	0.0914454	0.298964	1.70899	8.61922E-06
Slc4a10	0.0586484	0.191595	1.70789	1.06057E-05
Prss35	0.105233	0.343572	1.70702	7.06551E-05
Pitpnm3	0.0315705	0.102792	1.70307	0.000302296
Spata22	0.0505667	0.16436	1.7006	0.0334771
A230057D06Rik	0.237636	0.772255	1.70032	1.57347E-06
Lrp1b	0.204682	0.66499	1.69995	1.33227E-15
Akr1c14	0.0354879	0.115063	1.69702	0.0118505
Atp1b1	10.0872	32.628	1.69358	0
Hic1	0.232707	0.752354	1.6929	4.92186E-06
Abca12	0.0163922	0.0527583	1.68639	0.00171411
Bhlhe41	0.484883	1.55831	1.68427	1.82414E-07
Kcna1	0.0366004	0.117272	1.67993	1.23407E-05
Fam131a	2.935	9.37891	1.67606	5.4845E-14
Agpat9	0.0374706	0.119712	1.67574	0.00591925
Esr2	0.0242349	0.0774022	1.67529	0.0257169
Rbp1	1.34243	4.28208	1.67346	2.02061E-14
Syt4	0.0558578	0.178152	1.67327	0.000179025
Pdgfb	0.0199931	0.0637325	1.67253	0.0381478
Epb4.9	0.112807	0.359584	1.67247	3.19722E-05
Egfl6	0.120968	0.385266	1.67123	1.95023E-05
Fn3k	0.149417	0.47573	1.6708	0.00774935
Islr	0.150686	0.478608	1.6673	0.00189373
Tlr5	0.0519977	0.164363	1.66036	0.000947922
Cp	1.65276	5.22086	1.65941	4.15823E-12
Lama3	0.0228708	0.0721909	1.65831	0.000110044
Ajap1	0.208548	0.651355	1.64306	3.92535E-07
Fam20a	0.304334	0.950329	1.64277	1.02786E-07
Kcnt1	0.203685	0.635575	1.64172	4.46013E-05
Abat	8.92364	27.7446	1.6365	0
Igtp	0.369092	1.14666	1.63539	1.87269E-07

Pmaip1	3.19457	9.89306	1.6308	0
Tmem200a	0.354073	1.09441	1.62804	3.51997E-10
Sytl2	0.984854	3.04381	1.6279	1.78837E-08
Tlr4	0.0532083	0.164251	1.62618	0.000417946
Calb1	0.0268134	0.0827202	1.62528	0.0217076
Htra3	0.300562	0.926225	1.6237	1.29301E-05
Sdc4	5.71032	17.5828	1.62252	0
Fam101a	3.37129	10.3568	1.6192	0
P2rx7	3.76064	11.5262	1.61587	2.39808E-14
Acot11	0.512885	1.56803	1.61225	1.11022E-13
Osmr	0.0518316	0.157566	1.60405	0.000170725
Grm1	0.101341	0.307717	1.60238	0.000908446
Gbp9	0.692495	2.09775	1.59897	1.60094E-12
Hbegf	4.01069	12.0617	1.58851	0
Palm3	0.258661	0.775984	1.58497	1.06566E-05
Pdcd4	6.60458	19.8121	1.58484	7.06604E-09
Hrc	0.190094	0.569922	1.58405	1.44046E-05
Arhgef37	0.0338579	0.100945	1.57601	0.009003
Afap1l2	0.951877	2.83119	1.57256	1.98752E-12
Rai2	1.6334	4.832	1.56474	3.38871E-11
Chac1	3.12007	9.205	1.56084	1.9984E-15
Synpr	0.803791	2.36898	1.55937	8.22988E-11
Bfsp2	0.740172	2.18007	1.55844	3.2943E-08
Lrp2bp	0.136644	0.401763	1.55592	1.02888E-05
Kcnt2	0.152562	0.445792	1.54697	2.65674E-06
Spock1	0.0405505	0.118331	1.54504	0.0367156
Slc24a4	0.0543866	0.158526	1.5434	0.0104228
Cacna1e	0.0697064	0.202635	1.53952	2.01998E-07
Hif3a	0.0735119	0.21301	1.53487	8.72322E-06
Slc17a8	0.0395961	0.114536	1.53237	0.00186715
St8sia5	0.499097	1.44096	1.52964	1.32311E-05
Anxa5	8.21784	23.652	1.52513	0
Fcgrt	0.0800634	0.230139	1.52329	0.00658745
Mylk3	0.0355768	0.101988	1.51939	0.0122612
Nlrc5	0.0707463	0.202386	1.51638	1.11194E-05
Ccdc153	0.144367	0.412392	1.51428	0.00560226
4931408A02Rik	1.45201	4.13686	1.51049	2.63216E-10
Rgs16	2.98784	8.49754	1.50794	0

Bbc3	1.7024	4.8395	1.50728	2.80087E-12
Ptprt	1.79567	5.09908	1.50572	0
Epha2	0.714084	2.02457	1.50345	1.68006E-11
Cox7a1	3.37774	9.57307	1.50292	2.56062E-06
Apoe	21.1874	60.006	1.5019	0
Gbp2	0.324312	0.916967	1.49949	1.17409E-06
Sept4	5.16031	14.5693	1.4974	0
Trim12	0.0473863	0.133485	1.49413	0.0496445
Rnase1	0.134035	0.377383	1.49341	0.0127947
Ikbke	0.17536	0.493712	1.49335	9.38954E-06
Tmtc1	0.346799	0.975116	1.49147	0.00325372
Npy2r	0.0400908	0.112676	1.49084	0.00749091
P2ry2	0.0488806	0.137309	1.49009	0.0056055
Slc5a8	0.0207456	0.0582228	1.48878	0.0131814
Far2	0.68272	1.91443	1.48755	0.0106948
Tmem132b	0.322685	0.903906	1.48605	3.9075E-11
Cyp27a1	0.129228	0.361402	1.48368	0.000762212
BC031353	2.77622	7.75908	1.48276	0
H2-Ab1	0.324919	0.907962	1.48255	0.00013476
Fosb	0.0385603	0.10751	1.47929	0.00559956
Slc35f3	0.271529	0.755261	1.47587	2.38985E-06
C3	0.0219666	0.06096	1.47255	0.0169246
Ryr2	0.110699	0.307176	1.47242	1.79468E-09
Aox1	0.415243	1.15006	1.46968	3.34908E-09
Fgf1	4.46894	12.3502	1.46653	0
Mxd4	14.5422	40.1303	1.46445	0
Efhc1	0.112729	0.310913	1.46366	0.000752987
Grin2a	0.0840398	0.231665	1.4629	0.000101372
Sulf1	0.611814	1.68277	1.45967	3.9627E-11
Il34	0.146236	0.401274	1.45629	0.00136097
Fst	0.344976	0.946356	1.45589	2.68041E-06
Ifit1	0.0321633	0.0882032	1.45541	0.0388322
Fgd4	0.279586	0.766476	1.45495	0.000256074
Bace2	0.71135	1.94724	1.4528	1.08977E-10
Ddr2	1.66305	4.55182	1.45261	0
Anxa3	5.74598	15.7206	1.45203	0
Krt1	0.0662174	0.180679	1.44815	0.00521511
Rnasel	0.454645	1.24031	1.44789	9.40724E-10

Ryr3	0.409844	1.11772	1.44741	1.33227E-15
Angpt2	8.75081	23.8351	1.4456	0
Klf4	0.452305	1.22972	1.44296	8.42543E-08
A3galt2	0.215976	0.585975	1.43997	4.77249E-06
Rgs4	0.132372	0.358444	1.43715	0.000122002
Slc7a11	1.92066	5.20034	1.43701	0
6030405A18Rik	3.41387	9.24242	1.43686	0
Dapk1	4.27006	11.5535	1.436	0
Pik3ip1	1.97854	5.33046	1.42982	8.8396E-13
Krt222	0.0464004	0.125005	1.42977	0.0125524
Cytip	0.0148454	0.0399587	1.42849	0.0388582
Slc6a3	0.0313204	0.0840485	1.42412	0.0198773
Abcg1	0.0379795	0.101644	1.42024	0.00172753
Cacna1g	0.354478	0.947617	1.41861	8.81412E-08
Lgals4,Lgals6	0.341619	0.906699	1.40823	0.000193084
Tekt2	0.328107	0.869787	1.4065	0.000093262
Htr2a	0.227984	0.603982	1.40557	1.37277E-05
5031414D18Rik	0.0422656	0.111963	1.40547	0.0207303
Trp53inp1	25.3755	67.0182	1.40112	0
Slc16a14	0.286963	0.756427	1.39834	1.74836E-05
Enpp6	0.165306	0.435725	1.39828	8.19566E-05
Gm973	0.269871	0.711123	1.39783	2.03812E-06
Nkain2	0.945396	2.48921	1.3967	5.61701E-08
Lif	0.39093	1.02901	1.39628	2.20009E-07
Ctsf	3.8784	10.2034	1.39552	3.55271E-15
Gpc5	0.244769	0.643796	1.39518	1.23259E-05
Ldhd	0.0377522	0.0989445	1.39006	0.0455389
Ptprn	0.249027	0.652615	1.38993	4.19042E-06
Sorl1	0.536585	1.40122	1.38481	2.81144E-11
Il6ra	0.0570564	0.148915	1.38402	0.00410178
Mfap3l	2.85663	7.45149	1.38322	2.22045E-16
Dmrtb1	11.9155	31.0171	1.38023	0
Isg20	0.551958	1.43677	1.3802	0.00828716
Phyh	4.99384	12.992	1.3794	1.46549E-14
Ddit4	16.3602	42.5274	1.3782	0
Pstpip1	0.061116	0.158512	1.37497	0.0255539
Tuba8	0.12473	0.32344	1.37469	0.00789363
Ptpn14	3.43435	8.90527	1.37462	0

Txlnb	0.462879	1.19848	1.3725	1.22634E-08
Ano3	3.63701	9.40807	1.37115	5.66658E-13
C030044B11Rik	6.74068	17.425	1.3702	4.44089E-16
Clca1	0.0589519	0.152223	1.36858	0.00578415
Aass	0.0663694	0.171149	1.36666	0.00170759
Adrbk2	5.60673	14.4169	1.36253	1.55431E-15
Scn3a	0.133992	0.342682	1.35472	5.95217E-07
Prr16	0.104748	0.267768	1.35406	0.00298305
Plcd4	22.5595	57.6182	1.35279	3.49136E-08
Mapkapk3	3.74156	9.54066	1.35045	2.22045E-16
Serpinb5	0.512707	1.30609	1.34905	8.60569E-07
P2rx5	0.0638544	0.162594	1.34842	0.0133415
Tm4sf1	0.635111	1.61653	1.34782	2.06175E-06
Synm	0.234315	0.595356	1.34531	9.94947E-06
Kcnk3	0.112787	0.286105	1.34294	0.000225358
Klhdc8a	0.0671561	0.170151	1.34122	0.00111585
Tceal5	0.193477	0.48986	1.3402	0.00780574
Upk1a	0.440569	1.11335	1.33746	0.000125567
Pigz	0.0703425	0.177536	1.33565	0.0124459
Myt1l	0.135826	0.342609	1.33481	1.28706E-05
Mamdc2	3.78962	9.55841	1.33472	0
Scn1b	3.89523	9.81793	1.33371	2.88436E-12
Adc	0.755279	1.89904	1.33019	9.67517E-07
Tyr	0.0466039	0.117166	1.33003	0.0116782
Oplah	0.929449	2.33562	1.32936	2.58394E-10
Rnf182	0.833386	2.09395	1.32917	2.58261E-09
Foxj1	2.73077	6.84397	1.32553	1.50102E-13
Ptgfr	0.105119	0.262743	1.32162	0.000255309
Cyp27b1	0.0436463	0.109015	1.32059	0.0350946
Kcp	0.0216154	0.0539797	1.32036	0.0336265
Tiam2	0.49528	1.23519	1.31842	9.38845E-07
Ifi27l1	0.392199	0.976975	1.31673	0.00519476
Sesn2	19.1339	47.6428	1.31613	0
Adamts14	1.57891	3.91667	1.3107	4.24105E-14
Stard5	4.49177	11.1302	1.30912	1.9984E-15
Ccdc3	0.294959	0.72957	1.30653	3.12448E-05
Slc2a9	1.40886	3.48327	1.30591	2.13214E-09
Adora2a	0.318875	0.786241	1.30198	3.85684E-05

Cav1	2.03852	5.01375	1.29837	2.81959E-11
Pdk2	2.55781	6.28884	1.29788	6.11777E-12
Golga7b	1.10909	2.72143	1.29499	3.8001E-09
Ddit4l	12.0958	29.6764	1.29481	0
P4ha3	0.154962	0.379785	1.29327	0.000779524
Arhgef5	0.0192387	0.0471072	1.29194	0.0385063
Kcnq3	0.26879	0.65681	1.289	4.84738E-05
Rab40b	0.431748	1.05332	1.28669	4.37433E-05
Arpp21	0.993737	2.42292	1.28581	7.31335E-06
Gpr68	0.324185	0.788442	1.28219	0.0025655
1500015O10Rik	1.56965	3.81686	1.28195	5.08112E-06
Tec	0.178736	0.434169	1.28043	0.026265
Ccng1	92.2311	223.878	1.27939	7.99361E-15
Vwa1	0.701931	1.7035	1.2791	9.97712E-08
Kcnj11	0.131972	0.31985	1.27717	0.000605963
Slc35d2	0.0961563	0.232633	1.2746	0.00578553
Cacng5	2.83326	6.84649	1.2729	3.39728E-14
Sparcl1	48.9043	118.114	1.27214	0
Ccrl1	0.920978	2.22359	1.27165	0.00158962
Ak1	27.298	65.863	1.27067	0
Scn3b	2.86235	6.90464	1.27037	1.09912E-13
Atp2a3	0.0719333	0.173368	1.26911	0.0149167
Parp14	0.081321	0.195955	1.26882	0.000150412
Nmnat2	3.36463	8.07979	1.26387	2.22045E-16
Ang,Rnase4	0.32685	0.784419	1.263	0.00650779
Tmem88b	0.150281	0.36039	1.2619	0.000284677
Ccdc106	1.40393	3.36461	1.26097	2.95776E-08
Rasal1	0.0669957	0.160463	1.2601	0.00657082
Plp1	2.83525	6.78896	1.25971	2.54663E-12
Kcnc4	1.62661	3.89347	1.25919	1.29317E-10
Ercc5	11.2166	26.7707	1.25503	0
9230114K14Rik	2.00626	4.7823	1.2532	8.45995E-10
Chrna4	7.77078	18.4606	1.24832	0
Isoc2b	0.305548	0.72549	1.24756	0.00322693
Styk1	0.544637	1.29285	1.24719	7.01478E-07
Rnf169	4.4301	10.5155	1.2471	0
Gpc4	7.96504	18.8895	1.24583	0
Snph	0.856672	2.02939	1.24423	1.26255E-09

Elovl7	0.416993	0.987284	1.24344	1.51729E-07
Dkk3	0.426488	1.00948	1.24304	3.80912E-06
Arhgap6	0.452584	1.06901	1.24002	8.16144E-05
Stard10	2.36349	5.5758	1.23826	8.81325E-08
Rerg	0.274535	0.646902	1.23656	0.0108762
H2afj	5.43352	12.7569	1.23131	3.32623E-13
Abhd4	48.8479	114.66	1.231	0
Cmya5	0.110619	0.25965	1.23097	7.75792E-06
Slc22a4	0.14141	0.331531	1.22925	0.00253506
Ptgr2	5.45145	12.7783	1.22898	6.66134E-16
Pyroxd2	0.314311	0.736623	1.22874	3.37777E-05
Klhdc8b	1.08871	2.5505	1.22816	0.0010152
Cacna1i	0.0110923	0.0259494	1.22614	0.0433648
Osgin1	0.0914368	0.213568	1.22385	0.0163102
Ston1	1.57972	3.68857	1.2234	6.87037E-10
As3mt	0.662832	1.54592	1.22175	0.000021857
Mcf2	0.0707676	0.16499	1.22122	0.00449644
Sec16b	0.18407	0.427656	1.2162	0.00112753
Aqp4	1.00067	2.32469	1.21607	3.74515E-10
Nacc2	3.17451	7.36765	1.21467	4.44089E-16
Slc16a9	0.211395	0.489908	1.21257	0.000132177
Ociad2	1.37526	3.1871	1.21254	8.98798E-08
Adamts19	0.365904	0.846287	1.20968	2.52446E-06
Npvf	0.623693	1.44232	1.20949	0.00491006
Kcnma1	1.5565	3.59931	1.20942	5.54379E-12
4930486G11Rik	0.0833349	0.19245	1.20749	0.00552086
Kcnn2	0.963636	2.22148	1.20496	1.48247E-06
Plcxd3	0.201821	0.46501	1.20418	0.00183295
Slitrk6	0.0862907	0.198617	1.20271	0.00170432
Cyp7b1	1.211	2.78715	1.20259	2.18189E-07
Fam83h	0.116824	0.268317	1.1996	0.000661894
Itgb5	16.9155	38.7411	1.19552	0
Ipw	5.28838	12.1026	1.19442	7.48322E-08
Aspa	0.311923	0.713536	1.1938	0.00105985
Nrxn3	0.325945	0.744553	1.19175	8.00671E-07
Bdkrb2	0.252503	0.576389	1.19074	0.00184155
Disp2	0.9961	2.27045	1.18861	8.57194E-11
Gck	0.120502	0.274411	1.18728	0.00557179

Layn	0.747032	1.70051	1.18673	2.08064E-05
Ypel2	0.328307	0.747084	1.18623	5.09041E-06
Cyp4v3	0.2461	0.559992	1.18616	0.000244772
Rarg	1.27584	2.89863	1.18392	3.56808E-07
Galt	1.08031	2.45401	1.18369	1.37486E-06
Eno2	0.716683	1.62709	1.18289	2.82441E-06
Lrrc28	5.01151	11.3653	1.18132	7.56424E-10
Neu4	0.0269097	0.0609895	1.18043	0.0459186
Gpr123	0.860903	1.95087	1.1802	8.54214E-09
Mertk	1.46487	3.31759	1.17937	1.12196E-09
Chgb	0.181615	0.411065	1.17849	0.00093867
C1qtnf6	5.46447	12.3582	1.17732	1.04612E-11
Nptx1	8.28801	18.7404	1.17705	0
Phlda3	26.3583	59.5741	1.17643	0
Mfsd7c	0.151916	0.343344	1.17638	0.000812433
P4htm	1.90288	4.29929	1.17591	6.95171E-08
Fam13a	2.26184	5.10835	1.17536	2.48646E-12
Aldh4a1	9.78053	22.0452	1.17248	0
Nfkbid	0.165631	0.37297	1.17109	0.00360263
Gm1060	0.330173	0.742485	1.16914	0.000182678
Fam189a2	1.05264	2.36375	1.16706	4.31916E-07
Pex5l	1.11048	2.49173	1.16596	1.08854E-06
Klhl4	0.136754	0.306711	1.1653	0.00184251
Dysf	0.266437	0.597297	1.16465	2.97871E-05
Abca4	0.0296772	0.0665029	1.16406	0.0112296
Tmem37	1.36438	3.05636	1.16358	4.25873E-05
Trim66	0.271921	0.607253	1.15911	5.07901E-05
Cth	3.45661	7.71126	1.15761	9.07128E-10
Mgmt	4.97227	11.0842	1.15653	9.05494E-08
Ppfibp2	2.82984	6.30681	1.15619	4.05047E-11
Sepp1	22.0127	49.0431	1.15571	6.66134E-16
Cplx1	6.33013	14.0923	1.15461	2.92433E-13
Mpeg1	0.196273	0.436712	1.15382	0.000171069
Lama2	0.0492448	0.109431	1.15199	0.00116946
Pdlim4	1.68225	3.73471	1.1506	9.96643E-06
Ereg	0.0324493	0.0719524	1.14886	0.0431917
Dennd2c	0.480399	1.0626	1.14529	1.16336E-06
Parp3	1.25787	2.78094	1.14459	1.76862E-07

Larp6	0.224268	0.49577	1.14445	0.0015235
Esrrg	0.316867	0.700245	1.14398	1.02369E-05
Zfp641	1.36683	3.01877	1.14312	5.11044E-09
Kcng4	0.0376411	0.0829997	1.1408	0.039303
Cpne7	2.10311	4.63437	1.13984	8.86836E-09
Eda2r	21.4103	47.1679	1.1395	1.28766E-11
Pnrc1	3.49335	7.69398	1.13912	6.88462E-10
Gas6	10.3218	22.7333	1.13911	3.33067E-15
Fam19a1	0.14608	0.321725	1.13907	0.00199918
Apc2	1.78506	3.92972	1.13845	1.18709E-09
Lzts1	0.303299	0.667552	1.13814	0.00123415
Casp12	0.0587033	0.129113	1.13712	0.0385684
Acaa1b	1.4648	3.22023	1.13646	2.0478E-06
Rapgef4	3.73597	8.20816	1.13558	5.16653E-12
Cpt1c	10.3558	22.7364	1.13457	2.22045E-15
Igfbp5	2.3049	5.05553	1.13316	7.36078E-13
Procr	0.178813	0.392097	1.13276	0.0099563
Sorcs2	6.83448	14.9606	1.13027	8.88178E-16
Pde4a	0.245942	0.538025	1.12935	0.00181562
Atf3	0.552462	1.20645	1.12682	0.000134211
Sgcd	0.246513	0.538302	1.12675	0.00564518
Dio2	0.335792	0.732893	1.12603	5.96451E-06
Creg2	0.178551	0.389076	1.12372	0.000123579
Ifitm3	3.89399	8.47968	1.12276	7.80007E-06
Gstt1	14.3268	31.1572	1.12085	2.39853E-12
Tmem53	0.540113	1.17457	1.12079	0.00239635
Kcnk1	2.3351	5.07002	1.11851	8.46282E-09
Rassf5	0.104999	0.227843	1.11766	0.00407661
Sparc	32.9041	71.3708	1.11707	2.22045E-15
Emid2	0.288316	0.625073	1.11637	0.000449005
Pck2	6.85783	14.8587	1.11548	2.93099E-14
Dnahc8	0.0792555	0.171484	1.11349	8.41015E-05
Csdc2	4.85183	10.4909	1.11253	9.41314E-12
Dnahc7b	0.240678	0.520141	1.1118	6.16878E-07
Egr3	0.362187	0.782457	1.11128	0.00208015
Cav2	3.09058	6.67343	1.11055	5.33238E-10
Bhlhe22	0.0425408	0.0918221	1.11	0.0496931
Lrrc17	0.16378	0.353329	1.10925	0.00594447

Fos	4.07652	8.7885	1.10828	2.69914E-10
Mcf2l	0.949723	2.04553	1.10689	7.22315E-06
Gbp4	0.104877	0.225735	1.10593	0.0023282
Ctgf	0.4157	0.893536	1.10398	0.000254369
Grina	20.2762	43.579	1.10384	6.21725E-15
Olfr1314	0.177413	0.380729	1.10165	0.0464061
Camta2	3.65744	7.83562	1.09921	1.27582E-11
Plekha6	0.194823	0.417155	1.09842	0.00179372
Reps2	0.314731	0.673463	1.09748	3.18514E-06
Hyal1	1.0849	2.3206	1.09694	4.90387E-06
Cpne2	9.11261	19.4184	1.09149	2.57794E-13
Zfp874	2.01504	4.29235	1.09096	3.42575E-09
Hist2h3c2-ps	0.246709	0.525133	1.08987	0.0187107
H2-M3	0.158508	0.337159	1.08888	0.0213865
Ssh3	0.348792	0.741565	1.08821	0.000323956
1200009I06Rik	0.11252	0.239029	1.08701	0.00709263
Fa2h	0.0891575	0.189225	1.08568	0.0196256
Fbxw9	8.67211	18.3977	1.08507	3.33422E-12
Efemp1	0.186089	0.3944	1.08367	0.00527077
Mdm2	18.2903	38.7133	1.08175	1.9984E-15
Pcolce	0.89185	1.8875	1.08161	0.000105764
Hnmt	0.337784	0.714749	1.08133	0.00212304
Samd9l	0.101191	0.214098	1.08118	0.0018828
Nrg1	0.609314	1.28888	1.08086	0.000129509
Npy1r	0.114493	0.241969	1.07956	0.00633093
4933437F05Rik	0.268543	0.567315	1.079	0.00678868
Mxra7	3.54571	7.48645	1.07821	1.45901E-08
Abhd3	1.20251	2.5374	1.0773	9.85002E-06
Pdgfrl	0.472258	0.996049	1.07664	0.0011849
Lrdd	6.77654	14.2783	1.0752	7.10099E-13
Fhit	0.410805	0.865476	1.07504	0.023796
Rab3b	13.1803	27.745	1.07385	1.67644E-13
Ptrf	5.13639	10.7907	1.07097	3.96061E-12
Fam129a	0.0405578	0.084867	1.06522	0.0433314
Pacrg	1.867	3.906	1.06497	9.1591E-06
Loxl4	0.0731984	0.1531	1.06459	0.0265027
Polk	3.28997	6.87751	1.06381	1.45477E-11
Adamts15	0.0924203	0.193063	1.06279	0.00241097

Scn7a	0.04619	0.0963893	1.06129	0.00691414
Rfx5	4.42241	9.22125	1.06013	1.73417E-12
Tnip2	1.84116	3.83474	1.05851	9.81753E-07
Rab26	2.72841	5.68139	1.05818	1.51743E-06
1700003E16Rik	0.152283	0.31709	1.05814	0.010429
Serpinb9	0.089798	0.186948	1.05788	0.0101214
Parm1	0.528429	1.0994	1.05694	0.000335223
9030617O03Rik	8.48435	17.6467	1.05652	1.52545E-13
Bdh2	0.588135	1.22076	1.05356	0.0243015
Fam167a	0.261828	0.543296	1.05312	0.000396329
Tap2	1.21363	2.51566	1.05161	3.26799E-06
Arhgap28	0.0918861	0.190408	1.05117	0.00350837
Aifm2	1.54279	3.19569	1.05058	0.0298219
Bzrap1	0.468547	0.969788	1.04947	9.18624E-07
Syt17	0.407579	0.843594	1.04947	0.001901
Tob1	8.14636	16.8538	1.04885	4.20508E-12
Mtm1	3.0696	6.35061	1.04885	2.44039E-09
Man2b2	2.68664	5.55368	1.04764	1.05158E-09
Tifa	0.478777	0.9897	1.04764	0.000452537
Frmpd4	0.0410686	0.0848891	1.04754	0.00731547
Spsb1	1.37632	2.84417	1.04719	4.67488E-07
Pvalb	0.212482	0.439089	1.04717	0.0483575
Cdc42bpg	1.75476	3.62556	1.04693	2.9025E-10
Fbln7	1.3323	2.75087	1.04597	7.26162E-07
4922501L14Rik	0.582046	1.2012	1.04527	0.000298002
Id1	4.10576	8.46946	1.04462	2.48826E-06
Wipi1	2.3236	4.7918	1.04421	5.40594E-07
Fmn1	0.0408926	0.084291	1.04354	0.00382913
Ankrd45	0.177765	0.366267	1.04292	0.00178786
Sgsm2	4.47536	9.21657	1.04222	1.69686E-12
Chd5	0.413965	0.85227	1.0418	2.83303E-06
Ttyh2	4.21322	8.66912	1.04096	3.31555E-11
Avil	0.0809557	0.166218	1.03787	0.0220876
Fam189a1	1.2019	2.46588	1.03678	3.48196E-05
Sema5a	1.07949	2.21458	1.03669	2.54758E-10
Slc24a2	0.0950668	0.194883	1.0356	0.00815968
Mansc1	0.186334	0.3818	1.03493	0.00564563
Arl5c	0.314255	0.643434	1.03385	0.00477677

Lpo	9.43649	19.305	1.03265	6.71241E-13
A230065H16Rik	0.450909	0.921577	1.03127	0.0239351
Cyp4f17	1.34823	2.75272	1.02979	2.64448E-05
Rasl10b	5.03936	10.2786	1.02833	1.54547E-11
Plau	1.08446	2.2101	1.02713	1.39398E-05
Fam38a	1.78714	3.64	1.02628	7.03993E-08
Zfp456	0.288255	0.587056	1.02615	0.000350126
4930402H24Rik	5.40622	11.0069	1.02571	4.86167E-12
Lrrc7	1.70012	3.45875	1.02461	1.09159E-09
Fam83f	0.0727175	0.147625	1.02156	0.0287584
Cpeb1	0.289909	0.588439	1.02129	0.00152216
Snhg11	0.291666	0.591835	1.02088	8.07424E-05
Mir705,Rab11fip5	2.115	4.29058	1.02051	2.81763E-07
Scn11a	0.0757739	0.153672	1.02008	0.00542049
Tmem108	0.404934	0.820914	1.01954	0.000177781
Pde1c	1.88392	3.81888	1.01941	2.78812E-07
1700120K04Rik	0.721426	1.46217	1.01919	0.0164374
Ptchd2	0.463415	0.938404	1.0179	9.00233E-07
Cml1	2.74958	5.55789	1.01533	2.05027E-05
Whrn	3.45098	6.97272	1.01472	5.59231E-07
Zmat3	10.9752	22.1697	1.01434	2.09166E-13
E130309D14Rik	0.118835	0.239562	1.01144	0.00515585
Folh1	0.0905498	0.182537	1.01141	0.0254753
Il33	0.453305	0.913618	1.01111	0.000944661
Ubtd1	4.04771	8.14436	1.00869	1.69864E-07
Adm	7.55983	15.2107	1.00866	4.01345E-09
Nid1	1.20553	2.42464	1.00811	2.34705E-08
Ppm1h	0.920635	1.85118	1.00775	6.81582E-07
Amy1	0.315805	0.634798	1.00727	0.00541427
6330403K07Rik	3.89016	7.81697	1.00678	1.29044E-07
Slc30a10	0.469751	0.943524	1.00616	1.28809E-05
Celsr3	0.69099	1.38668	1.00489	1.13454E-08
Zbtb7b	3.36815	6.75618	1.00425	5.85E-10
Psmb8	0.310248	0.621661	1.00271	0.0116093
Galntl4	1.45274	2.91089	1.00268	3.47288E-06
Igdcc4	11.8978	23.8275	1.00193	1.54765E-13
Ctsd	97.212	194.685	1.00193	6.53055E-12
Col18a1	2.09386	4.18765	0.999979	2.71971E-08

Mocos	0.0918041	0.183538	0.99945	0.0208781
Kcnc2	0.0439738	0.0878549	0.998477	0.0182431
Prkcd	0.0982452	0.196202	0.997882	0.0253971
Adamtsl1	0.0646225	0.128984	0.997085	0.00478897
Gpr146	0.427549	0.85231	0.995287	0.0278997
Tubb3	4.81267	9.59292	0.995131	2.72773E-08
Slc27a3	4.52497	9.01767	0.994846	4.42095E-09
Csmd1	0.144348	0.287443	0.993719	5.61747E-05
Fam70a	1.31711	2.61953	0.991935	1.05824E-06
Camk2b	33.1112	65.8238	0.991291	3.09406E-10
Cox6b2	6.45716	12.8286	0.99039	0.000410397
Mical2	4.7228	9.37836	0.989695	1.54136E-10
Gabrr2	0.281545	0.559007	0.989498	0.00610884
Dsc2	1.63409	3.24416	0.989356	4.67134E-08
Synj2	4.47112	8.87433	0.989	1.09154E-08
Myrip	0.0987454	0.195947	0.988682	0.00653894
Stk32c	1.1215	2.22391	0.987673	0.00192671
Rgs6	0.0880079	0.174506	0.987569	0.0321857
Gstm1	33.8326	66.9877	0.985483	1.9682E-12
Car12	0.453373	0.897314	0.984915	0.000177351
Gm4349	0.33883	0.670267	0.984176	0.0176505
Sh2d4a	0.137221	0.271425	0.984054	0.0112554
Kcnk2	2.04766	4.04595	0.982501	8.24732E-07
Kcnd1	0.167206	0.330329	0.982275	0.016299
Cdkn2b	2.31442	4.57053	0.981706	0.000015793
Vwa5b1	0.187055	0.369084	0.980486	0.00260277
Als2cl	1.29675	2.55739	0.979776	2.99886E-07
Ghitm	59.1384	116.618	0.979623	3.23985E-12
Cd14	0.569194	1.12166	0.978644	0.00207901
Rhod	4.09828	8.07499	0.978441	8.50981E-07
Slc37a2	3.15522	6.21521	0.978061	6.46782E-10
Cdk18	0.090471	0.178201	0.977979	0.0215842
Cpped1	15.7716	31.065	0.977964	2.33769E-12
Ccnd2	144.074	283.549	0.976792	2.63857E-06
Fbxl20	1.56908	3.08806	0.976786	7.08928E-10
Slc19a2	8.75262	17.2248	0.976702	4.94693E-12
Npnt	1.86915	3.67688	0.976103	5.80404E-06
Ano1	0.0704115	0.138508	0.97609	0.019649

Scml4	0.565135	1.11063	0.974707	2.77342E-05
Lrfn2	0.225762	0.442923	0.972251	0.00335324
Greb1	0.454496	0.891193	0.971471	5.10215E-06
Usp2	4.37729	8.57831	0.970655	3.53422E-10
Dhrs11	1.93996	3.80128	0.970461	4.08718E-05
Il15ra	2.11027	4.13431	0.970215	0.000318293
Lrrc16a	5.35076	10.4719	0.968713	1.19316E-11
Fam65b	0.21559	0.421751	0.968105	0.0151334
Renbp	2.64695	5.17765	0.96797	0.000067544
Frmpd1	2.78858	5.44601	0.96567	1.29801E-09
Olfr1317	0.252412	0.492469	0.964254	0.043951
Tmem38a	19.6712	38.3603	0.963529	6.96043E-12
Rimbp2	0.344897	0.672317	0.962976	0.000387919
Mgat5b	3.10258	6.03742	0.960461	2.11373E-09
Stard8	0.108609	0.210912	0.957491	0.00619249
Jhdm1d	1.96985	3.82318	0.956686	1.76555E-10
Mmd2	11.3291	21.9878	0.956672	6.04701E-11
Luzp2	3.28491	6.37498	0.956565	3.70702E-10
Txnip	0.649479	1.25959	0.955602	0.00473614
Stxbp2	0.0797742	0.15461	0.95464	0.0434885
Tmem163	0.0986276	0.190867	0.952505	0.0361586
Ecm2	0.480453	0.929476	0.952023	0.0105776
Micalcl	0.241149	0.465741	0.949603	0.00546292
Faim2	0.103058	0.198878	0.948433	0.0111403
Tns1	1.53856	2.96828	0.948046	9.8701E-10
Acad11	3.40045	6.56014	0.948	5.2729E-08
Adamtsl4	0.0609863	0.117527	0.946433	0.037005
D10Bwg1379e	0.0449336	0.0865619	0.945936	0.014806
Megf10	2.51262	4.83927	0.945596	2.97871E-10
Efhd1	3.89322	7.49465	0.944897	3.80624E-07
Ttpa	4.23381	8.14676	0.944271	4.72024E-09
Fblim1	0.632288	1.2158	0.943252	0.00025071
Myh14	1.1821	2.2729	0.943179	1.57066E-07
Tlr2	0.104881	0.201595	0.942704	0.0237713
1300014I06Rik	4.10459	7.87676	0.940362	2.79278E-07
Frem1	0.126373	0.242408	0.939756	0.0010149
S1pr1	7.35093	14.0913	0.938812	1.98957E-10
9330129D05Rik	0.514979	0.986993	0.938527	0.00110649

Astn2	3.15985	6.0537	0.93796	2.55307E-05
Serpina3n	0.656842	1.258	0.93752	0.00160787
Akap17b	3.0839	5.90337	0.936781	4.60238E-10
A430110N23Rik	0.493403	0.944308	0.93649	0.00017362
Pcp4l1	32.429	62.0257	0.93558	1.21527E-11
Card10	0.242844	0.463825	0.933552	0.00130647
Ctsh	1.97856	3.77766	0.93304	0.000058857
Abcg4	3.29589	6.28909	0.932184	1.20022E-08
Ldhb	77.3383	147.569	0.932137	7.93365E-12
H2-DMa	1.85297	3.53414	0.931518	0.00122691
Dpp6	5.36732	10.2364	0.931429	2.17231E-10
Rnf43	0.125019	0.238409	0.931289	0.0085594
Tspan18	0.245502	0.468057	0.930947	0.00292839
Ctso	3.11702	5.94207	0.9308	2.48312E-08
Lgals3bp	0.350752	0.668635	0.930768	0.00424824
AA415398	0.443776	0.845756	0.930409	0.0034833
Slc5a3	5.72341	10.9071	0.930324	6.38134E-12
Cul9	1.38176	2.63035	0.928748	2.22162E-08
Tcfcp2l1	0.024991	0.0475635	0.928443	0.0393856
Slc6a15	0.678347	1.28841	0.925501	0.000106128
Irak2	0.247928	0.470862	0.925385	0.0236403
Dixdc1	0.407093	0.772948	0.925013	0.000122407
Tcn2	12.9041	24.5008	0.924998	3.52546E-09
Ache	0.295395	0.560592	0.924304	0.00666481
Fzd1	6.11945	11.6054	0.923328	1.78027E-10
Gucy1a3	1.53457	2.91005	0.923208	4.68345E-07
Smad3	5.43361	10.2981	0.922395	1.3474E-10
Ccdc88c	11.047	20.9336	0.92217	1.80853E-11
Srsf13b	0.534138	1.01179	0.921623	0.000602702
Mpa2l	0.0938808	0.177796	0.921319	0.0152241
Samd12	1.60466	3.03828	0.920984	0.00112118
Arntl	10.146	19.1805	0.918729	1.12526E-10
Atp2b2	0.228769	0.432399	0.918474	0.00238767
Cx3cl1	5.68814	10.7511	0.918456	1.72394E-09
Tnfrsf25	0.194463	0.367484	0.918185	0.0323676
Lmna	5.02525	9.48572	0.916562	2.74997E-05
Chst8	0.140529	0.265086	0.91559	0.0241707
Itga3	0.113789	0.214528	0.914804	0.00882995

Ntm	20.2493	38.1524	0.913901	7.50044E-11
Itga2b	0.110884	0.208804	0.913101	0.0200454
Rtn4rl1	2.10002	3.95357	0.912751	9.29437E-07
Sv2a	2.90113	5.45775	0.911689	3.52101E-08
Slc25a18	42.7546	80.4245	0.911556	2.22351E-11
Car5b	0.336474	0.632788	0.911227	0.00169172
Cdkl3	1.89591	3.5653	0.911137	0.000574314
Efna5	0.206218	0.387388	0.909607	0.0104225
AI854703	0.27595	0.518334	0.909475	0.00258746
Plcl1	1.62218	3.0455	0.908743	4.96384E-08
Fmnl1	0.199591	0.374074	0.906279	0.00572959
Fgl2	0.41599	0.779603	0.906191	0.000803229
Pfkp	5.08586	9.5285	0.905758	0.00263554
Ednrb	85.971	160.916	0.904386	3.20087E-07
Mpped1	0.116553	0.218026	0.903514	0.0201243
AA986860	0.33846	0.633003	0.903228	0.00288524
Gm8615	3.54231	6.62395	0.903002	8.95074E-07
Aqp9	0.185233	0.346277	0.902581	0.0134635
Palm2	0.192551	0.359871	0.902238	0.000706032
Cpeb3	0.448689	0.838352	0.901842	0.000118617
Ppargc1a	8.45014	15.7725	0.900364	1.10136E-10
Fahd1	6.94699	12.9629	0.899924	2.20676E-07
Dnahc1	0.0300463	0.0560571	0.899708	0.0193439
BC066028	0.382299	0.713193	0.899594	0.000912571
Neurod1	0.349251	0.65079	0.897928	0.00456117
Mtap1b	7.16043	13.336	0.897203	4.24767E-11
Atp2b4	1.80287	3.35757	0.897119	7.2279E-07
Cybrd1	9.01048	16.7611	0.895442	5.90628E-11
C130074G19Rik	0.188225	0.349468	0.892704	0.0120778
B930059L03Rik	0.223192	0.414325	0.892478	0.040966
Rnls	0.46254	0.858511	0.892259	0.0428367
Vldlr	4.62048	8.55794	0.889221	1.52798E-09
Scn2b	0.200752	0.371577	0.888246	0.00400243
Postn	0.213732	0.395513	0.887922	0.00796165
Dhdpsl	0.397814	0.735495	0.886623	0.0134188
Gria3	9.13397	16.8792	0.885932	9.09048E-11
Usp53	1.18258	2.18519	0.885817	1.13871E-05
Gem	0.529514	0.978361	0.885699	0.00233103

Tceal6	1.50159	2.76807	0.882394	0.00124105
Gnpda1	11.1458	20.5453	0.882302	1.31118E-09
Pbxip1	36.929	68.0714	0.882294	6.03448E-10
St6galnac5	3.11785	5.74196	0.880989	3.96415E-06
Nos1ap	0.637469	1.1736	0.880508	0.0253193
Iffo1	4.57091	8.4045	0.878682	7.63587E-07
Plxna4	0.380772	0.699269	0.876922	1.25059E-05
Cela1	0.510261	0.936389	0.875872	0.0157581
Ano4	0.309517	0.567916	0.875657	0.00201534
Ampd3	0.894663	1.637	0.871636	0.000053832
Gpr156	0.144534	0.264455	0.871613	0.0092133
Slc3a2	56.7604	103.852	0.871568	9.88919E-10
Ddc	0.23483	0.429391	0.870675	0.0209762
Ramp1	6.35529	11.6204	0.870632	3.35983E-05
Flnc	1.30694	2.38864	0.869999	1.11638E-07
Ehd4	3.8474	7.02852	0.869336	9.13052E-08
Oxr1	27.9267	51.0059	0.869018	1.59633E-08
Dbx2	13.6285	24.8833	0.868546	1.07916E-09
Ifi30	2.2238	4.06008	0.868478	0.000728554
Atp5sl	2.38523	4.35273	0.86779	8.47412E-06
Rasgrp1	0.0740441	0.135096	0.867528	0.0251762
N4bp2l1	0.650978	1.18719	0.866866	0.00270441
Cyp46a1	0.700912	1.2766	0.865001	0.00168822
Ampd2	15.6219	28.4317	0.863934	2.33601E-10
Pde3a	0.830681	1.51042	0.862585	8.61292E-05
Hspb8	2.55142	4.63765	0.862095	3.47507E-05
Hmox1	24.893	45.2417	0.861913	7.68449E-10
Ppp1r3b	0.312695	0.568086	0.861354	0.00230411
Crim1	3.44846	6.2631	0.860923	8.52962E-09
Tbc1d2	0.104746	0.190129	0.860087	0.0208075
Ednra	1.38375	2.51129	0.85985	1.64411E-05
A330023F24Rik,Mir29b-2,Mir29c	0.0727327	0.13186	0.858333	0.0277713
Thsd1	0.34552	0.62639	0.858292	0.00531864
Cdc42ep3	0.772087	1.39938	0.857955	0.00188115
Fam161a	0.229683	0.416145	0.857444	0.0230196
Slc25a45	0.720075	1.30444	0.857209	0.00266991
Tgfbr3	0.134266	0.243225	0.857201	0.00675166

Fam46a	1.09373	1.98102	0.856989	0.000073736
Cyp2u1	0.978766	1.77273	0.856939	0.000505945
Dennd3	0.3696	0.666918	0.851545	0.000816525
Prkar1b	1.15456	2.08274	0.851145	0.000202946
Mylk	1.10983	2.00087	0.850289	1.13407E-06
Gmpr	3.16336	5.69993	0.849488	3.62095E-05
Chst2	20.2043	36.4038	0.849428	9.04685E-10
Asah2	0.377321	0.679091	0.84781	0.00104376
Ifitm2	6.75129	12.1402	0.84656	0.000174748
Flt1	0.0658113	0.11831	0.84616	0.0254953
Wdr52	0.0489762	0.0879729	0.844976	0.0384759
Vamp8	0.987163	1.77124	0.843401	0.0133645
Dnaja4	1.10086	1.97473	0.843019	0.000157834
Cobll1	5.07693	9.1029	0.842369	3.12843E-08
Muc1	0.984072	1.76314	0.841313	0.000743435
Gpr179	0.269451	0.482614	0.840846	0.000439569
Klhl24	6.66105	11.9274	0.840463	8.9493E-10
4933426M11Rik	12.877	23.0528	0.840143	5.6237E-10
Susd4	4.34555	7.77776	0.839816	2.15758E-06
Tmem19	6.65606	11.9123	0.839716	2.42094E-08
Dnaic2	0.13641	0.244076	0.839382	0.0310393
Pygl	0.124821	0.223329	0.839308	0.0360509
Npr2	1.43431	2.56512	0.838667	2.29478E-05
2210403K04Rik,Mir22	0.953849	1.70507	0.837998	0.00188648
Kcnc1	21.9976	39.3074	0.837453	4.74861E-08
Slc7a5	58.2393	103.979	0.836232	1.32934E-08
Pik3r3	14.274	25.4567	0.83466	6.39775E-10
Gm10825	0.462725	0.824757	0.833815	0.000824148
Stac2	0.1255	0.223333	0.831506	0.03517
Cdhr1	0.348253	0.619017	0.829842	0.00233113
Kank4	0.891869	1.58511	0.829682	6.65706E-05
Kcnn1	0.371346	0.659847	0.829368	0.00234136
Acy3	0.971021	1.72521	0.829198	0.00316016
Cygb	0.206202	0.366352	0.829174	0.0249878
Nbeal2	0.827065	1.46941	0.829165	5.3823E-06
Pgcp	3.90869	6.94376	0.829033	1.18707E-05
1500015A07Rik	1.23642	2.19268	0.826522	0.000849156
Ogdhl	10.0273	17.779	0.826239	3.90173E-09

Trafd1	13.6091	24.0707	0.822712	4.24049E-08
Usp35	1.2844	2.2717	0.822673	3.72527E-05
Pkib	0.0951343	0.168106	0.82133	0.0247858
Carns1	0.129072	0.227806	0.819624	0.023495
Nefl	0.986675	1.74003	0.818462	0.00155294
Lhfpl2	4.56668	8.05324	0.818425	5.31361E-08
Rev1	10.0067	17.6466	0.818425	0.000419611
Arhgap23	0.740261	1.30507	0.818021	0.000107277
Snhg10	1.67886	2.95699	0.816648	0.0198616
Pla2g16	2.33544	4.10644	0.814196	5.23596E-06
Fosl2	0.969964	1.70511	0.813862	0.000027729
Adrb1	3.39761	5.97262	0.813842	5.05357E-06
Matn4	0.21267	0.37364	0.813033	0.0390952
Ccdc30	0.206432	0.362607	0.812742	0.0239547
Lgals3	0.421937	0.740782	0.812021	0.0298206
Cpe	98.5774	173.062	0.811958	2.33484E-08
Egr2	0.852293	1.49565	0.811356	0.000716969
Leprel1	1.98949	3.49074	0.81113	0.000104328
Aatk	2.45153	4.29672	0.809557	6.17219E-07
Slc4a11	0.168021	0.294316	0.808725	0.023037
Cd151	18.5618	32.5007	0.808133	2.5716E-07
Syne1	1.29859	2.27326	0.807816	8.60157E-06
Aldh1l1	67.7269	118.499	0.807079	2.74948E-08
Zfp677	0.175558	0.306932	0.805973	0.0277353
Srgap3	7.37045	12.8829	0.805633	2.55918E-09
Pnpo	0.370701	0.647816	0.805328	0.014643
Plekha4	0.572889	1.00055	0.804471	0.00325445
Cfb	0.331319	0.578575	0.804283	0.0104141
Mt3	298.934	521.15	0.801873	5.27574E-09
Trp53inp2	35.5843	62.0214	0.801524	8.00056E-09
Tnfaip2	0.201326	0.350793	0.801082	0.0155907
Dusp14	2.15017	3.745	0.800516	0.000584127
Cd36	0.263935	0.459624	0.800271	0.0164141
Mitf	0.822384	1.43184	0.799991	0.000155058
Slc43a2	2.25554	3.92679	0.79988	3.2465E-06
Rnf144b	0.595866	1.03697	0.799314	0.00605493
Bdnf	0.421944	0.734271	0.799261	0.0221299
Tek	0.0803912	0.139862	0.798895	0.0409021

Mkl2	5.19331	9.02867	0.79786	0.00105439
Pim2	2.71727	4.72388	0.797814	5.57242E-05
Smox	11.7472	20.4142	0.797251	6.72583E-06
Igfbp2	369.224	641.619	0.797221	2.4286E-06
C2	1.65551	2.87634	0.796958	0.000134806
Alpk1	0.217473	0.377423	0.795344	0.00774708
1700084C01Rik	0.853446	1.48091	0.795117	0.00680533
0610010O12Rik	3.41194	5.91796	0.794509	0.00386922
Dcaf4	10.3995	18.0206	0.793139	3.68735E-07
Tmem35	34.915	60.4796	0.7926	4.8812E-09
Pdk1	1.125	1.94866	0.792557	4.08354E-05
Park2	0.163338	0.282811	0.791976	0.0279405
Fam135b	0.881435	1.52456	0.790467	0.000191687
Dyx1c1	0.274449	0.474597	0.790165	0.049593
Tmco4	0.248501	0.429687	0.790035	0.0136375
Kirrel3	5.75449	9.94994	0.79	2.59101E-06
Axl	3.55984	6.15144	0.789115	5.50605E-07
Slc4a4	22.7989	39.37	0.788136	5.52711E-08
Mfap2	5.49946	9.4956	0.787969	7.83073E-05
Svep1	0.912748	1.57566	0.787666	3.16377E-06
Arfgef2	4.85472	8.37799	0.787217	1.06863E-08
Ptpre	0.509225	0.878674	0.787026	0.000773322
Mtus2	0.069449	0.119743	0.785917	0.0343473
Col4a2	0.428989	0.73965	0.785901	0.000765377
Grn	17.2371	29.6967	0.784786	2.00146E-08
Ndrg2	12.7849	22.0231	0.784577	4.39525E-07
Ppp1r13b	0.405353	0.697653	0.783332	0.00283328
Prkcc	0.230204	0.396055	0.782785	0.0233147
Dnajc6	0.15675	0.269671	0.782732	0.0149295
Cadm2	1.57392	2.70704	0.782358	6.45434E-07
Scrg1	4.89489	8.41483	0.781656	0.000929081
Ephx1	63.5022	109.158	0.781542	9.34496E-09
Kcnip1	3.60957	6.20454	0.781495	2.80885E-05
Adcy2	1.28437	2.20693	0.780981	7.32759E-05
Dlgap1	1.246	2.1405	0.780649	0.000287796
Nek3	2.5727	4.41963	0.780643	0.000432475
Myo5b	0.0744453	0.127836	0.780045	0.0343334
Fam195a	10.3867	17.8276	0.779378	2.79471E-05

Celf3	0.399831	0.686146	0.779123	0.00934764
Steap1	0.531011	0.911112	0.778887	0.0266773
Adamts8	0.645511	1.10714	0.778319	0.00146582
Esrrb	1.73419	2.97325	0.777775	2.74814E-05
Plekha7	2.85124	4.88819	0.777712	2.04811E-06
Lrrk2	1.09759	1.8817	0.777699	7.60245E-06
Il11ra1	4.70828	8.06924	0.777232	2.36952E-05
Elavl3	3.44576	5.89956	0.775783	4.53366E-07
Vwa5a	4.07003	6.96499	0.77508	5.16461E-07
Gse1	5.37838	9.20143	0.774686	7.80261E-06
Phyhipl	16.9055	28.8945	0.773302	1.21381E-05
Jag1	6.53449	11.1685	0.773289	3.89563E-08
Tnfrsf12a	16.543	28.2601	0.772548	0.00029436
Phf21b	6.16119	10.5226	0.772206	2.03283E-07

APPENDIX D - RNA-sequencing MATS analysis in MEFs

Event	Gene Name	ExonID	IncLevEtOH	IncLevOHT	IncLevDifference	PValue	Direction	Replicate
A3SS	2500003M10Rik	ENSMUSG00000001017#chr3#-#90310029l90311180l 90310029l90310183l90311466l90311548#I#A3SS	0.524	1	-0.476	2.27E-11	Inclusion	161
A3SS	2500003M10Rik	ENSMUSG00000001017#chr3#-#90310029l90311180l 90310029l90310183l90311466l90311548#I#A3SS	0.491	1	-0.509	6.99E-09	Inclusion	163
A3SS	Tsc2	ENSMUSG00000002496#chr17#-#24741772l24741937l 24741772l24741934l24744381l24744476#I#A3SS	0.571	0.938	-0.367	0.04829085	Inclusion	159
A3SS	Tsc2	ENSMUSG00000002496#chr17#-#24741772l24741937l 24741772l24741934l24744381l24744476#I#A3SS	0.143	0.846	-0.703	0.006973165	Inclusion	161
A3SS	Yars2	ENSMUSG00000022792#chr16#+#16306555l16306711l 16306590l16306711l16304628l16304796#I#A3SS	0.529	0.777	-0.248	0.028688997	Inclusion	159
A3SS	Yars2	ENSMUSG00000022792#chr16#+#16306555l16306711l 16306590l16306711l16304628l16304796#I#A3SS	0.621	1	-0.379	0.001039232	Inclusion	163
A3SS	Tcf7l2	ENSMUSG00000024985#chr19#+#55991828l55991969l 55991843l55991969l55987048l55987135#E#A3SS	0.405	0.053	0.352	0.005158893	Exclusion	159
A3SS	Tcf7l2	ENSMUSG00000024985#chr19#+#55991828l55991969l 55991843l55991969l55987048l55987135#E#A3SS	0.421	0.112	0.309	0.045271401	Exclusion	161
A3SS	2400003C14Rik	ENSMUSG00000031729#chr8#-#112199275l112200750l 112199275l112199324l112201385l112201586#I#A3SS	0.678	1	-0.322	0.001495469	Inclusion	159
A3SS	2400003C14Rik	ENSMUSG00000031729#chr8#-#112199275l112200750l 112199275l112199324l112201385l112201586#I#A3SS	0.571	1	-0.429	0.005378088	Inclusion	163
A3SS	Plekhg2	ENSMUSG00000037552#chr7#-#29155256l29156061l 29155256l29155516l29156133l29156264#I#A3SS	0.234	0.549	-0.315	0.013388647	Inclusion	159
A3SS	Plekhg2	ENSMUSG00000037552#chr7#-#29155256l29156061l 29155256l29155516l29156133l29156264#I#A3SS	0.332	1	-0.668	0.023213596	Inclusion	161
A3SS	Iffo1	ENSMUSG00000038271#chr6#+#125101812l125102789l 125102631l125102789l125101402l125101543#I#A3SS	0.487	0.928	-0.441	0.016862446	Inclusion	159
A3SS	Iffo1	ENSMUSG00000038271#chr6#+#125101812l125102789l 125102631l125102789l125101402l125101543#I#A3SS	0.31	1	-0.69	0.001315389	Inclusion	161
A3SS	Pprc1	ENSMUSG00000055491#chr19#+#46136630l46136780l 46136633l46136780l46135892l46136066#I#A3SS	0.182	0.432	-0.25	0.043830745	Inclusion	159
A3SS	Pprc1	ENSMUSG00000055491#chr19#+#46136630l46136780l 46136633l46136780l46135892l46136066#I#A3SS	0	0.286	-0.286	0.0062657	Inclusion	161
A3SS	Pprc1	ENSMUSG00000055491#chr19#+#46136630l46136780l 46136633l46136780l46135892l46136066#I#A3SS	0	0.414	-0.414	0.007167437	Inclusion	163
A3SS	Psma3	ENSMUSG00000060073#chr12#+#72084305l72084429l 72084310l72084429l72079719l72079802#I#A3SS	0	0.921	-0.921	0	Inclusion	159
A3SS	Psma3	ENSMUSG00000060073#chr12#+#72084305l72084429l 72084310l72084429l72079719l72079802#I#A3SS	0	0.931	-0.931	0	Inclusion	163
A5SS	Mll1	ENSMUSG00000002028#chr9#-#44641980l44642103l 44641989l44642103l44640943l44641128#E#A5SS	0.431	0.073	0.358	0.018109848	Exclusion	159
A5SS	Mll1	ENSMUSG00000002028#chr9#-#44641980l44642103l 44641989l44642103l44640943l44641128#E#A5SS	0.525	0	0.525	0.025635193	Exclusion	161
A5SS	Usp9x	ENSMUSG00000031010#chrX#+#12742397l12742658l 12742397l12742610l12743757l12743853#E#A5SS	1	0.079	0.921	2.14E-08	Exclusion	159
A5SS	Usp9x	ENSMUSG00000031010#chrX#+#12742397l12742658l 12742397l12742610l12743757l12743853#E#A5SS	1	0.024	0.976	1.9E-11	Exclusion	161
A5SS	Psma3	ENSMUSG00000060073#chr12#+#72079719l72079826l 72079719l72079802l72084305l72084429#E#A5SS	1	0.038	0.962	2.22E-16	Exclusion	159

A5SS	Psma3	ENSMUSG00000060073#chr12#+#72079719l72079826l72079719l72079802l72084305l72084429#E#A5SS	1	0.033	0.967	0	Exclusion	163
MXE	Cct4	ENSMUSG00000007739#chr11#+#22894297l22894387l22895929l22896038l22893266l22893319l22896314l22896457#E#MXE	0.658	0.368	0.29	0	Exclusion	161
MXE	Cct4	ENSMUSG00000007739#chr11#+#22894297l22894387l22895929l22896038l22893266l22893319l22896314l22896457#E#MXE	0.647	0.391	0.256	1.11E-16	Exclusion	163
MXE	Rbx1	ENSMUSG00000022400#chr15#+#81301381l81301452l81304272l81304358l81298584l81298663l81305515l81306149#I#MXE	0.046	0.418	-0.372	6.93E-09	Inclusion	159
MXE	Rbx1	ENSMUSG00000022400#chr15#+#81301381l81301452l81304272l81304358l81298584l81298663l81305515l81306149#I#MXE	0.277	0.533	-0.256	0.000194349	Inclusion	161
MXE	Galnt7	ENSMUSG00000031608#chr8#-#60021308l60021491l60021631l60021814l60018816l60018934l60024125l60024205#I#MXE	0.171	0.373	-0.202	0.026503409	Inclusion	159
MXE	Galnt7	ENSMUSG00000031608#chr8#-#60021308l60021491l60021631l60021814l60018816l60018934l60024125l60024205#I#MXE	0.114	0.393	-0.279	0.029024912	Inclusion	161
MXE	Galnt7	ENSMUSG00000031608#chr8#-#60021308l60021491l60021631l60021814l60018816l60018934l60024125l60024205#I#MXE	0.133	0.545	-0.412	0.026135553	Inclusion	163
MXE	Djc8	ENSMUSG00000054405#chr4#+#132094101l132094203l132097696l132097753l132091495l132091578l132099970l132100037#E#MXE	0.717	0	0.717	6.2E-05	Exclusion	161
MXE	Djc8	ENSMUSG00000054405#chr4#+#132094101l132094203l132097696l132097753l132091495l132091578l132099970l132100037#E#MXE	0.832	0.492	0.34	0.001933732	Exclusion	163
MXE	Tia1	ENSMUSG00000071337#chr6#+#86369094l86369127l86369687l86369806l86368871l86368926l86370317l86370405#E#MXE	0.891	0.641	0.25	0.002312727	Exclusion	161
MXE	Tia1	ENSMUSG00000071337#chr6#+#86369094l86369127l86369687l86369806l86368871l86368926l86370317l86370405#E#MXE	0.869	0.634	0.235	0.035714643	Exclusion	163
MXE		ENSMUSG00000072566#chr15#+#61980793l61980907l61991551l61991683l61938702l61939020l62007021l62007103#E#MXE	0.919	0.574	0.345	0.003464714	Exclusion	159
MXE		ENSMUSG00000072566#chr15#+#61980793l61980907l61991551l61991683l61938702l61939020l62007021l62007103#E#MXE	0.914	0.576	0.338	0.003481267	Exclusion	161
RI	2500003M10Rik	ENSMUSG00000001017#chr3#-#90310029l90311548l90310029l90310183l90311466l90311548#I#RI	0.5	1	-0.5	9.91E-12	Inclusion	161
RI	2500003M10Rik	ENSMUSG00000001017#chr3#-#90310029l90311548l90310029l90310183l90311466l90311548#I#RI	0.474	1	-0.526	3.88E-09	Inclusion	163
RI	Mettl17	ENSMUSG00000004561#chr14#+#52508416l52509310l52508416l52508511l52509202l52509310#E#RI	0.864	0.407	0.457	0.01552353	Exclusion	159
RI	Mettl17	ENSMUSG00000004561#chr14#+#52508416l52509310l52508416l52508511l52509202l52509310#E#RI	1	0.534	0.466	0.036967053	Exclusion	161
RI	Rasa4	ENSMUSG00000004952#chr5#+#136577113l136577559l136577113l136577264l136577494l136577559#I#RI	0.215	0.498	-0.283	2.86E-06	Inclusion	159
RI	Rasa4	ENSMUSG00000004952#chr5#+#136577113l136577559l136577113l136577264l136577494l136577559#I#RI	0.199	0.514	-0.315	0.000117487	Inclusion	161
RI	Rasa4	ENSMUSG00000004952#chr5#+#136577113l136577559l136577113l136577264l136577494l136577559#I#RI	0.197	0.41	-0.213	0.027462934	Inclusion	163
RI	Tctex1d2	ENSMUSG00000014075#chr16#+#32425326l32427007l32425326l32425396l32426943l32427007#I#RI	0.041	1	-0.959	1.14E-07	Inclusion	159
RI	Tctex1d2	ENSMUSG00000014075#chr16#+#32425326l32427007l32425326l32425396l32426943l32427007#I#RI	0.075	1	-0.925	0.048520477	Inclusion	163
RI	Fhod1	ENSMUSG00000014778#chr8#-#107855541l107856092l107855541l107855724l107855936l107856092#I#RI	0.163	0.457	-0.294	0.000507332	Inclusion	159
RI	Fhod1	ENSMUSG00000014778#chr8#-#107855541l107856092l107855541l107855724l107855936l107856092#I#RI	0.093	0.559	-0.466	1.95E-05	Inclusion	161

RI	Adamts10	ENSMUSG00000024299#chr17#+#33675012l33675355l33675012l33675118l33675208l33675355#I#RI	0.483	0.734	-0.251	0.02227738	Inclusion	159
RI	Adamts10	ENSMUSG00000024299#chr17#+#33675012l33675355l33675012l33675118l33675208l33675355#I#RI	0.391	0.769	-0.378	0.030084472	Inclusion	163
RI	Lrdd	ENSMUSG00000025507#chr7#-#148627510l148628463l148627510l148627720l148628049l148628463#I#RI	0.602	1	-0.398	0.021545053	Inclusion	159
RI	Lrdd	ENSMUSG00000025507#chr7#-#148627510l148628463l148627510l148627720l148628049l148628463#I#RI	0.321	0.84	-0.519	0.031974202	Inclusion	161
RI	0610011F06Rik	ENSMUSG00000025731#chr17#+#26013605l26014114l26013605l26013684l26013894l26014114#I#RI	0.375	0.671	-0.296	0.014822168	Inclusion	161
RI	0610011F06Rik	ENSMUSG00000025731#chr17#+#26013605l26014114l26013605l26013684l26013894l26014114#I#RI	0.375	0.666	-0.291	0.030938342	Inclusion	163
RI	Wdr75	ENSMUSG00000025995#chr1#+#45874107l45875109l45874107l45874288l45875014l45875109#I#RI	0.045	1	-0.955	7.39E-10	Inclusion	161
RI	Wdr75	ENSMUSG00000025995#chr1#+#45874107l45875109l45874107l45874288l45875014l45875109#I#RI	0.03	1	-0.97	1.72E-11	Inclusion	163
RI	Fam98b	ENSMUSG00000027349#chr2#+#117083369l117085091l117083369l117083515l117084956l117085091#E#RI	1	0.016	0.984	0.00946378	Exclusion	159
RI	Fam98b	ENSMUSG00000027349#chr2#+#117083369l117085091l117083369l117083515l117084956l117085091#E#RI	1	0.009	0.991	0.034267236	Exclusion	163
RI	Stoml2	ENSMUSG00000028455#chr4#-#43041809l43042230l43041809l43041938l43042150l43042230#I#RI	0.059	0.316	-0.257	0.003094312	Inclusion	159
RI	Stoml2	ENSMUSG00000028455#chr4#-#43041809l43042230l43041809l43041938l43042150l43042230#I#RI	0.103	1	-0.897	0.014584486	Inclusion	163
RI	Aebp2	ENSMUSG00000030232#chr6#+#140599276l140601347l140599276l140599303l140599836l140601347#I#RI	0.427	1	-0.573	1.46E-09	Inclusion	159
RI	Aebp2	ENSMUSG00000030232#chr6#+#140599276l140601347l140599276l140599303l140599836l140601347#I#RI	0.352	1	-0.648	1.87E-08	Inclusion	161
RI	Phkg2	ENSMUSG00000030815#chr7#+#134721048l134721543l134721048l134721224l134721488l134721543#I#RI	0.19	0.396	-0.206	0.020375842	Inclusion	159
RI	Phkg2	ENSMUSG00000030815#chr7#+#134721048l134721543l134721048l134721224l134721488l134721543#I#RI	0.179	0.602	-0.423	0.005852126	Inclusion	163
RI	Nono	ENSMUSG00000031311#chrX#+#98640026l98640673l98640026l98640129l98640633l98640673#I#RI	0.035	1	-0.965	0	Inclusion	159
RI	Nono	ENSMUSG00000031311#chrX#+#98640026l98640673l98640026l98640129l98640633l98640673#I#RI	0.028	1	-0.972	0	Inclusion	161
RI	Nono	ENSMUSG00000031311#chrX#+#98640026l98640673l98640026l98640129l98640633l98640673#I#RI	0.035	1	-0.965	0	Inclusion	163
RI	Parl	ENSMUSG00000033918#chr16#-#20285837l20287142l20285837l20285908l20286992l20287142#I#RI	0.019	1	-0.981	5.36E-09	Inclusion	161
RI	Parl	ENSMUSG00000033918#chr16#-#20285837l20287142l20285837l20285908l20286992l20287142#I#RI	0.025	1	-0.975	1.58E-06	Inclusion	163
RI	Mrps17	ENSMUSG00000034211#chr5#+#130221558l130222741l130221558l130221785l130222601l130222741#I#RI	0.256	0.501	-0.245	0.002485041	Inclusion	159
RI	Mrps17	ENSMUSG00000034211#chr5#+#130221558l130222741l130221558l130221785l130222601l130222741#I#RI	0.193	0.429	-0.236	0.000676491	Inclusion	161
RI	Galt	ENSMUSG00000036073#chr4#+#41703385l41703684l41703385l41703434l41703554l41703684#I#RI	0.16	0.483	-0.323	1.4E-05	Inclusion	159
RI	Galt	ENSMUSG00000036073#chr4#+#41703385l41703684l41703385l41703434l41703554l41703684#I#RI	0.262	0.48	-0.218	0.033746741	Inclusion	161
RI	Galt	ENSMUSG00000036073#chr4#+#41703385l41703684l41703385l41703434l41703554l41703684#I#RI	0.282	0.526	-0.244	0.043508979	Inclusion	163
RI	Ankrd13b	ENSMUSG00000037907#chr11#-#77285950l77286379l77285950l77286114l77286226l77286379#I#RI	0.168	0.496	-0.328	0.023447806	Inclusion	159

RI	Ankrd13b	ENSMUSG00000037907#chr11#-#77285950l77286379l77285950l77286114l77286226l77286379#I#RI	0.047	0.392	-0.345	0.011284512	Inclusion	161
RI	2410002F23Rik	ENSMUSG00000045411#chr7#+#51505678l51507682l51505678l51505710l51505982l51507682#I#RI	0.281	1	-0.719	4.12E-05	Inclusion	161
RI	2410002F23Rik	ENSMUSG00000045411#chr7#+#51505678l51507682l51505678l51505710l51505982l51507682#I#RI	0.255	1	-0.745	0.000157901	Inclusion	163
RI	Ppox	ENSMUSG00000062729#chr1#-#173209560l173210132l173209560l173209705l173209999l173210132#I#RI	0.43	0.697	-0.267	0.003046848	Inclusion	159
RI	Ppox	ENSMUSG00000062729#chr1#-#173209560l173210132l173209560l173209705l173209999l173210132#I#RI	0.452	0.743	-0.291	0.01594661	Inclusion	161
RI	Fxc1	ENSMUSG00000089847#chr7#+#112789275l112789742l112789275l112789371l112789541l112789742#I#RI	0.159	0.427	-0.268	2.49E-06	Inclusion	159
RI	Fxc1	ENSMUSG00000089847#chr7#+#112789275l112789742l112789275l112789371l112789541l112789742#I#RI	0.089	0.333	-0.244	2.4E-07	Inclusion	161
RI	Fxc1	ENSMUSG00000089847#chr7#+#112789275l112789742l112789275l112789371l112789541l112789742#I#RI	0.224	1	-0.776	1.36E-08	Inclusion	163
SE	Med25	ENSMUSG00000002968#chr7#-#52135936l52136008l52135621l52135840l52136292l52136481#E#SE	0.937	0.489	0.448	0.000505472	Exclusion	161
SE	Med25	ENSMUSG00000002968#chr7#-#52135936l52136008l52135621l52135840l52136292l52136481#E#SE	1	0.401	0.599	0.002366841	Exclusion	163
SE	Mettl17	ENSMUSG00000004561#chr14#+#52508821l52508892l52508416l52508511l52509202l52509310#E#SE	0.938	0.567	0.371	0.009800963	Exclusion	159
SE	Mettl17	ENSMUSG00000004561#chr14#+#52508821l52508892l52508416l52508511l52509202l52509310#E#SE	1	0.635	0.365	0.012873464	Exclusion	161
SE	Mettl17	ENSMUSG00000004561#chr14#+#52508821l52508892l52508416l52508511l52509202l52509310#E#SE	1	0.659	0.341	0.034602983	Exclusion	163
SE	Mettl17	ENSMUSG00000004561#chr14#+#52508821l52509072l52508416l52508511l52509202l52509310#E#SE	0.901	0.488	0.413	0.015678773	Exclusion	159
SE	Mettl17	ENSMUSG00000004561#chr14#+#52508821l52509072l52508416l52508511l52509202l52509310#E#SE	1	0.528	0.472	0.021804689	Exclusion	161
SE	Ptbp1	ENSMUSG00000006498#chr10#+#79322861l79322939l79322525l79322700l79323568l79323714#E#SE	0.647	0.122	0.525	0	Exclusion	161
SE	Ptbp1	ENSMUSG00000006498#chr10#+#79322861l79322939l79322525l79322700l79323568l79323714#E#SE	1	0.188	0.812	1.69E-06	Exclusion	163
SE	Mdm2	ENSMUSG00000020184#chr10#-#117146709l117146840l117142210l117142285l117147001l117147084#E#SE	0.786	0.563	0.223	0.000162174	Exclusion	159
SE	Mdm2	ENSMUSG00000020184#chr10#-#117146709l117146840l117142210l117142285l117147001l117147084#E#SE	0.716	0.506	0.21	0.013302913	Exclusion	161
SE	Tlk2	ENSMUSG00000020694#chr11#+#105071858l105071954l105071107l105071151l105082499l105082667#E#SE	0.584	0	0.584	4.37E-08	Exclusion	161
SE	Tlk2	ENSMUSG00000020694#chr11#+#105071858l105071954l105071107l105071151l105082499l105082667#E#SE	1	0.701	0.299	0.008860646	Exclusion	163
SE	Erbb2ip	ENSMUSG00000021709#chr13#-#104620267l104620411l104614799l104615006l104623577l104625108#E#SE	1	0.634	0.366	0.017961793	Exclusion	159
SE	Erbb2ip	ENSMUSG00000021709#chr13#-#104620267l104620411l104614799l104615006l104623577l104625108#E#SE	0.791	0.317	0.474	0.021143176	Exclusion	161
SE	Dph3	ENSMUSG00000021905#chr14#-#32898092l32898167l32896354l32896432l32898595l32898795#E#SE	0.7	0.406	0.294	0.00016138	Exclusion	161
SE	Dph3	ENSMUSG00000021905#chr14#-#32898092l32898167l32896354l32896432l32898595l32898795#E#SE	0.826	0.533	0.293	0.001426256	Exclusion	163
SE	Dph3	ENSMUSG00000021905#chr14#-#32898092l32898293l32893754l32896432l32898595l32898795#E#SE	0.348	0.116	0.232	0.000126514	Exclusion	159
SE	Dph3	ENSMUSG00000021905#chr14#-#32898092l32898293l32893754l32896432l32898595l32898795#E#SE	0.344	0.082	0.262	5.04E-06	Exclusion	161

SE	Dph3	ENSMUSG00000021905#chr14#-#32898092l32898293l 32893754l32896432l32898595l32898795#E#SE	0.537	0.11	0.427	2.1E-06	Exclusion	163
SE	Prmt5	ENSMUSG00000023110#chr14#-#55132127l55132291l 55130829l55130991l55133433l55133483#E#SE	1	0	1	0	Exclusion	159
SE	Prmt5	ENSMUSG00000023110#chr14#-#55132127l55132291l 55130829l55130991l55133433l55133483#E#SE	1	0	1	0	Exclusion	161
SE	Prmt5	ENSMUSG00000023110#chr14#-#55132127l55132291l 55130829l55130991l55133433l55133483#E#SE	1	0	1	0	Exclusion	163
SE	Bin1	ENSMUSG00000024381#chr18#+#32585877l32586006l 32584473l32584621l32591324l32591396#I#SE	0.511	0.902	-0.391	0.001632665	Inclusion	161
SE	Bin1	ENSMUSG00000024381#chr18#+#32585877l32586006l 32584473l32584621l32591324l32591396#I#SE	0.512	1	-0.488	0.023492464	Inclusion	163
SE	Tcof1	ENSMUSG00000024613#chr18#-#60991819l60991963l 60991427l60991649l60992080l60992278#E#SE	0.96	0.453	0.507	1.21E-05	Exclusion	159
SE	Tcof1	ENSMUSG00000024613#chr18#-#60991819l60991963l 60991427l60991649l60992080l60992278#E#SE	0.932	0.661	0.271	0.046558874	Exclusion	161
SE	Tcf7l2	ENSMUSG00000024985#chr19#+#56001173l56001246l 56000466l56000539l56005923l56006699#I#SE	0.132	1	-0.868	0.049763268	Inclusion	159
SE	Tcf7l2	ENSMUSG00000024985#chr19#+#56001173l56001246l 56000466l56000539l56005923l56006699#I#SE	0	1	-1	0.006657726	Inclusion	161
SE	Pycr1	ENSMUSG00000025140#chr11#-#120504472l120504601l 120504205l120504276l120504993l120505018#E#SE	1	0.746	0.254	0.011179095	Exclusion	161
SE	Pycr1	ENSMUSG00000025140#chr11#-#120504472l120504601l 120504205l120504276l120504993l120505018#E#SE	1	0.754	0.246	0.035487878	Exclusion	163
SE	R3hd m2	ENSMUSG00000025404#chr10#+#126918748l126918811l 126913575l126913754l126921031l126921274#I#SE	0.087	1	-0.913	7.48E-07	Inclusion	161
SE	R3hd m2	ENSMUSG00000025404#chr10#+#126918748l126918811l 126913575l126913754l126921031l126921274#I#SE	0.085	1	-0.915	0.000271221	Inclusion	163
SE	R3hd m2	ENSMUSG00000025404#chr10#+#126918748l126918850l 126913575l126913754l126921031l126921274#I#SE	0.13	1	-0.87	2.23E-09	Inclusion	161
SE	R3hd m2	ENSMUSG00000025404#chr10#+#126918748l126918850l 126913575l126913754l126921031l126921274#I#SE	0.068	1	-0.932	3.6E-05	Inclusion	163
SE	Mllt10	ENSMUSG00000026743#chr2#+#18047760l18047856l 18045345l18045439l18068403l18068499#E#SE	1	0.563	0.437	0.037612404	Exclusion	159
SE	Mllt10	ENSMUSG00000026743#chr2#+#18047760l18047856l 18045345l18045439l18068403l18068499#E#SE	1	0.516	0.484	0.009089319	Exclusion	161
SE	Fam18 8a	ENSMUSG00000026767#chr2#-#12325624l12325795l 12322685l12322703l12327486l12327547#E#SE	0.941	0.636	0.305	0.02836364	Exclusion	161
SE	Fam18 8a	ENSMUSG00000026767#chr2#-#12325624l12325795l 12322685l12322703l12327486l12327547#E#SE	1	0.639	0.361	0.016127839	Exclusion	163
SE	Mtfr1	ENSMUSG00000027601#chr3#+#19108490l19108527l 19106451l19106550l19111467l19111583#E#SE	1	0.085	0.915	2.01E-06	Exclusion	159
SE	Mtfr1	ENSMUSG00000027601#chr3#+#19108490l19108527l 19106451l19106550l19111467l19111583#E#SE	1	0.11	0.89	1.91E-05	Exclusion	163
SE	Tpm3	ENSMUSG00000027940#chr3#+#89894934l89895013l 89893931l89894001l89903449l89904487#E#SE	1	0.068	0.932	0	Exclusion	159
SE	Tpm3	ENSMUSG00000027940#chr3#+#89894934l89895013l 89893931l89894001l89903449l89904487#E#SE	1	0.068	0.932	2.63E-13	Exclusion	163
SE	Pacrgl	ENSMUSG00000029089#chr5#+#48771362l48771470l 48770568l48770703l48773025l48773106#E#SE	0.586	0.236	0.35	0.007569231	Exclusion	161
SE	Pacrgl	ENSMUSG00000029089#chr5#+#48771362l48771470l 48770568l48770703l48773025l48773106#E#SE	1	0.266	0.734	0.000227565	Exclusion	163
SE	Tpm4	ENSMUSG00000031799#chr8#+#74670955l74671018l 74670350l74670426l74671096l74671166#I#SE	0.791	1	-0.209	0.000353879	Inclusion	159

SE	Tpm4	ENSMUSG00000031799#chr8#+#74670955l74671018l74670350l74670426l74671096l74671166#I#SE	0.722	1	-0.278	0.000335202	Inclusion	161
SE	Tbc1d24	ENSMUSG00000036473#chr17#-#24319730l24319794l24319394l24319490l24320638l24320797#E#SE	1	0.77	0.23	0.033548402	Exclusion	159
SE	Tbc1d24	ENSMUSG00000036473#chr17#-#24319730l24319794l24319394l24319490l24320638l24320797#E#SE	1	0.543	0.457	0.00362161	Exclusion	161
SE	Upf3b	ENSMUSG00000036572#chrX#-#34639060l34639099l34636852l34637013l34639501l34639684#E#SE	0.529	0.153	0.376	0.001349992	Exclusion	161
SE	Upf3b	ENSMUSG00000036572#chrX#-#34639060l34639099l34636852l34637013l34639501l34639684#E#SE	0.247	0.032	0.215	0.039314304	Exclusion	163
SE	Ubap2l	ENSMUSG00000042520#chr3#-#89835217l89835292l89832246l89832299l89837986l89838099#E#SE	1	0.586	0.414	0	Exclusion	161
SE	Ubap2l	ENSMUSG00000042520#chr3#-#89835217l89835292l89832246l89832299l89837986l89838099#E#SE	1	0.611	0.389	3.85E-09	Exclusion	163
SE	Ubap2l	ENSMUSG00000042520#chr3#-#89835232l89835292l89832246l89832299l89837986l89838099#E#SE	1	0.614	0.386	0	Exclusion	161
SE	Ubap2l	ENSMUSG00000042520#chr3#-#89835232l89835292l89832246l89832299l89837986l89838099#E#SE	1	0.637	0.363	7.39E-09	Exclusion	163
SE	Zfp740	ENSMUSG00000046897#chr15#+#102035659l102035736l102035001l102035314l102038201l102038351#E#SE	0.701	0.402	0.299	0.037814574	Exclusion	161
SE	Zfp740	ENSMUSG00000046897#chr15#+#102035659l102035736l102035001l102035314l102038201l102038351#E#SE	1	0.321	0.679	0.00210974	Exclusion	163
SE	Immt	ENSMUSG00000052337#chr6#+#71816719l71816734l71813134l71813264l71818573l71818797#I#SE	0	0.393	-0.393	3.71E-12	Inclusion	159
SE	Immt	ENSMUSG00000052337#chr6#+#71816719l71816734l71813134l71813264l71818573l71818797#I#SE	0	0.39	-0.39	1.75E-09	Inclusion	161
SE	Tia1	ENSMUSG00000071337#chr6#+#86373599l86373665l86369922l86370405l86374338l86374417#I#SE	0.105	0.384	-0.279	0.000310484	Inclusion	161
SE	Tia1	ENSMUSG00000071337#chr6#+#86373599l86373665l86369922l86370405l86374338l86374417#I#SE	0.066	0.269	-0.203	0.008705428	Inclusion	163
SE	Rpl23	ENSMUSG00000071415#chr11#-#97643119l97643203l97642647l97642776l97643657l97643751#E#SE	0.946	0.719	0.227	0.000938556	Exclusion	161
SE	Rpl23	ENSMUSG00000071415#chr11#-#97643119l97643203l97642647l97642776l97643657l97643751#E#SE	1	0.746	0.254	0.004915888	Exclusion	163
SE	Rpl23	ENSMUSG00000071415#chr11#-#97643119l97643355l97642717l97642776l97643657l97643696#E#SE	0.87	0.411	0.459	4.37E-06	Exclusion	161
SE	Rpl23	ENSMUSG00000071415#chr11#-#97643119l97643355l97642717l97642776l97643657l97643696#E#SE	1	0.476	0.524	0.003301076	Exclusion	163
SE	Ppia	ENSMUSG00000071866#chr11#+#6318103l6318317l6315878l6315982l6319115l6319288#E#SE	1	0.15	0.85	1.22E-14	Exclusion	161
SE	Ppia	ENSMUSG00000071866#chr11#+#6318103l6318317l6315878l6315982l6319115l6319288#E#SE	1	0.068	0.932	6.66E-16	Exclusion	163

APPENDIX E - RNA-sequencing differential gene expression analysis in MEFs

Gene Name	RPKM EtOH	RPKM OHT	log2 Fold Change	p-value
Tacstd2	0	0.0303614	1,7977E+308	0.0334078
Cxcl13	0	0.0477452	1,7977E+308	0.0361027
Atp12a	0.139931	0.569464	2.02489	0.00420945
Fstl4	0.0227818	0.084724	1.89489	0.0289782
Fhl5	0.0926733	0.343413	1.88972	0.0215137
Stx1b	0.0441243	0.16198	1.87617	0.0382404
Odz1	0.0727036	0.242652	1.73879	0.013117
Rxfp1	0.102136	0.312853	1.61499	0.0297757
Wscd2	0.100913	0.296347	1.55417	0.0260662
Adamts17	0.0257874	0.0740318	1.52148	0.0357099
B4galnt3	0.0505701	0.140948	1.47881	0.0466124
Npr3	1.61094	4.1743	1.37363	0.00158393
Svop	0.447327	1.10699	1.30724	0.018683
Ppp2r2c	0.113451	0.277208	1.2889	0.0412102
Arhgap20	1.10346	2.64705	1.26236	0.00416448
Ptprv	0.693821	1.64581	1.24616	0.00691612
St8sia2	0.59413	1.38888	1.22507	0.0201751
Hecw1	0.0714833	0.1642	1.19978	0.046185
Rgs4	8.90464	20.0584	1.17158	0.000724996
Rsad2	1.23833	2.76211	1.15738	0.0401883
Cobl	0.638261	1.40369	1.13701	0.0211189
Myh2	0.969693	2.04349	1.07543	0.0156773
Myh11	8.24732	17.2164	1.06179	0.000901497
Rgs5	3.76049	7.73211	1.03994	0.0157622
Dsp	0.81854	1.66983	1.02858	0.0138056
Arsi	3.63422	7.40905	1.02764	0.0284811
Eln	25.3039	51.1334	1.01491	0.013654
Ano3	4.3123	8.68382	1.00987	0.0166723
Oasl2	4.49211	9.01476	1.0049	0.0424619
Nrk	1.4056	2.81048	0.999628	0.0149673
9930111J21Rik1	1.75252	3.46801	0.984678	0.0222986
Ptprq	1.85436	3.66334	0.982241	0.0120129
Nell2	1.76514	3.45896	0.970557	0.034331
Grid2	2.00129	3.85399	0.945423	0.0374579

Pappa	3.4297	6.57532	0.938979	0.0034493
Slc5a7	2.64796	5.0672	0.936307	0.014472
Mest	71.6641	136.362	0.928115	0.0404224
Adamtsl1	1.37344	2.58095	0.910109	0.0219848
Itga8	8.28484	15.4837	0.902203	0.00662816
Hmcn1	1.06943	1.98536	0.892563	0.0123426
Kank4	4.2849	7.8282	0.869418	0.0162982
Adamts12	9.1692	16.5103	0.848496	0.00714401
Parm1	5.47556	9.78147	0.837044	0.03186
Prrg4	4.26624	7.60609	0.834189	0.0316062
Hcn1	1.38482	2.44098	0.817759	0.043332
Dmd	1.19443	2.08385	0.802926	0.0268856
Ptprd	4.03077	7.02217	0.800862	0.0233514
Jag1	5.15148	8.77508	0.768424	0.0233608
Fat4	10.0276	16.9437	0.756778	0.0206636
Ptprz1	1.69252	2.84921	0.751391	0.043784
Sorbs1	13.3546	22.0709	0.724802	0.0317293
Prelp	21.0046	34.712	0.724731	0.0228304
Mylk	4.04263	6.59222	0.705471	0.0363073
Adamts10	8.22209	13.3416	0.69835	0.0343244
Limch1	6.27819	10.1383	0.691398	0.0402788
Adamtsl3	11.9411	18.7418	0.65032	0.0423629
Cdk1	26.2514	16.7182	-0.650975	0.0440137
Fam162a	304.179	190.105	-0.678123	0.046474
Tacc3	22.559	14.0828	-0.679776	0.0402007
Hmgn2	55.3778	34.5395	-0.681061	0.0439556
Mcm5	15.8966	9.79982	-0.697887	0.0366464
Mcm3	21.1849	13.0475	-0.699265	0.03347
Phyh	40.9464	25.0288	-0.710148	0.0468132
Stmn1	50.5804	30.2537	-0.741467	0.0313387
Top2a	34.2268	20.4477	-0.743191	0.017107
Mad2l1	18.1809	10.8542	-0.744172	0.0426701
Mif	199.533	118.652	-0.749898	0.0302281
Fkbp11	39.8184	23.6651	-0.750672	0.0492266
H2afz	103.702	60.7806	-0.770769	0.0164272
Aurkb	10.8272	6.30994	-0.778964	0.0474733
Pdk1	12.2814	7.08908	-0.79281	0.0281187
Pold1	5.79077	3.34138	-0.793313	0.0446752

Melk	6.8331	3.91924	-0.801967	0.0440782
Cenpa	19.2792	11.0299	-0.805624	0.0369871
Fam64a	12.7679	7.2982	-0.806905	0.0470281
Ube2c	32.1624	18.1688	-0.823915	0.0297321
Bnip3	58.5182	32.8033	-0.835046	0.0250806
Cbr2	177.669	99.0383	-0.843137	0.0225261
Ccnb2	20.1048	11.1416	-0.851586	0.0224155
Tnfsf11	25.045	13.7701	-0.862987	0.0264277
Fbxo5	9.48801	5.21159	-0.864382	0.0376515
Cdca3	23.7327	12.9647	-0.872291	0.0171457
2700094K13Rik	34.1401	18.5886	-0.877045	0.0491597
Birc5	39.5336	21.4229	-0.883924	0.0212829
Slc16a1	31.2609	16.904	-0.886999	0.0213703
Cdca5	5.52812	2.92313	-0.919272	0.0442206
Zc3h12a	15.5439	8.20195	-0.92231	0.0338929
Rnd1	26.9907	14.2336	-0.92316	0.0124259
Irak3	5.61935	2.9508	-0.929297	0.043878
Hmgb2	11.8318	6.21234	-0.929459	0.0116522
Slc16a3	41.8726	21.9627	-0.930955	0.0195588
Ptx3	241.389	125.415	-0.944644	0.0300247
Ccl20	141.689	72.8744	-0.959248	0.0484533
Mybl2	2.682	1.36117	-0.978467	0.0334606
D2Ertd750e	7.65623	3.87782	-0.981388	0.0118728
Cdkn3	9.39876	4.63735	-1.01917	0.0472117
Mt1	263.993	128.02	-1.04413	0.00492678
2610002D18Rik	4.02322	1.93059	-1.05931	0.0452433
Tk1	18.9498	8.80188	-1.1063	0.00986533
Enpp2	12.1137	5.476	-1.14545	0.0165817
Hp	76.243	34.4357	-1.1467	0.0195752
Wfdc2	5.18083	2.17748	-1.25053	0.0411823
Chi3l1	6.41443	2.60056	-1.3025	0.0308098
Cxcl3	20.7705	8.2938	-1.32443	0.00938076
Mt2	503.458	200.556	-1.32787	0.00230525
Rasl12	1.70011	0.660826	-1.36328	0.0225872
Traf1	1.28574	0.471385	-1.44762	0.0484318
U90926	70.0902	21.8933	-1.67873	0.00148449
Gm4349	0.295966	0.0880027	-1.74981	0.0442952
Pgr	0.0244941	0.00609293	-2.00722	0.0431482

Prmt5	20.9639	3.76423	-2.47748	2.51893E-10